C-51-68

TM 5-855-1

TECHNICAL MANUAL

FUNDAMENTALS OF PROTECTIVE DESIGN
FOR CONVENTIONAL WEAPONS

HEADQUARTERS, DEPARTMENT OF THE ARMY
3 NOVEMBER 1, 1986

REPRODUCTION
AUTHORIZATION/RESTRICTIONS

This manual has been prepared by or for the Government and is public property and not subject to copyright.

Reprints or republications of this manual should include a credit substantially as follow: "Department of the Army Technical Manual TM 5-855-1, Fundamentals of Protective Design for Conventional Weapons, 3 November 1986."

TM 5-855-1

TECHNICAL MANUAL
No. 5-855-1

HEADQUARTERS
DEPARTMENT OF THE ARMY
Washington, DC, 3 November 1986

FUNDAMENTALS OF PROTECTIVE DESIGN FOR CONVENTIONAL WEAPONS

---

*This manual supersedes TM 5-855-1, dated July 1965.

TM 5-855-1

List of Figures

LIST OF FIGURES   (cont'd)

LIST OF FIGURES (cont'd)

LIST OF TABLES

LIST OF TABLES (cont'd)

v

CHAPTER 1

INTRODUCTION

1-1. Purpose and scope.

This manual provides procedures for the design and analysis of protective structures subjected to the effects of conventional weapons. It is intended for use by engineers involved in designing deliberately hardened facilities. Users should have a basic knowledge of weapons effects and structural dynamics. Depending on the type of facility and the threat, the structure may be required to protect personnel and equipment against the effects of a penetrating weapon, a contact detonation, or the blast and fragmentation from a standoff detonation. In the last case, if the structure responds in a predominantly flexural mode, it is assumed that the element can be represented by a single-degree-of-freedom (SDOF) system. Transformation factors needed to represent beams and slabs as equivalent SDOF systems are provided in the manual. If the loading or the geometry of the structure is such that a simple SDOF representatiuon is inadequate to determine response, the analyst should consider using a multi-degree-of-freedom (MDOF) system or a finite element representation for calculations.

1-2. Design philosophy.

Since protective structures are usually designed for a single high-intensity transient load, some nonlinear response is permitted. Nonlinear response can be easily represented in the resistance functions for SDOF or MDOF analysis. Nonlinear models for reinforced concrete in finite element codes are not recommended for preliminary design of the type of structures considered in this manual.

1-3. Research.

Little information is available on the synergistic effects of blast and fragmentation. Research presently under way to study these effects on protective structures indicates that fragmentation may deteriorate the concrete cover on the reinforcing steel and make the steel locally ineffective. Reinforement in three directions could minimize this effect by confining the concrete. The use of stirrup is recommended herein in all cases to achieve such confinement. Research is also being conducted to determine the effectiveness of rock rubble / boulder screens to defeat penetrating weapons. Tests show that boulder screens are very effective in degrading the penetration capability of such weapons, especially those with a high slenderness ratio.

1-4. References.

Appendix A contains a list of references used in this document.

2336

CHAPTER 2

NONNUCLEAR WEAPONS CHARACTERISTICS

2-1. General.

Basic weapons information which is necessary for the development of protective structure designs is presented in this chapter. In many cases, generic rather than specific characteristics are presented due to the enormous variety of weapen systems available and the frequency with which they are developed or modified. For this reason, it is recommended that the most current and detailed reference sources containing weapons information be consulted prior to the development of specific structural designs.

2-2. Projectiles.

a. Small arms and aircraft cannon projectiles. Projectiles intended for use in pistols, rifles, machine guns, and aircraft cannon are included in this category. Cartridges most often available to these weapons include ball, tracer, armor-piercing (AP), and armor-piercing-incendiary (API) ammunition (fig 2-1). These projectiles are used against personnel, concrete structures, light armored and unarmored targets, and similar bullet-resisting targets, caliber, projectile weight, and velocity characteristics for typical small arms and aircraft cannon are presented in table 2-1.

BULLET JACKET ─┘   SLUG ─┘

7.62 MM

─GILDING METAL JACKET

MILD STEEL CORE ─┐   ─LEAD ALLOY
                        FILLER

0.50 CAL

BALL

─BASE FILLER

─POINT FILLER

CORE ─┐
BULLET JACKET ─┘

7.62 MM

─CHROME MOLYBDENUM
 STEEL CORE

0.50 CAL

ARMOR-PIERCING
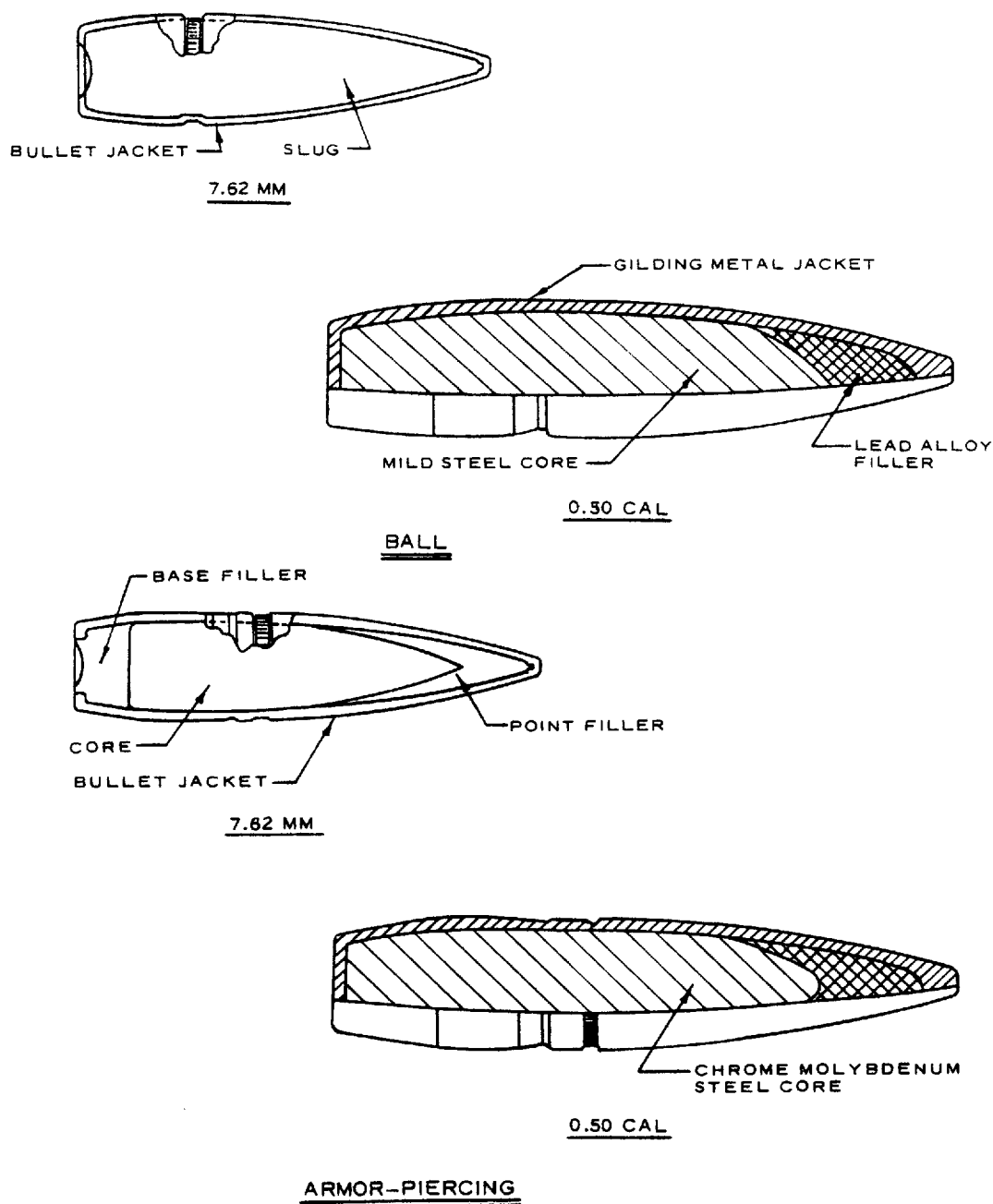
US Army Corps of Engineers

Figure 2-1.   Typical small arms projectiles.

2338

2-2

Table 2-1.   Characteristics of small arms and aircraft cannon.

| Caliber | Type | Projectiles | |
		Weight grains	Muzzle Velocity fps
	Pistols		
7.62 mm	Ball	74–106	950–1,500
9 mm	Ball	125–160	990–1,275
0.45 in.	Ball	208–234	820–850
	Rifles		
5.56 mm	Ball, Tracer	43–56	3,100–3,300
7.62 mm	Ball, Tracer, AP	74–187	1,380–2,880
	Machine Guns		
7.62 mm	Ball, AP, Tracer	149–182	2,680–2,850
12.7 mm (0.50 cal)	Ball, AP, Tracer, Incendiary	620–710	2,750–3,050
14.5 mm	Ball, AP, Tracer, Incendiary	919–980	3,200
	Aircraft		
23 mm	HE, AP, Incendiary	3,080	2,260
30 mm	HE, AP, Incendiary	6,320	2,560
37 mm	HE, AP, Incendiary	11,350	2,260
40 mm	HE, AP, Incendiary	15,000	3,280

  b. Direct and indirect fire weapon projectiles.   Projectiles for mortar, artillery, or direct fire gun cannons (fig 2-2) generally contain a sufficient amount of high explosive (HE) to cause severe blast and fragmentation effects.   The greatest damage from this type of shell is obtained from the explosive action which shatters the concrete, shears the reinforcing bars, and, after repeated hits, perforates the concrete wall.   Considerable damage may result from spalling of concrete interior surfaces. High-explosive antitank (HEAT) shells are effective against hardened targets such as reinforced concrete, armor plate, etc.   HEAT shells generally use a base-detonating delay inertia or piezoelectric-type fuze.

TM 5-855-1

ROTATING BAND
FUZE AND BOOSTER
BASE PLATE
HE FILLER

HIGH EXPLOSIVE

ROTATING BANDS
STEEL PROJECTILE BODY
TRACER
BALLISTIC WINDSHIELD

ARMOR PIERCING SOLID SHOT

STEEL PROJECTILE
BURSTING CHARGE
ARMOR PIERCING CAP
BASE DETONATING FUZE
ROTATING BAND
BALLISTIC WINDSHIELD

ARMOR PIERCING CAP FED

BASE DETONATING FUZE
HE SHAPED CHARGE
ROTATING BAND
SHAPED CHARGE LINER

HIGH EXPLOSIVE ANTITANK

ROCKET PROPELANT
FUZE AND BOOSTER
DELAY ASSEMBLY
ROCKET MOTOR BODY
HE FILLER

HIGH EXPLOSIVE ROCKET-ASSISTED

US Army Corps of Engineers

Figure 2-2. *Typical cannon projectiles.*

2-4

(1) AP projectiles are extremely effective in perforating armor plate and reinforced concrete. AP solid shot is effective against homogeneous armor plate at normal impact; however, against face-hardened and homogeneous plate at more than 10 degrees obliquity, the solid shot is not as effective as a capped projectile unless the striking velocity is very high. Against concrete, the solid shot is not as effective as a capped projectile containing an explosive charge, as the solid shot does little more than crater the concrete. The purpose of the cap is to provide a tough hardened alloy steel nose to withstand the high impact stress and to distribute the impact stresses over the forward body of the projectile. AP capped projectiles are fuzed with delay action inertia-type base fuzes which detonate the explosive after maximum penetration have been achieved. AP projectiles are used principally for direct fire where accuracy is reasonably assured. Oblique impact decreases penetration and causes projectiles to ricochet: hence the rounded and sloping surfaces of tanks and other armored vehicles. Exposed surfaces of protective structures should be designed to present the maximum angle relative to the direction of fire and to the trajectory of the design weapon.

(2) Typical HE shells used in artillery cannons contain an explosive content amounting to approximately 15 percent of the weight of the projectile as fired. They may be fitted with an instantaneous, delay action, or time fuze. Against concrete, a special concrete-penetrating nose fuze may be employed. When fitted with time or instantaneous fuzes, fragments are thrown outward by the explosion and are effective against exposed personnel, supplies, and equipment. When fitted with delay-action fuzes, they may penetrate earth or concrete and detonate in a confined state, thereby causing more damage to a protective structure.

(3) Mortar shells containing 20 to 40 percent explosive cause essentially the same type of damage as artillery shells, although the penetration and range of small-to-medium-mortars are usually less, due to their high trajectory and low velocities. Some of the large breech-loading mortars such as the Soviet 240 mm are known to be capable of delivering very large concrete-penetrating shells (over 630 pounds) which could be expected to cause severe damage to some buried structures.

(4) A summary of typical U. S. and Soviet artillery, mortar, and tank weapon characteristics is presented as table 2-2. The information contained in the table is primarily for HE shells; however, rocket-assisted projectiles (AP) are available or under development for some of the artillery weapons, which will significantly extend their velocity and range capabilities.

Table 2-2. *Characteristics of typical U. S. and Soviet mortar, artillery, and tank rounds*

Caliber	Rate of Fire rounds per minute	Muzzle Velocity fps	Maximum Range m	Projectile			
				Type	Total Weight, lb	Explosive Type	Weight of Explosive, lb
				U.S. Mortars			
60 mm	18–30	522	1,814	HE	3.2	TNT	0.34
81	18–30	875	4,595	HE	9.4	COMP B	2.1
4.2 in.	5–20	960	5,650	HE	27	TNT	7.1
				Soviet Mortars			
82 mm	15–25	693	3,000	HE	6.8	TNT/AMATOL	0.91
120	12–15	893	5,700	HE	35.2	AMATOL	3.48
160	2–3	1,126	8,040	HE	90.7	AMATOL	17.03
240	1	1,189	9,700	HE	288.2	TNT	70.34
240	1	----	----	Concrete Penetrating	632.0	TNT	---
				U. S. Artillery			
105 mm	3–1	1,621	11,500	HE	33	COMP B	5.08
155	1–2	1,852	14,600	HE	94.6	TNT	15.4
175	1	3,000	32,700	HE	147	COMP B	31.0
8 in.	0.5	1,950	16,800	HE	200	TNT	36.75
				Soviet Artillery			
122 mm	6–7	2,956	21,900	HE	47.8	AMATOL	8.1
130	6–7	3.054	31,000	HE	73.6	TNT	10.2
152	4	2,150	17,300	HE	95.8	TNT	12.7
180	1	2,600	30,000	HE	225.0	---	---
203	0.5	1,990	18,000	Concrete Penterating	220.5	TNT	33.9
				U.S. Tank			
90	8–9	2,400	17,900	HEAT	23.4	TNT	2.15
				Soviet Tank			
115	5	---	---	HEAT	39.08	TNT	6.0

2342

c. *Grenades*. Grenades are small projectiles weighing between 1 and 1.5 pounds designed for use against enemy equipment or personnel. The two types—hand and launcher-thrown grenades—are filled with HE or chemical mixtures. The introduction of special-purpose launchers for use by individuals or mounted on combat equipment has made it possible to deliver grenades to targets at greatly extended ranges. A summary of grenade characteristics is presented in table 2-3.

Table 2-3. Characteristics of typical grenades

| Type | Projectile Weight lb | Range, m | Filler | | Remarks |
			Type	Weight lb	
Fragmentation	0.86	40	COMP B	0.40	Hand delivery
Concussion	0.97	30–40	TNT	0.50	Hand delivery
Rifle–HEAT	1.48	115–195	COMP B	0.61	Penetrates approximately 10-in. armor and 20-in. concrete
40–mm Launcher	0.61	350–400	COMP B	0.08	Shoulder fired

2-3. Bombs.

Bombs are divided into four principal groups; high-explosive, fire and incendiary, dispenser and cluster, and special-purpose weapons. Since the blast and fragmentation effects of HE bombs represent the greatest threat to protective structures more attention will be directed toward them than the three remaining bomb categories.

a. *High-explosive (HE) bombs*. HE bombs comprise all types containing HE material primarily for demolition. General-purpose (GP) bombs are designed for general destruction by blast and fragmentation. They will perforate light reinforced concrete and this armor. After penetrating in earth, they will cause considerable damage to nearby structures due to the confined explosion. Light-case (LC) bombs contain a large percentage of HE and, consequently, the thin cases readily deform upon striking resistant materials. For this reason, fuzes are generally instantaneous or non-delay and the principal damage results from blast. Fragmentation (FRAG) bombs cause heavy concentrations of fragments to be distributed around the point of detonation, and are effective against personnel and light equipment. Little damage results from their blast effects. AP bombs have heavy cases which resist deformation when striking heavily protected targets such as warships and reinforced concrete structures. Semi-armor-piercing (SAP) bombs have characteristics similar to AP bombs; however they are not as effective against thick armor. Fuel-air explosive (FAE) bombs, which consist of a thin metal canister filled with a flammable gas, are used to clear helicopter landing areas, detonate mines and booby traps, and destroy above-ground structures.

(1) Charge weight ratios of HE bombs are approximately as follows: AP, 5-15 percent; SAP, 30 percent; GP, 50 percent; and LC, 75-80 percent. FRAG bombs contain only sufficient explosives to fracture the case and cause maximum fragment velocities.

(2) The characteristics of one typical HE bombs are summarized in table 2-4. The bombs annotate as high-slenderness-ratio bombs in the table are representative of the more modern bombs currently in inventories. Figure 2-3 shows sectional views of typical bombs.

Table 2-4. Characteristics of typical generic high-explosive bombs

Designation and Classification	Total Weight (W_T) lb	Diameter (d) in.	Length (L) in.	Charge-Weight Ratio %	Slenderness Ratio (L/d)	Sectional Pressure pp psi $\frac{4W}{\pi d^2}$
GP 100	110	8	29	51	3.6	2.2
GP 250	260	11	36	48	3.3	2.7
GP* 280	280	9	75	35	8.3	4.4
GP 500	520	14	45	51	3.2	3.4
GP* 500	550	11	90	35	8.2	5.8
GP* 750	830	16	85	44	5.3	4.1
GP 1,000	1,020	19	53	54	2.8	3.6
GP* 1,000	1,000	14	120	42	8.6	6.5
GP 2,000	2,090	23	70	53	3.0	5.0
GP* 2,000	2,000	18	150	48	8.3	7.9
GP* 3,000	3,000	24	180	63	7.5	6.6
SAP 500	510	12	49	30	3.9	4.5
SAP 1,000	1,000	15	57	31	3.8	5.6
SAP 2,000	2,040	19	66	27	3.5	7.2
AP 1,000	1,080	12	58	5	4.8	9.5
AP 1,600	1,590	14	67	15	4.8	10.3

* High slenderness ratio bombs.

ARMING WIRE
SUSPENSIONS LUG
BOMB CASE
NOSE FUZE
BURSTING CHARGE
SURROUNDS
AUXILIARY BOOSTER
TAIL FUZE
BOX TYPE FIN

GENERAL PURPOSE

L
TAIL FUZE
NOSE FUZE PLUG

SEMI-ARMOR PIERCING

L
AUXILIARY BOOSTER
TAIL FUZE

ARMOR PIERCING

L
TAIL FUZE AND BOOSTER
CHARGING TUBES
NOSE FUZE AND BOOSTER
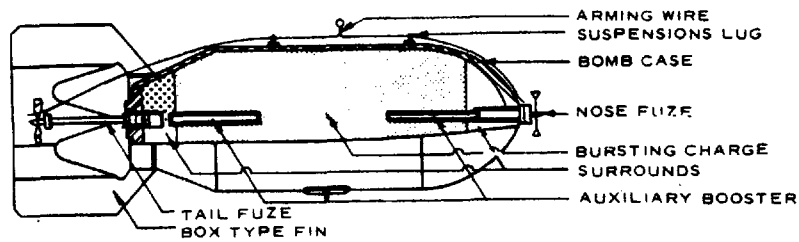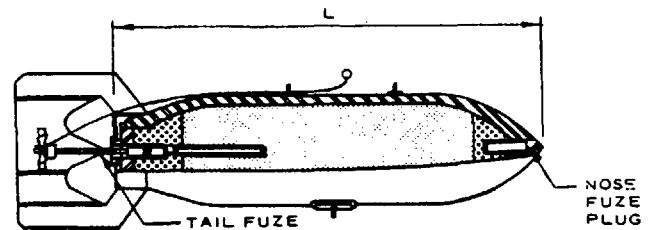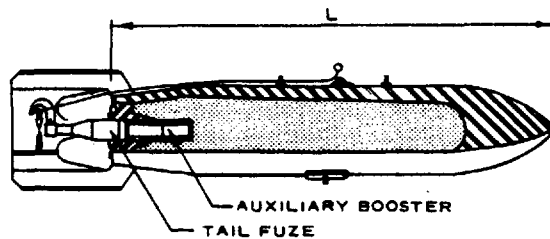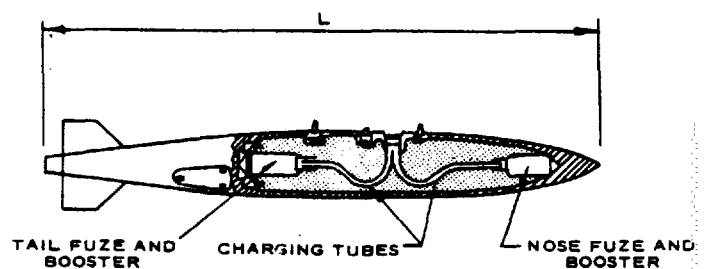
**GENERAL PURPOSE
(HIGH SLENDERNESS RATIO)**

US Army Corps of Engineers

Figure 2–3. Typical high-explosive bombs.

b. Fire and incendiary bombs. Firebombs are large thin-walled metal containers of thickened fuels designed to perforate light to medium structures. They are designed to burst on impact with little or no penetraion. Incendiary bombs are relatively small steel cases filled with metal are petroleum incendiary mixtures that are usually used against hard targets. The incendiary bombs are frequently delivered in clusters and their solid iron noses cause them to fall nose downward and penetrate without deforming. Fire ad incendiary bombs would not normally be employed against well designed protective structures. They are better adapted for the attack of imflammable targets such as built-up industrial and residential areas, troop and equipment assemply areas, fuel storage facilitites, etc. An exception is the gasoline gel firebomb which may be used effectively against entrancers or other openings of protective structures to burn out or deoxidize the interior.

c. Special-purpose bombs. Included in this category are such bombs as leaflet, flare, smoke, and other chemical munitions. In general, these bombs pose very little threat to properly designed and constructed protective structures.

d. Dispenser and cluster bombs. These bombs are normally used against surface targets such as armor, personnel, assembly and storage areas, vehicles, industrial or residential buildings, etc. They consist of large metal dispensers filled with clusters of small HE, HEAT, chemical, FAE, etc., bomblets. The dispensers are fuzed to open and release the bomblets at a predetermined height over the target areas.

2-4. Rockets and missiles.

a. Tactical rockets and missiles. These weapons are designed primarily for use against armored vehicles; however, alternative warheads are available for some of them which make them suitable for use against personnel, equipment, or hardened protective structures. A launcher is used to aim the rockets along a definite trajectory and also provides a means for initiating ignition of the rocket propellant. Launchers are also used to aim and initiate the flight of missiles; however, a guidance system is used to influence the flight of the missile to its target. Most weapons and their launchers are so light and portable that they can be handled by infantry. They can also be aircraft launched. Characteristics of typical U. S. and Soviet surface-launched rockets and missiles are presented in table 2-5.

2346

Table 2-5. Characteristics of typical U. S. and Soviet surface-launched rockets and missiles

Diameter mm	Warhead			Muzzle Velocity fps	Maximum Effective Range, m	Weapon System
	Type	Explosive Filler				
		Weight, lb	Type			
66	HEAT	0.66	OCTOL	476	200	U. S.–LAW
85	HEAT	1.25	RDX	985	300	Soviet–RPG–7
102	HEAT	3.5	OCTOL	250	1,000	U.S. DRAGON
120	HEAT	––		394	3,000	Soviet SAGGER
140	HE	8.10	TNT	1,320	9,810	Soviet MULTIROCKET LAUNCHER
221	HEAT	5.2	OCTOL	657	3,750	U. S. –TOW
240	HE	59.81	TNT	969	10,300	Soviet MULTIROCKET LAUNCHER

b. Battlefield support missiles. Large battlefield support missiles represent a serious threat to protective structures. Missiles such as the U. S. LANCE or Soviet SCUD or FROG series have a nuclear as well a high-explosive capability. They can reliably and accurately deliver large amounts of HE (comparable to the amount contained in bombs) to battle sites hundreds of miles away. It is recommended that appropriate literature (not included in this manual) be referred to for characteristics of these missiles.

2-5. Special-purpose weapons.

a. Fuel-air munitions. These weapons act on the principle of dispersing fuel into the atmosphere so as to form a fuel-to-air ratio which is detonable. The fuel (e.g., propylene oxide) is usually contained in a metal canister. Detonation of a central burster charge causes the canister to rupture and disperses the fuel, forming a fuel-air mixture is detonated. Peak pressure within the cloud is approximately 300 psi. Outside the cloud, the pressure-distance curve is much the same as that for conventional explosives. Fuel-air munitions can create large area loadings on a structure as compared to more localized loadings from an equal weight of HE. Therefore, special consideration is needed for proper protective structure design when these weapons are considered a threat.

b. Demolition materials. Demolition materials are used for the destruction of structures and facilities, for the creation and removal of barriers, and for minefield clearing. They include hand-emplaced breaching or cratering charges, shaped charges, and line charges. Rocket-assisted and tank-mounted minefield clearing devices are also available as is a special 165-mm demolition round that is fired from the Combat Engineer Vehicle (CEV). For information on demolition materials (excluding the 165-mm round), refer to FM 5-25. Characteristics of the 165-mm CEV munition are given in table 2-6. Design methods for protection against the 165-mm round are the same as those used for conventional artillery rounds.

Table 2-6. Characteristics of 165-mm demolition round

Total Weight	65 lb
Explosive type	A-3
Explosive weight	36 lb
Muzzle velocity	840 fps
Range	1,000 yd

c. Flame throwers. Flamethrowers produce intense heat and noxious gases which readily neutralize accessible fortifications. The intense flame may also exhaust the oxygen content of the air inside a structure and thereby cause respiratory injuries to occupants shielded from the flaming fuel. Inproved fuels for use in flamethrowers permit longer ranges for flamethrower operations and increased temperatures and burning time.

2-6. Weapon development trends.

With ever-increasing technology, the designer of protective structures will be faced with providing protection form more sophisticated weapons. Significant improvements are being made in the areas of weapons accuracy, fuzing, and damage mechanisms. As an example, weapons are being developed with hardness-sensing fuzes which allow for delayed detonations against soft targets such as soil, so that the round can penetrate. These hardness-sensing fuzes function instantaneously when impacting a hard target such as concrete. In the area of damage mechanisms, dual-stage munitions are currently being developed. These munitions use a shaped charge to create a hole into which a high-explosive follow-through warhead can more easily penetrate and detonate, resulting in increased damage. Thus, the designer must be aware of new weapons development so that structures that are built for a long life span will not become obsolete.

CHAPTER 3

AIRBLAST EFFECTS

3-1. Introduction

The blast effects of an explosion are in the form of a shock wave composed of a high-pressure shock front which expands outward from the center of the detonation, with the pressure intensity decaying with distance. As the wave front impinges on a protective structure, a portion of the structure or the structure as a whole will be engulfed by the shock pressures. The magnitude and distribution of the blast loads on the structure are a function of the type of explosive material, weight of explosive, the location of the explosion relative to the protective structure, and the interaction of shock front with the ground or the protective structure itself.

3-2 Types of explosive and comparative effects

a. Explosives vary in a number of ways that determine their effectiveness, including not only detonating rate or velocity, but also other characteristics such as density and heat production. Various explosive are compared by their various characteristic for demolition charges or by their blast pressure and impulses for bombs and shells. TNT is used as the standard or reference explosive for equating the effects of various explosives. The free-air equivalent weight of a particular explosive is the weight of the standard explosive TNT required to produce a selected shock wave parameter of magnitude equal to that produced by a unit weight of the explosive in question.

b. The equivalent weight of an explosive based on blast pressure or impulse varies at different pressure levels. Generally an average value for the equivalency is used. Averaged free-air equivalent weights for common military explosives are given in table 3-1.

Table 3-1.   Averaged free-air equivalent weights based on blast pressure and impulse

Explosive	Equivalent Weight Pressure	Equivalent Weight Impulse	Pressure Range, ps i
ANFO (9416 Am Ni/ Fuel oil)	0.82		1-100
Composition A-3	1.09	1.07	5-50
Composition B	1.11	0.98	5-50
Composition C-4	1.37	1.19	10-100
Cyclotol (70/130)[a]	1.14	1.09	5-50
HBX-1	1.17	1.16	5-20
HBX-3	1.14	0.97	5-25
H-6	1.38	1.10	5-100
Minol II 70/30[b]	1.20	1.11	3-20
Octol 75/25	1.06		
PETN	1.27		5-100
Pentolite	1.42	1.00	5-100
	1.38	1.14	5-600
Tetryl 75/25[c]	1.07		3-20
Tetrytol 70/30 65/35	1.06		
TNETB	1.36	1.10	5-100
TNT	1.00	1.00	Standard for pressure ranges shown
Tritonal	1.07	0.96	5-100

[a] RDX/TNT
[b] HMX/TNT
[c] TETRYL / TNT

3-3. Cube-root scaling.

Hopkinson or cube-root scaling is used to relate the characteristic properties of the airblast wave from an explosion of one energy level to that of another energy level. According to cube-root scaling, a given pressure will occur at a given distance from an explosion that is proportional to the cube root of the energy yield. This has been proven true experimentally for explosive weights ranging from a few ounces to hundreds of tons. Using cube-root scaling, if R is the distance from a reference explosion of weight W pounds, then parameters such as overpressure, dynamic pressure, and particle velocity for the reference explosion would occur for an explosion weight W_2 pounds at a distance R_2 given by:

$$R/R_2 = (W/W_2)^{1/3} \text{ or }   R/W^{1/3} = R_2/W_2^{1/3} \qquad \text{(eq 3-1)}$$

The term $R/W^{1/3}$ is the scaled distance and is represented in this manual by the symbol λ . Likewise, the scaled time of arrival is $t_a/W^{1/3}$, and the scaled impulse is $i_s/W^{1/3}$. Cube-root scaling implies that all quantities with dimensions of pressure and velocity are unchanged in the scaling .   Using the scaling relations, a large amount of data on the parameters associated with the blast wave can be shown on relatively simple plots. The scaling relations apply when there are: (a) identical ambient conditions, (b) identical charge shapes,   (c) identical charge-to-surface geometries. However, reasonable values can be obtained using the scaling relations even when only similar conditions exist.

2350

3-4. Blast wave phenomena.

   a. General. The violent release of energy from a detonation in a gaseous medium gives rise to a sudden pressure increase in that medium. The pressure disturbance, termed the blast wave, is characterized by an almost instantaneous rise from the ambient pressure to a peak incident pressure P_{so}. Incident pressure is the pressure on a surface parallel to the direction of the blast wave. This pressure increase or shock travels radially from the burst point with a diminishing velocity U which is always in excess of the sonic velocity of the medium. Gas molecules, making up the front, move at lower velocities u . This latter particle velocity is associated with a dynamic pressure or the pressure formed by the winds produced by the shock fronts. As the shock front expands into increasingly larger volumes of the medium, the peak incident pressure at the front decreases and the duration of the pressure increases

   (1) At any point away from the burst, the pressure disturbance has the shape shown in figure 3-1. The shock front arrives at time t_a and, after the rise to the peak value, the incident pressure decays to the ambient value in the time t_o which is the positive phase duration. This is followed by a negative phase with a duration t_o longer than the positive phase and characterized by a pressure below the preshot ambient pressure and a reversal of the particle flow. The negative phase is usually less important in a design than the positive phase. The incident impulse density (hereafter referred to as unit incident impulse associated with the blast wave is the integrated area under the pressure-time curve. It is denoted as i_s for the positive phase.

OVERPRESSURE

P_{so}

i_s, IMPULSE (i.e., AREA UNDER CURVE)

AMBIENT
PRESSURE
(P_a)

TIME

t_A t_o $t_o + t_o^-$

POSITIVE PHASE   NEGATIVE PHASE

(t_o) (t_o^-)
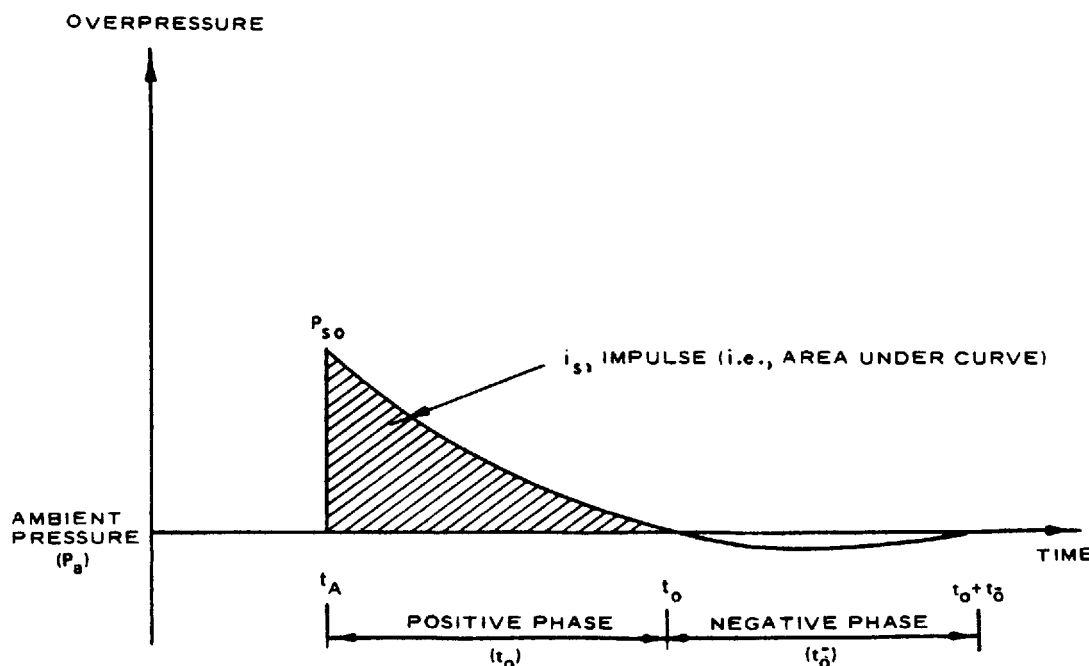
US Army Corps of Engineers

Figure 3-1.   Free-field pressure-time variation.

(2) If the shock wave impinges on a rigid surface oriented at an angle to the direction of propagation of the wave, a reflected pressure is instantly developed on the surface, and the pressure is raised to a value in excess of the incident pressure. The reflected pressure is a function of the pressure in the incident wave and the angle formed between the rigid surface and the plane of the shock front. For a reflector, where flow around an edge or edges occurs, the duration of the reflected pressures is controlled by the size of the reflecting surface. The high reflected pressure seeks relief toward the lower pressure regions, and this tendency is satisfied by the propagation of rarefaction waves from the low-to the high pressure region. These waves, traveling at the velocity of sound in the reflected pressure region, reduce the reflected pressures to the stagnation pressure, which is the value that is in equilibrium with the high-velocity air stream associated with the incident pressure wave. When such a relief is not possible (for example, when an incident wave strikes an infinite surface) the incident pressure at every point in the wave will be reflected. These reflected pressures will last for the duration of the wave.

(3) The peak positive reflected pressure is designated P_r and the unit impulses associated with a completely reflected incident wave are i_n for the positive phase.

(4) An additional parameter of the blast wave, the wave length, is required in the analysis of structures. The positive phase wave length L_w is that length at a given distance from the detonation which, at a particular instant of time, is experiencing positive pressures

b. *Reflected overpressure.*

(1) When the incident pressure wave moves radially away from the center of an explosion and comes in contact with a surface, the pressures and impulses of the initial wave are reinforced and reflected. The reflected pressure pulse of figure 3-2 is typical for infinite plane reflectors. When the shock wave impinges on a surface that is perpendicular to the direction of travel of the shock wave, then the point of initial contact will be subjected to the maximum reflected pressure and impulse. The reflected pressure varies from this maximum to a minimum pressure where the reflecting surface is parallel to the direction of travel of the blast wave. This minimum will be the same as the incident pressure. The variation of the pressure and impulse patterns on a reflecting surface is a function of the angle on incidence α and the magnitude of the incident pressure P_{so}

2 3 5 2

Pr

Pso

t₀

t₀ + t₀⁻

TIME

POSITIVE
PHASE
DURATION

NEGATIVE PHASE
DURATION, t₀⁻

US Army Corps of Engineers
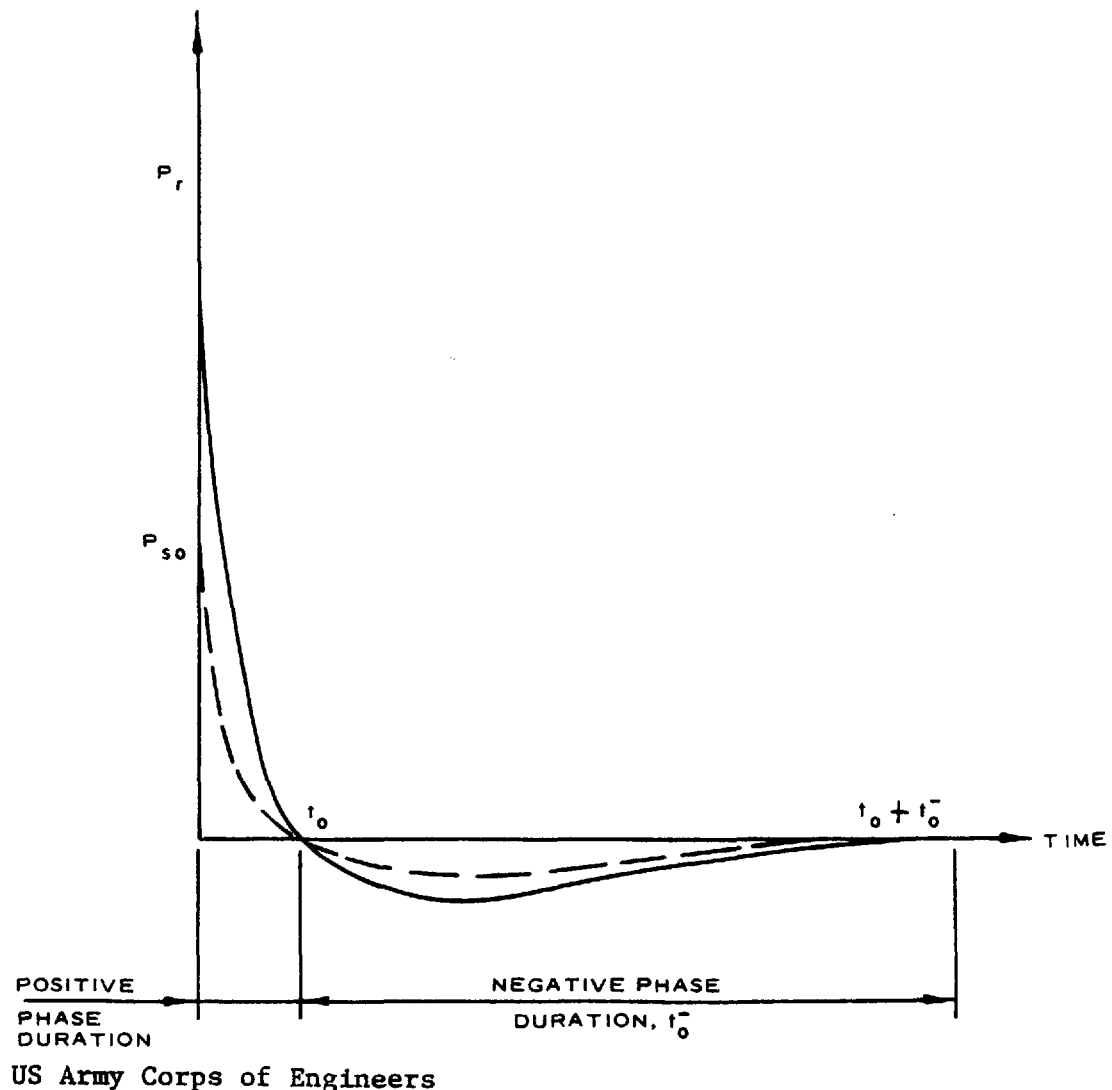
Figure 3-2. Typical reflected pressure-time history.

(2) The effect of the angle of incidence on the peak reflected pressure is shown in figure 3-3, a plot of the angle of incidence versus the peak reflected pressure coefficient for various peak incident pressures. The peak reflected pressure P_r is obtained by multiplying the peak reflected pressure coefficient $C_{r\alpha}$ by the peak incident pressure P_{so} . For design purposes, the other blast parameters (except the duration of the wave) may be taken as those corresponding to the reflected pressure P_r . The duration of the blast wave should correspond to the duration of the free air pressure.
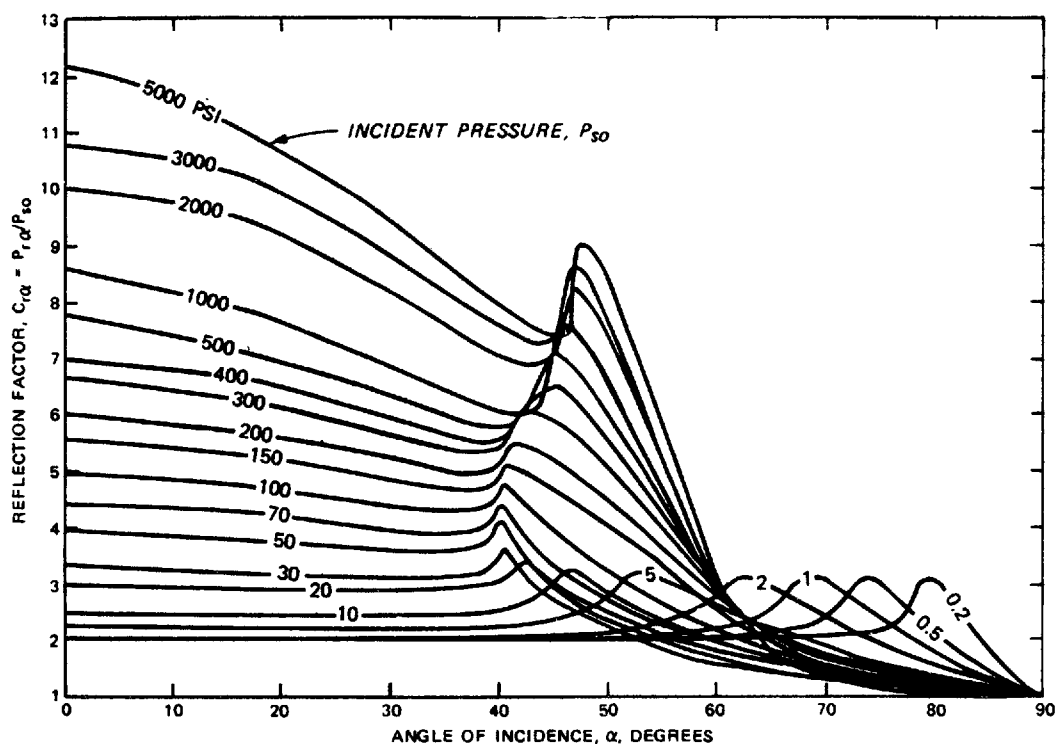
SOURCE: Air Force Weapons Laboratory, "Protection from Nonnuclear Weapons," AFWL TR 70-127.

Figure 3-3. Reflected pressure coefficient versus angle of incidence.

   c. Airburst. Peak pressure, impulse, velocity, and other parameters for a spherical TNT explosion in air as a function of scaled distance ($\lambda = R/W^{1/3}$) are given in figure 3-4. Although the curves presented in figure 3-4 were developed from the detonation of bare spherical TNT charges, they can also be used for cased charges where the TNT equivalency of the actual explosive weight is used to calculate the scaled distance. Casing effects on reducing the effective weight of the explosive should be ignored since they are not well defined and could produce an unconservative design if considered.
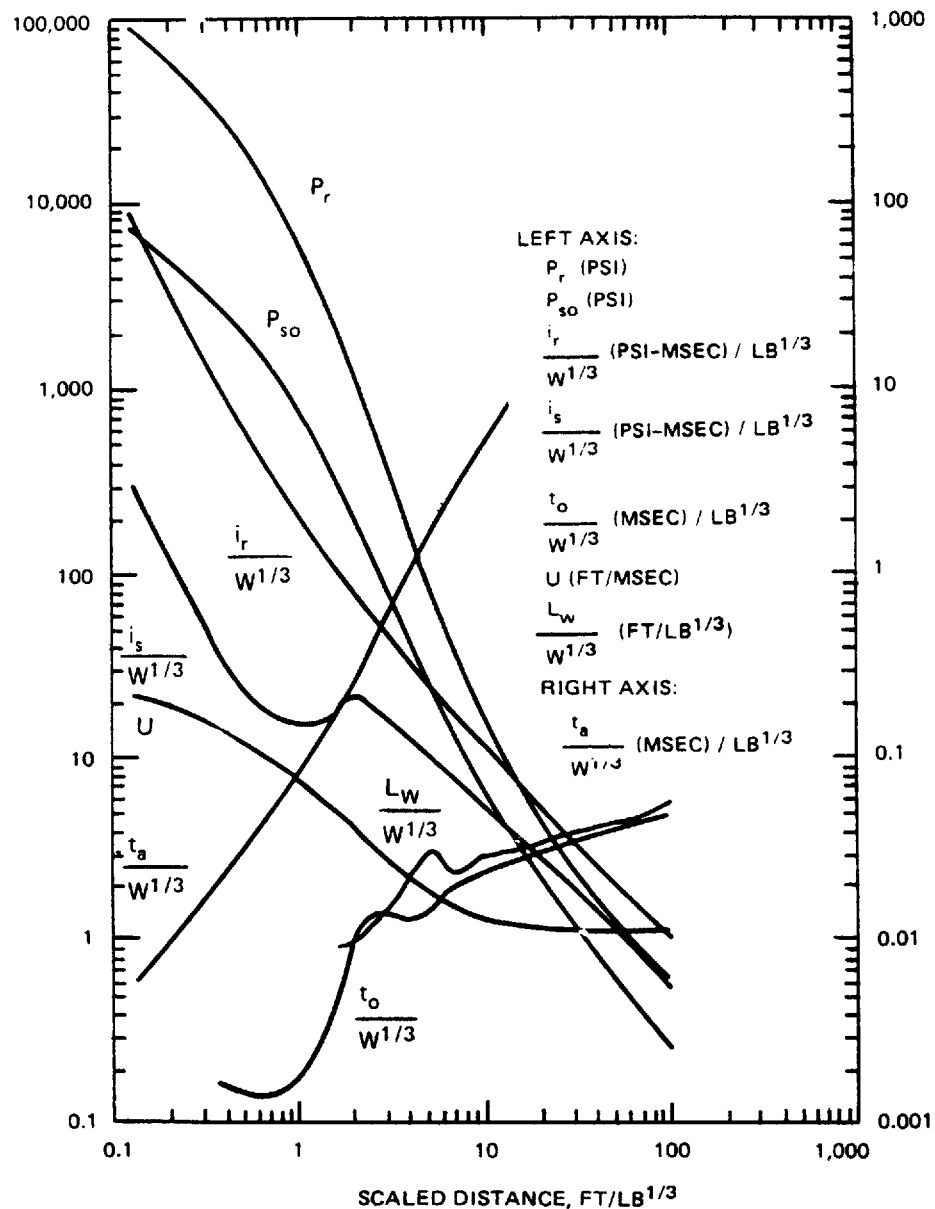
U.S. Army Ballistic Research Laboratory

Figure 3-4. Shock wave parameters for spherical TNT explosions in free air

(1) Two loading cases are to be considered with an airburst: (a) explosions that occur above a protective structure such that no amplification of the initial shock wave occurs between the explosion and the structure and (b) an explosion which occurs at some distance from the structure so that the initial shock wave propagating away from the explosion impinges on the ground surface prior to arrival at the protective structure. Loadings for the first case can be determined using the curves shown in figure 3-4 along with the appropriate reflection factor from figure 3-3.

(2) Loadings for the second case are slightly more complicated to obtain since there is an interaction of the blast wave with the ground surface prior to the blast wave's arrival at the structure. As the blast wave propagates out ward, a front known as the Mach front (fig 3-5) is formed by the interaction of the initial wave (incident wave) and the reflected wave which is the result of the reinforcement of the incident wave by the ground. Some variation of pressure occurs over the height of the Mach front but, for design purposed, this variation can be neglected and the shock considered as a plane wave over the full height of the front. The pressure-time variation of the Mach front is similar to that of the incident wave except that magnitude of the pressure is somewhat larger.
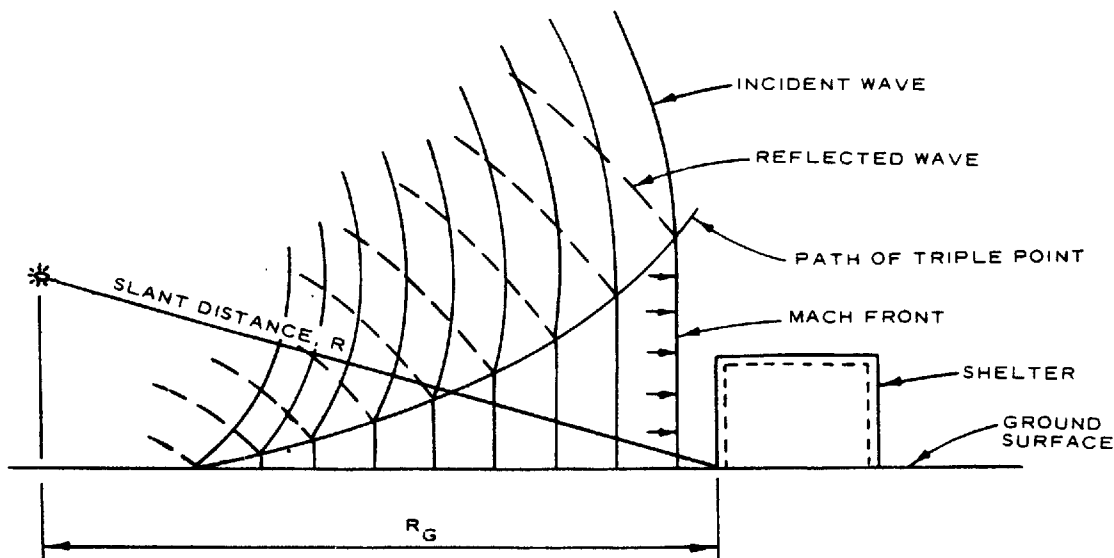
US Army Corps of Engineers

Figure 3-5. Blast environment from an airburst.

(3) The height of the Mach front increases as the wave propagates away from the center of the detonation. This increase in height is referred to as the path of the triple point and is formed by the intersection of the initial, reflected, and Mach waves. A protective structure is subjected to a plane wave (uniform pressure) when the height of the triple point exceeds the height of the structure.

(4) If the height of the triple point does not extend above the height of the structure. then the magnitude of the applied loads will vary with the height of the point considered. Above the triple point, the pressure-time variation consists of an interaction of the incident and reflected incident wave pressures resulting in a pressure-time variation different from that of the Mach incident wave pressures. The magnitude of pressures above the triple point is smaller than that of the Mach front. In most practical design situations, the location of the detonation will be far enough away from the structure so as not to produce this pressure variation. An exception may exist for multistory buildings. although these buildings are usually located at very low pressure ranges where the triple point is high.

(5) For determining the magnitude of the blast loads acting on the surface of an aboveground protective structure, the peak incident blast pressures in the Mach wave acting on the ground surface immediately before the structure are calculated first. The peak incident free-air pressure is determined for this point from figure 3-4 using the distance R (fig 3-5) which corresponds to the path of the initial shock wave between the explosive source and any point on the ground surface beyond the point at which the Mach wave is formed. Once the incident free-air pressure is obtained, then the peak reflected pressure P_r is computed from figure 3-3, using the predetermined values of the angle of incidence α and the peak incident free-air pressure. Other blast parameters of the Mach wave are determined form figure 3-4 in a manner similar to that used for reflected free-air pressures.

d. Surface burst. A charge located on or very near the ground surface is considered to be a surface burst. The initial wave of the explosion is reflected and reinforced by the ground surface to produce a reflected wave. Unlike the airburst, the reflected wave merges with the incident wave at the point of detonation to form a single wave similar in nature to the reflected wave of the air-burst but essentially hemispherical in shape (fig 3-6).

2357

TM 5-855-1
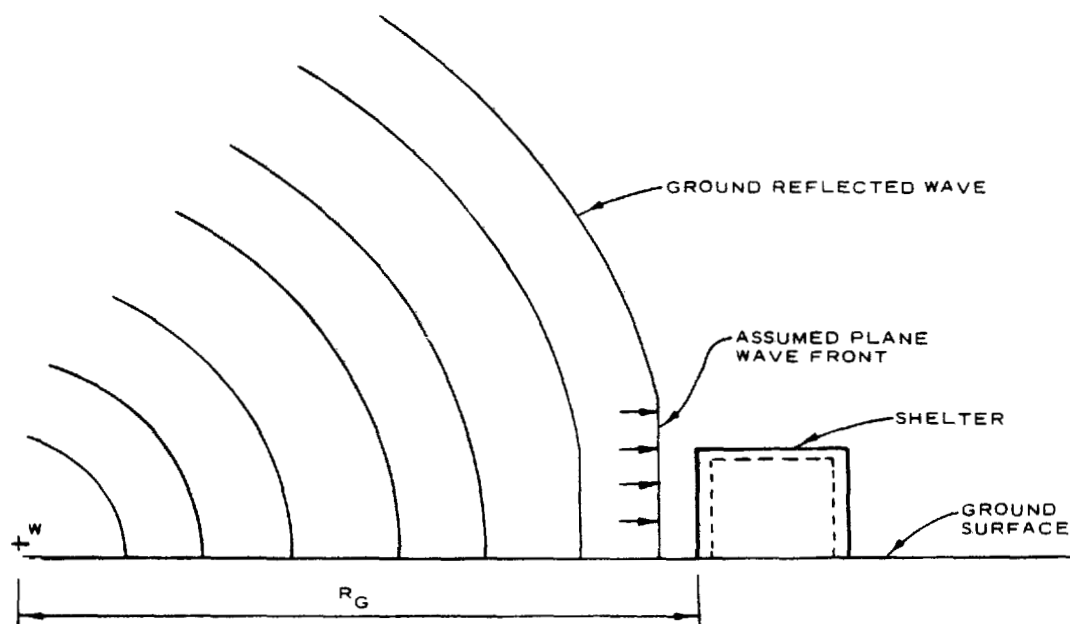
US Army Corps of Engineers

Figure 3-6. Surface burst blast environment.

(1) The parameters of the surface burst environment for TNT explosions are given in figure 3-7. A comparison of figures 3-4 and 3-7 shows that, at a given distance from a detonation of the same weight of explosive, all of the parameters of the surface burst environment are larger than those for the free-air environment.

2358
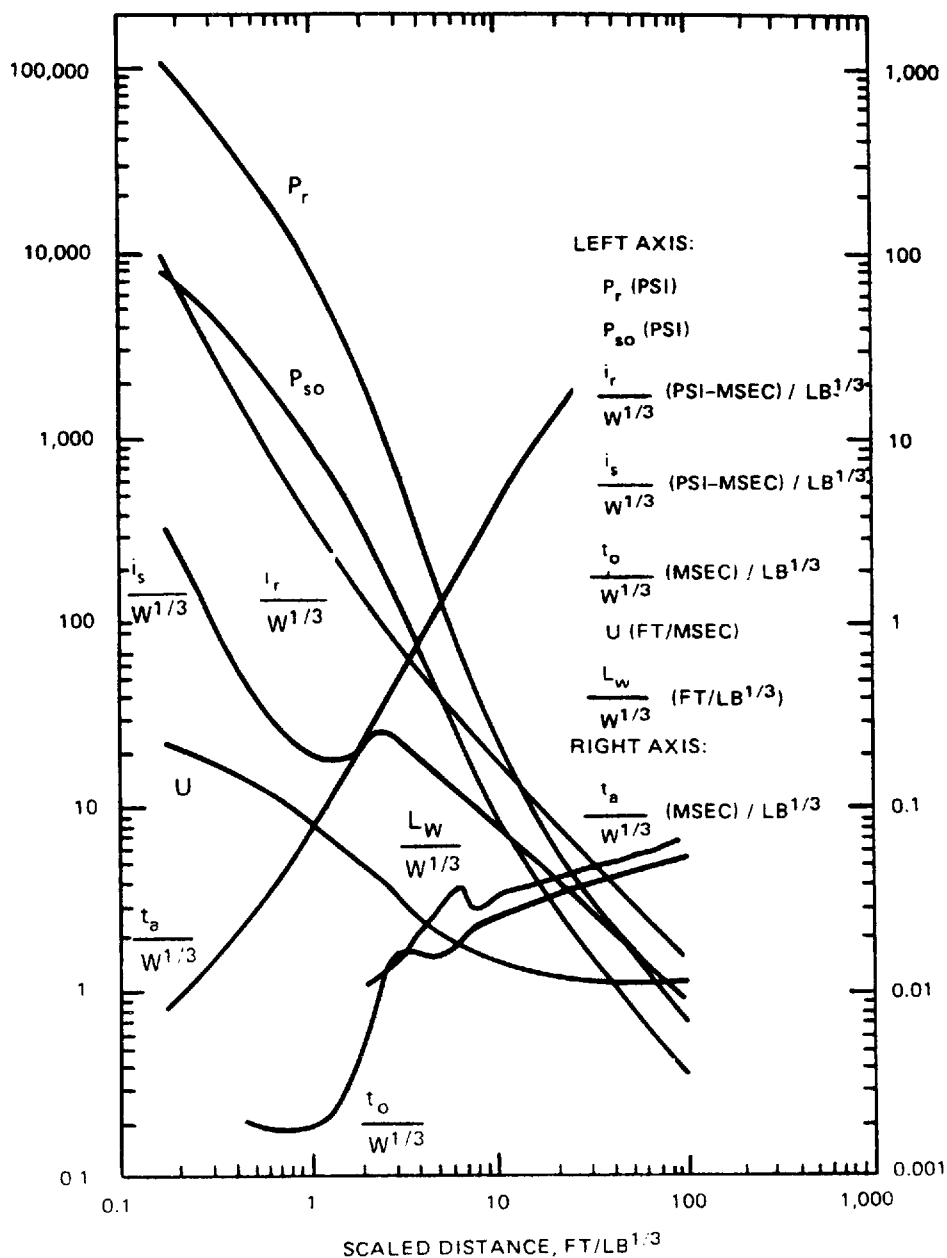
U.S. Army Ballistic Research Laboratory ...

Figure 3-7. Shock wave parameters for hemispherical TNT surface bursts at sea level

2359

Provided by IHS
No reproduction or networking permitted without license from IHS

Sold to:ARSALAN GHAHRAMANI, W0685154
Not for Resale,2009/5/25 8:10:11 GMT

3-11

(2) As for the case of airbursts, protective structures subjected to the explosive output of a surface burst will usually be located in the pressure regions where the plane wave (fig3-6) concept can be applied. Therefore, for surface bursts, the blast loads acting on structure surfaces are calculated as described for the airburst, except that the incident pressures and other parameters of the free-field shock environment are obtained from figure 3-7.

e. Dynamic pressure. The forces acting on a structure associated with a a plane shock wave are dependent upon both the peak values and the pressure-time variation of the incident and dynamic pressures acting in the free field. The peak values of the free-field pressures for the several blast loading categories were treated previously. For each pressure range, there is a particle or wind velocity associated with the blast wave that causes a dynamic pressure on objects in the path of the wave. In the free field, these dynamic pressures are essentially functions of the air density and particle velocity . For typical conditions, standard relationships have been established between the peak incident pressure P_{so} and the peak dynamic pressure q_0 . The magnitude of the peak dynamic pressure is solely a function of the peak incident pressure and, therefore, independent of the size of the explosion. Figure 3-8 gives the values of the peak dynamic pressure versus peak incident pressure.
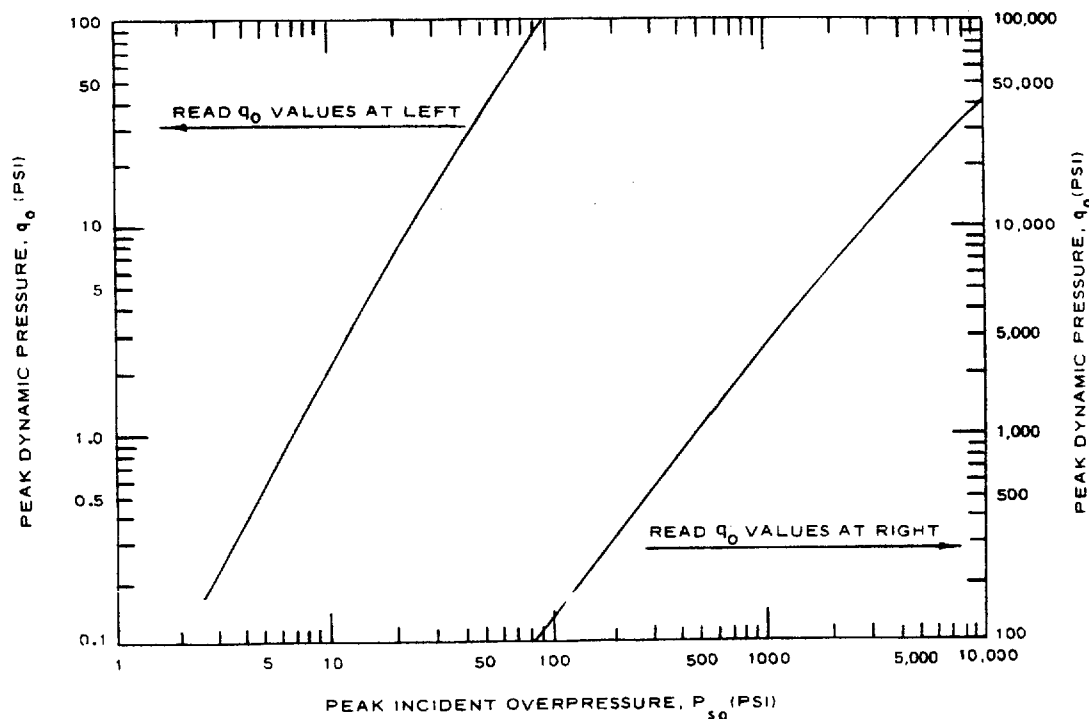
US Army Corps of Engineers

Figure 3-8.   Peak incident pressure versus peak dynamic pressure.

2360

f. Equivalent triangular pulse. For design purposes, it is necessary to establish the variation or decay of both the incident and dynamic pressures with time since the effects on a structure subjected to a blast loading depend upon the intensity-time history of the loading as well as on the peak intensity. The idealized form of the incident blast wave (fig 3-1) is characterized by an abrupt rise in pressure to a peak value, a period of decay to ambient pressure and a period in which the pressure drops below ambient (negative-pressure phase).

(1) The rate of decay of the incident and dynamic pressures, after the passage of the shock front, is a function of the peak pressure and the size of the detonation. For design purposes, the actual decay of the incident pressure may be approximated by the use of an equivalent triangular pressure-time pulse. The accrual duration of the positive pressure phase is replaced by a fictitious positive duration t_{of} which is a function of the total positive impulse and the peak pressure:

$$t_{of} = \frac{2i_s}{P_{so}}$$

(eq 3-2)

(2) The above relationship for the equivalent triangular pulse is applicable to the incident pressures as well as the reflected blast pressures; however, in the case of the latter, the value of the impulse used with equation 3-2 is equivalent to that associated with the reflected wave. The fictitious duration of the dynamic pressures may be assume to be equal to that of the incident pressures.

3-5. Suppressed airblast (delay-fuzed rounds)

When a bomb or shell explodes after penetration into the earth, the majority of the energy released is used in forming the crater and producing ground shock. Penetration is discussed in chapter 4 and crater formation and ground shock are discussed in chapter 5. If the explosion occurs at shallow depths of burial, some of the explosive gasses are released into the atmosphere, producing airblast. The peak airblast at various distances from the ground surface directly above the explosion can be predicted using the curve in figure 3-9.

$$\bar{\lambda} = \lambda_x \cdot \rho' \cdot \lambda_D$$

$$\lambda_x = R/W^{1/3}$$

$$\lambda_D = D/W^{1/3}$$

X = ADJUSTED SCALED GROUND RANGE
R = GROUND RANGE IN FEET
D = DEPTH OF EXPLOSION IN FEET
W = WEIGHT OF TNT IN POUNDS
ρ' = SPECIFIC GRAVITY OF SOIL

(NOTE: THIS CURVE IS VALID FOR
VALUES OF $\lambda_D < 2$ FT/LB$^{1/3}$

PEAK INCIDENT AIRBLAST PRESSURE, PSI

ADJUSTED SCALED GROUND RANGE, $\bar{x}$ (FT/(LBS TNT)$^{1/3}$)
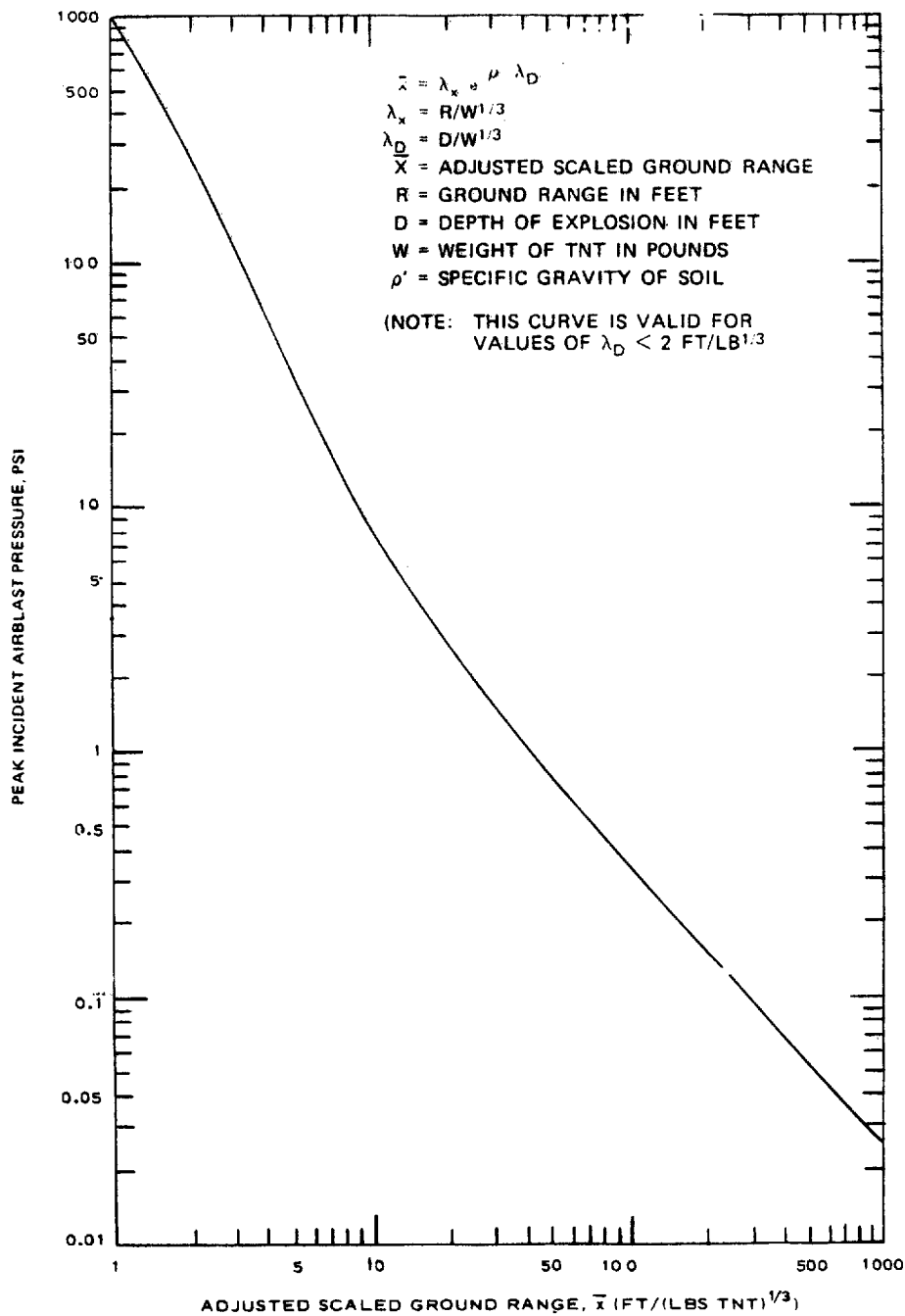
SOURCE: Naval Surface Center, "Explosion Effects and Properties, Part I – Explosion Effects in Air," Technical Report No. 75-116.

Figure 3-9. Peak incident airblast pressure from underground explosion.

2362

3-6. Pressure increases within a structure

a. Leakage through openings . When a structure is enveloped in a blast wave, a leakage of the pressures through any openings in the structure occurs. The interior of the structure experiences an increase in its ambient pressure in a time that is a function of the structure volume, area of openings, and applied exterior pressure and duration. Since personnel exhibit a tolerance limit to such pressure increases, a method of determining the average pressure inside the structure is needed. It should be noted that the interior pressures immediately adjacent to the openings will be higher than the average pressure. The following method for calculation the average pressure increase is applicable for structures with small area of opening/volume ratios and applied blast pressures of less than 150 psi. The change in pressure ΔP_i inside the structure within a time interval Δt is a function of the pressure difference at the openings $P - P_i$ and the area-volume ratio A_0 / V_0

$$\Delta P_i = C_L\left(\frac{A_0}{V_0} \right) \Delta t \qquad\qquad (eq\ 3\text{-}3)$$

where

ΔP_i = interior pressure increment, psi

C_L = leakage pressure coefficient (a function of pressure difference $P - P_i$ where P = pressure applied to the exterior of the structure)

A_0 = area of openings, ft ^{2}

V_0 = volume of structure, ft^3

Δt = time increment, ms

Figure 3-10 shows the variation of C_L versus $P - P_i$. The interior pressure-time curve is calculated as follows:

(1) Determine the pressure-time of the applied blast pressures P acting on the surface surrounding the opening as presented in paragraph 3-4f.

(2) Divide the duration t_0 of the applied pressure into n equal intervals Δt , each interval being approximately $t_0/10$ to $t_0/20$, and determine the pressures at the end of each interval.

(3) For each time interval, compute the pressure differential $P - P_i$, determine the corresponding value of C_L from figure 3-10, and calculate ΔP_i from equation 3-3 using the proper values of A_0/V_0 and Δt . Add ΔP_i to P_i for the interval being considered to obtain the new value of P_i for the next interval. At time $t = 0$,the pressure differential will be equal to P , the peak overpressure incident on the entrance.
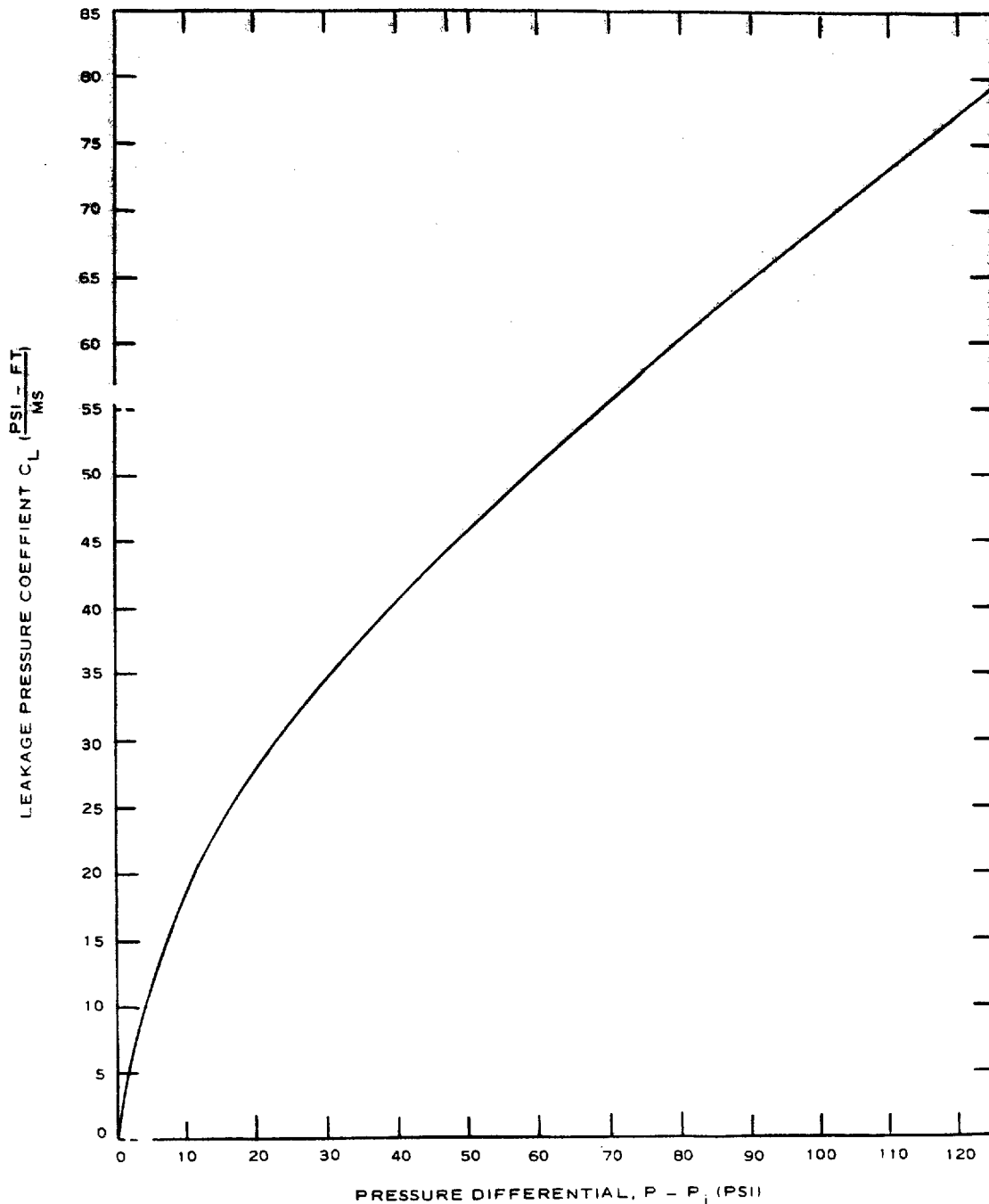
US Army Corps of Engineers

Figure 3-10. Leakage pressure coefficient versus pressure differential.

(4) Repeat for each interval using the proper values of P and P_i. Note that when $P - P_i$ becomes negative during analysis, the value of C_L must be taken as negative also.

2364

3-16

b. Confined blast. The loading from an explosion occurring inside a structure consists of two phases. The first phase is the reflected blast loading consisting of an initial high-pressure, short-duration reflected wave plus perhaps several later reflected pulses that have already interacted with other parts of the inclosed area. The later reflected wave are very complicated to define. A schematic representation of shock reflections from the wall of an inclosed area is shown in figure 3-11. The second loading phase is a quasi-static pressure pulse caused by the overpressure settling to a slowly decaying level. The quasistatic overpressure is dependent on the charge -weight-to-room volume ratio for its peak value and depends on the vented area of the inclosure for its decay characteristics.
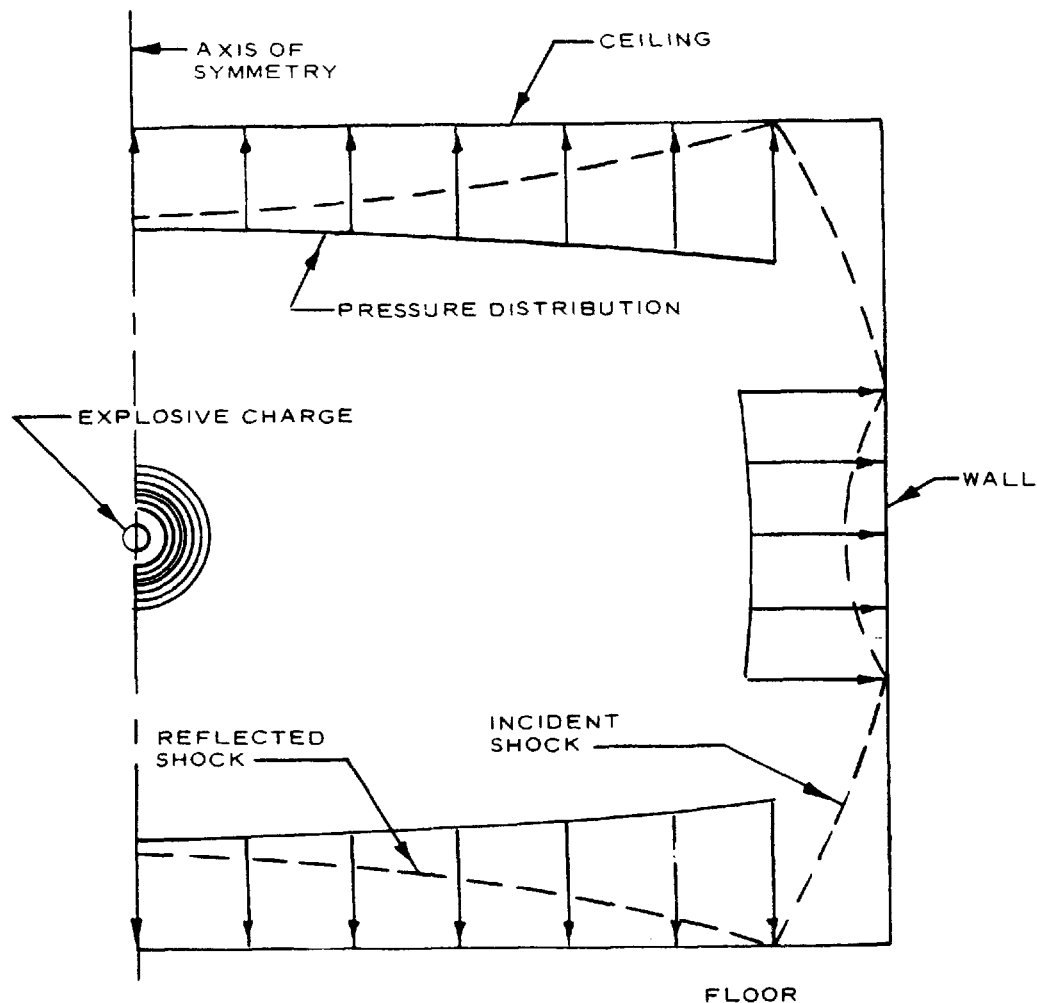
US Army Corps of Engineers

Figure 3-11. Schematic representation of shock reflection from interior walls of a structure.

(1) Initial reflected overpressure. The air shock loading on interior surfaces is quite complex for all structural geometries. Approximate loading predictions suitable for preliminary design or analysis can be made with several simplifying assumptions. First, it is assumed that the initial *reflected airblast parameters* can be taken as the ideal normally reflected parameters even for oblique reflections from the structure walls. This assumptions reasonable for strong shock waves (greater than ambient pressure) up to an angle of incidence of about 40 degrees and for weak shock waves (less than ambient pressure) about 70 degrees. The slant range from the center of the charge to the point of interest should be used to calculate the scaled distance used to determine the reflected pressure P_r and impulse i_s from the curves presented in figure 3-4. The duration of the initial reflected pulse is taken as

$$t_r = 2i_r/P_r \qquad \text{(eq 3-4)}$$

The re-reflected aftershock is neglected for preliminary analysis or design. If a more exact calculation of loading is required, then it is necessary to consider arrival times of the shock front and re—reflected aftershock as a function of position in the structure.

(2) **Quasi-static pressures.**

(a) When an explosion occurs within a structure, the over pressure eventually settles to a slowly decaying level, which is a function of the volume and vent area of the structure and the nature and energy release of the explosion. A typical time history of overpressure at the wall of a structure after an internal explosion is shown in figure 3-12a. This pressure-time history can be idealized as the two triangle pulses shown in figure 3-12b. Determination of the initial impulsive portion of the idealized loading curve can be determined from the methods presented in paragraph 3-6b. Prediction of the idealized long duration quasi-static portion of the loading is presented below.
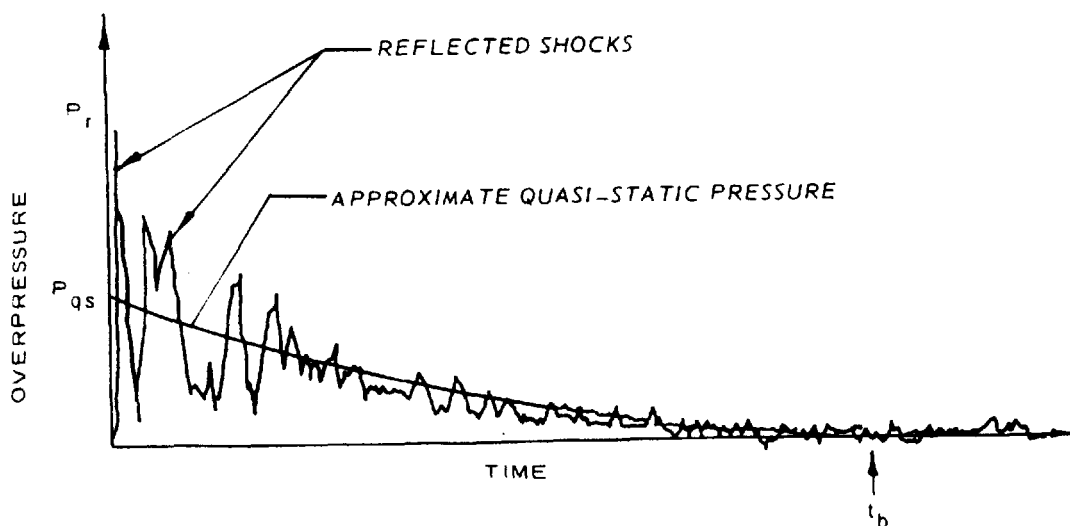
a. TYPICAL PRESSURE-TIME HISTORY
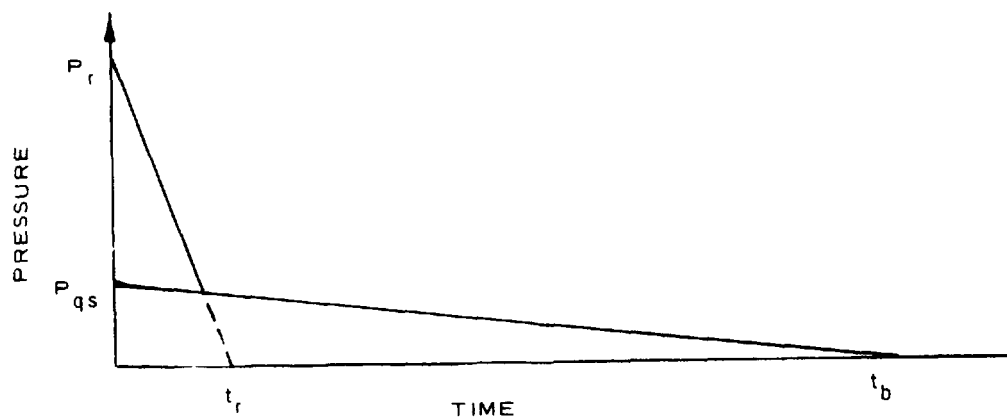
b. IDEALIZED PRESSURE-TIME HISTORY

US Army Corps of Engineers

Figure 3-12. Pressure loading on inner surface of structure.

(b) The tow parameters of interest for construction of the quasi-static portion of the idealized loading function are the peak quasi-static pressure P_{qs} and the time t_b at which the quasi-static pressure returns to ambient. The maximum value for the quasi-static pressure in the long-duration phase of the loading is the pressure rise which would occur in an unvented enclosure. Figure 3-13 has been shown to yield good predictions of P_{qs} as a function of the charge-to-volume ratio, W/V_I. The time for the internal pressure to return to ambient pressure can be determined from figure 3-14 once P_{qs} had been established. In figure 3-14.

P_a = ambient pressure, psi

C = speed of sound, 1,100 fps

V_I = internal volume of structure, ft^3

A_i = internal vented surface area, ft^2

∂_e = vent area ratio

The internal vented surface area is the total surface area of those surfaces which are vented. For example, if the side walls are vented, but the roof and floor are not, A_i is equal to the total interior surface area of the walls only. The vent area ratio is

$$\partial_e = A_V / A_W \qquad \text{(eq 3-5)}$$

where A_V and A_W are the vent areas and wall areas of the structure, respectively. The vent area is the area of all openings and the wall area is the total internal area of the walls.

2368

3—20

PEAK QUASI-STATIC PRESSURE, P$_{qs}$ (PSI)

W/V$_I$ (LB/FT³)

SOURCE: U.S. Army Corps of Engineers
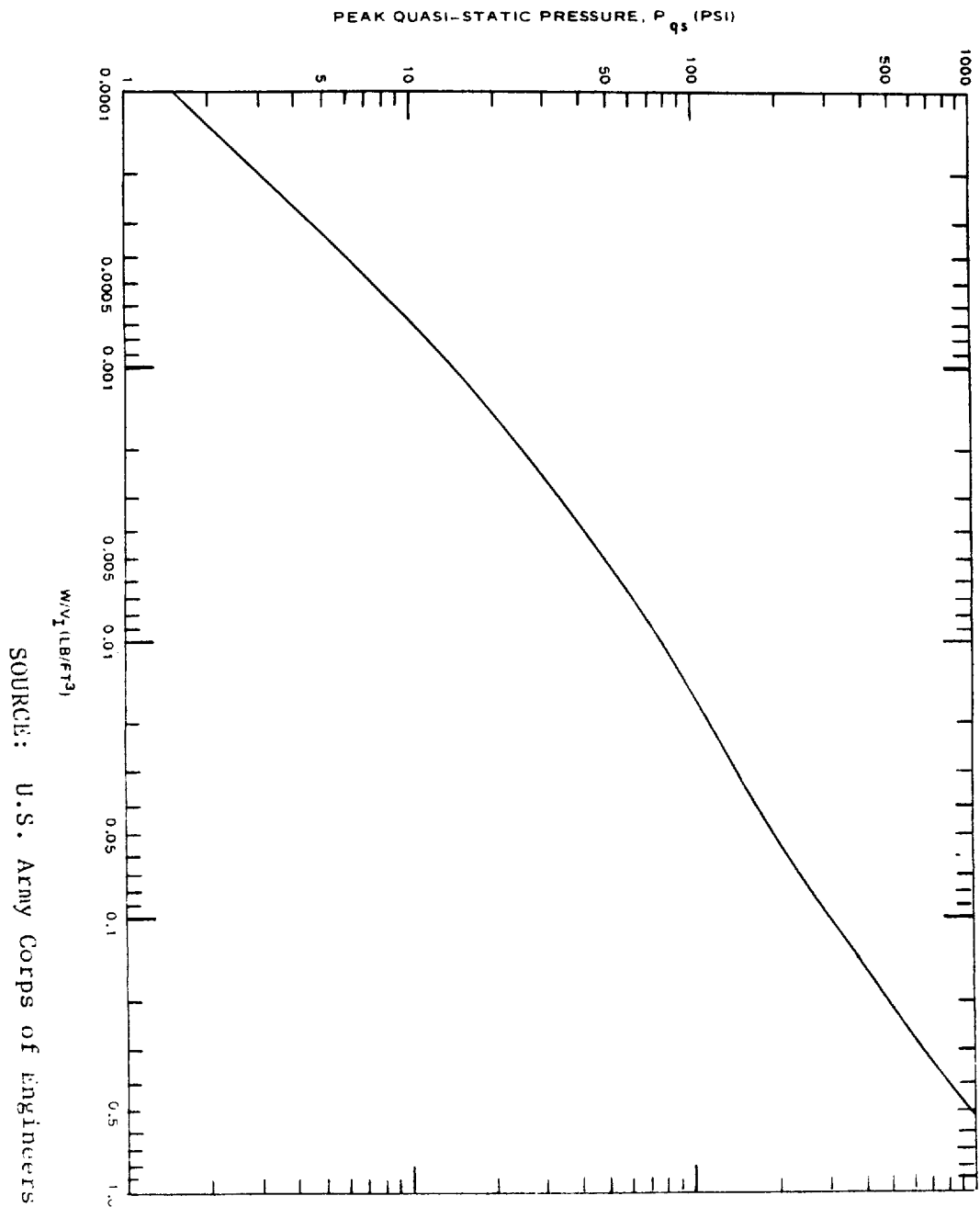
Figure 3-13. Peak quasi-static pressure.
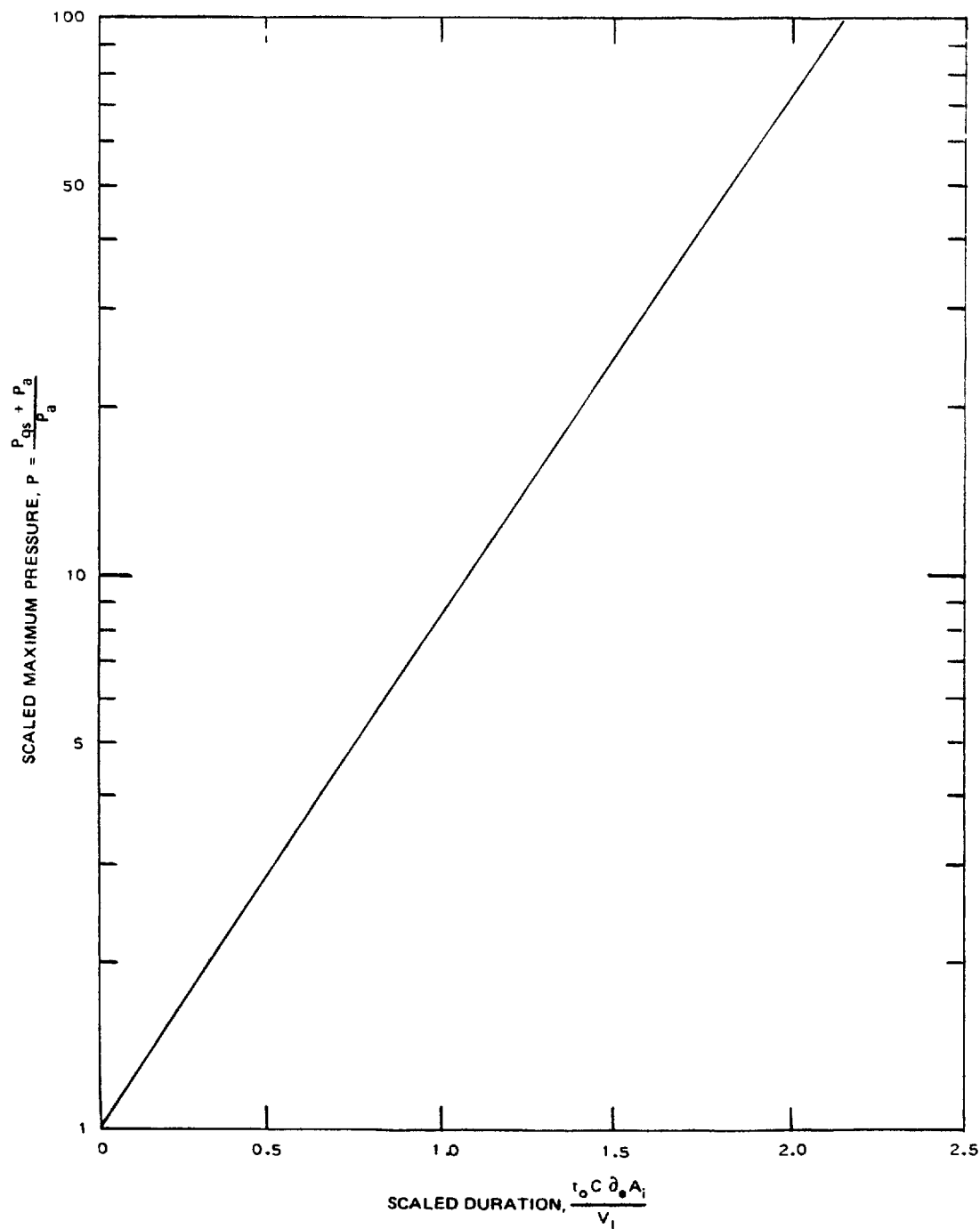
Figure 3-14. Scaled durations versus scaled maximum pressure.

US Army Corps of Engineers

2370

3-7. Airblast transmission through tunnels and ducts.

It is necessary to know how a blast wave propagates through a tunnel or duct in order to define the loading on blast closures for the entranceway or ventilation system of a buried shelter. The formation of the flow field at the entrance to a tunnel is very complex and is dependent on the orientation and configuration of the opening as well as the surrounding topography. Overpressures within the tunnel may be increased or decreased by the tunnel geometry. A decrease in the area of the tunnel's cross section will cause an increase in overpressure.
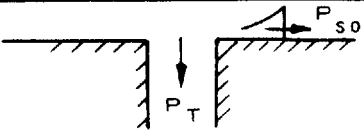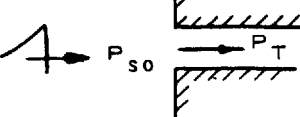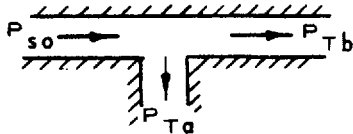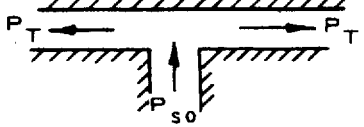
a. Most of the available data on the attenuation of blast pressure in tunnels have been obtained through shock tube tests which were conducted using long-duration loads to simulate a nuclear blast wave. The shock tube data, when compared to the limited data available for short-duration loads, give reasonable results. Therefore, the long-duration shock tube data are presented herein to be used to predict the blast loadings from conventional weapons. Neither empirical data nor analytical methods are available for all conceivable tunnel configurations. However, there is sufficient information for designers to make reasonable estimates of tunnel pressure for many variations in tunnel geometry knowing the free stream conditions at the tunnel entrance.

b. Sharp turns or bends will reduce the peak pressure in a tunnel of uniform cross section. Shock tube studies have shown that a 90-degree bend in a tunnel will reduce the peak pressure by approximately 6 percent. Thus, the peak pressure P_n after n such turns is

$$P_n = P_{so} (0.94)_n \qquad \text{(eq 3-6)}$$

where P_{so} is the peak overpressure in the tunnel just ahead of the first turn. The above equation assumes that there are no losses from friction or pressure attenuation between bends. It also assumes that the positive phase duration t_o is greater than or equal to $50 D_t/C$ where D_t is the tunnel diameter in feet and C is the ambient sound velocity in feet per second. Shock tube data for various tunnel configurations are summarized in figure 3-15. The data in figure 3-15 apply up to about 50 psi only. For overpressures greater than 50 psi, curves such as the one in figure 3-16 should be used.

CASE	RATIO OF TRANSMITTED TO PEAK OVERPRESSURE P_T/P_{so}
	0.5
	1.0
	1.5
	(a) 0.5 (b) 0.8
	0.8
90° BENDS	$(0.94)^n$ WHERE n IS THE NUMBER OF TURNS

US Army Corps of Engineers

Figure 3–15. Transmitted overpressure in tunnels $(P_{so} \leq 50\,psi)$.
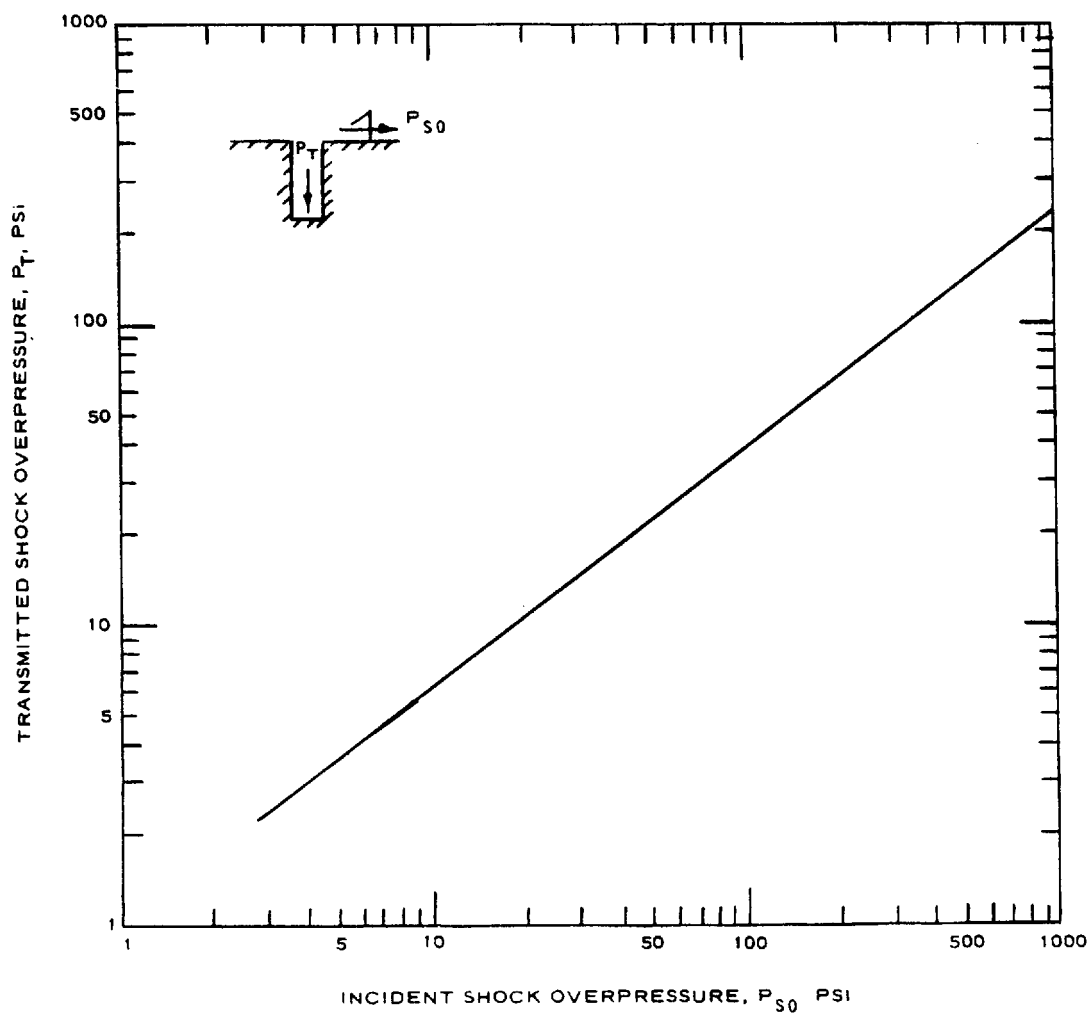
Figure 3-16. *Incident shock overpressure versus transmitted shock overpressure for side-on tunnel.*

2373

c. As a blast wave progresses through a straight tunnel of uniform cross section, the peak overpressure decreases due to friction losses along the tunnel walls, viscosity of the fluid, and the rate *of decay of the shock front.* Attempts have been made to develop analytical models for the prediction of overpressure losses in straight tunnels due to wall roughness and the advance of the rarefaction wave toward the shock front. These analytical procedures have not been developed sufficiently to be included in this manual.

d. The attenuation of the peak overpressure as function of the distance into a smooth tunnel can be predicted using the curves given in figure 3–17. The curves are normalized plots of an equation developed by Robert Broh (BRL MR 1809). The dominant parameter of the Broh equation is the time intercept τ_i. This P is the pressure at some point down the tunnel, time is a function of the charge weight and distance from the explosion to the tunnel entrance and can be obtained from the curve shown in figure 3–18. This curve is for a surface tangent explosion where a spherical charge was placed on the ground surface. The Broh equation is insensitive to the diameter of the tunnel for tunnel diameters in the range of 2 to 15 feet.

2374
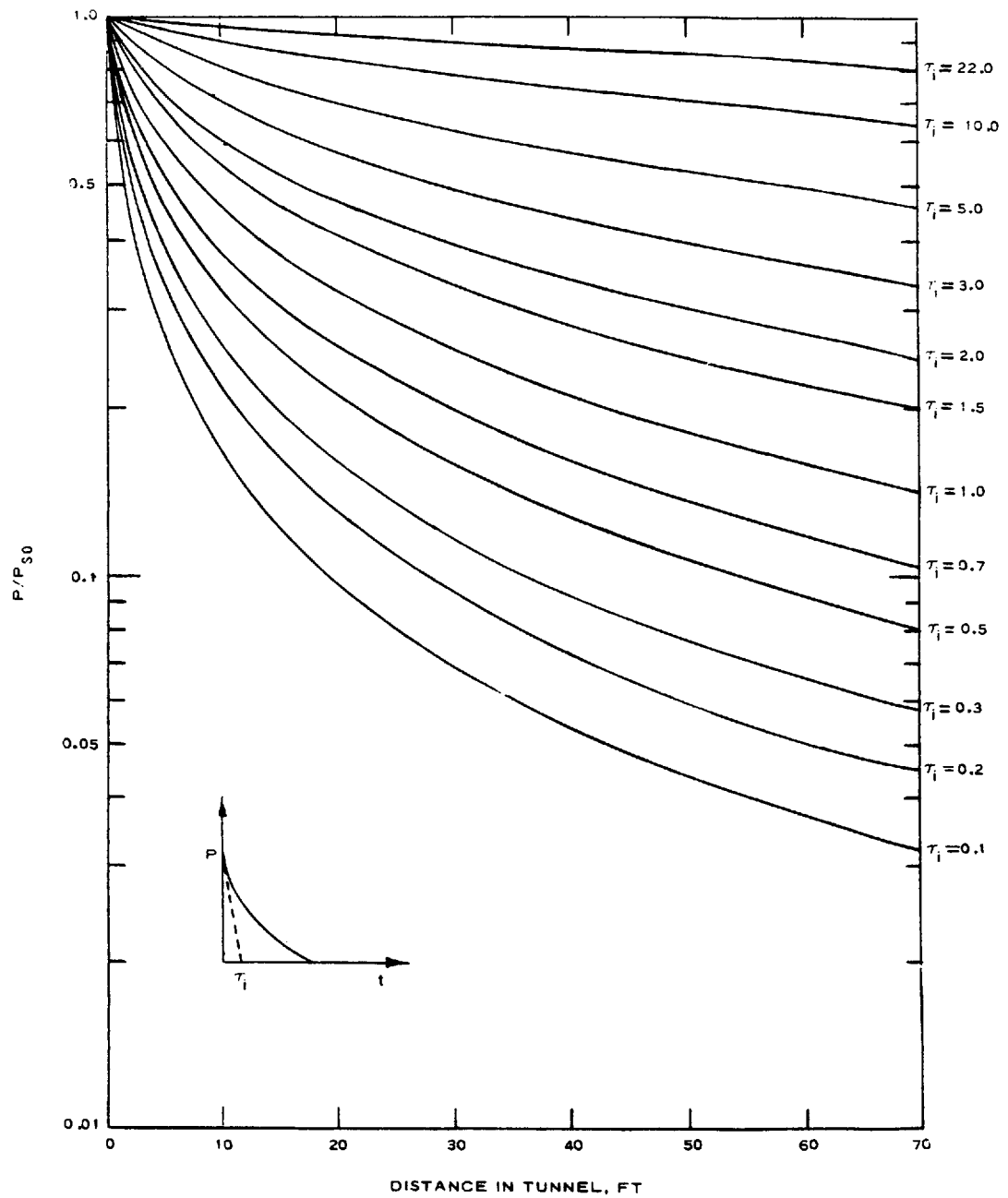
Figure 3-17. Pressure attenuation versus distance for smooth tunnels.

US Army Corps of Engineers

2375

TM 5-855-1
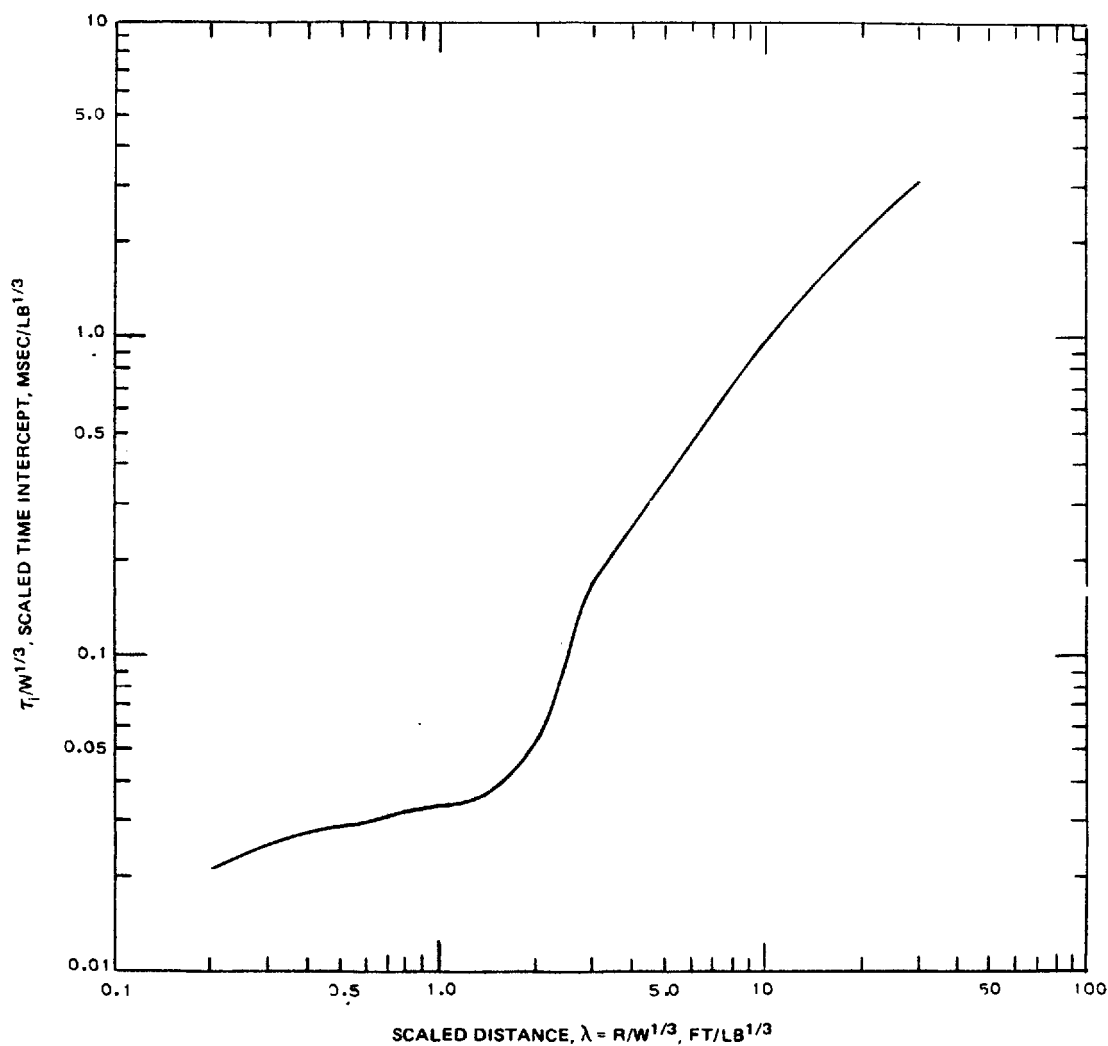
Figure 3-18. *Scaled time intercept versus scaled distance from a surface-tangent explosion.*

US Army Corps of Engineers

2376

3-28

e. The shock strength is reduced in going from one tunnel section *to another of larger diameter.* This dependence for long duration pulses in shock tubes is roughly proportional to the square root of the ratio of the areas of the tunnel sections,

$$P_2 \approx (A_1/A_2)^{1/2} P_1 \qquad \text{(eq 3–7)}$$

for $A_1/A_2 \geq 0.1$. As the ratio decreases to 0.01, the relation approaches a linear dependence on the ratio

$$P_2 \approx (A_1/A_2) P_1 \qquad \text{(eq 3–8)}$$

Little, if any, data is available for short-duration pulses expanding into larger tunnel sections or rooms.

Chapter 4

Penetration

4-1. Impact

a. General. Bombs and HE projectiles cause the greatest damage to structures if detonation occurs after maximum penetration is achieved. The ideal fuzing condition is for detonation to occur at the instant of maximum penetration.

(1) The computed kinetic energy of a bomb projectile striking at a high velocity is enormous, and it would obviously be impractical to design structures in the usual manner to withstand such stresses. The energy is dissipated primarily in deforming the case, producing strain and heat, and displacing target material. Due to the high velocity, materials such as concrete, rock, and brick are disintegrated and pulverized in the immediate vicinity of the point of impact, with the energy expended principally through local action. A nominal amount of energy is transmitted to the structural system, with magnitude and distribution depending on the characteristics of the system and on the nature of the impulse. In general, the greater the duration of the impulse, the more energy will be distributed through the system. For thin slabs or plates of ductile materials, the damage from impact is limited, the hole of entry being only slightly larger than the diameter of the bomb or projectile.

(2) Impact may cause scabbing (the disruption and throwing off of material from the rear face of a target resulting from either impact or explosion or both on the opposite face) whether the resisting material is perforated or not. Tests indicate that scabbing develops in concrete when the penetration of a bomb becomes greater than about 50 percent of the slab thickness, and perforation may occur at about 70 percent penetration.

b. Structural effects. While the energy of a bomb striking a structure is of great magnitude, the impact loads imparted to it are not critical; the structure as a whole does not deflect greatly to absorb the loads caused by a bomb striking a portion of it. Tests and analyses of reinforced concrete structures show that heavy structures will absorb the energy of impact without failure. On the basis of elastic analyses for end-supported concrete beams and slabs, the computed fiber stresses at failure under impact loads appear to be about 10 times as large as the usual ultimate stress capacity. It should be understood that while stresses of this magnitude do occur, the strains are very much smaller than those resulting from comparable static loads.

2378

4-2. Penetration.

a. General. Penetration and perforation depend on the following:

Characteristics of missile	Striking conditions (fig 4-1)	Properties of target material
Weight (W_T)	Impact Velocity	Strength or hardness
Caliber or diameter (d)	Angle of incidence	Density
Shape	Yaw	Ductility
Fuzing		Porosity
Structural resistance		

The effects of penetration on the target and on the projectile are quite different in frangible and ductile materials. Figure 4-2 illustrates the type of failure resulting when a 155-mm nondeforming projectile perforates a 5.5 foot wall of reinforced concrete. The craters, front and back, are typical of the behavior of frangible targets. Figure 4-2 also shows a section of a steel plate perforated by a nondeforming projectile. There is ductile flow of the plate material resulting in petals front and back.
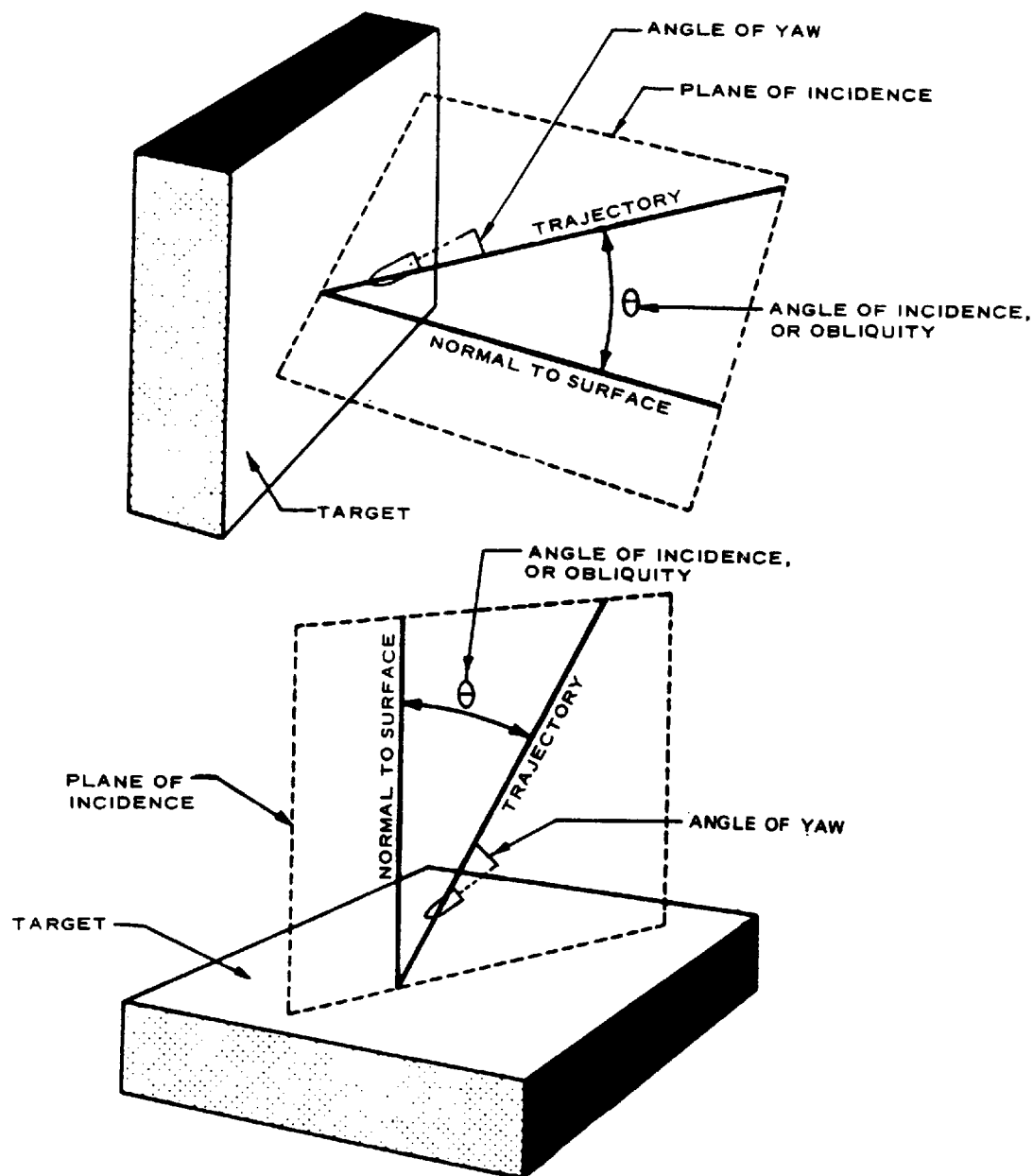
US Army Corps of Engineers

Figure 4-1. Geometry of impact.
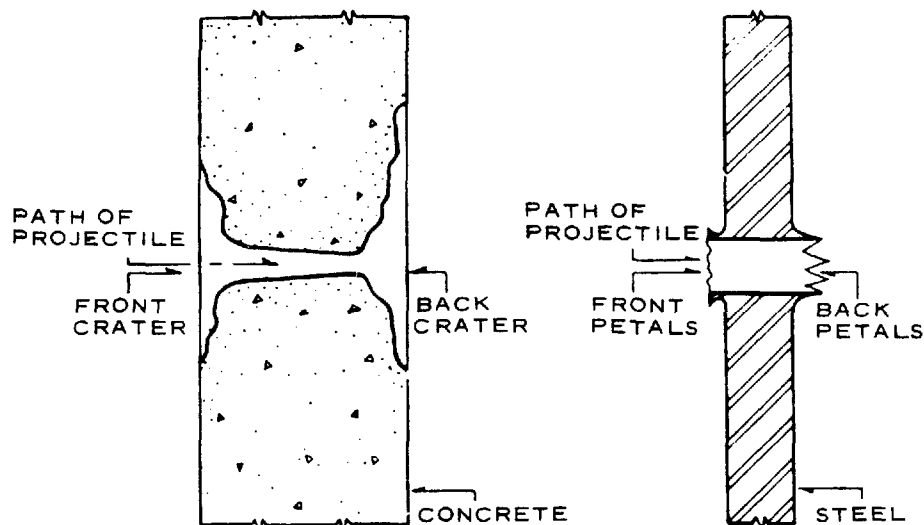
US Army Corps of Engineers

Figure 4-2.   Perforation of concrete & steel

b. Deformability and shattering of projectiles.

(1) If the projectile or some part of it yields or deforms on striking the target, its penetration into the target is much less than that of a similar nondeforming projectile. Most AP types remain undeformed against concrete and produce the same penetration as AP capped types of the same caliber and weight. Small-caliber jacketed, lead "ball" ammunition (e.g., 0.30 caliber) deforms completely against concrete, and the penetration of this type of ammunition is 50 percent (or less) of that for the corresponding AP ammunition. The jacket of a small AP bullet is torn completely off within the first inch or two of penetration into concrete; hence, it is better to consider the AP core alone in estimating penetration. HE projectiles and bombs with relatively thin noses tend to deform or even burst open on striking concrete; the degree of deformation depends on the rigidity and wall thickness of the nose section. Special concrete-penetrating nose fuzes can make HE projectiles effective against concrete. Deformation of projectiles and bombs is most likely at high velocities, at large angles of impact, and against hard targets (e.g., hard homogeneous and face-hardened armor plate).

(2) The discussion of penetration in the following paragraphs deal with frangible materials such as reinforced concrete and with plastic armor, masonry, soil, and rock, as well as the more ductile materials such as mild steel and armor plate. The results presented are mainly taken from test data. It is important that the data be used and supplemented by sound engineering judgment in practical applications to the design of protective structures and to military operations involving the breaching and destruction of such structures.

4-3. Concrete penetration characteristics.

a. General. As a structural material, concrete is strong in compression and weak in tension. When overstressed by static loading or under the impact of projectiles or bombs, it fails in a brittle rather than in a ductile manner. When a massive concrete slab suffers a direct hit, the forces generated at impact and during the penetration process are able to easily break up large masses of concrete, unless sufficient reinforcing steel is present to inhibit the spread of the cracks. Inadequate reinforcing may allow a projectile to breach a wall or roof completely by structural collapse due to cracking. Therefore, reinforcement tends to counteract the brittleness of the concrete and to provide tensile strength.

2381

b. Quality of concrete. Normally, factors such as selection of materials, mix design, and methods of placing and curing that govern the quality of concrete for civil construction also govern its resistance to projectiles in military protective structures. Small-caliber tests and some evidence at larger calibers indicate that the resistance to penetration increases with the compressive strength of the concrete as measured on standard test cylinders. For a given projectile and a given striking velocity, the penetration in concrete is approximately inversely proportional to the square root of the compressive strength. There is also some evidence that penetration is decreased somewhat by an increase in maximum aggregate size, especially when the latter is greater than the diameter of the projectile.

c. Reinforcement. The principal functions of steel reinforcement in concrete protective structures are to carry tensile stresses and to inhibit cracking splintering, scabbing, and spalling which result from a direct hit or explosion. However, the increased resistance to penetration along the path of the projectile is not sufficient to warrant any increase in the percentage of steel or in the complication of the reinforcement pattern for this purpose. In general, steel reinforcement will consist of the following three components, each of which contributes its share toward inhibiting mass cracking and breaching of the concrete slabs, walls, or roofs subjected to direct hits:

(1) Front face mat—tends to reduce the spall area around the point of impact and to hold some of the shattered front crater material in place. This action on the whole increases the resistance of the slab to repeated shots in the same general area.

(2) Back face mat—tends to reduce back scabbing and to raise the scabbing limit velocity. The back face mat gives resistance to inward bending.

(3) Shear steel—ties both face mats to each other and to the body of the concrete slab.

d. Antiscabbing plates. Steel antiscabbing or backing plates consisting of steel plates anchored to the inside face of concrete surfaces are of some value in protecting personnel and equipment by reducing the probability of scab ejection from the back face. For this purpose the antiscabbing plate must be tied to the concrete by an adequate number of welded shear studs as illustrated in figure 4-3. Tests have shown the shock of a deep penetration to be enough to cause inadequate welds to fail over a large area, thus adding the whole plate itself to the potential concrete scab. A very strongly attached plate increases the perforation resistance of a concrete slab by about 10 percent. When a structure is covered with soil and a burster slab is then placed on the soil surface, antiscabbing plates are not required.

TM 5-855-1

SHEAR STUDS
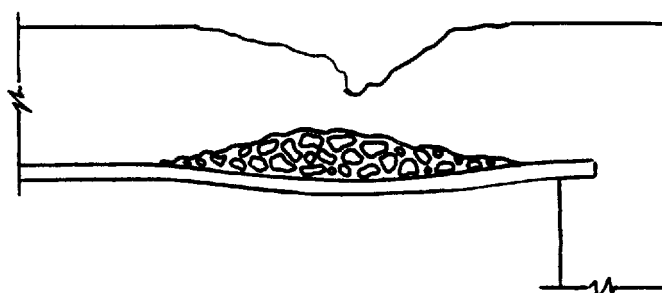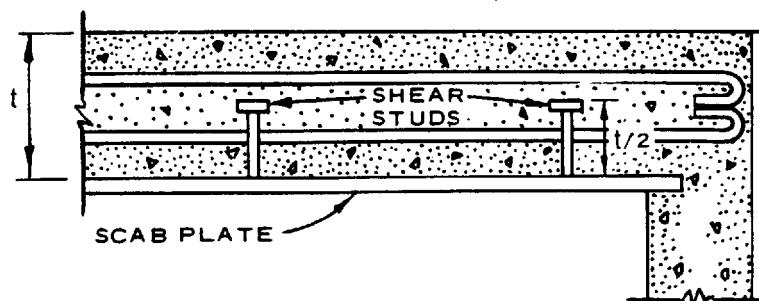
SCAB PLATE

RETENTION OF SCAB MATERIAL

US Army Corps of Engineers

Figure 4-3.   Scab plate.

e. Layers and laminations. A thick slab constructed in several layers in generally less resistant to perforation than a single slab of the same thickness and strength. It is estimated that the perforation limit velocity is lowered by not more than 5 percent per construction joint if the outer layers are at least 2 or 3 calibers thick and reasonable care is taken to secure a good mechanical bond between layers. Hence, it is important that the number of lift joints be kept to a minimum and that a good bond be provided.

f. Methods of computation.

(1) General. The formulas and nomograms presented in this section enable one to obtain approximate estimates of the effects of projectiles and bombs on concrete targets. The formulas and the penetration nomograms yield penetration values for nondeforming projectiles and bombs striking massive (semi-infinite) concrete slabs. The scabbing and perforation nomograms indicate slab thicknesses which will be scabbed and perforated, respectively, under specified conditions.

(2) Penetration formula. The empirical formula for normal penetration of inert AP projectiles and AP and SAP bombs into massive reinforced concrete is:

$$X = \frac{222 \times P_p \times (d)^{0.215} \times V^{1.5}}{(f'_c)^{0.5}} + 0.5\,d \qquad \text{(eq 4-1)}$$

where

X = penetration, in.

P_p = sectional pressure of the bomb or projectile (weight in pounds divided by the maximum cross-sectional area in square inches)

d = diameter or caliber of bombs or projectile, in.

V = striking velocity in units of 1,000 fps, that is, 1,100 fps = 1.1

f'_c = compressive strength of concrete, psi

Values derived from the above formula may be considered accurate within±15 percent for single hits. In using equation 4-1, for the more modern high slenderness ratio bombs at striking velocities below 1,000 fps, the penetration depth should be increased by 30 percent.

(3) Nomograms for reinforced concrete, the nomograms in figures 4-4, 4-5, and 4-6 give the penetration, the thickness which will be scabbed, and the thickness which will be perforated by inert, armor-piercing, or semi-armor-piercing projectiles or bombs. To use these nomograms properly, the weight and diameter of the projectile, the compressive strength of the concrete, and the striking velocity and obliquity must be known. When one or more of these factors is unknown, but is believed to lie between certain limits, the nomogram may be used for each of the limiting values, the result being between the two values so determined. Alternatively, the limit offering the greater safety may be selected. These nomograms are for nondeformable inert projectiles or bombs. The penetration, thickness scabbed, or thickness perforated by deformable projectiles is somewhat less than predicted by the nomograms; but for design purposes it will be safer to treat the projectile or bomb as nondeformable. For design against the explosive effects of projectiles and bombs, such as breaching and cratering, the results given by the formula and the nomograms must be supplemented by the added effect of explosion as described in chapter 5.

NOMOGRAM

Figure 4-4. Penetration by inert AP or SAP projectiles or bombs in reinforced concrete.

US Army Corps of Engineers

2-385
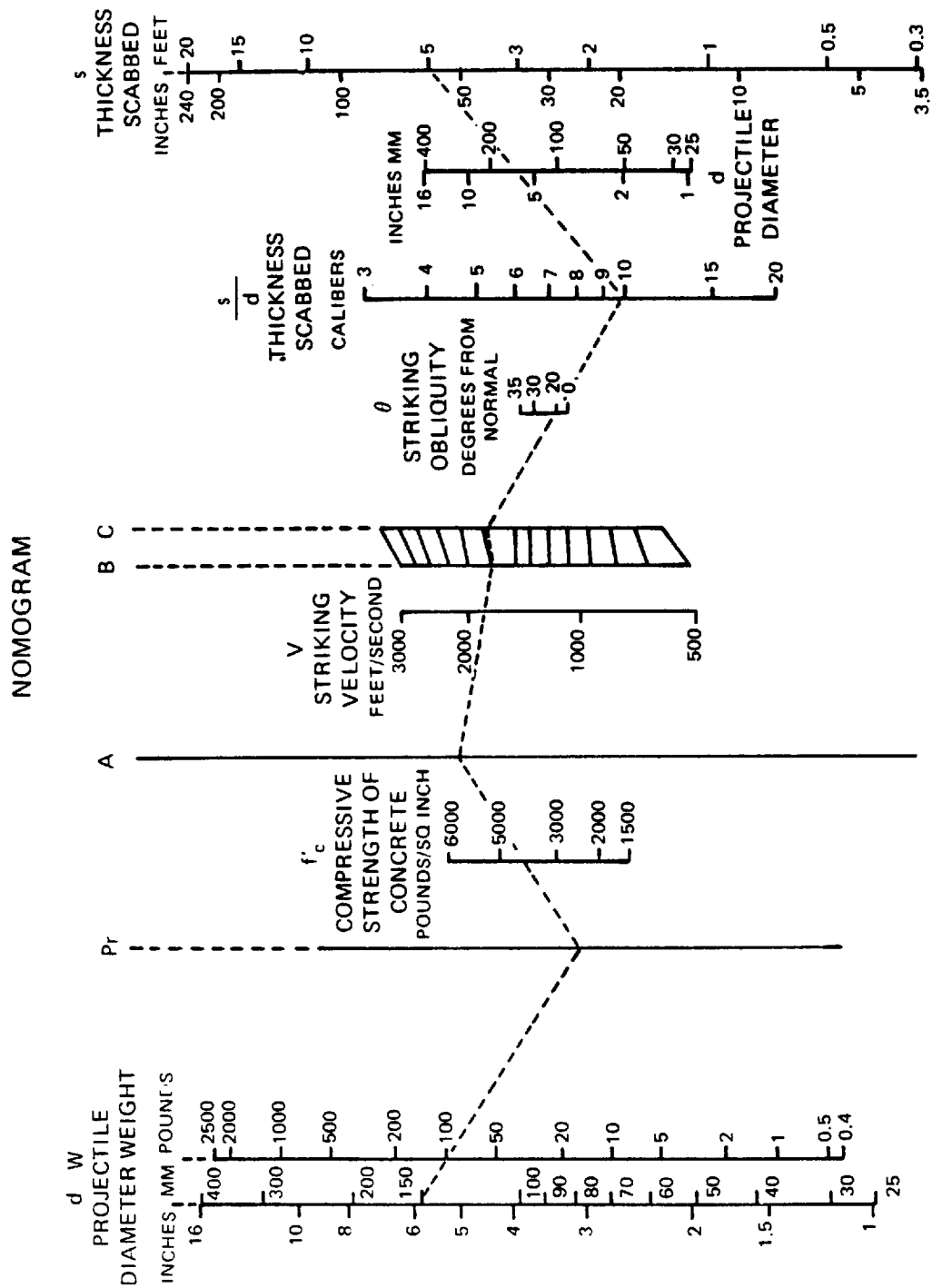
Figure 4-5. Scabbing by inert AP or SAP projectiles or bombs in reinforced concrete.
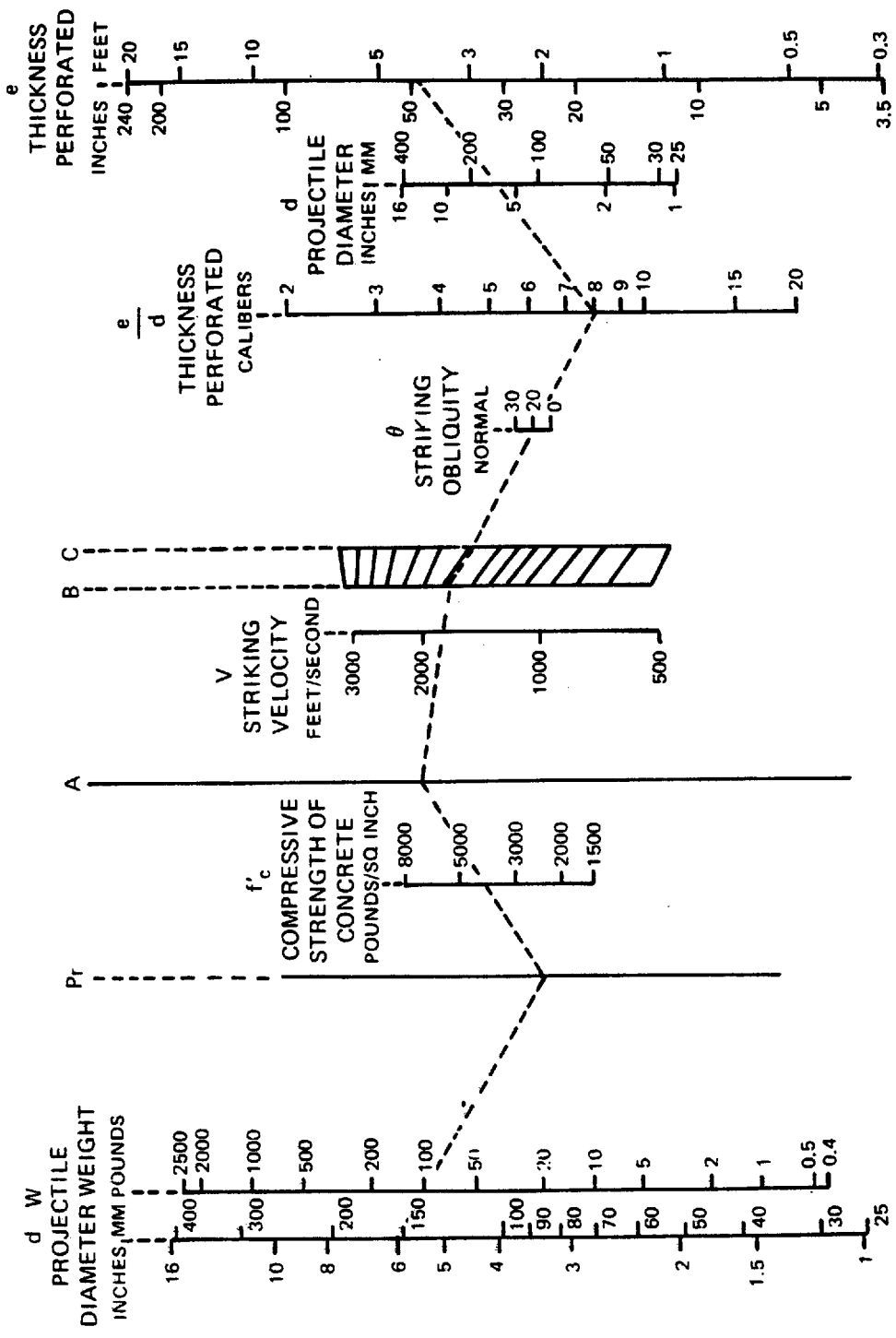
US Army Corps of Engineers

Figure 4-6. Perforation by inert AP or SAP projectiles or bombs in reinforced concrete.

US Army Corps of Engineers

(a) The penetration nomogram, figure 4-4, gives the average penetration into massive concrete. If the target is so thin that scabbing occurs on the back face, the actual penetration will be more than that predicted. If the penetration determined by the nomogram is less than the length of the nose of the projectile, the result is only approximate, and actual penetrations may be as much as 25 percent more or less than this value. The scabbing nomogram, figure 4-5, gives the limiting value of thickness that can be scabbed. The perforation nomogram, figure 4-6, gives the limiting value of thickness that can be perforated.

(b) The obliquity at which bombs and projectiles will ricochet is dependent on the nose shape, striking velocity, and target characteristics, as discussed previously. Values shown in figures 4-4 through 4-6 probably extend beyond the point at which ricochet will occur under average conditions, making the results conservative.

4-4. Rock penetration characteristics.

a. General. Penetration data are scarce for rock targets in which material properties have actually been measured. Moreover, the available data seem to indicate that rock penetrability is related to standard engineering properties of the rock as well as the in situ condition of the bulk target. This stands to reason since natural rock deposits often contain joints, fractures, and other irregularities not accounted for in standard laboratory test. The net result is that the penetrability of in situ rock is somewhat less predictable than that of concrete. It has been found, however, that by introducing the so-called Rock Quality Designation (RQD) as a material property, it becomes possible to estimate penetrability for large projectiles. The RQD is determined from boring log data as follows:

(1) All solid pieces of core that 4 inches long or longer are summed, and this length is called the modified core recovery.

(2) The modified core recovery is divided by the total length of core run, and the quotient multiplied by 100 is the value of the RQD in percent.

b. Penetration formula.

(1) An empirical rock penetration equation has been developed, based on penetration data for which RQD and material property measurements are available:

$$X = 6.45 \frac{W_T}{d^2} \frac{V_S}{(\rho Y)^{0.5}} \frac{100^{0.8}}{RQD} \qquad \text{(eq 4-2)}$$

where

X = final penetration depth, in.

W_T = projectile weight, lb

d = projectile diameter, in.

V_s = striking velocity, fps

ρ = target bulk density, pcf

Y = unconfined compressive strength of the intact rock, psi

(2) Due to limitations on the rock-penetration data base, the following restrictions must be observed in using equation 4-2:

(a) The equation is valid only when the calculated depth is greater than three projectile diameters.

(b) For nearly intact rock (RQD > 90), the equation is applicable for projectiles 1 to 12 inches in diameter, with an accuracy of ± .20 percent.

(c) For rock with RQD < 90, the equation has been verified only for projectiles in the 4- to 12-inch-diameter range, with accuracy of ± 50 percent.

(d) If RQD < 20, the equation should not be used at all.

(e) Although the effect of nose shape seems to be slight, the equation is not recommended for blunt or near-blunt projectiles.

(f) The equation is not valid if the projectile "mushrooms" or breaks up.

(g) The equation is not valid if the projectile tumbles, or if the penetration path is sharply curved.

(3) If possible, the target strength should be determined from static unconfined compression tests of intact rock samples, and the values used for Y and RQD should correspond to the same borehole. If only the strength and density are known, then a lower bound on penetration can be obtained by setting RQD = 100.

(4) Tables 4-1 through 4-3 contain information that can be used to make rough estimates of ρ, Y, and RQD in those cases where only a word description of the target is available. However, in such cases only very rough estimates of penetration depth can be made. If any previous penetration data for the site in question exist, these data should be used as benchmarks for checking the results obtained from equation 4-2 and (indirectly) the target parameters used therein.

Table 4-1. Rock quality designation

RQD, %	Rock Quality
0–25	Very poor
25–50	Poor
50–75	Fair
75–90	Good
90–100	Excellent

Table 4-2. Engineering classification for intact rock

Class	Description	Compressive Strength psi
A	Very high strength	Over 32,000
B	High strength	16,000–32,000
C	Medium strength	8,000–16,000
D	Low strength	4,000–8,000
E	Very low strength	Less than 4,000

Table 4-3. Common intact rock descriptions

Rock Types	Typical Density ρ pcf	Strength Range Y psi
Soft Shale (clay shales, poorly cemented silty or sandy shales)	143	200–2,000
Tuff (nonwilded)	118	200–3,000
Sandstone (large grain, poorly cemented)	125	1,000–3,000
Sandstone (fine to medium Grain)	130	2,000–7,000
Sandstone (very fine to medium grain, massive, well cemented)	143	6,000–16,000
Shale (hard, tough)	143	2,000–12,000
Limestone (Coarse, porous)	143	6,000–12,000
Limestone (fine grain, dense massive)	162	10,000–20,000
Basalt (vesicular, glassy)	162	8,000–14,000
Basalt (massive)	180	>20,000
Quartzite	162	>20,000
Granite (course grains, altered)	162	8,000–16,000
Granite (competent, fine to medium grain)	162	14,000–28,000
Dolomite	156	10,000–20,000

4-5. Soil and other material penetration characteristics

a. General. The penetration of small-arms bullets, artillery projectiles, and aircraft bombs in materials other than concrete and steel is extremely variable. The variation in penetration into any one type of material results from the inconsistency of the material. This makes it extremely difficult to fit the data into some general law of penetration for miscellaneous materials as a whole.   Of the miscellaneous materials the most resistant are certain types of hard stone, followed by brickwork, stabilized soil, gravel, sand, asphalt, and all kinds of soil. The penetration in the least-resistant soil may be from five to ten times greater than that in stone. For granular target materials, several general tendencies have been noted:

(1) For materials of the same density, the finer the grain the greater the penetration.

(2) Penetration decreases with increase in density.

(3) Penetration increases with increasing water content.

b. Method of computation

(1) Nomograms. In view of the erratic behavior of bombs and projectiles penetrating into nonhomogeneous and yielding materials such as soil, gravel, etc., computations of path length and offsets can only be considered as approximations.

(a) Bombs penetrating in earth frequently follow J-shaped paths, the final depth of burial being somewhat less than the path length. For bombs which follow a J-shaped path, the straight portion will usually be about two-thirds of the total path length and the curved portion one-third. The radius of the curved portion is usually about one-fifth to one-third of the total path length. The penetration path of a heavy bomb is shown in figure 4-7 together with the time increments for various depths of penetration after the fuze is initiated on impact.
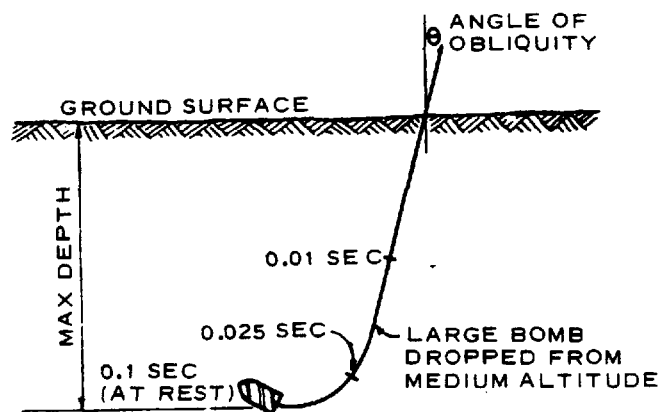
US Army Corps of Engineers

Figure 4-7.   Course of bombs which form "J"-shaped paths in earth

(b) The charts shown in figure 4-8 give an approximation of the penetration of bombs and projectiles into various types of soil and indicate the effect of nose shape on penetration. Explanatory notes for use of the charts are included below the graphs.

2391
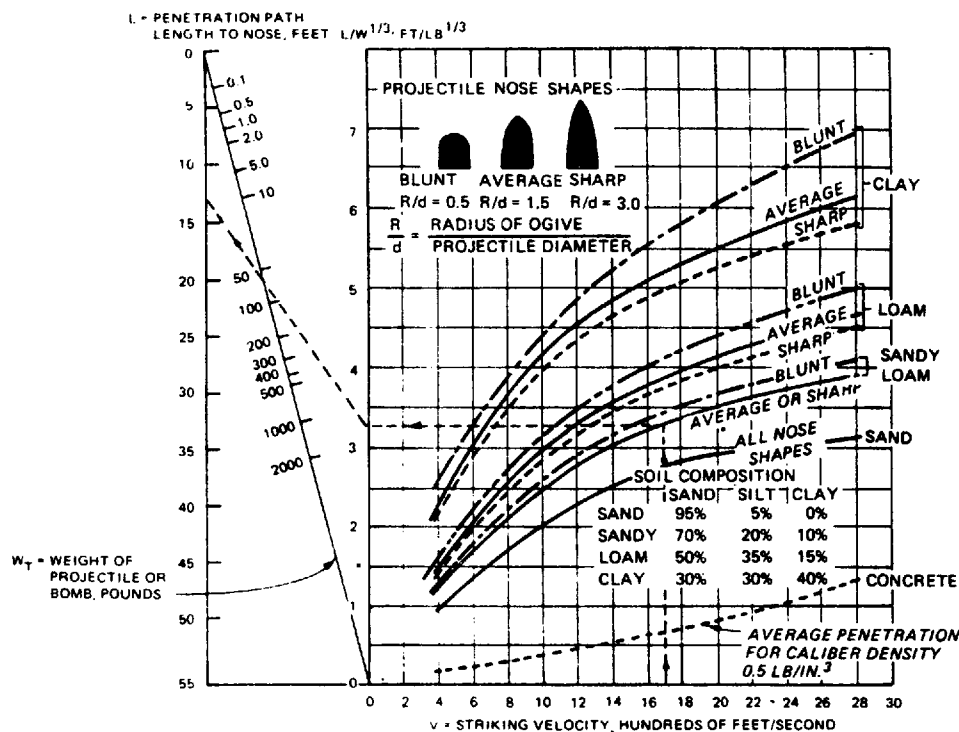
The graph and nomogram give the relation between striking velocity and penetration path length, measured to the nose, for projectiles or bombs of various weights penetrating into several soils. Curves marked blunt, average, and sharp are for projectiles of different nose shapes as sketched. Where no appreciable effect of nose shape on penetration has been observed only a single curve is drawn. The dependence of penetration path length on projectile weight, as given by the nomogram, agrees with observations for projectiles or bombs having caliber densities from 0.15 to 0.65 lb/in.³. Most bombs and artillery projectiles have caliber density values (weight of projectile in pounds divided by the cube of the diameter in inches) within the above range.

Trajectories in soils are usually straight for two-thirds or more of the path length, but curve near the end of the path (see sketch). For this reason final distance from the surface is usually 10% to 30% less than the penetration path given here.

Curves given are for average soil types. Penetrations into rich plastic clay are approximately 30% greater than those observed in clay. The dotted curve at the bottom of the graph gives average penetration into good quality reinforced concrete, and is added here for rough comparison.

EXAMPLE   The dotted line shows that a projectile of average nose shape and weight of 60 lb striking sandy loam soil with a velocity of 1700 ft/sec will have a path length of approximately 12.5 ft, measured to the nose. Because of the curvature of the underground trajectory the actual penetration from the surface will be somewhat less.

SOURCE   British and American tests with bombs and large caliber projectiles at velocities below 1100 ft/sec. Small caliber tests for the Corps of Engineers, USA, extending over entire velocity range. The curves agree with measurements to +20%.
NDRC Weapon Data
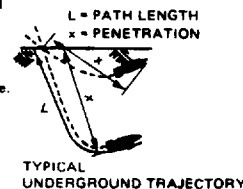
US Army Corps of Engineers

Figure 4-8.   Penetration of bombs and projectiles into soil.

TM 5-855-1

(2) Penetration formula for long projectiles. The slenderness ratio (ratio of bomb length to bomb diameter) for most conventional bombs ranges from approximately 3 to 6. This type of projectile is not terradynamically stable and, as was pointed out previously, the underground trajectory usually follows a J-shaped path. Penetration experiments, however, have indicated that long projectiles (slenderness ratios of approximately 10) are stable and that their underground trajectories are approximately straight. An empirical penetration equation has been developed, based on experimental data for long projectiles, with the following form

$$X_f = 0.0031 \, S_i N_s \, (W_T/A_m)^{0.5} \, (V_s - 100) \qquad \text{(eq 4-3)}$$

where

$\quad X_f \;=\;$ final penetration depth, ft
$\quad S_i \;=\;$ soil penetrability index
$\quad N_s \;=\;$ nose shape factor
$\quad W_T \;=\;$ projectile weight, lb
$\quad A_m \;=\;$ Maximum cross-sectional area of projectile, in.^{2}
$\quad V_s \;=\;$ striking velocity, fps

The following restrictions must be observed in using equation 4-3:
(a) The striking velocity must be greater than 200 and less than 3,000 fps.
(b) The equation is not applicable for projectiles weighing less than 60 and more than 5,700 pounds
(c) The equation was developed for projectiles with slenderness ratios of 10 or greater.
(d) The equation should not be used for shallow penetration (depth of penetration less than three body diameters plus one nose length).
(e) At best, the accuracy of the equation is ± 20 percent.
(f) The equation is not valid if the projectile deforms or breaks up or if the penetration path is sharply curved. Table 4-4 shows a generalized description of several natural earth materials with their associated range of the penetrability index S_i. This table can be used to make a rough estimate of S_i when a broad description of the target material is available. If any previous penetration data exist for the site in question, these data should be used in conjunction with equation 4-3 to calculate the value S_i for the site. Nose shape factors for various nose calibers (nose length/diameter) are given in table 4-5.

2393

Table 4-4.   Typical soil penetrability index for natural earth materials

Soil Index S_i	Materials
2–3	Massive gypsite deposits. Well-cemented coarse sand and gravel. Caliche, dry. Frozen moist silt or clay.
4–6	Medium dense, medium or coarse sand, no cementation, wet or dry. Hard, dry, dense silt or clay. Desert alluvium.
8–12	Very loose fine sand, excluding topsoil. Moist stiff clay or silt, medium dense, less than about 50% sand.
10–15	Moist topsoil, loose, with some clay or silt. Moist medium-stiff clay, medium dense, with some sand.
20–30	Loose moist topsoil with humus material, mostly sand and silt. Moist to wet clay, soft, low shear strength.
40–50	Very loose dry sandy topsoil. Saturated very soft clay and silts, with very low shear strengths and high plasticity. (Great Salt Lake Desert and bay mud at Skaggs Island) Wet lateritic clays.

Table 4-5.   Nose shape factors

Nose Shape	Nose Caliber[a]	N_a
Flat	0	0.56
Hemisphere	0.5	0.65 [b]
Cone	1	0.82 [b]
Tangent ogive	1.4	0.82
Tangent ogive	2	0.92
Tangent ogive	2.4	1.0
Cone	2	1.08
Tangent ogive	3	1.11
Tangent ogive	3.5	1.19
Cone	3	1.33

NOSE CALIBER = $\sqrt{\dfrac{R}{d} - \dfrac{1}{4}}$

TANGENT OGIVE
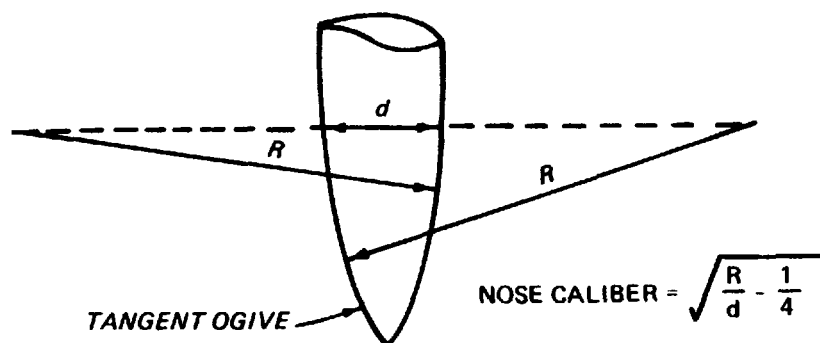
[a] Nose length /diameter.
[b] Estimated.

4-6. Armor penetration characteristics

a. General properties of steel. Of the materials commonly used for protective purposes, steel offers the greatest resistance to projectile perforation and the best structural characteristics for resisting collapse after sustaining damage. Comparison with good-quality reinforced concrete furnishes an idea of its effectiveness. To afford equal protection against nondeforming projectiles of small and intermediate calibers, armor plates need to be only one-sixth the thickness of concrete. In terms of weight, steel is favored in the ratio of 1 to 2. As the caliber of the projectile is increased, concrete becomes relatively less effective. In addition, steel being hard, is more likely to deform or shatter the projectile and thus further reduce its ability to perforate. Since good-quality armor does not scab, spall, or crack as easily as concrete, it is better able to withstand repeated attacks.

b. Armor classifications

(1) General.

(a) Classifications in general refer to the hardness of the plates, distinguishing between face-hardened and homogeneous armor. Ordinarily specifications for armor plate do not prescribe the composition of the materials; they only require that the plate pass certain physical and ballistic tests. Both rolled and cast armor are satisfactory. Cast armor is only slightly less effective than rolled and is more easily fabricated in implicated shapes.

(b) The hardness of a plate usually is specified in terms of the Brinell Hardness Number (BHN). This is obtained by pressing a 10-mm diameter steel ball into the surface of the plate under a load of 3,000 kg. The BHN equals the load divided by the area of the spherical surface of the impression measured in square millimeters. Thus, BHN represents units of pressure, kilograms divided by square millimeters. Up to the point where the plate becomes brittle, an increase in BHN indicates increased resistance to bullet penetration.

(2) Face-hardened armor. This class includes any armor which has a hard face combined with a softer back and is thus nonhomogeneous. Armor of this class also is known as cemented plate, Class A plate, and face-hardened bullet proof (FHBP) or merely bulletproof. Face-hardened armor, being unmachinable except on the softer face, is the most difficult to manufacture and consequently the most expensive. Its usefulness comes from the ability of the hardened face to shatter or deform the projectile. Against a projectile having an AP cap, it offers roughly the some protection as homogeneous plate does against an uncapped projectile. Projectiles without AP caps are inferior in penetration performance against face-hardened plate.

(3) Homogeneous hard armor. As the name implies, this material is of the same hardness and composition throughout. It is sometimes known as homogeneous bulletproof (BP). The plate is effective against small-arms attack, especially at angles of obliquity.

(4) Homogeneous soft armor. Often this is referred to as machinable quality (MQ) Class B, special-treatment steel (STS). This is the armor most commonly used because of its ease of manufacture and relatively high resistance to perforation.

(5) Mild steel. Structural steel is much softer than armor plate and hence offers less protection. It has a further disadvantage in that, as a rule, its manufacture is not so closely controlled as that of armor plate; consequently, it is more likely to contain imperfections, which result in poor ballistic performance. These disadvantages are crucial where weight must by conserved. However, when weight is not highly important, it may be used because of the relative simplicity of its manufacture and the greater facilities available for its production; the cost is less and procurement easier. To give equal protection, from 20 to 40 percent more mild steel is required than homogeneous soft armor. Table 4-6 summarizes some of the properties of these materials.

Table 4-6. *Properties of armor plate and mild steel*

Name	Abbreviations	BHN	Remarks
Face-hardened armor	Class A FHBP	Face 550–650	Unmachinable
		Back 250–440	Unmachinable
Homogeneous hard armor	BP	400–475	Unmachinable
Homogeneous soft armor	Class B STS	220–350	Machinable
Mild Steel	MS	110–160	Machinable

*Unmachinable except with special tools.

(6) Composite plate. When two or more plates are used in contact with one another, the arrangement is known as composite armor. This arrangement is used to obtain the benefits of face-hardened plate without its difficulties of manufacture., Such combinations are never as effective, however, as a single plate. For series of plates with similar ballistic characteristics the efficiency of the combination may be expressed as:

Total effective thickness $(t_t) = t_1 + 0.7 t_2 + 0.7 t_3$, etc.

It may thus be seen that the resistance of composite plate varies between 70 and 85 percent of that for single plates of the some total thickness.

(7) Spaced plates. When two or more plates are spaced with a distance between them somewhat greater than the length of the projectile or bomb selected for establishing the design, advantage sometimes is gained if the first plate either shatters the projectile or causes it to yaw badly. However, such spacing requires additional material to keep the plates separated and to maintain structural strength. Furthermore, the back plate in such construction is more likely to bulge than is a single thick plate. In addition, the first plate is readily made ineffective by repeated attacks or by the use of high-explosive projectiles. Spaced plated appear to offer certain advantages against shaped charges and rocket projectiles; the space may be filled with a material exhibiting suitable resisting characteristics against the weapon under consideration.

c. *Types of failure.*

(1) General. In applying reasonable safety factors in design, an idea of the type of failure that may occur is important. There have been numerous reports of personnel being injured by ejections of material from the plate itself even when the projectile was arrested completely.

(a) In general, the plate fails locally at the point of impact; so unless the plate cracks badly, only small areas are affected, provided enough attention has been directed to how the plate was mounted.

(b) Cracking of the plate is most likely if the point of impact is a near a hole or outer edge of the plate, particularly if the plate is hard and subjected to large-caliber attack at high obliquities. Shock tests are carried out during the proof firing of armor plates for acceptance to eliminate, as far as possible, plates defective in this respect. There are indications, however, that plates may shatter at low temperatures even though they behave satisfactorily at normal temperatures.

(c) No type of resilient support, such as a system of springs or a rubber mounting, is effective in increasing the resistance of a plate to perforation. Numerous experiments have shown that a plat of reasonable size has the same resistance to penetration regardless of whether it is freely hung or rigidly mounted. Nevertheless, armor should be securely attached to prevent it from being dislodged.

TM 5-855-1

(2) *Petalling.* If a soft homogeneous plate is attacked at small angles of obliquity or by a nondeforming projectile, a clean hole is made, plate material being pushed aside following plastic deformation. Petals are formed about the hole on both the front and back surfaces (fig 4-2). This is the least dangerous type of failure from the point of view of the defense. Greatest resistance to perforation is offered to the projectile during penetration, and no plate material is thrown from the back face into the protected area.

(3) *Plugging.* A plug may be formed ahead of the bullet and ejected from the back face. With nondeforming projectiles the diameter of the plug varies from about one-third the caliber of the projectile to full caliber at the back of the plate. The probability of plug formation increases with increase in plate hardness and nose bluntness.

(a) For plates 1 caliber thick, impacted with 0.30 caliber AP bullets at normal incidence, brittle failures begin to occur at approximately 350 to 400 BHN. This brittle limit apparently decreases with increase in caliber thickness; for this reason thick homogeneous plate usually is made comparatively soft. Plugs are usual occurrences with homogeneous hard and face-hardened plates.

(b) Even with soft homogeneous plate struck at normal incidence, plugs are formed by projectiles which shatter or deform excessively on impact. Ball ammunition produces this type of failure. The diameter of the hole produced in the plate is greater than the caliber of the projectile. Much more energy is required for perforation with this ammunition than with an AP projectile whose core remains intact; so if a plate is designed to stop AP projectiles, there is no danger of perforation with the corresponding ball ammunition.

(4) *Disking or flaking.* This circular disks or irregular flakes considerably larger than the caliber of the projectile may be thrown from the back face if the plate, particularly if the plate is of inferior quality. This is the most dangerous type of failure, but it seldom occurs with plate of good quality.

d. Ballistic limits. The ability of a given type and thickness of plate to withstand attack by a given projectile is usually specified by the limit velocity. This is the lowest velocity of the projectile which just defeats the plate, several limit velocities being possible depending upon the criteria used to judge plate failure.

(1) Although the limit for complete perforation (the projectile passing completely through the plate and emerging with zero velocity is the one most commonly specified, and the one from which the design thickness must be inferred, it does not represent the velocity for which the plate offers complete protection. This is particularly true with plates in which plugging occurs. A lower velocity is required to produce a pinhole perforation (a situation in which light can be seen through the hole), and this corresponds more closely to a value for reasonable safety. The difference in required plate thickness specified by the two limits is slightly less than 0.50 caliber. The distinction between the two limits is less clear for plates subject to brittle failures.

(2) *General performance based on caliber.* Against small-arms attack (0.50 caliber and less), about 25 percent less face-hardened armor than that listed in table 4-7 is required. Uncapped shot in larger calibers tend to shatter and are relatively ineffective against face-hardened plate. Against capped shot in larger calibers the thickness required is about the same as for soft homogeneous plate.

(3) *Approximation to extend known data.* Often the limit velocity for a particular projectile is known for a certain plate thickness, and it is desired to know the armor thickness required to stop a similar projectile of slightly different caliber and mass. Even for the ideal case in which a nondeforming projectile strikes normal to the surface of the plate, there is no exact simple formula applicable to all plate thickness. However, for small interpolations and extrapolations there is a rule of thumb which gives reasonable results for soft homogeneous plate over 1 caliber thick.

2397

Table 4-7. Plate thickness of homogeneous soft armor, Class B, STS BHN 250-300

4 Calibers	2 Calibers	1-1/2 Calibers	1 Calibers
Practical immunity	Favorable to defense	Favorable to attack at short range and small obliquity.	Distinctly favorable to attack at Medium range and large obliquities.
Thickness required to resist attack at normal impact at striking velocity of 3,500 fps or less. Hypervelocity weapons perforate thicknesses up to 8 calibers based on caliber of core, or at about the value above, based on caliber of gun.	Thickness required to resist attack at normal impact at striking velocity of 2,400 fps or less.	Not immune against attack at obliquities less than 20 deg and striking velocities above 2,200 fps.	Not immune against attack at normal impact for striking velocities above 1,700 fps and just resists attack at 40-deg obliquities at 2,000 fps.

TM 5-855-1

(1) Estimates from limited data. At times, estimates for the perforating power of a projectile may be required when little more than its caliber and type are known. With standard projectiles, the value of the caliber density (weight divided by the cube of the diameter) is approximately constant for most calibers. Hence, if the projectile is a conventional type, a value of the caliber density can be assumed; and if no account is given to the unpredictable effects of breakup of the projectile, some indication of its performance can be obtained. Table 4-7 is drawn up on this basis.

(2) Because of variation in plate quality, a given thickness of plate does not necessarily give complete protection even against a velocity equal to its specified pinhole perforation limit. The specified limit being merely an average value. However, since the manufacturing variation is within relatively narrow limits in terms of limit thickness, the probability of complete perforation occurring for designs based on the pinhole limit is extremely small.

e. Safety factor. Careful design is necessary where weight is an important consideration, as it is with mobile units such as tanks and ships; under such conditions a high factor of safety is inadmissible. In fixed fortifications, more adequate protection can be provided with an ample safety factor applies to thicknesses based on average ballistic limit values. For plates over 0.75 caliber thick, the safety factor should consist of the addition of a constant thickness for all velocities. An increase in plate thickness of 0.50 caliber over the calculated limit thickness usually affords reasonable safety.

f. Plate performance.

(a) The energy required per unit volume of the hole produced is approximately a constant for plates of greater than 0.50-caliber thickness. The energy (kinetic energy of the projectile) is applied over the cross-sectional area of the hole, and this may be taken to be the same as that of the projectile. With this assumption, the thickness of plate perforated is proportional to the energy of the projectile—a rule which leads to a 20-percent error when extending data from plate 1 caliber thick to plate 4 calibers thick.

(b) Considering all variables, the thickness of plate perforated is:
- Proportional to the mass of the projectile.
- Proportional to the square of the striking velocity.
- Inversely proportional to the square of the caliber.

(c) For example, if 3 inches of armor is the limit thickness against perforation by a given projectile at 1,640 fps, then the limit thickness against perforation by the same projectile at 2,000 fps would be estimated as:

$$3 \times \left(\frac{2000}{1640} \right)^2 = 4.46 \text{ in}$$

(d) It is true in general that this rule, since it involves velocity, predicts thicknesses greater than actually needed when going from low to higher velocities. However, this margin of safety is not provided with some types of jacketed ammunition. As another example, if a 75-mm AP projectile weighing 13.9 pounds perforates 3.7 inches of armor at 1,800 fps, a 57-mm AP projectile weighing 6.28 pounds and with the same striking velocity would perforate:

$$3.7 \times \frac{6.28}{13.9} \times \left(\frac{75}{57} \right)^2 = 2.89 \text{ in.}$$

The above rules are approximate and should not be used for large extrapolations.

(4) Oblique attack. The thickness of a plate required to defeat an oblique attack is much less than that needed if the impact is normal. Hence, for reasons of safety, plate usually is designed to withstand normal attack; its exact behavior under oblique impact is of secondary interest from the point of view of defense. However, if the angle of attack is specified, slanting plates may be used to increase obliquity and encourage ricochet.

(5) Small arms. Results which are representative of the conventional service rifle, automatic rifle, and machine gun fire can be obtained with 0.30-caliber and 0.50-caliber AP projectiles. If adequate protection is provided against AP projectiles, there need be no concern over the effects of ball ammunition except that additional precautions should be taken against bullet splash, such as the installation of shields, deflectors, or baffles. Hypervelocity rifles with exceptional AP qualities are used against heavily armored tanks and vehicles. They hold a real advantage in penetrating power over the conventional rifle only at short range, due to their extremely high velocity loss with distance

(6) Guns of intermediate caliber. Guns as large as 155-mm have been mounted on tank chassis and can therefore be made completely mobile. Although the damage done by an HE AP shell is much greater than that produced by AP shot (Monobloc) if perforation is achieved, it is unlikely that this will occur if the plate is bulletproof against the shot. The shell is weaker and therefore much more likely to deform on impact with the plate. In any case, the explosion adds little to its perforating ability; in fact, it may detract if the explosion occurs instantaneously on impact. Protection should be designed against the most effective shot in each caliber range.

g. Methods of computation.

(1) Small-caliber projectiles. The ballistic limit velocity for small-caliber projectiles (0.50 caliber or smaller) can be calculated from the following relationship:

$$V_1 = 19.72 \left\{ \frac{7800\, d^3\, [(e_h/d)\sec\theta\,]^{1.6}}{W_T} \right\}^{0.5} \qquad \text{(eq 4-4)}$$

where

V_1 = ballistic limit velocity, fps

d = caliber, in.

e_h = thickness of homogeneous armor (BHN 360-440), in.

θ = angle of obliquity

W_T = weight of projectile, lb

(2) Intermediate-caliber projectiles. For intermediate-caliber projectiles, the data given in figure 4-9 on nondeforming projectiles will usually give good results.

SYMBOLS

W_T = WGT OF PROJECTILE, POUNDS
d = CALIBER OF PROJECTILE, INCHES
V_ℓ = PERFORATION LIMIT VELOCITY, FEET/SECOND
e = THICKNESS OF PLATE, INCHES
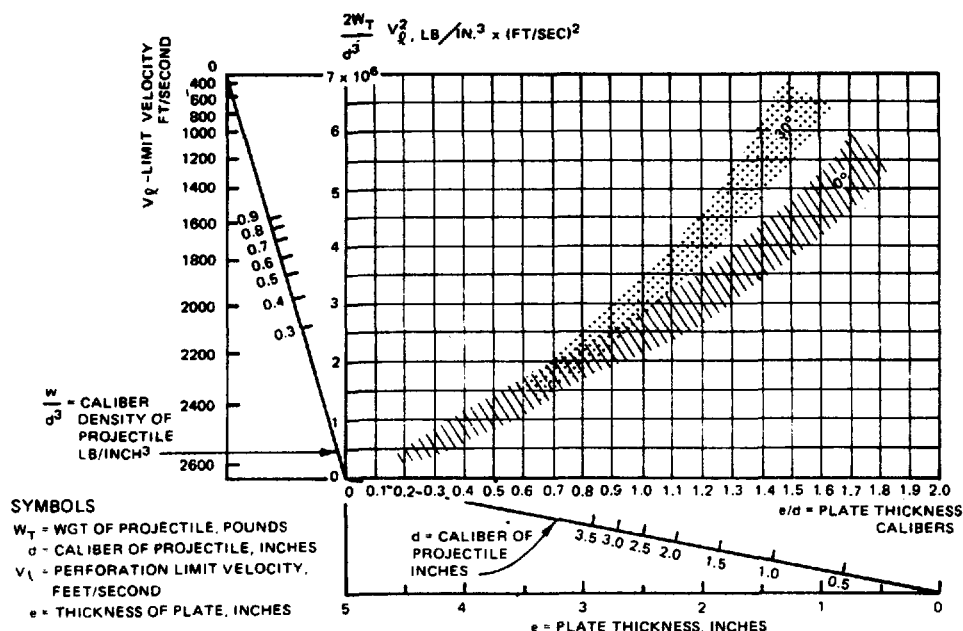
THE GRAPH SHOWS THE RELATION BETWEEN PERFORATION LIMIT VELOCITY AND THICKNESS OF PLATE PERFORATED. THE LIMIT VELOCITY CONCERNED IS THAT AT WHICH THE PROJECTILE JUST PASSES COMPLETELY THROUGH THE PLATE (Navy Limit). THE DATA REPRESENT ARMOR PIERCING (AP) UNCAPPED PROJECTILES RANGING FROM 1.45 INCHES TO 3.44 INCHES FIRED AGAINST HOMOGENEOUS ARMOR OF BHN 250-300 AT BOTH NORMAL INCIDENCE AND AN OBLIQUITY OF 30 DEGREES.

BECAUSE OF INHERENT SCATTER OF THE DATA, THE RESULTS FOR EACH OF THE TWO ANGLES OF INCIDENCE ARE PRESENTED IN THE FORM OF A BAND. EACH BAND, THEREFORE, MAY BE LOOKED UPON AS SEPARATING TWO REGIONS OF THE GRAPH, CORRESPONDING TO VULNERABILITY (ABOVE) AND SAFETY (BELOW)

A

EXAMPLES

Given a 75 mm M72 projectile striking at 30° obliquity with a velocity at 2000 ft/sec., two values of plate thickness, about 3-3/8 inches and 3-7/8 inches, are read by following the line to each of the two borders of the band. It is reasonable to assume that plate thicknesses greater than 3-7/8 inches will be safe against the given projectile, while thicknesses less than 3-3/8 inches will be vulnerable.
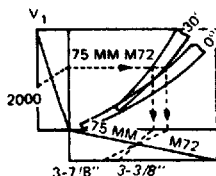
B

Similarly, for the given projectile (example A) fired at a plate 3-7/8 inches thick, two values of the striking velocity result by reading to the two borders of the band, namely about 2000 and 2230 ft/sec. The plate referred to is likely to be safe against striking velocities less than 2000 ft/sec. and vulnerable to velocities greater than 2230 ft/sec.
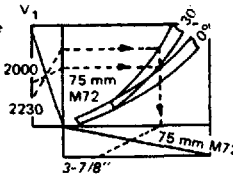
SOURCE: National Defense Research Committee, "Effects of Impact and Explosion," Volume I.

Figure 4-9. Perforation of homogeneous armor (BHN 250-300) by uncapped AP projectiles

(3) **Bombs.** The thickness of homogeneous armor perforated by bombs is given if figure 4-10 with an explanation given in the accompanying notes.

$$\frac{2W_T}{d^3}\ V^2\frac{LB}{\ell\ IN.^3}\cdot x\left(\frac{FT}{SEC}\right)^2$$

$$\frac{W}{d^3} = \text{CALIBER DENSITY OF BOMB, LB/IN.}^3$$
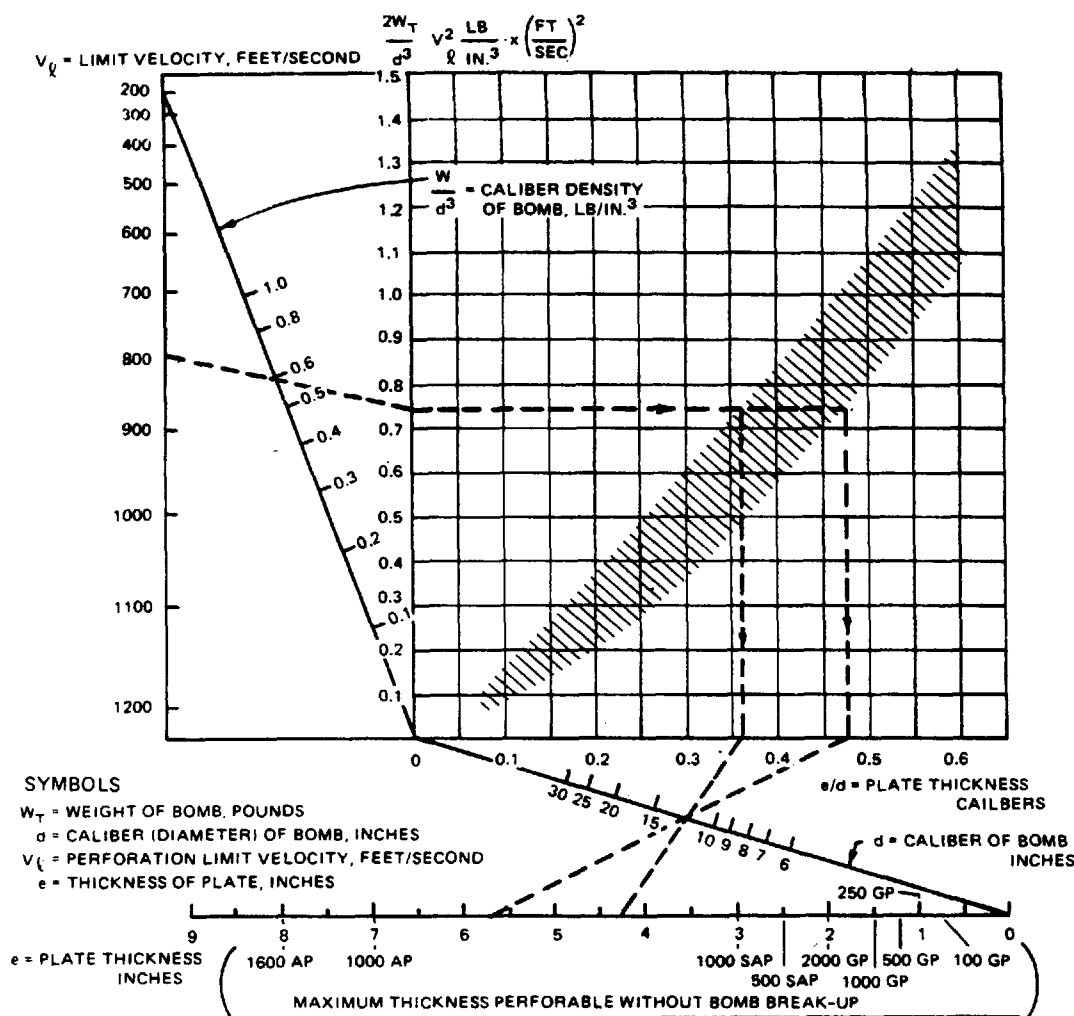
SYMBOLS

W_T = WEIGHT OF BOMB, POUNDS
d = CALIBER (DIAMETER) OF BOMB, INCHES
V_ℓ = PERFORATION LIMIT VELOCITY, FEET/SECOND
e = THICKNESS OF PLATE, INCHES

e = PLATE THICKNESS INCHES

1600 AP   1000 AP   1000 SAP | 2000 GP | 500 GP   100 GP
                        500 SAP   1000 GP

MAXIMUM THICKNESS PERFORABLE WITHOUT BOMB BREAK-UP

The graph gives the relation between the striking velocity of a bomb and the thickness of homogeneous armor which it will perforate. Due to inherent scatter of the data, the relationship is represented in the form of a band, and strikes at obliquities from 0° to 30° are included in it.

EXAMPLE: Given a 12-inch diameter, 1000-lb AP bomb striking with a velocity of 800 ft/sec; it can be expected to remain intact and to have a perforation limit thickness of 4-1/4 to 5-3/4 inches of armor.

SOURCE: National Defense Research Committee, "Effects of Impact and Explosion," Volume I.

Figure 4-10.   Perforation of homogeneous armor by bombs.

4-7. Plastic armor performance characteristics

a. Description and use. Plastic armor, a material developed by the British, is a mechanical mixture of asphaltic binder, finely ground limestone, and crushed granite, in proportions of about 10:30:60, by weight, respectively. It is used as a substitute for steel protection, and, if properly applied, is slightly superior to an equal weight of medium steel against some forms of attack. Mixed hot and poured into forms, it requires a backing plate of mild steel, usually between 1/8 and 1/4 inch thick. To increase structural strength and prevent excessive spalling, chicken wire or expended metal is embedded at the center or near the exposed surface of the slab. Plastic armor weighs about 170 pcf.

(1) If poured into forms of mild steel, the mixture may be made up into slabs. The slabs may be fitted together around objects to be protected, such as gun emplacements, or many be used to form portable pillboxes.

(2) The material is easily repaired by chipping out the damaged portion and refilling. If the insert is dovetailed carefully, there is no difficulty in obtaining a homogeneous joint.

b. Resistance to small-arms fire and projectile and bomb splinters. Compared with other materials, the ballistic effectiveness of 4 inches of plastic armor weighing 57 pounds per square foot (psf) is equivalent to:

Material	Weight psf
1 in. of special-treatment steel	41
1.5 in. of mild steel	61
12 in. of reinforced concrete	150
13.5 in. of brick mortar wall	160
15 in. of unreinforced concrete	180

c. Resistance to shaped charges. On a weight basis, plastic armor with certain combinations of backing plate fives more protection against shaped charges than does steel. The advantage is more clearly marked from normal impact up to 30 degrees obliquity. Due to the critical nature of steel production in wartime, plastic armor has been used extensively and successfully providing added protection to ships and armored vehicles and in protecting open gun positions. It has also been used for protecting observation posts, towers, etc.

4-8. Performance of combinations of materials

a. Concrete and earth. Many fortifications will be so constructed that a projectile or bomb would have to pass through two or more materials to pierce the structure. In limited small-caliber tests made to determine the resistance of a concrete slab covered with earth, there appeared to be some advantage in such combinations. One advantage is the tendency of a projectile to yaw when passing through earth; thus the projectile strikes the concrete surface at an angle which is likely to reduce further penetration. A disadvantage, however, is that the earth may be displaced by an artillery barrage or by bombing and thus some protection may be removed. Tests were made with 0.50-caliber projectiles and the results did not exhibit a degree of consistency. The action of bombs may indicate different results. It is recommended that in the case of bombs containing a considerable amount of explosive, the thickness of th concrete walls be made sufficient to withstand a side-on buried contact explosion at the center of the span.

b. Concrete and steel. Combinations of concrete and steel showed some advantage when tested with mild steel plate used as a scab plate. The advantage was lost, however, and the performance was somewhat deficient when homogeneous plate was used, both as a scab and as a face plate.

4-9. Performance of construction materialed against repeated hits

a. Concrete. Repeated hits in concrete tend to increase the depth of craters and expand the damaged area. A concentrated attack may produce repeated hits in the zone of previous damage and rapidly disintegrate the concrete. A number of repeated hits on concrete fortifications will soon breach a wall which is otherwise bulletproof against single hits by the weapons used. Table 4-8 shows the cumulative effect on concrete of repeated hits from various weapons. In tests on concrete pillboxes, a 5 foot thick concrete wall was perforated in approximately 6 minutes by a 37-mm antitank gun firing 15 rounds per minute. The normal penetration in concrete by single hits from this weapon is about 13 inches.

Table 4-8. Cumulative effect of weapons

Weapons	Number of Rounds to Perforate Pillbox Indicated at 1,000-Yard Range (Strength of Concrete, 5,000-7,000 psi)	
	5-ft Concrete Walls	7-ft Concrete Walls
155-mm gun, M1	1	2
155-mm gun, GPF	2	4
90-mm gun, M1	3-4	8-10
3-in. gun, M3	8-10	15-16
76-mm gun, M1	8-10	15-16
75-mm gun, M3	15-18	--
57-mm gun, M1	18-20	--
37-mm gun, M3	60-80	--
105-mm howitzer, HEAT	25-35	--

b. Steel. The effect of repeated hits on steel is much less damaging than on concrete. The damage from a hit is localized in an area approximately that of the projectile's sectional area, and failure through shear of the plate is confined to the area in contact with the projectile itself. Hence, for cumulative penetration, it is necessary for repeated hits to strike in the existing crater, which is very difficult to achieve.

c. Plastic armor. The mastic characteristics of plastic armor do not prevent surface spalling and the material is vulnerable to repeated hits. Single-shot craters generally are localized with little secondary damage from cracking. However, repeated hits in existing craters tend to reduce protective thickness and may separate the scab plate from the mastic prior to perforation. The mild steel backing plate alone offers little protection against perforation even by small-caliber projectiles.

d. Earth, stone, wood, and other material. In brittle materials such as stone and brick and to a lesser extent in bitudobe brick, repeated hits cause extensive cracking and spalling and opening of joints with consequent increases in penetration. Wood, though less extensively damaged, offers little resistance to penetration and generally tends to split. Earth, sand, and gravel, if untamped and comparatively dry, fill the voids caused by the passage of a projectile; hence, in such materials the successive damage from repeated hits is little more than for single hits.

4-10. Defense against shaped charge attack

a. General. The shaped charge is known by a variety of names: Monroe charge, hollow charge, lined cavity charge, and HEAT projectile. Its primary application as a weapon is to defeat massive targets such as steel or concrete and it is used extensively in recoilless rifle projectiles, antitank rockets and missiles, and engineer demolition charges. The most common shaped charge (fig 4-11) is a right circular cylinder of high explosive, with a detonator-booster explosive train at one end and a copper-lined conical cavity at the opposite end. On detonation of the explosive, the conical liner collapses and a high-velocity (20,000-30,000 feet per second) (fps) molten metallic jet is formed. This jet has the ability to perforate large thicknesses of high-density material (e.g., armor) and after perforation continues in a straight line along its original path. The energy of the remaining jet is sufficient to set ammunition and fuel afire and personnel in its path will be severely injured or killed.

BOOSTER — — DETONATOR

EXPLOSIVE

ALUM BODY

42°

COPPER
LINER

ALUM RETAINING RING
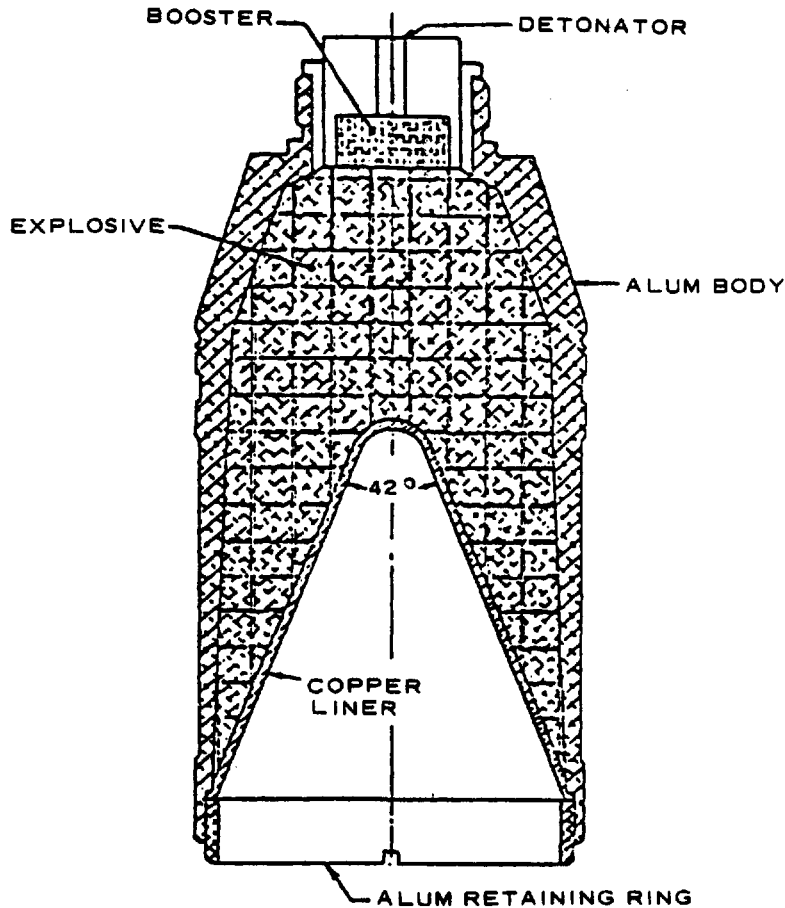
US Army Corps of Engineers

Figure 4-11. Cross section of a typical cylindrical shaped charge.

b. Protection. Although new types of armor concepts designed to disrupt the high-velocity jet have been studied, the most economical and practical method for protection of structures is to place a sufficient thickness of a given material in the path of the jet. Table 4-9 gives the penetration into steel armor for various munitions and figure 4-12 is a plot of steel penetration versus diameter. The lower curve is a fit to test data, but the upper line represents penetration close to the theoretical maximum and is the recommended design curve. Penetration into other materials can be obtained by multiplying the armor penetration by the factors given in table 4-10. For materials not listed in this table, a good rule to follow is to calculate the penetration in the mild steel and then multiply that number by the square root of ρ_s/ρ_t where ρ_s is the density of steel and p_t is the density of the material for which the penetration is desired.

Table 4-9.   Armor penetration data for various shaped charge munitions

Country	Weapons	Warhead Diameter mm	Armor Penetration mm
Argentina	Recoilless Gin Model 1968	105	200
Belgium	RL-83 Rocket Launcher	83	300
Belgium	Rocket Launcher MPA75	75	270
Belgium	PRB 415 Antitank Rocket	89	200
Belgium	MECAR Light Gun	90	350
China	Type 56 Antitank Grenade launcher	80	265
China	Type 69 Antitank Grenade Launcher	85	320
China	Recoilless Rifle Type 36	57	63.5
China	Recoilless Rifle Type 52	75	228
China	Antitank Rocket Launcher Type 51	90	267
China	Recoilless Gun Type 65	82	240
Czechoslovakia	Antitank Grenade Launcher Type P-27	120	250
Czechoslovakia	Recoilless Gun Type T-21	82	228
Czechoslovakia	Recoilless Guns M59 and M59A	82	250
Finland	Recoilless Antitank Grenade Launcher M-55	55	200
Finland	Recoilless Antitank Gun M58	95	300
France	SARPAC Antitank Missile	68	500
France	STRIM Antitank Rocket Launcher	89	400
France	ENTAC Antitank Missile	150	650
France	SS11 Antitank Missile	164	600
Federal Republic of Germany	PZF44 Portable Antitank Weapon	67	370
Federal Republic of Germany	B)810 Cobra 2000 Antitank Missile	100	500
Federal Republic of Germany	Mamba Portable Antitank Weapon System	120	475
International	HOT Vehicle Mounted Antitank Weapon System	136	800
International	Milan Portable Antitank Weapon	90	352
Spain	Antitank Rocket Launcher M-65	88.7	330
Sweden	Miniman Light Antiarmor Weapon	74	300
Sweden	Carl Gustaf M2RCL Gun and Carl Gustaf System 550	84	400
Sweden	Recoilless Rifle PV-11110	90	380
USSR	RPG-2 Portable Rocket Launcher	82	180
USSR	RPG-7 Portable Rocket Launcher	85	320
USSR	SPG-9 Recoilless Gun	73	>390
USSR	SPG-82 Rocket Launcher	82	230
USSR	B-10 Recoilless Gun	82	240
USSR	B-11 Recoilless Gun	107	380
USSR	Sagger Antitank Guided Missile	120	>400
USA	HEAT Rocket Launcher's M72, M72A1, M72A2	66	305
Yugoslavia	M60 Rifle Grenade	60	200
Yugoslavia	M57 Antitank Launcher	90	300
Yugoslavia	M60 Recoilless Gun	82	220
Yugoslavia	M65 Recoilless Gun	105	330

TM 5-855-1
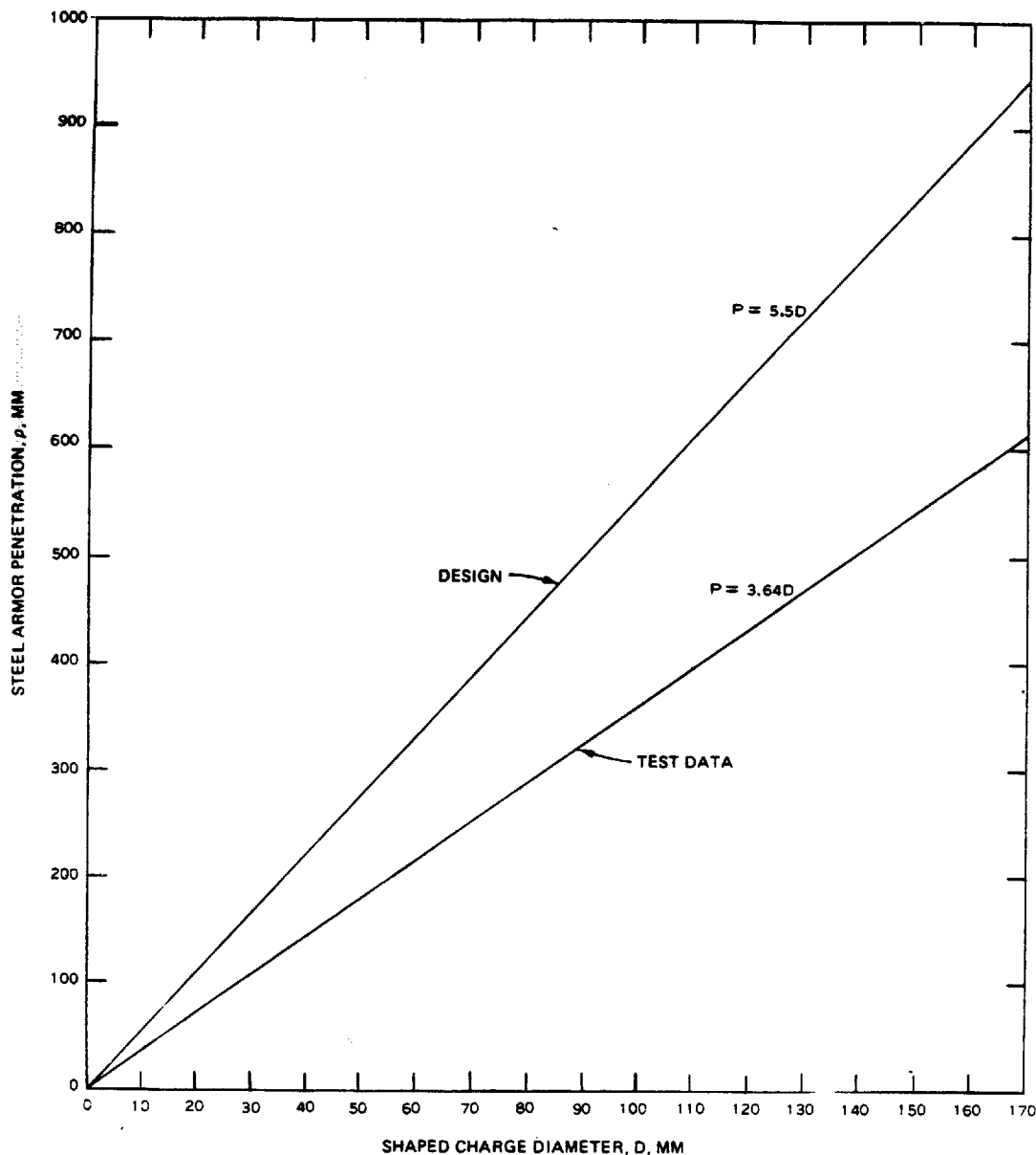
US Army Corps of Engineers

Figure 4-12. *Penetration of steel armor vs. shaped charge diameter.*

Table 4-10. *Armor penetration multiplication factors for various materials*

Material	Multiplication Factor
Steel armor	1.00
Mild steel	1.25
Aluminum	1.75
Lead	0.84
Concrete	2.00
Earth	6.00
Granite	1.50
Rock	1.75
Water	2.80
Green wood	3.60
Kiln-dried white oak (12% moisture)	6.70

CHAPTER 5

GROUNDSHOCK, CRATERING, AND EJECTA

5-1. Ground shock

   a. General. The ground shock produces by bombs exploding on or within the ground near buried structures generally represents the dominant threat to these facilities. Stresses from buried bursts are usually greater in magnitude and of much longer duration than coresponding bursts in air.

   (1) Significant enhancement of the stresses and ground motions will occur if the weapon penetrates more deeply into the surrounding soil or backfill before it detonates. Protective layers of concrete or rock rubble are often placed over the structure to limit weapon penetration, thus reducing the effective coupling of the explosion into the ground and increasing the weapon standoff distance.

   (2) Important variables affecting the intensity of the loading are:

   (a) weapon size and distance from the structure

   (b) mechanical properties of the soil or rock between the detonation point and the structure

   (c) depth of weapon penetration at the time of detonation (depth of burst).

Of these factors, the effect of soil or rock properties is least predictable by simple handbook methods. Ground shock intensity may vary by more than two orders of magnitude for wide variations in soil type; e.g., from low-intensity dry soils to saturated clays.

   (3) There are two important cases to consider in assessing ground shock threat to buried vacilities:

   (a) bombs that explode overhead, generally on or within the protective concrete or rock rubble overlay, causing a direct loading of the roof slab, and

   (b) weapons that penetrate into the surrounding soil and detonate adjacent to the facility, loading the walls and floor. While the some general ground shock prediction equations apply for both cases, the effects of the site geology and the protective overlay required a somewhat different application of these equations. These cases are shown in figure 5-1.

TM 5-855-1
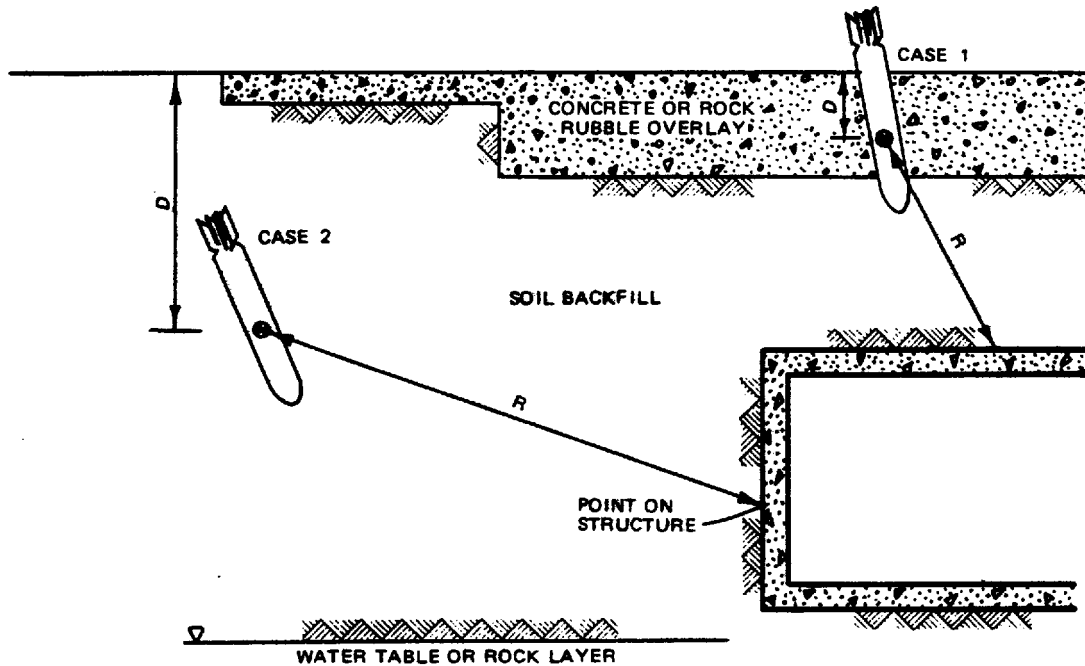
Figure 5-1. Geometry for explosion against a buried facility.

US Army Corps of Engineers

b. Soil property effects. Ground shock propabation in earth media is a complex function of the dynamic constitutive properties of the soil, the detonation products, and the geometry of the explosion. No single soil index, or combination of indices, can adequately describe the process in a simple way for all cases.

(1) Soil water content can have a profound influence on ground shock propagation in cohesive soils, particularly if the degree of soil saturation is 95 percent or greater. Water is typically bound within the skeletal structures of these soils, providing a significant contribution to the overall stiffness and strength of the soil structure. A soil saturation approaches 100 percent, pronounced increases in peak stresses and accelerations have been observed in wet clays, clay shales, and sandy clays. In fact, stress levels similar to those from shock waves in free water have been noted in saturated clays. In some locations, the depth to the surface of a saturated soil layer may be inferred by the level of standing water in boreholes. However, this is not always an accurate measure of the true saturation depth, particularly where seasonal water table fluctuations introduce small amounts of air into the soil. Seismic surveys generally will show a sharp jump in the soil seismic velocity, to more than 5,000 fps, at the depth of a saturated zone.

2409

(2) Granular soils with high relative density are generally not as strongly influenced by water saturation as are cohesive soils. The stiffness of granular soil is provided by the grain-to-grain contacts in the skeleton, with only a small contribution by the free water. Consequently, controlled laboratory and field experiments in dense, nearly saturated sands have not shown a large influence of the pore water on shock wave propagation. However, the effects of water in sands with low relative densities can produce effects similar to those seen in cohesive soils. In these cases, the soil skeleton can collapse, and the loss of grain-to grain contacts results in high pore pressures as the sand liquifies. Therefore, sites having sands of low relative density would not normally be considered for construction of hardened facilities.

(3) Seismic velocity, c , is often used as a crude index of soil or rock properties for ground shock prediction purposes. It provides a simple measure of the stiffness and the density of the soil through the relationship

$$c = \sqrt{\frac{M}{\rho_0}}$$

(eq 5-1)

where M is the stiffness or modulus of the soil and ρ_0 is its mass density. The seismic velocity also provides a relationship between distance and time.

(4) Caution must be used in generalizing the use of seismic velocity as a ground shock index. Cementation in granular soils, such as dry desert alluvium, may result in abnormally high seismic velocities (approaching 4,000 fps). Yet these materials may also exhibit a very high volume of air-filled voids and low relative densities—qualities that classify them as very poor transmitters of ground shock. Low seismic velocities, on the other hand, automatically indicate poor ground shock transmission qualities.

(5) The attenuation rate with range of the ground shock magnitude is controlled by the irreversible crushing of the void volume within a soil matrix by the passage of a stress wave. In cohesive soils, the volume of the air-filled voids is an index for the rate of attenuation of ground motions, while the best index for attenuation rates in granular media is the relative density, . Because relative density is not always available, dry unit weight can be an effective index for ground shock attenuation. Soils with high relative density or a low volume of air voids will attenuate the ground shock more slowly than low-relative-density or high-air-void materials. Figure 5-2 shows peak stresses and particle velocities from fully contained explosions in typical soils.
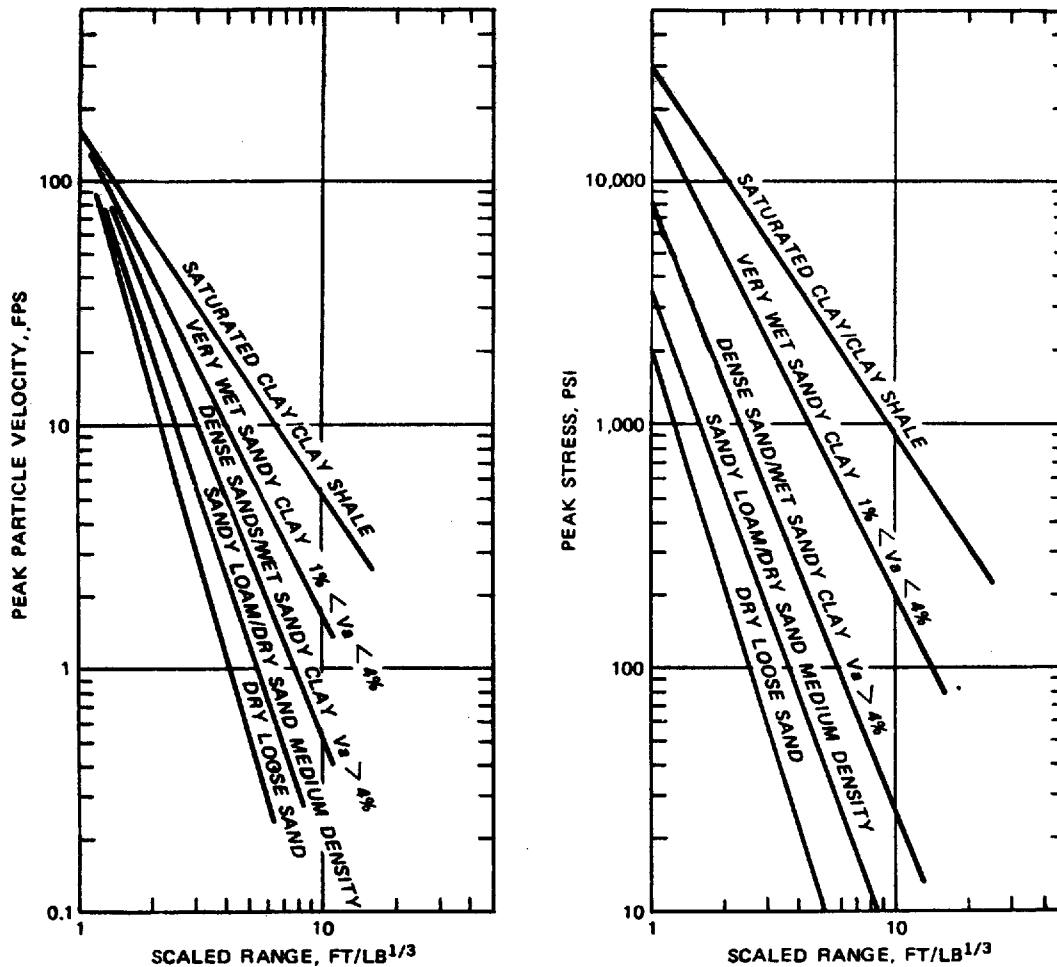
US Army Corps of Engineers

Figure 5-2.   Peak stress and particle velocity from contained explosions in various soils

c. *Ground shock predictions.* Stress and particle velocity pulses can be characterized by exponential-type time histories that decay rapidly in amplitude and broaden as they propagate outward form the explosion. The arrival time, t_a, is the elapsed time form the instant of detonation to the time at which the ground shock arrives at a given location, and

$$t_a = \frac{R}{c} \qquad \text{(eq 5-2)}$$

where

R = distance from the explosion

c = average seismic or propagation velocity the distance R

Typically, these wave forms rise sharply to their peak value, such that the rise time t_r can be expressed as

2411

$$t_r = 0.1 \, t_a \qquad \text{(eq 5-3)}$$

(1) From its peak value, the shock pulse decays monotonically to nearly zero over a time period equal to one to three times the value of t_a, as given by the following equations:

$$P(t) = P_o e^{-\alpha t/t_a} \qquad t \geq 0 \qquad \text{(eq 5-3a)}$$

$$V(t) = V_o (1 - \beta t/t_a) e^{-\beta t/t_a} \qquad t \geq 0 \qquad \text{(eq 5-3b)}$$

where

$$P(t) = \text{shock stress}$$
$$V = \text{particle velocity}$$
$$\alpha, \beta = \text{time constants}$$

Although the time constants generally vary with specific site conditions, they can be taken as

$$\beta = \frac{1}{2.5}$$

$$\alpha = 1.0$$

for most applications. P_o and V_o are the peak values of the shock stress and particle velocity. Other wave form parameters, such as impulse, displacement, and accelerations may be derived from these functions.

(2) Since the characteristic arrival time is inversely proportional to seimic velocity, explosions in high-velocity media such as saturated clay will produce very short, high-frequency pulses with high accelerations and low displacements. On the other hand, detonations in dry, loose materials will produce ground motions of much longer duration and lower frequency. Peak particle velocity and peak stress are related by

$$P_o = \rho c V_o \qquad \text{(eq 5-4)}$$

where ρ is the mass density. Free-field stresses and ground motions from bombs detonating on or within burster layers, or in the soil near a structure, are given as follows:

$$P_0 = f \cdot (\rho c) \cdot 160 \cdot \left(\frac{R}{W^{1-3}}\right)^{-n} \qquad \text{(eq 5-5a)}$$

$$V_0 = f \cdot 160 \cdot \left(\frac{R}{W^{1/3}}\right)^{-n} \qquad \text{(eq 5-5b)}$$

$$a_0 \cdot W^{1/3} = f \cdot 50 \cdot c \cdot \left(\frac{R}{W^{1/3}}\right)^{(-n-1)} \qquad \text{(eq 5-5c)}$$

$$\frac{d_0}{W^{1/3}} = f \cdot 500 \frac{1}{c} \left(\frac{R}{W^{1/3}}\right)^{(-n+1)} \qquad \text{(eq 5-5d)}$$

$$\frac{I_0}{W^{1/3}} = f \cdot \rho_0 \cdot 1.1 \cdot \left(\frac{R}{W^{1/3}}\right)^{(-n+1)} \qquad \text{(eq 5-5e)}$$

where

P_0 = peak pressure, psi

f = coupling factor

(ρc) = acoustic impedance, psi/fps

R = distance to the explosion, ft

W = charge weight, lb

n = attenuation coefficient

V_0 = peak particle velocity, fps

a_0 = peak acceleration, g's

c = seismic velocity, fps

d_0 = peak displacement, ft

I_0 = impulse, lb-sec/in.2

ρ_0 = mass density, lb-sec^2 / ft^4 = 144 ρ (see table 5-1, ρc)

For preliminary design considerations, table 5-1 is suggested for use in selecting the seismic velocity, acoustic impedence, and attenuation coefficients.

Table 5-1.   Soil properties for calculating ground shock parameters

Material Description	Seismic Velocity c fps	Acoustic Impedance (ρc) psi/fps	Attenuation Coefficient n
Loose, dry sands and gravels with low relative density	600	12	3–3.25
Sandy loam, loess, dry sands, and backfill	1,000	22	2.75
Dense sand with high relative density	1,600	44	2.5
Wet sandy clay with air voids (greater than 4 percent)	1,800	48	2.5
Saturated sandy clays and sands with small amount of air voids (less than 1 percent)	5,000	130	2.25–2.5
Heavy saturated clays and clay shales	>5,000	150–180	1.5

(3) A more detailed dsescription is provided in table 5-2 for soils that have been encountered in explosion test programs.   Simple soil parameters such as wet and dry uni weights, volume of air-filled voids, and seismic velocity are shown to assist in relating the explosion effects parameters to the design soil conditions.   Note that the attenuation coefficient and seismic velocity are closely related to dry unit weight for granualr soils, while air void content is important for cohesive soils.

TM 5-855-1

Table 5-2. Soil propertries from explosion tests

Soil Description	Dry Unit Weight γ_{dry} pcf	Total Unit Weight γ pcf	Air-Filled Voids %	Seismic Velocity c fps	Acoustic Impedance ρc psi/fps	Attenuation Coefficient n
Dry desert alluvium and playa, partially cemented	87	93-100	>25	2,100-4,200[a]	40	3-3.25
Loose, dry poorly graded sand	80	90	>30	600	11.6	3-3.5
Loose, wet, poorly graded sand with free-standing water	97	116	10	500-600	12.5-15	3
Dense dry sand, poorly graded	99	104	32	900-1,300	25	2.5-2.75
Dense wet sand, poorly graded, with free-standing water	108	124	9	1,000	22	2.75
Very dense dry sand, relative density $\cong$100%	105	109	30	1,600	44	2.5
Silty-clay, wet	95-100	120-125	9	700-900	18-25	2.75-3
Moist loess, clayey sand	100	122	5-10	1,000	28	2.75-3
Wet sandy clay, above water table	85	120-125	4	1,800	48	2.5
Saturated sand, below water table in marsh	--	--	1-4[b]	4,900	125	2.25-2.5
Saturated sandy clay, below water table	78-100	110-124	1-2	5,000-6,000	130	2-2.5
Saturated sandy clay, below water table	100	125	<1	5,000-6,600	130-180	1.5
Saturated stiff clay, saturated clay-shale	--	120-130	0	>5,000	135	1.5

[a] High because of cementation.
[b] Estimated.

2415

5-8

d. Ground shock coupling factor. The magnitude of the stress and ground motions will be greatly enhanced as the weapon penetrates more deeply into the soil or a protective burster layer before it detonates. The concept of an <u>equivalent-effect coupling factor</u> is introduced to account for this effect on the ground shock parameters, and is defined as follows: The coupling factor f is defined as the ratio of the ground shock magnitude from a partially buried or shallow-buried weapon (near surface burst), to that from a fully buried weapon (contained burst) in the same medium.

(1) A single coupling factor is applicable for all ground shock parameters that depend upon the depth of burst (measured to the center of the weapon) and the medium in which the detonation occurs, i.e., soil, concrete, or air.

$$f = \frac{(P, V, d, I, a) \text{ near surface}}{(P, V, d, I, a) \text{ contained}}$$

It is important to note that the coupling factor concept used here <u>does not indicate the size of an equivalent charge</u>, but is a reduction factor applied to the ground shock computed for a contained burst to account for the effects of a shallow weapon detonation depth.

(2) Coupling factors are different for bursts in air, soil, and concrete, and depend upon the scaled depth of burst of the weapon. These factors are shown in figure 5-3. The coupling factor for a detonation in air does not vary with weapon position, but has a constant value

$$f = 0.14$$

The use of this factor is recommended for all contact bursts, regardless of the underlying medium.
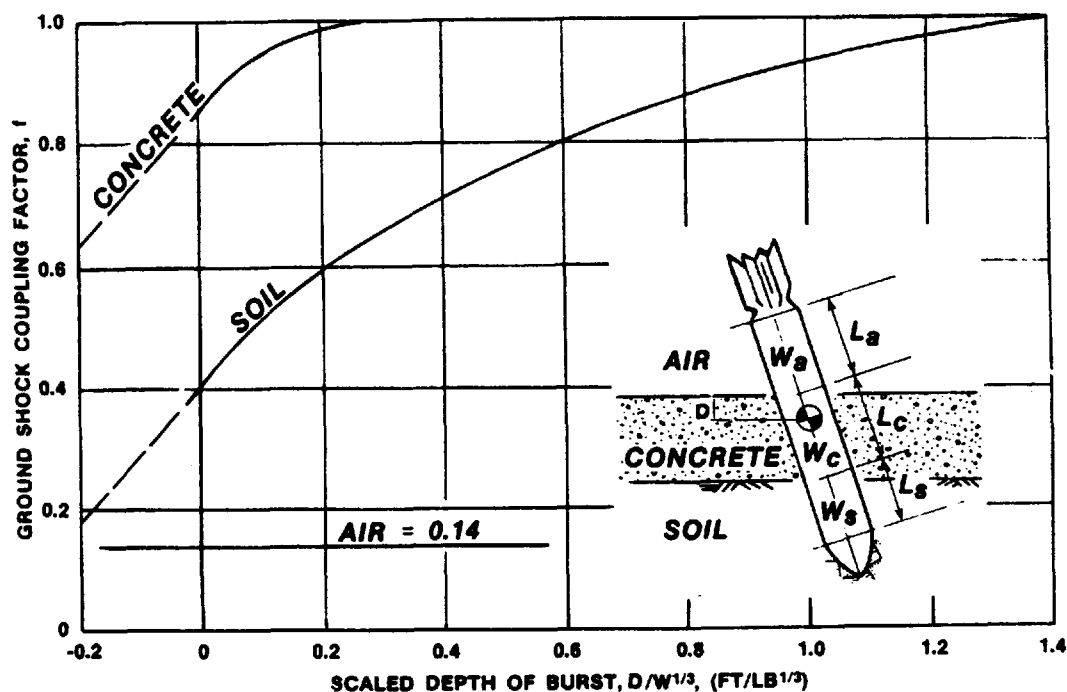
US Army Corps of Engineers

Figure 5-3.   Ground shock coupling factor as a function of scalled depth of burst for air, soil, and concrete.

(3) When a weapon penetrates into more than one material (e.g., a long bomb that passes partially through a concrete slab and into the soil beneath the slab), the coupling factor is computed as the sum of the coupling factors for each material, weighted according to the proportion of the charge contained within each medium. In other words,

$$f = \sum f_i \left(\frac{w_i}{W}\right)$$

(eq 5-6)

where

f = total coupling factor
f_i = coupling factor for each component material, i.e., air, soil, concrete
w_i = weight of the charge in contact with each component material
W = total charge weight

Since most bombs are cylindrical, the coupling factor can also be defined as

$$f = \sum f_i \left(\frac{L_i}{L}\right)$$

(eq 5-7)

where

L_i = length of weapon in contact with each material
L = total weapon length

e. *Reflections from interfaces.* When a buried weapon detonates near a structure, shock reflections from the ground surface (or from layers such as a water table or rock layer) can combine with the directly transmitted stress wave to cause a significant change in the magnitude and / or duration of the loading on the structure. Reflections from the ground surface will produce tensile waves that can combine with the incident wave to reduce the impulse load on the upper portions of the structure wall. Reflections from layers below the explosion will produce secondary compression waves, which can combine with the incident stress to significantly increase the total loading on lower sections of the walls.

(1) The path length travelled by the directly transmitted wave to any point on the wall is the straight line distance from the detonation center to the point, and is given by

$$R_d = \sqrt{(D - z)^2 + r^2}$$

(eq 5-8a)

The total path length of a wave reflected from the ground surface is given by

$$R_s = \sqrt{(D + z)^2 + r^2}$$

(eq 5-8b)

and the total path length of a wave reflected from a deeper layer is

2417

$$R_l = \sqrt{(2h - D - z)^2 + r^2}$$

(eq 5-8c)

where

h	=	thickness of layer
D	=	depth of bomb from ground surface
z	=	depth of the point on the structure from the ground surface
r	=	horizonal distance to the point on the structure

Figure 5-4 shows the propagation paths for a burst in a layered medium.
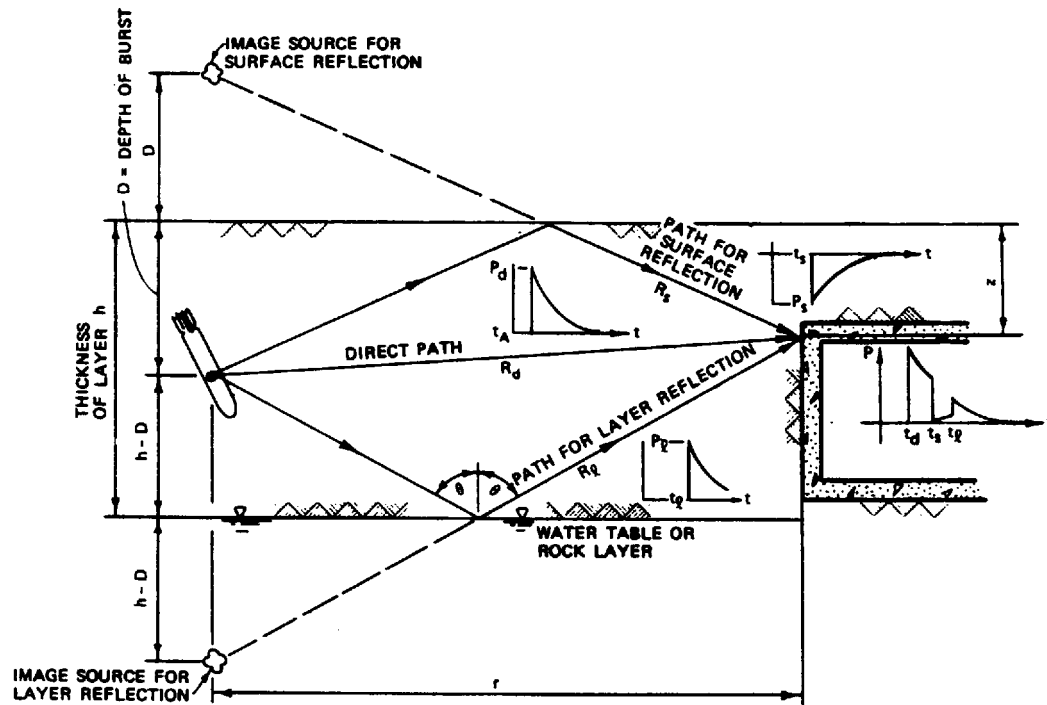
US Army Corps of Engineers

Figure 5-4.   Ray path for reflections from surface and lower layers.

TM 5-855-1

(2) Equation 5-5a can be used to compute the stress along both the direct and the reflected paths, using the path lengths given in equation 5-8. The computed magnitude along the reflected path is then multiplied by a reflection factor to determine the actual reflected wave magnitude. The direct and the reflected wave forms are combined to calculate the total stress-time history at the target location. Thus,

$$P_d = P_o (R_d) e^{-\alpha t/t_d} \qquad\qquad t \geq t_d \qquad\qquad \text{(eq 5-9a)}$$

$$P_s = -P_o (R_s) e^{-\alpha t/t_s} \qquad\qquad t \geq t_s \qquad\qquad \text{(eq 5-9b)}$$

$$P_\ell = K P_o (R_\ell) e^{-\alpha t/t_\ell} \qquad\qquad t \geq t_\ell \qquad\qquad \text{(eq 5-9c)}$$

where

P_d = directly transmitted stress

P_s = stress reflected from the surface

P_l = stress reflected from a lower layer

$$P_o(R_i) = (\rho c)160 \quad \bullet \quad \left(\frac{R_i}{W^{1/3}} \right)^{-n} \qquad , \text{peak stress at distance } R_i$$

for each of the three pulses

K = reflection coefficient from the lower layer.

Note that the coefficient for a surface reflection is -1, and the times of arrival are given as

$$t_d = \frac{R_d}{c_1} \qquad\qquad\qquad \text{(eq 5-10a)}$$

$$t_s = \frac{R_s}{c_1} \qquad\qquad\qquad \text{(eq 5-10b)}$$

$$t_\theta = \frac{R_\ell}{c_1} \qquad\qquad\qquad \text{(eq 5-10c)}$$

The reflection coefficient K is

$$K = \begin{cases} \dfrac{\cos\theta - K_o}{\cos\theta + K_o}, \text{ for } 1 - \left[\left(\dfrac{c_2}{c_1} \right)^2 \sin^2\theta \right] > 0 & \text{(eq 5-11a)} \\ 1 \quad , \qquad \text{otherwise} & \text{(eq 5-11b)} \end{cases}$$

where

$$K_o = \frac{\rho_1 c_1}{\rho_2 c_2} \sqrt{1 - \left[\left(\frac{c_2}{c_1} \right)^2 \sin^2\theta \right]}$$

(eq 5-11c)

and

ρ_1 = mass density of upper layer
c_1 = seismic velocity of upper layer
ρ_2 = mass density of lower layer
c_2 = seismic velocity of lower layer

The angle θ is defined such that

$$\sin \theta = \frac{r}{R_d}$$

and

$$\cos \theta = \frac{(2h - D - z)}{R_d}$$

(3) The total stress history of the shock load at the point of concern on the structure wall is defined by the superposition of these three waves with their proper times of arrival, and is expressed as the function

$$P(t) = P_d + P_s + P_\ell$$

TM 5-855-1

5-2. Cratering.

a. Terminology. A crater is defined as a hole in the ground formed by an explosion. Figure 5-5 illustrates the characteristic parts of a crater, each of which may have some military significance in various situations. General references to a crater normally mean the apparent crater, or the visible hole left after the explosion. The true crater is the hole actually excavated by the explosion, but normally masked by the fallback, i.e., the dirt or debris that falls back into the true crater. If the explosion occurs deep enough to be completely contained below the surface, the true crater will consist of a cavity called a camouflet. The rupture zone is a region immediately surrounding the true crater (or camouflet) in which the earth material remains in place, but has been severely disturbed by the force of the explosion. In turn, the rupture zone is surrounded by a larger region of lesser disturbance known as the plastic zone. On the surface, the rupture and plastic zones form a region of surface displacement, or upthrust. This is normally covered by ejecta, i.e., material thrown out of the crater by the explosion. The crater lip is the deposit of ejecta which completely covers the ground surface beyond the crater edge. Those pieces of ejecta which are thrown beyond the outer edge of the lip and are of sufficient size to present an impact hazard to personnel, structures, etc., are often called missiles.
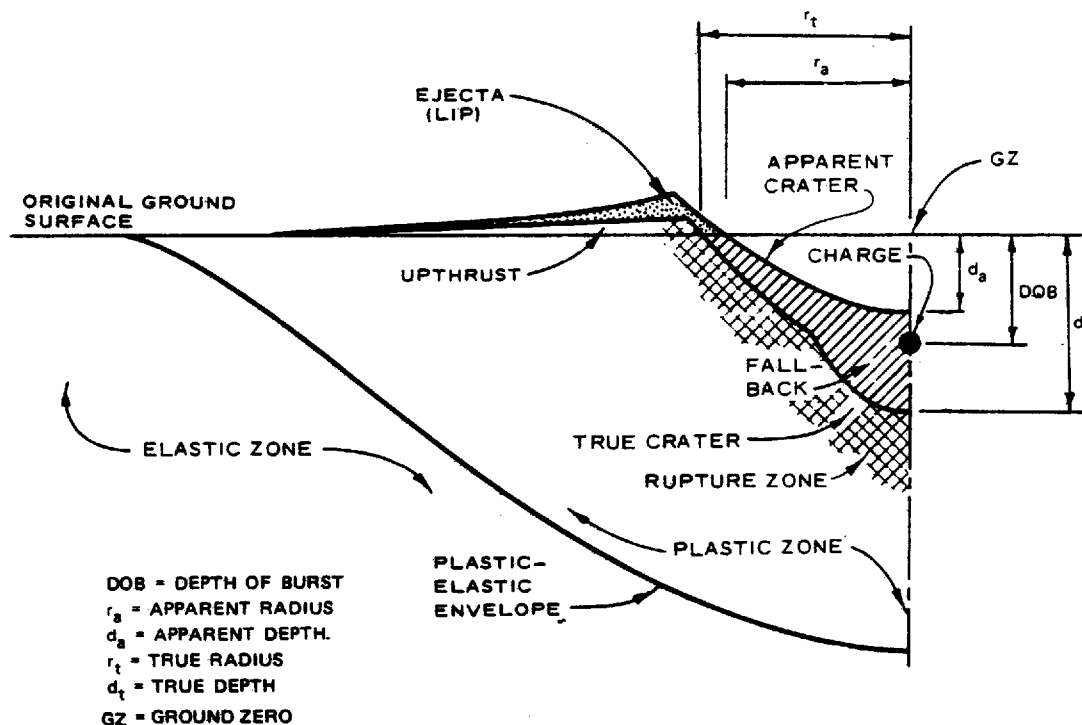
US Army Corps of Engineers

Figure 5-5.   Half-crater profile, taken about a vertical centerline through ground zero and showing crater nomenclature and notation.

2421

b. Crater prediction in earth. The primary variables which govern crater prediction are amount and type of explosive, depth of burst, and type of material in which the cratering occurs , e.g., soil, rock, layered earth, etc.

(1) Variation with depth of burst. For a given munition with a given explosive charge, crater size will at first increase steadily as the depth of burst (DOB) is increased. At some depth called the "optimum" DOB, the crater volume will reach a maximum. The apparent crater depth normally reaches a maximum value at a DOB slightly less than optimum, while the maximum apparent crater diameter occurs at a DOB slightly greater than optimum. For further increases in DOB, the weight of the soil overburden tends to suppress the formation of the crater. As the energy of the explosion becomes less able to throw ejecta beyond the edge of the crater, more material falls back within the crater boundary, thus reducing the apparent crater depth. The apparent crater radius r_a will decrease slightly until a DOB called the containment depth is reached, at which the crater completely disappears and is replaced by a mound of bulked soil. Finally, the camouflet depth is that DOB at which little or no surface disturbance occurs, and the explosion forms only a subsurface cavity. Figure 5-6 illustrates characteristic variations in craters as a function of DOB.
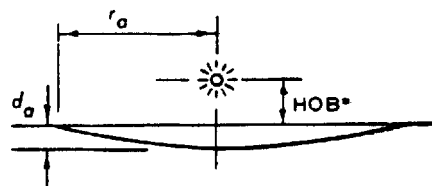
a. LOW AIRBURST
*HEIGHT OF BURST
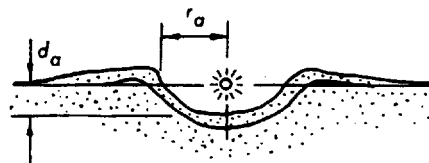
b. SURFACE BURST
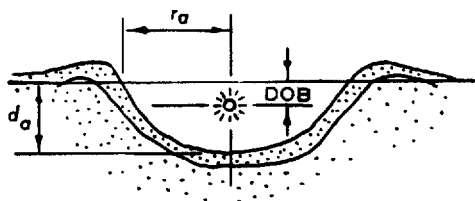
c. SHALLOW DOB
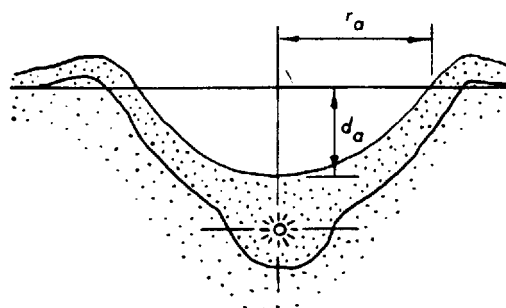
d. OPTIMUM DOB
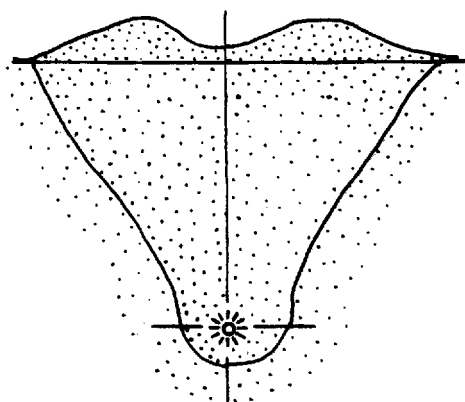
e. DEEPLY BURIED
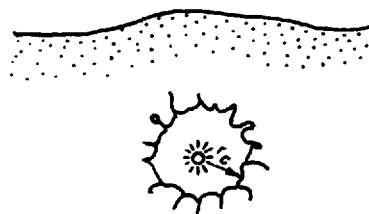
US Army Corps of Engineers

f. CAMOUFLET

*Figure 5-6. Variation in crater size and shape with depth of burst. Upper profile in each
figure indicates apparent crater; lower profile indicates true crater
(coincident in 5-6a.).*

(2) Variation with soil type. Craters formed in sandy soils are smaller than those in clay. Other soils (clayey sand, silt, loam, etc.) usually fall in between sands and clays. A wet soil will usually produce a larger crater than a dry soil; this is particularly true of clayey soils. Figure 5-7 shows apparent crater diameters and depths that should be expected for "bare" (uncased) explosive charges and munitions detonated in different soil types, as a function of DOB.
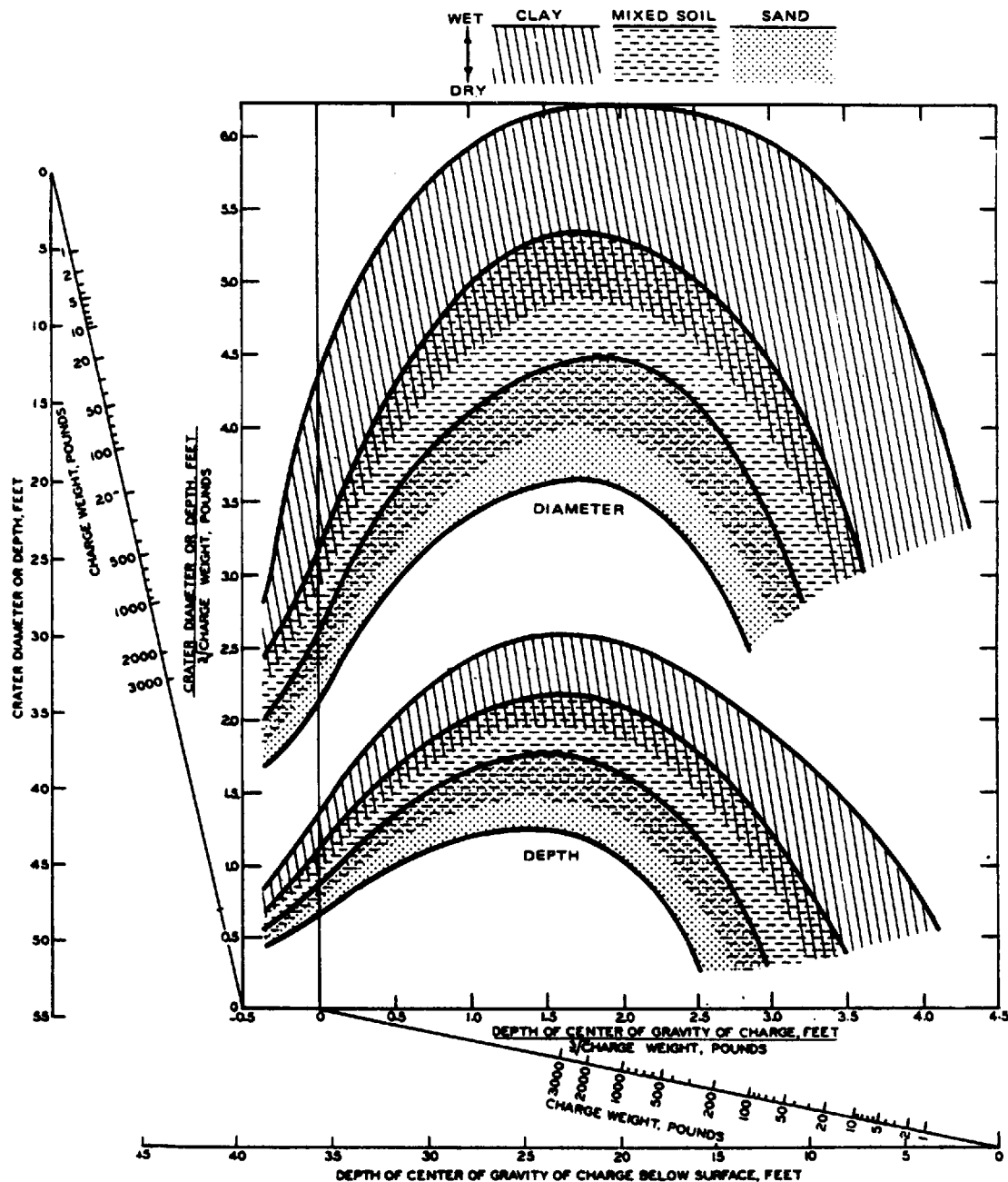
US Army Corps of Engineers

Figure 5-7.   Apparent crater dimensions from cased and uncased high explosives in various soils.

(3) **Variation with surface slope and soil structure.** The crater dimensions of figure 5-7 must be modified if the terrain has a definite slope or departure from a homogeneous condition. Craters formed in flat terrain are roughly circular in plan and symmetrical in cross section; in sloping ground, craters tend to be deeper in the up-slope direction, with a greater amount of ejecta thrown out in the down-slope direction. Subsurface layering in soil , such as a water table (especially in sandy soils) or underlying rock strata, may influence crater shape and dimensions. This occurs when the depth to the layer is less than 1.5 times the apparent crater depth predicted for a layer-free soil (fig 5-7), causing a shallower, wider crater. If the layer is actually intersected by the crater, the increase in crater diameter and the decrease in crater depth can be as much as 50 percent of the predicted values. If the detonation point lies below a water table, the crater should simply resemble one formed in wet soil. (Saturated sands of relatively low densities represent an exception; in this material, there is a possibility that the explosion shock and pressure may induce liquefaction of sand, causing the crater walls to collapse, leaving a wide, shallow crater.)

(4) **Variation with munition type.** Most crater prediction curves are based on test data for uncased (bare) explosive charges. Generally, the bare charges were spheres or short cylinders, centrally detonated, and described in terms of a TNT-equivalent explosive weight.

(a) Munitions, on the other hand, normally have cylindrically shaped explosive fillers with greater length-diameter ratios, are detonated at one end (nose or tail fuzed), have explosive weights given for a specific type of explosive filler, and are encased in a steel shell. These differences between bare charges and munitions can affect the cratering characteristics of the munitions in different ways, depending on the munition burst position relative to the ground surfac.e For example, a quick-fuzed artillery round or bomb which impacts the ground at a steep angle will form a shallower crater than one impacting at a very shallow angle, because the blast and fragments from a long, cylindrical charge are directed more to the sides of the cylinder than toward the ends.

(b) As the munition's burst position moves below the ground surface, however, the effects of explosive charge shape, initiation point location, and casing strength all become less noticeable with increasing detonation depth. For example, the energy expended in rupturing the casing is largely recovered in the cratering process by the kinetic energy of the moving shell fragments being transferred into the surrounding soil. Since all of these effects and relationships can become quite complex, particularly when various soil types must be taken into account, empirically based cratering curves are the most reliable and convrnient means for predicting crater dimensions from munitions. These curves, shown in figure 5-7, assume some degree of data scatter due to variations in munition designs, soil characteristics, etc., as reflected by the width of the shaded bands.

(c) Generally, munitions fired in dry soils with low explosive weight / total weight ratios, high length/diameter ratios, and explosive types with low TNT-equivalence factors will produce crater dimensions at the lower edges of the prediction bands. Craters from munitions having opposite characteristics will fall near the upper boundaries.

(d) The crater dimensions given in figure 5-7 are for __apparent__ craters, and do not necessarily indicate the size of the __true__ crater, i.e., the extent of excavation in the soil by the explosion. As a rule of thumb, the true crater radius will be about 10 to 15 percent greater than the apparent crater radius for all DOB which are less than optimum in soil. The true crater depth will normally be equal to the DOB plus about $0.4 \text{ ft} / W^{1/3}$, where W is the explosive weight in pounds. For explosions on or above the surface, the apparent and true craters will be roughly coincident, since most of the soil debris will be blown clear of the crater. For DOB's greater than optimum, the true crater radius will remain near that for optimum DOB, while the true crater depth will continue to increase with DOB.

c. Crater predictions in concrete and rock. Many fortifications consist of massive concrete, either reinforced or unreinforced. Reliable data on cratering effects of munitions upon such structures are sparse, partly due to the difficulty in determining the exact depth at which detonation occurs. Figure 5-8 is intended to permit estimates of crater sizes resulting from munitions employed against massive concrete and medium-strength rock. The curves are largely based on uncased charge data for both conctere and rock. The values given in this figure are for typical concrete strengths, i.e., 2,000–5,000 psi. Crater dimensions will be larger in weak concrete or rock, and less in high-strength materials. The curve for crater diameter applies to the __apparent__ crater. For explosions with DOB's less than about $1.5 \text{ ft} / W^{1/3}$, however, the __true__ craters should have similar diameters. A separate curve is given for true crater depth.
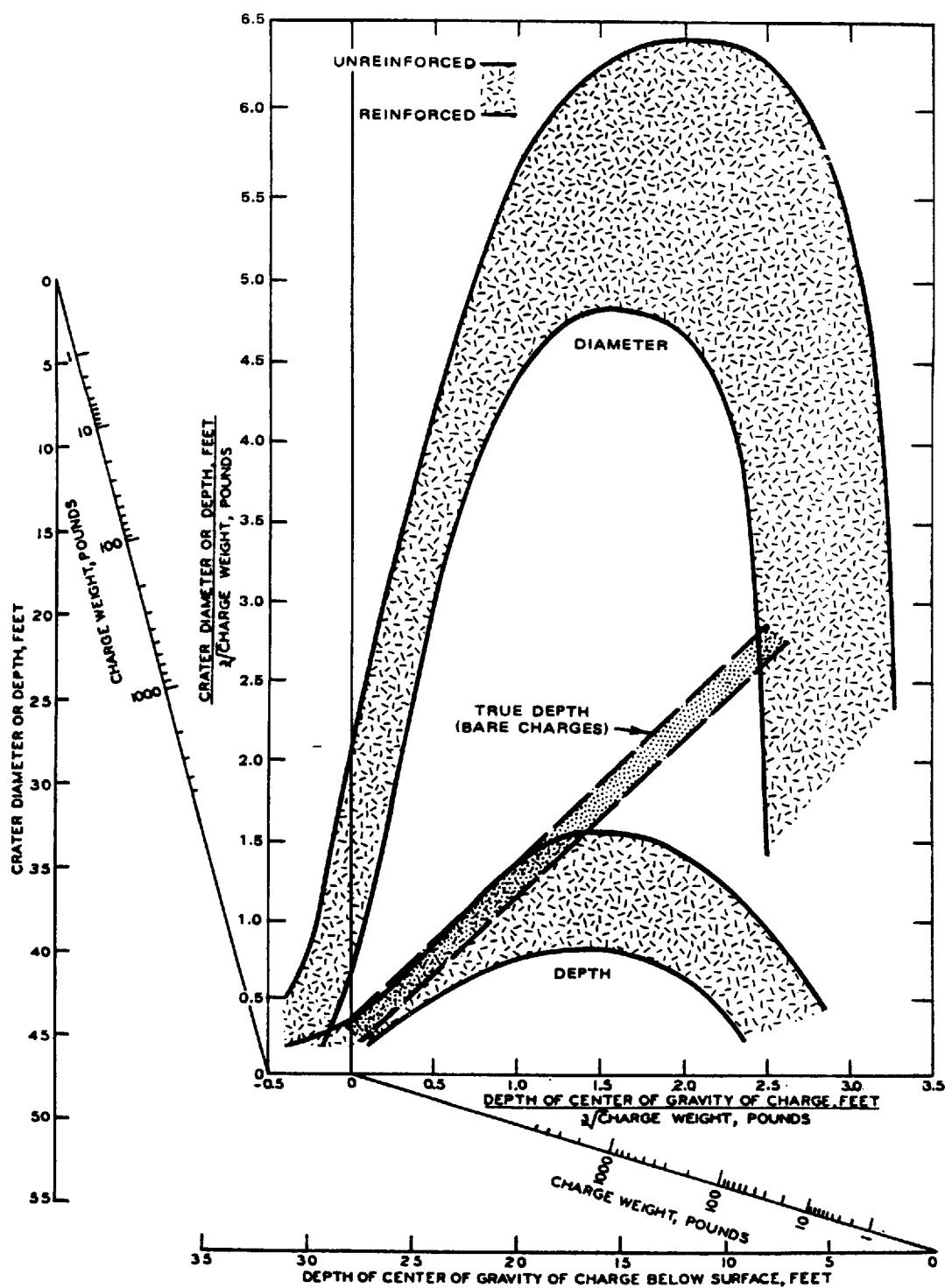
US Army Corps of Engineers

Figure 5-8. Estimated crater dimensions in massive concrete.

(1) Penetration and depth of burst. As in soil, crater size in concrete and rock is highly dependent upon DOB. Some munitions, such as concrete-piercing artillery projectiles and heavy-cased bombs, may penetrate massive concrete to produce craters as indicated by figure 5-8. It is very unlikely, however, that common munitions will be capable of penetrating to any significant depth before the bomb casing is destroyed by the force of impact. In the case of quick-fuzed or point-detonating projectiles or bombs, detonation will occur with little or no penetration, resulting in a very shallow crater. Against concrete structural elements of finite thickness such as slabs and bridge piers, point-detonating muntions may produce a breach by the combined action of cratering on the front face and spalling on the rear face. This action occurs when front-face true crater depth is approximately equal to one-third of the slab thickness. Figure 5-9 shows crater dimensions for attack of finite-thickness structural elements.
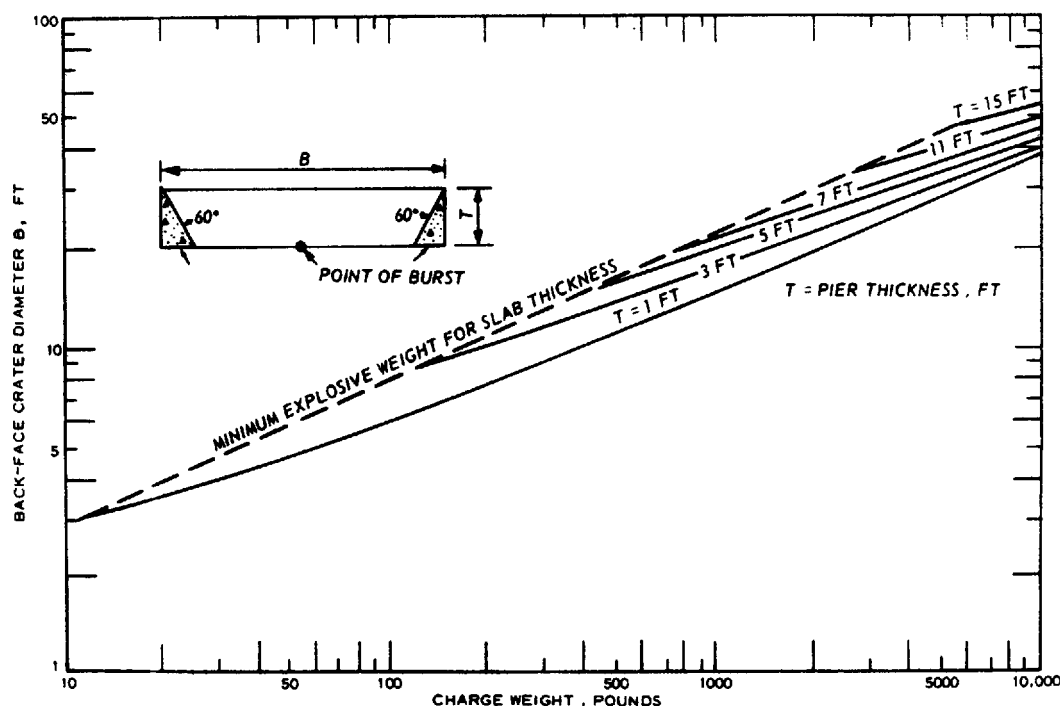
US Army Corps of Engineers

Figure 5-9. Charge weight for breach of bridge pier or similar reinforced concrete structure. Use dashed line for minimum breach and solid line to obtain the desired crater diameter.

(2) Reinforcing. Based on bare charge tests, reinforcing steel conforming to standard American construction practices has shown no observable effect on cratering for point-detonating munitions on reinforced concrete construction. For buried charges, however, reinforcing inhibits crater development by holding together sections of concrete that have cracked loose. In figure 5-8, the area near the upper boundary of each curve indicates the expected crater dimension for underreinforced concrete, and the area near the lower boundary the expected dimension for reinforced concrete.

5-3. Ejecta.

Earth material permanently ejected from the crater void is called "ejecta." For most bombs and warheads, and for small demolition charges, ejecta offers only a nuisance threat insofar as damage or injury is concerned; however, for large explosive charges detonated underground, it poses a more serious threat and must be taken into consideration in the design process.

    a. Ejecta volume and distribution. Graphs of crater and ejecta volumes are shown in figures 5-10 and 5-11 for earth media such as rock and cohesive soil, in which ejecta may present a long-range threat. About 40 to 90 percent (by weight) of this ejecta is deposited within a distance of 2 to 4 apparent crater radii from ground zero (GZ), with the smaller percentage pertaining to near-surface detonations and the larger to near-optimum (for crater volume) depths of burial. Deeper bursts may occur, but they pose an insignificant ejecta threat. The remainder of the ejecta field decreases, on the average, in both particle size and areal density to its outer limit. In soil, ejecta deposition is almost totally confined to 30 crater radii, but in rock, deposition may extend to 75 crater radii with very few particles beyond that range. Figure 5-12 shows maximum particle size as a function of range.
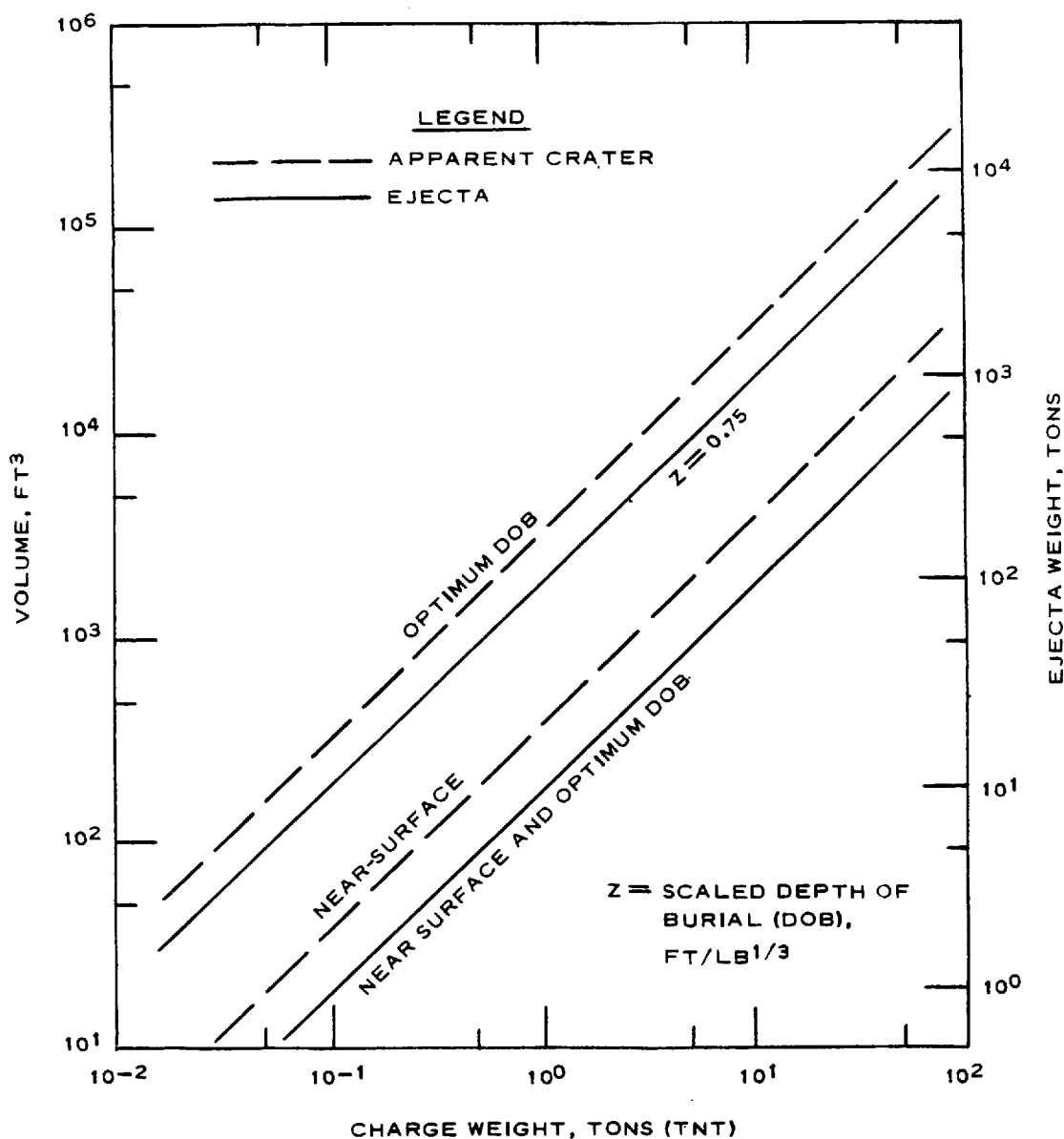
US Army Corps of Engineers

Figure 5-10.   Crater ejecta weight and volume relations for hard rock.

TM 5-855-1

106

LEGEND

— — — — APPARENT CRATER

———— EJECTA

10⁴

OPTIMUM DOB

Z = 0.5

NEAR-SURFACE

10³

Z = SCALED DEPTH OF
BURIAL (DOB)
FT/LB¹ᐟ³

VOLUME, FT³

EJECTA WEIGHT, TONS

10² 10⁻¹ 10⁰ 10¹ 10²

CHARGE WEIGHT, TONS (TNT)
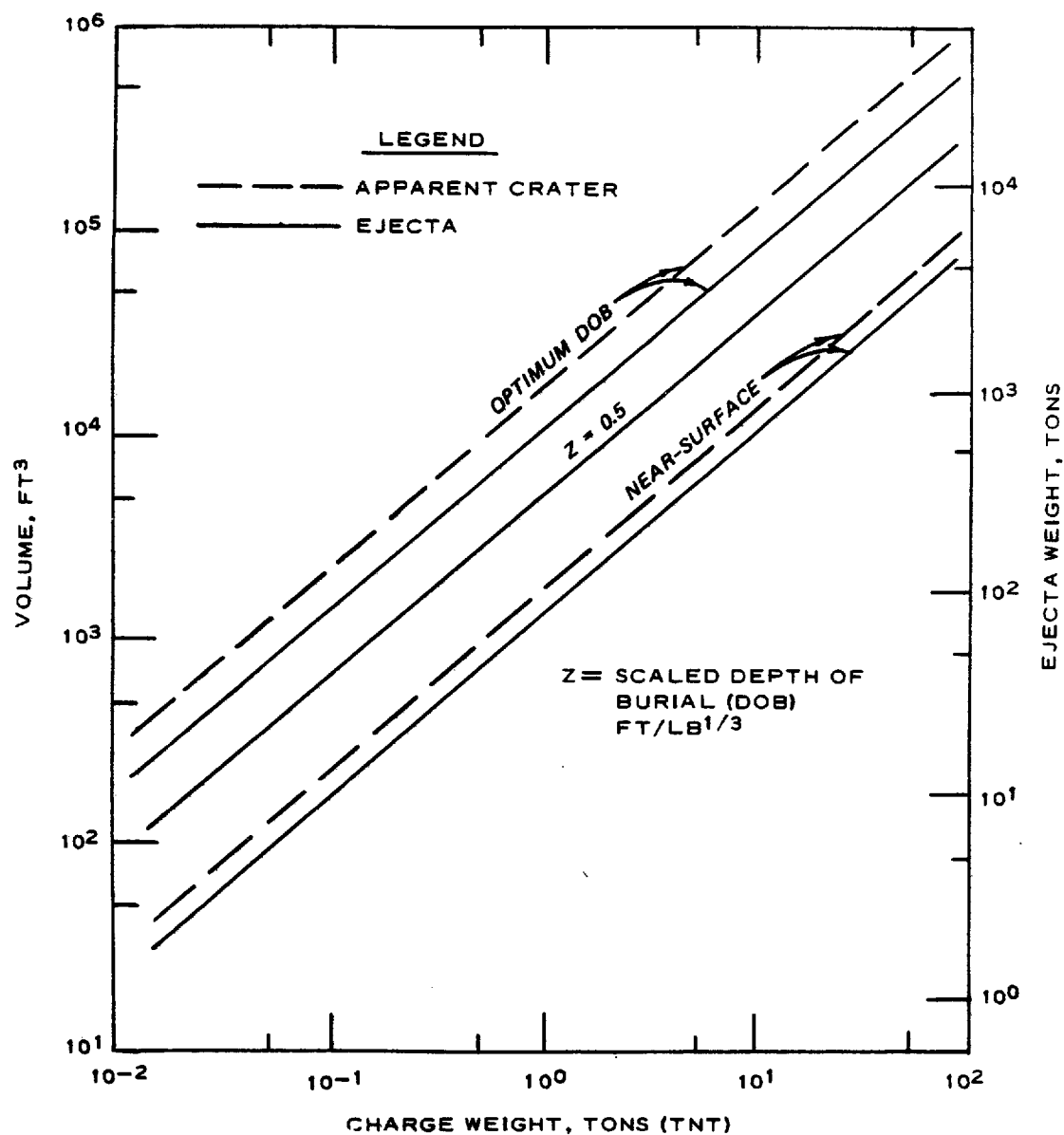
US Army Corps of Engineers

Figure 5-11.   Crater ejecta weight and volume relations for soft rock and cohesive soils.

2429

5-22
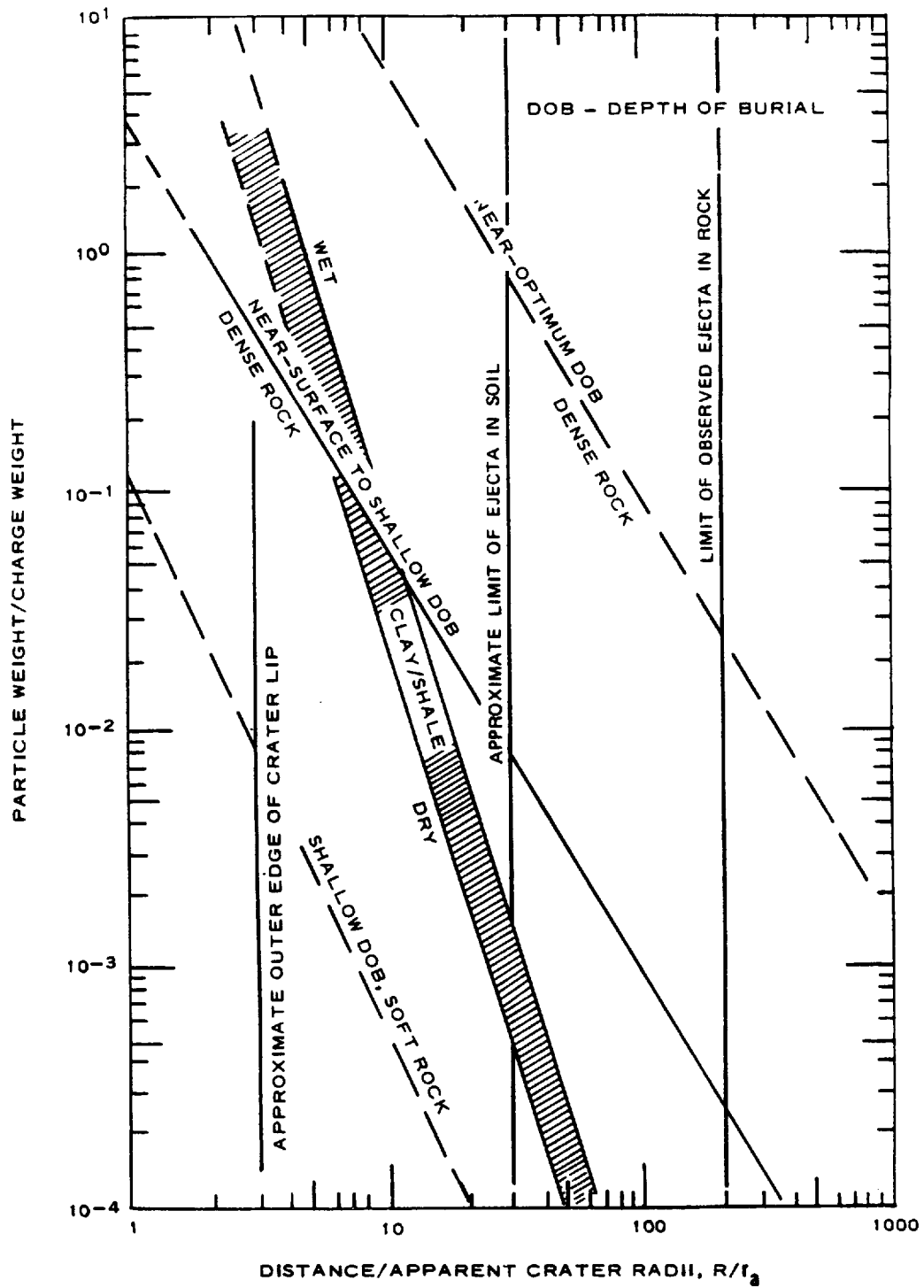
Figure 5-12. *Maximum expected ejecta particle size versus range.*

b. Damage potential. Damage from falling ejecta will be mostly confined to horizontal (or nearly horizontal) structural components, such as roofs, overhead cover for field fortifications, etc. Rock particles may penetrate such cover, while particles of cohesive soil (such as some clays) may cause damage by flexural failure. Most available data concern damage from rock and are confined to impacts against steel and concrete.

(1) Rock particles. Upon impacting steel plate, competent rock particles deliver a sharp blow, usually perforating the plate (by punching shear) or rebounding. Soft rock may shatter before or during penetration. Figure 5-13 is a perforation capability graph, showing the effects of rock against mild steel plate. The limited data available indicate a 7:1 ratio in perforation capability for hard versus soft rock, i.e., a 1-pound hard rock particle has about the same perforation capability against mild steel as a 7-pound soft rock particle. Figure 5-14 (right-hand ordinate scale) permits estimates of maximum perforation thickness for long-range, hard-rock ejecta impacting unreinforced concrete slabs. These curves are based upon empirical formulae for "nondeformable" missiles with assumed terminal velocities, and thus may be considered upper limit values for perforation, but to an unknown degree.

APPROXIMATE VELOCITY RANGE
OF EJECTA IMPACTS

LEGEND
——— GRANITE
— — — SANDSTONE
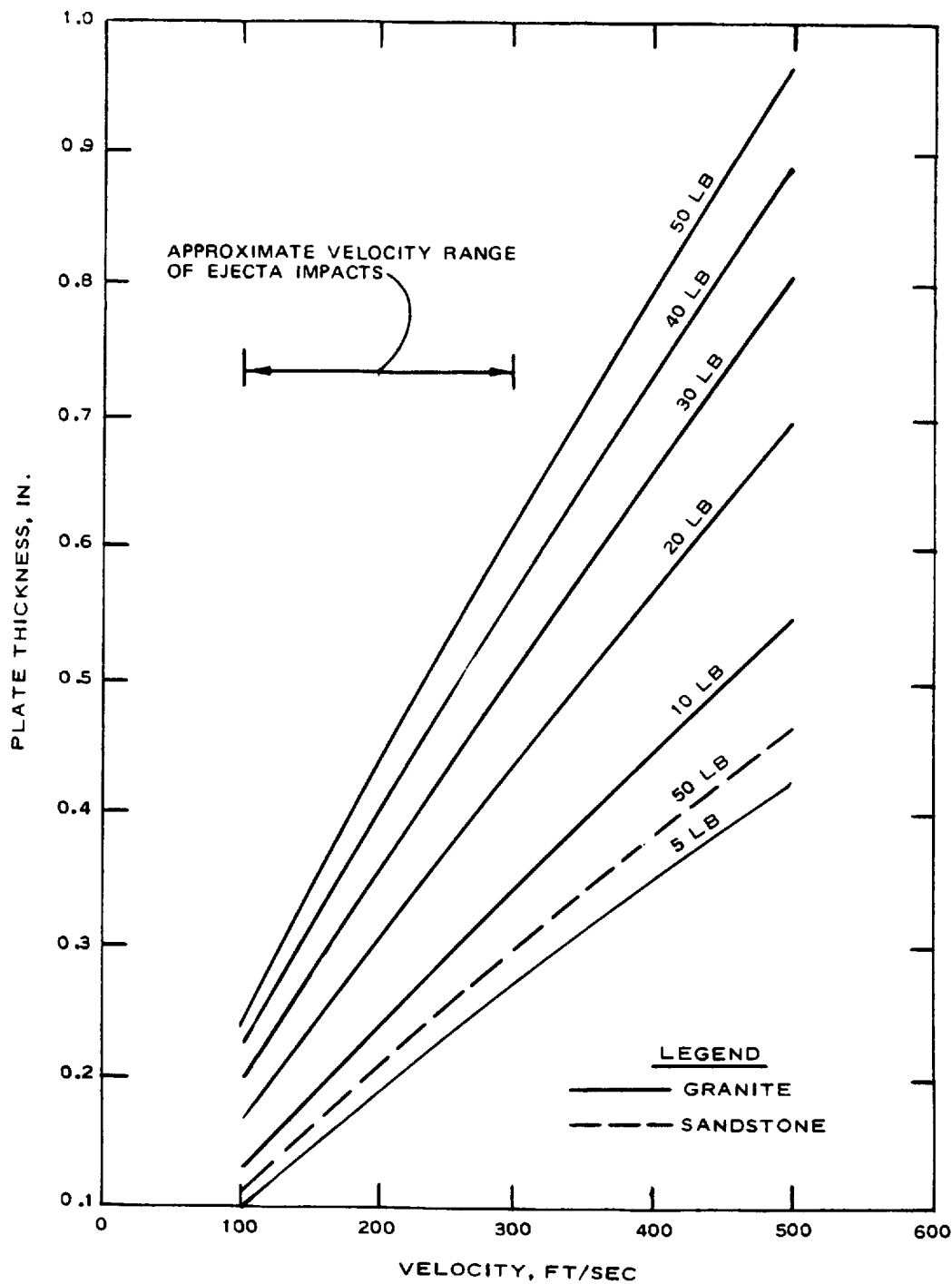
US Army Corps of Engineers

Figure 5-13.   Perforation of mild steel plate by rock particles.

2432
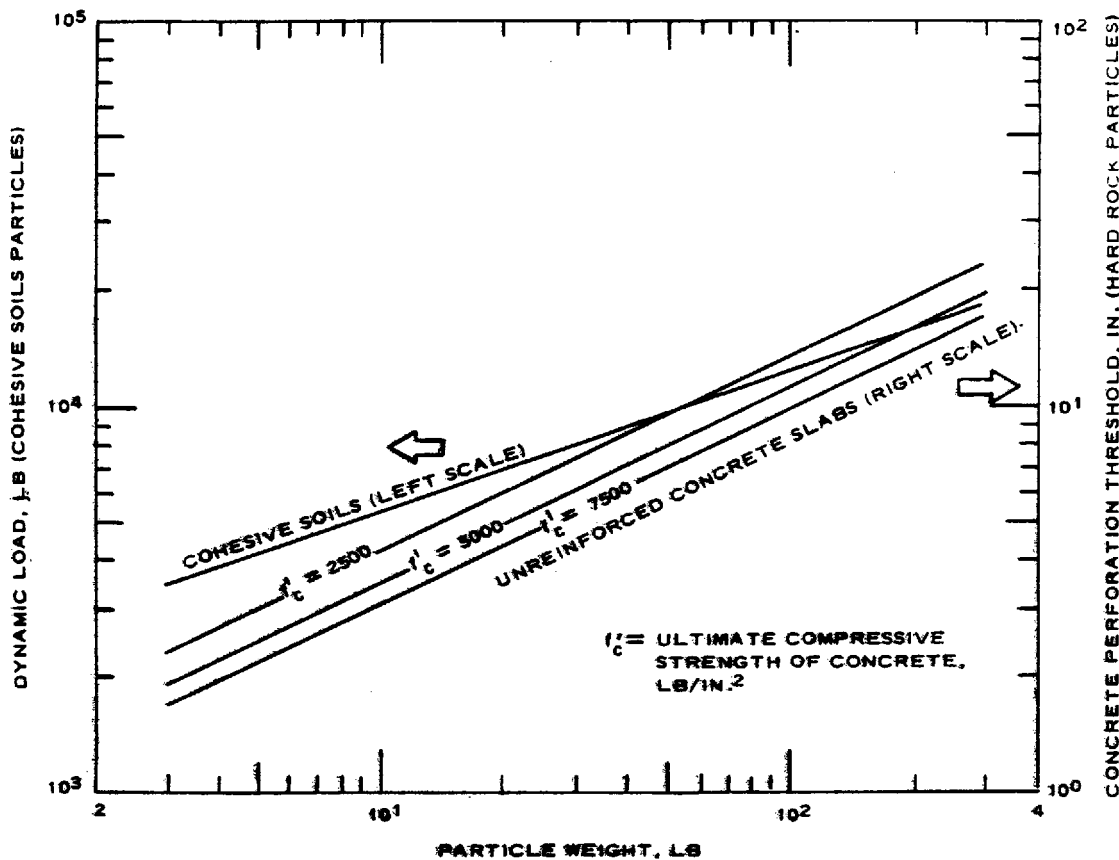
US Army Corps of Engineers

Figure 5-14.   Ejecta impact parameters.

(2) Cohesive soil particles. Moist clay particles deform upon impact, expending some of their kinetic energy in the process, and transmitting an impulse to the impacted structure that has a lower peak load than that of rock particles, but is longer in duration. Damage or failure is most likely attributable to localized flexure. There are insufficient experimental data available to define threshold levels of damage, but the use of certain simplifying assumptions make possible an estimate of dynamic loads by impacting particles.

Assuming

   (a) soil specific weight (moist clay) 120 pcf

   (b) an idealized particle shape (between sphere and cube) with linear dimension l_d

   (c) that the impacting particle deforms about 2/3 l_d (based upon field observations)

   (d) that an average vertical velocity V During deformation may be estimated as

2433

$$\overline{V} = \frac{V_i + V_f}{2} \qquad \text{(eq 5-12)}$$

where

V_i = impact velocity, for which some data are available

and

V_f = final velocity = 0

then the duration of dynamic loading t_{dy} can be estimate as

$$t_{dy} = \frac{2/3 \ell_d}{\overline{V}} \qquad \text{(eq 5-13)}$$

Average particle momentum M during deformation is

$$\overline{M} = \frac{W_p}{g} \overline{V} \qquad \text{(eq 5-14)}$$

where

W_p = particle weight

and

g = gravitational acceleration

Momentum is transmitted to the impacted structure as impulse I , so that

$$\overline{M} = \overline{I} \qquad \text{(eq 5-15)}$$

and the dynamic load

$$P_d = \frac{\overline{I}}{t_{dy}} \qquad \text{(eq 5-16)}$$

For long-range ejecta particles from large charges buried in moist clay, figure 5-14 (left-hand ordinate scale) shows estimated dynamic loads. These may be applied as point loads to structural components to compare with ultimate flexural stress. In so doing, use the following dynamic/static load factors to allow for the higher ultimate stresses which can be tolerated for the short durations associated with dynamic loads:

- Steel plate, 2.5
- Concrete, 2.5
- Wood, 1.75

CHAPTER 6

MUNITION FRAGMENTATION

6-1. Introduction.

An important consideration in the design of structures to resist conventional weapons effects is impact by relatively high-velocity fragments produced from the metal case of an explosive-loaded munition. Upon contact with a structure, these fragments will either pass through (perforate), become embedded in, or be deflected by the structural element. This chapter presents reliable design procedures for determining characteristics (mass, velocity, shape, and number) of fragments from a given munition and their penetration into various structural materials.

6-2. Primary fragment characteristics.

a. General. Design of structures against the effects of fragment penetration requires a knowledge of the characteristics of a critical design fragment at its point of impact with the structure. This section shows how to determine the number, mass distribution, and velocity of fragments created by the detonation of a given munition whose geometry and explosive and metal case material properties are known. In addition, a design fragment shape is defined.

b. Fragment mass distribution. Upon detonation of an explosive munition, the casing breaks up into a large number of fragments. In specially designed munitions (especially in missile warheads), fragment masses are controlled to certain weights either by using preformed fragments or by causing the casing to break in a predetermined fashion. In these cases, the design fragment weight is easily determined if the details of the munitions are known. Most artillery shells, mortar rounds, and bombs, however, have cases that fragment naturally, and determining a critical design fragment weight is more involved. Generally, the explosion of the naturally fragmenting munition will produce a comparatively large number of fragments. However, many of these are small and only the larger fragments are considered in the design of a protective structure since these may have the momentum necessary to perforate and damage the structure.

(1) The weight distribution of the fragments resulting from the detonation of the fragments resulting from the detonation of any evenly distributed explosive in a cylindrical metal case of uniform thickness is given by

$$N_m = \left(\frac{W_c}{2M} \right)_e - \left(\sqrt{\frac{m}{M}} \right) \qquad \text{(eq 6-1)}$$

where

N_m = the number of fragments with weight greater than the fragment weight m
W_c = total casing weight, oz

$$M = B_x^2 t_c^{5/3} d_i^{2/3} \left(1 + \frac{t_c}{d_i} \right)^2$$

B_x = explosive constant (table 6-1)

2435

t_c = average casing thickness, in.

d_i = average inside diameter of casing, in.

the total number of fragments generated is obtained by setting m = 0 , so that

$$N_T = \frac{W_c}{2M}$$ (eq 6-2)

The choice of design fragment weight is based upon a prescribed confidence level (CL) and is given by

$$W_f = M \ln^2 (1 - CL)$$ (eq 6-3)

In most cases a design confidence level of 0.95 or greater should be used. The confidence level is defined as the probability that the design fragment weight W_f is the largest weight fragment released. The number of fragments with weight greater than W_f is given by:

$$N_f = N_T (1 - CL)$$ (eq 6-4)

For ease in using equation 6-3, figure 6-1 presents the quantity $\sqrt{M}/B_x$ for a given cylindrical casing geometry and figure 6-2 gives W_f / M versus specified confidence levels. Finally, figure 6-3 gives the quantity $B_x^2 N_T / W_c$ for a given casing geometry.

Table 6-1. Explosive constants

Explosive	Bx (Equation 6-1) $(oz)^{1/2}/(in.)^{7/6}$	G (Equation 6-5) 10^3 fps
AMATOL	0.35	6.190
BARATOL	0.51	5.200
COMP. A-3	0.22	
COMP. B	0.22	8.800
COMP. C-4		8.300
CYCLONITE (RDX)		9.300
CYCLOTOL (75/25)	0.20	8.900
CYCLOTOL (20/80)		8.380
CYCLOTOL (60/40)	0.27	7.880
H-6	0.28	8.600
HBX-1	0.26	8.100
HBX-3	0.32	
HMX		10.200
HTA-3		8.500
OCTOL (75/25)		9.500
PENTOLITE (50/50)	0.25	8.100
PTX-2	0.23	
TNT	0.30	7.600
TORPEX		7.450
TRITONAL (80/20)		7.600

2436
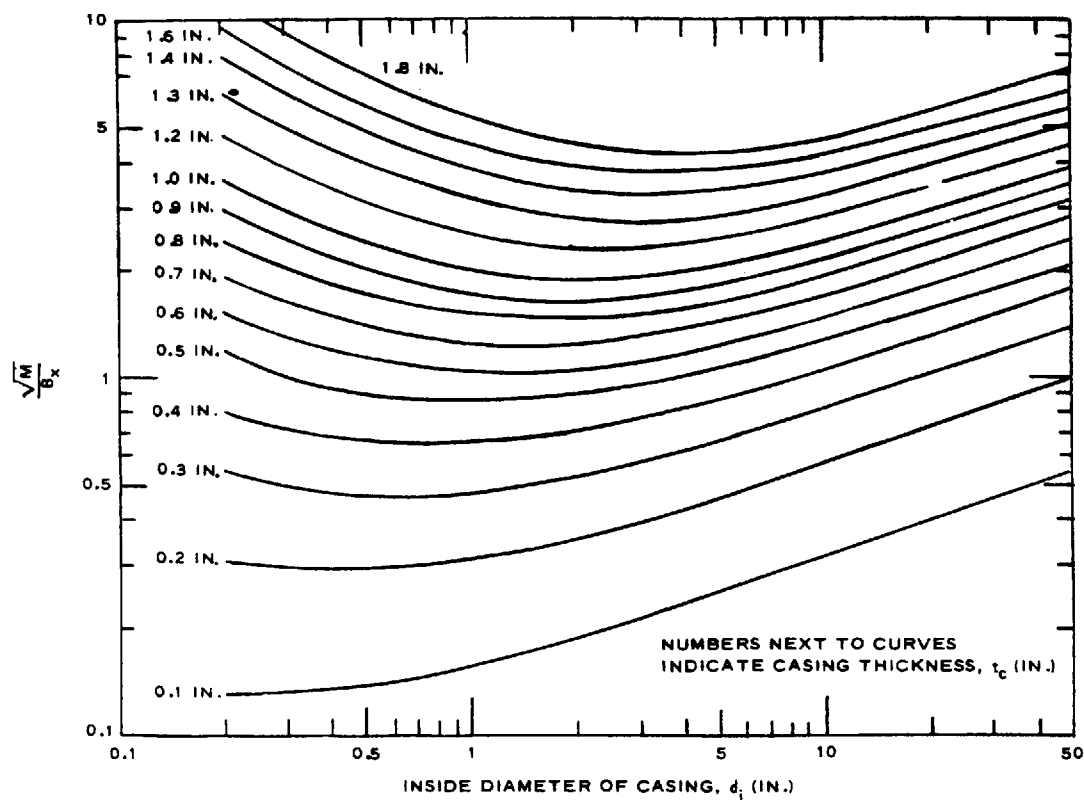
US Army Corps of Engineers

Figure 6-1. $\sqrt{M}/B_x$ versus casing geometry

DESIGN CONFIDENCE LEVEL, CL
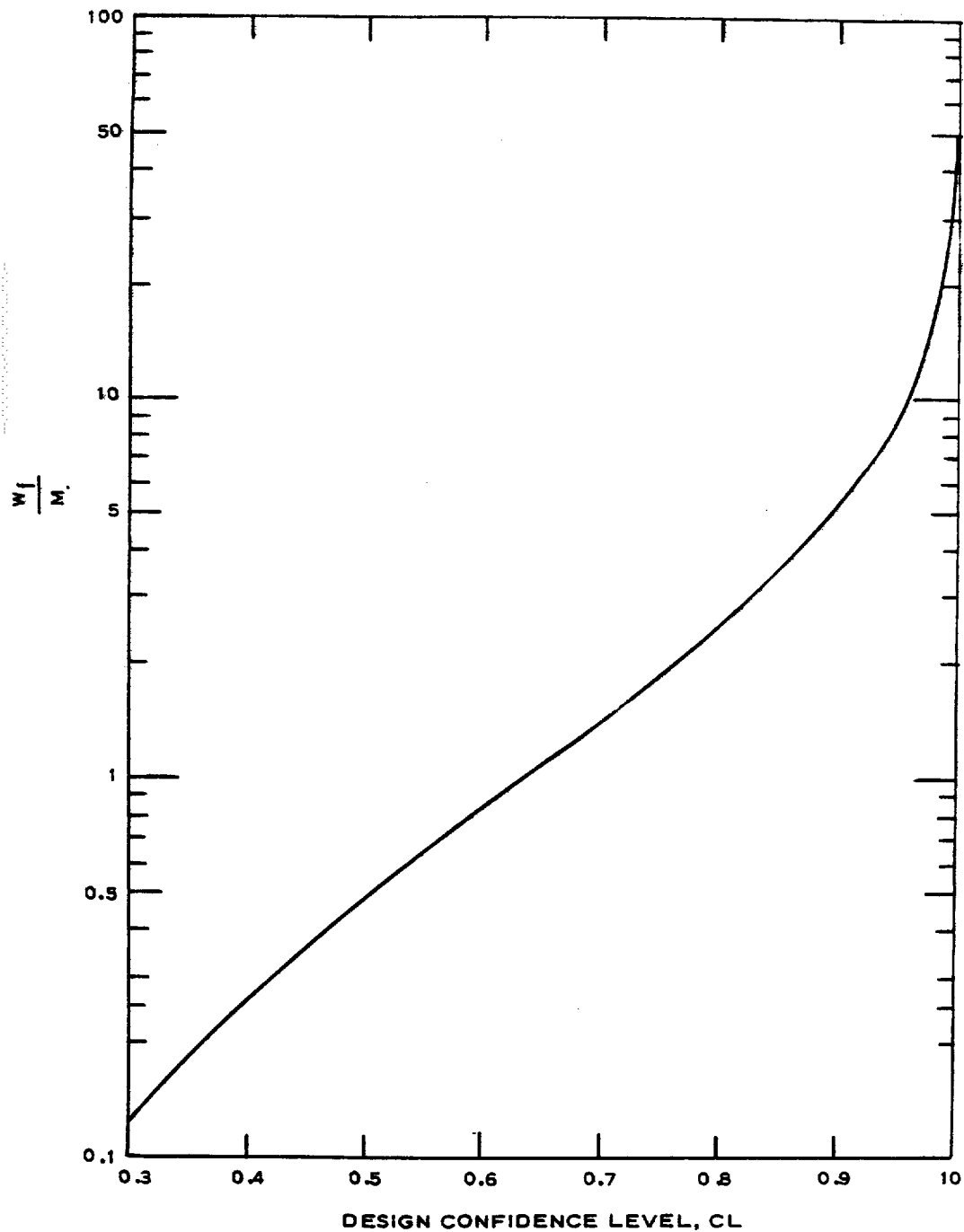
US Army Corps of Engineers

Figure 6-2. *Design fragment weight versus design confidence level.*

NUMBERS NEXT TO CURVES INDICATE CASING THICKNESS t_c

Vertical axis: $\dfrac{B_x^2 N_T}{W_c}$

Horizontal axis: INSIDE DIAMETER OF CASING, d_i, IN.
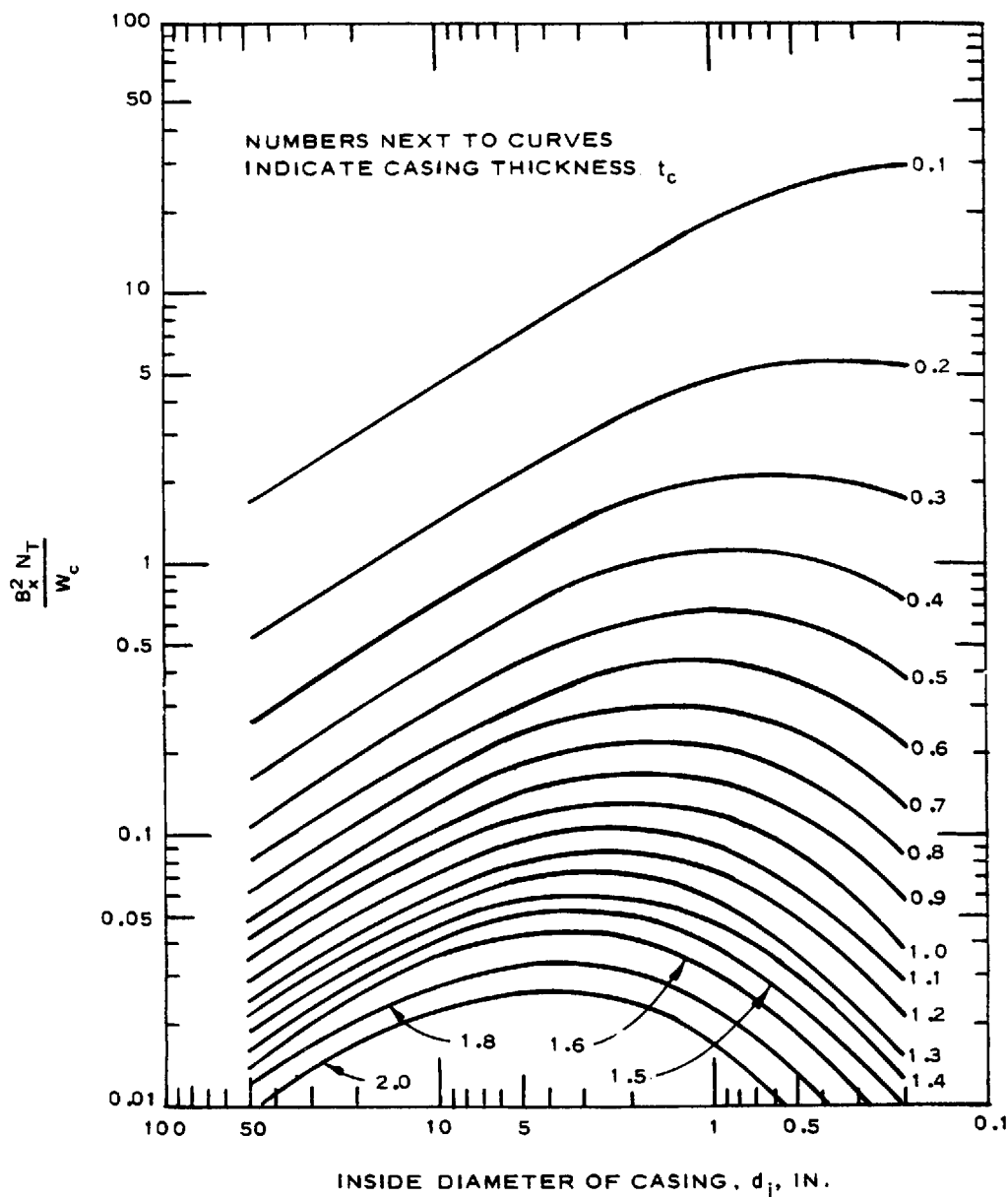
US Army Corps of Engineers

Figure 6-3. $B_x^2 N_T / W_c$ *versus casing geometry.*

(2) Strictly speaking, the preceding development is accurate only for encased explosives with cylindrical geometry. Most munitions, however, are of more complicated geometry, for which prediction equations are not presently available. As such, it is recommended that the calculation given be performed with average cross-sectional dimensions, considering the munition as an equivalent cylindrical container and neglecting the weight of the case at the ends of the munition.

c. *Initial fragment velocity*. The initial velocity of fragments resulting from the detonation of a cased munition is a function of the ratio of the explosive weight to the case weight and of the type explosive. For a cylindrical charge with a uniform casing wall thickness, the initial velocity is given by the Gurney equation

$$V_{oI} = G\left[\frac{W}{W_c} \bigg/ \left(1 + 0.5\frac{W}{W_c}\right)\right]^{0.5} \qquad \text{(eq 6-5)}$$

where

V_{oI} = initial fragment velocity, 10^3 fps
G = the Gurney explosive energy constant (table 6-1)
W = weight of explosive
W_c = weight of casing

A plot of V_{oI}/G versus W/W_c is given in figure 6-4. Actual munitions are seldom cyclindrical and the approximate procedure described previously must be used in conjuction with equation 6-5. Table 6-2 demonstrates use of the procedure for some selected weapons.
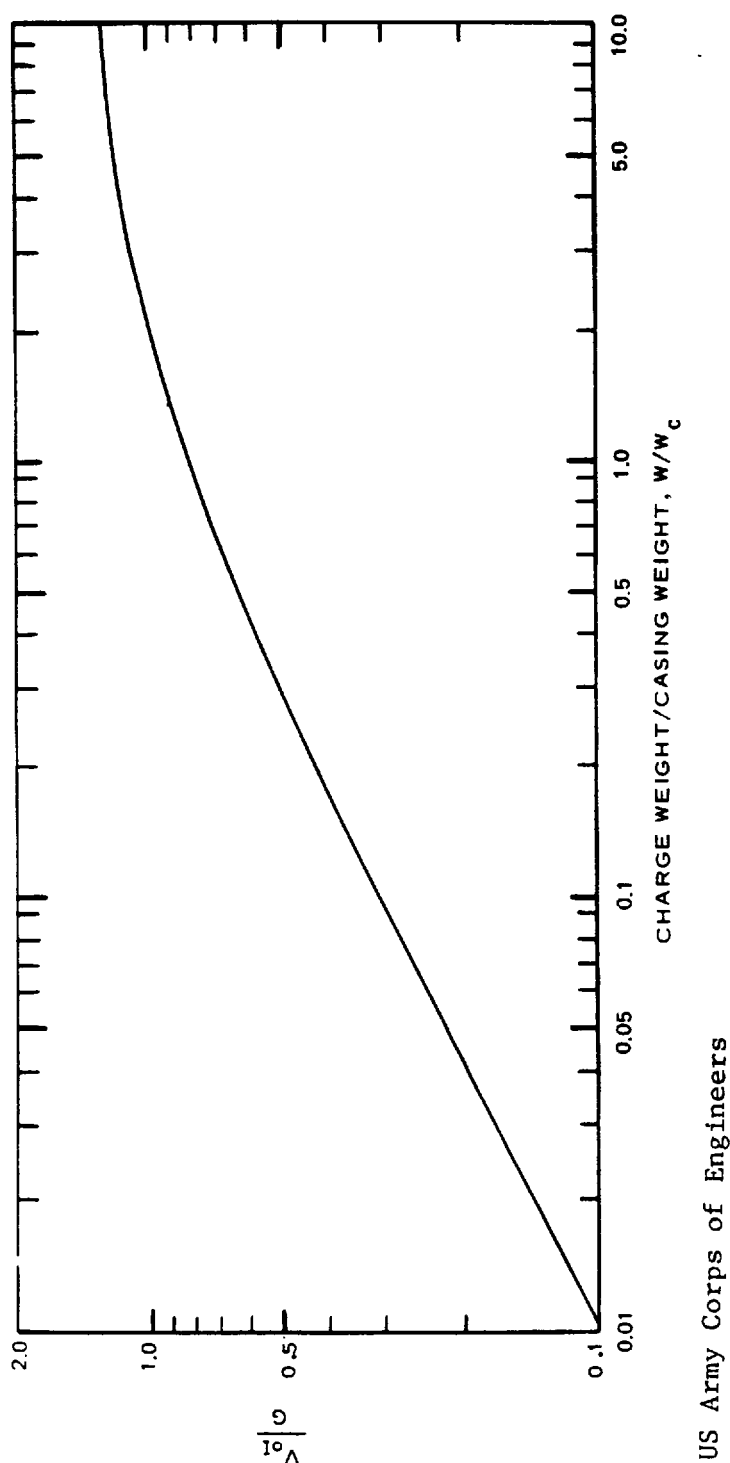
Figure 6-4. *Initial velocity of primary fragments for cylindrical casing.*

Table 6-2. Design fragment characteristics of some selected munitions

Munition Type	Country / Size	Model No. or Type	M (Equation 6-1) oz	W_f (CL = 0.95) oz	V_{ol} 10^3 fps
Mortar round	USSR/82 mm	O-832D	0.030	0.27	4.34
	USSR/120 mm	OF 843A	0.192	1.73	2.66
	USSR/160 mm	F-853A	0.210	1.89	3.28
	USSR/240 mm	F-864	0.277	2.49	4.74
	US/60 mm	M49	0.009	0.084	4.82
	US/81 mm	M362A1	0.0075	0.068	6.34
	US/4.2 in.	M327A2	0.024	0.219	5.55
Artillery round	USSR/122 mm	OF 472	0.163	1.47	3.30
	USSR/130 mm	OF 482M	0.282	2.54	2.78
	USSR/152 mm	OF 540	0.249	2.24	3.45
	US/105 mm	M1	0.051	0.463	4.06
	US/155 mm	M107	0.253	2.27	3.38
	US/175	M437A2	0.146	1.32	4.55
	US/8 in.	M106	0.383	3.44	3.78
Tank round	USSR/115 mm	OF-18	0.195	0.86	3.85
Rocket round	USSR/140 mm	M-14-OF	0.134	1.21	3.93
	USSR/240 mm	9	0.058	0.52	6.93
Bomb	US/100 lb	GP	0.0175	0.16	8.03
	US/250 lb	GP	0.05	0.45	7.96
	US/500 lb	GP	0.072	0.65	7.88
	US/1000 lb	GP	0.204	1.84	7.41
	US/2000 lb	GP	0.25	2.25	7.76
	US/1600 lb	AP	1.80	16.18	3.46
	US/2000 lb	SAP	1.05	9.49	5.16

2442

6-8

d. Variations of fragment velocity with distance. When the point of fragment impact on the structure is less than or equal to 20 feet from the point of the detonation of the munition, the initial velocity V_{oI} given by equation 6-5 can be used as the striking velocity; however, for distances greater than 20 feet the effect of air drag on the fragment should be considered. An estimate of the decrease in velocity with distance is given by

$$V_{sf} = V_{oI}e^{-0.004\left(\dfrac{R_f}{W_f^{1/3}}\right)}$$ (eg 6-6)

where

V_{sf} = striking velocity, 103 fps

R_f = distance traveled by fragment, ft

W_f = weight of design fragment, oz

Figure 6-5 shows the value of V_{sf} / V_{oI} versus W_f for various distances R_f.
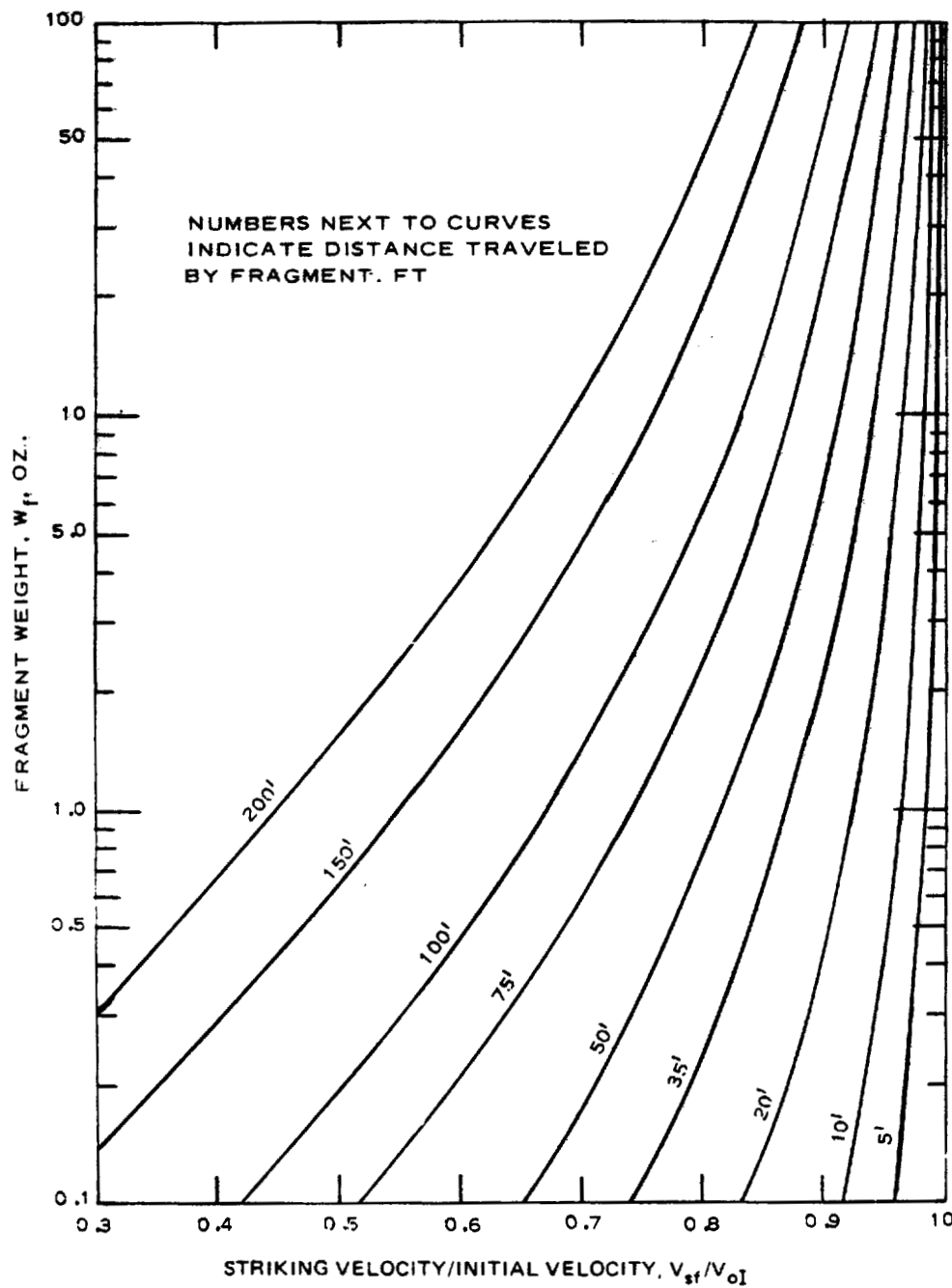
Figure 6-5. *Variation of primary fragment velocity with distance.*

US Army Corps of Engineers

e. Fragment shape, caliber density, and impact angle. The assumed fragment shape for design purposes is shown in figure 6-6. This shape is not necessarily the most critical since it is *statistically possible* that some fragments will have a sharper shape than that shown. However, the number of these fragments is usually very small and the majority of fragments will have a more blunt shape than that shown. Therefore, the penetration predicted for the bullet-shaped fragment shown will be assumed as critical. Caliber density D_d is defined as

$$D_d = \frac{W_f}{d^3} \qquad \text{(eq 6-7)}$$

and the nose-shape factor N_s is defined by

$$N_s = 0.72 + 0.25 \sqrt{n - 0.25} \qquad \text{(eq 6-8)}$$

For the shape shown, $D_d = 0.186 \, \text{lb} / \text{in}^3$, $n = 0.5$, and $N_S = 0.845$. The impact angle is defined as the angle between the path of the fragment and the plane of the surface. In order to design for the most severe conditions, a normal (90-degree) impact angle is assumed.
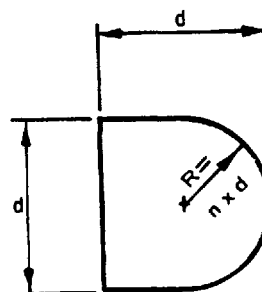
US Army Corps of Engineers

Figure 6-6. Primary fragment shape.

6-3. Penetration.

a. General. The impact of a fragment on a structure can have various effects ranging from possible shatter or ricochet of the fragment with essentially no damage to the structure to complete perforation of the elements. In addition to direct penetration effects, the impact may crater the structure on the front face and cause spalling on the rear face, especially in the case of concrete. The important parameters affecting damage to the structure are the characteristics of the fragment, the striking conditions, and the properties of the barrier material. The first two parameters were devined in paragraph 6-1. Design equations for perforation of various materials commonly used in construction and limits of spalling for concrete are presented below.

b. Penetration of steel. For the design fragment shape given in paragraph 6-1e and for normal impact conditions, penetration into common structural steel is given by

TM 5-855-1

$$X = 0.21 \ W_f^{0.33} \ V_{sf}^{1.22} \qquad \text{(eq 6-9)}$$

where

X = penetration depth, in.
W_f = fragment weight, oz.
V_{sf} = striking velocity, 10^3 fps

Thus, if the steel plate thickness t_s is less than X , the steel will be completely perforated. The residual velocity of the fragment after perforation, in 10^3 fps, is given by

$$V_r = \left[V_{sf}^2 - 12.92 \left(\frac{t_s}{W_f^{1/3}} \right)^{1.64} \right]^{1/2} \bigg/ \left(1 + 1.44 \frac{t_s}{W_f^{1/3}} \right) \qquad \text{(eq 6-10)}$$

For other than common structural steel, perforation depth can be found from

$$X' = X \exp [8.77 \times 10^{-6} (B'^2 - B^2) - 5.41 \times 10^{-3} (B' - B)] \qquad \text{(eq 6-11)}$$

where

X' = penetration into other than mild steel
B' = Brinell hardness of other than mild steel
B = Brinell hardness of common mild structural steel (taken as 150)

Figure 6–7 is a plot of X versus V_{sf} for various values of W_f . Figure 6–8 is a plot of V_r versus V_{sf} for various values of $t_s/W_f^{1/3}$. Finally, figure 6–9 is a plot of X'/X versus B'.

2446

6-12

NUMBERS NEXT TO CURVES
INDICATE FRAGMENT WEIGHT. OZ
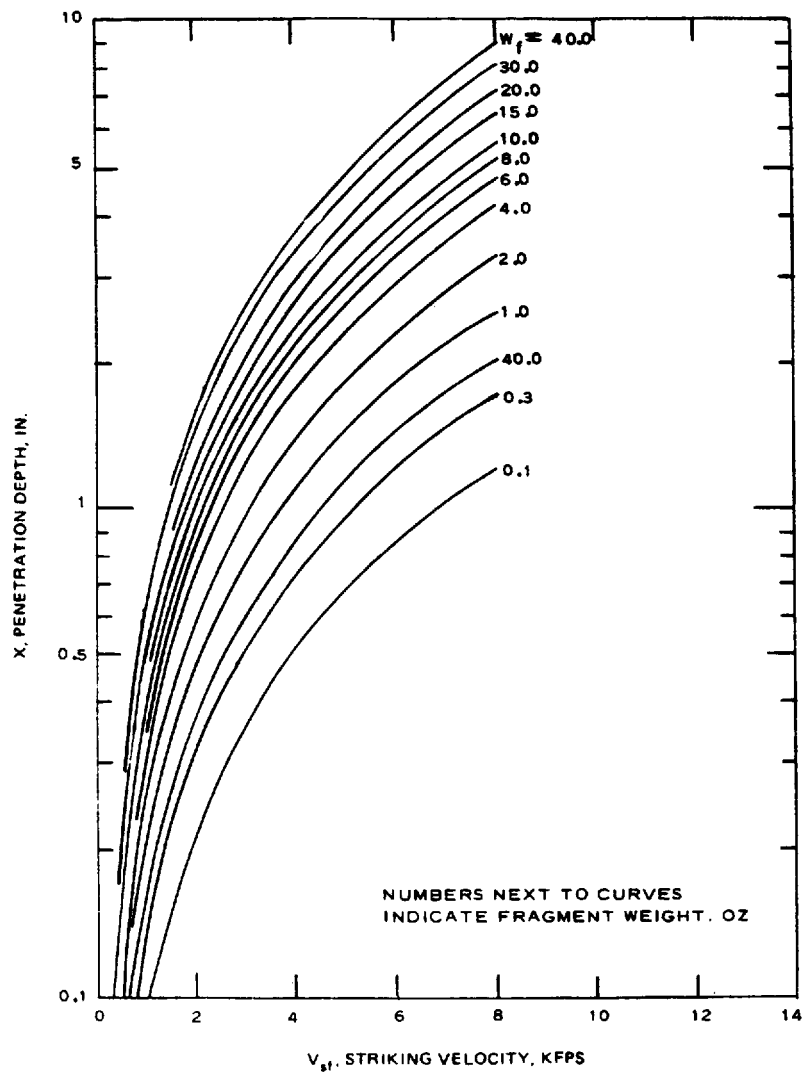
US Army Corps of Engineers

Figure 6–7. Steel penetration design chart — mild steel fragments penetrating mild steel plates.
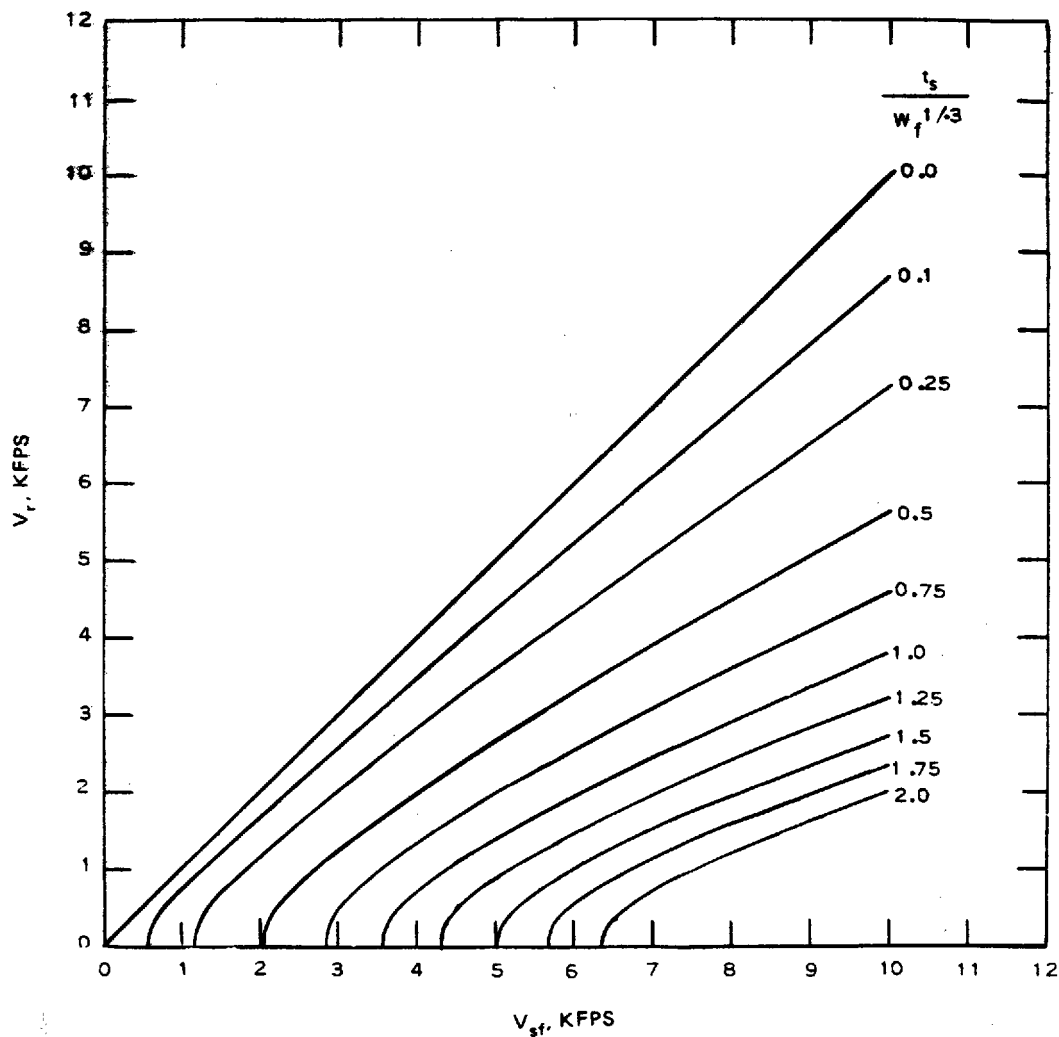
US Army Corps of Engineers

Figure 6–8. Residual velocity after perforation of steel.
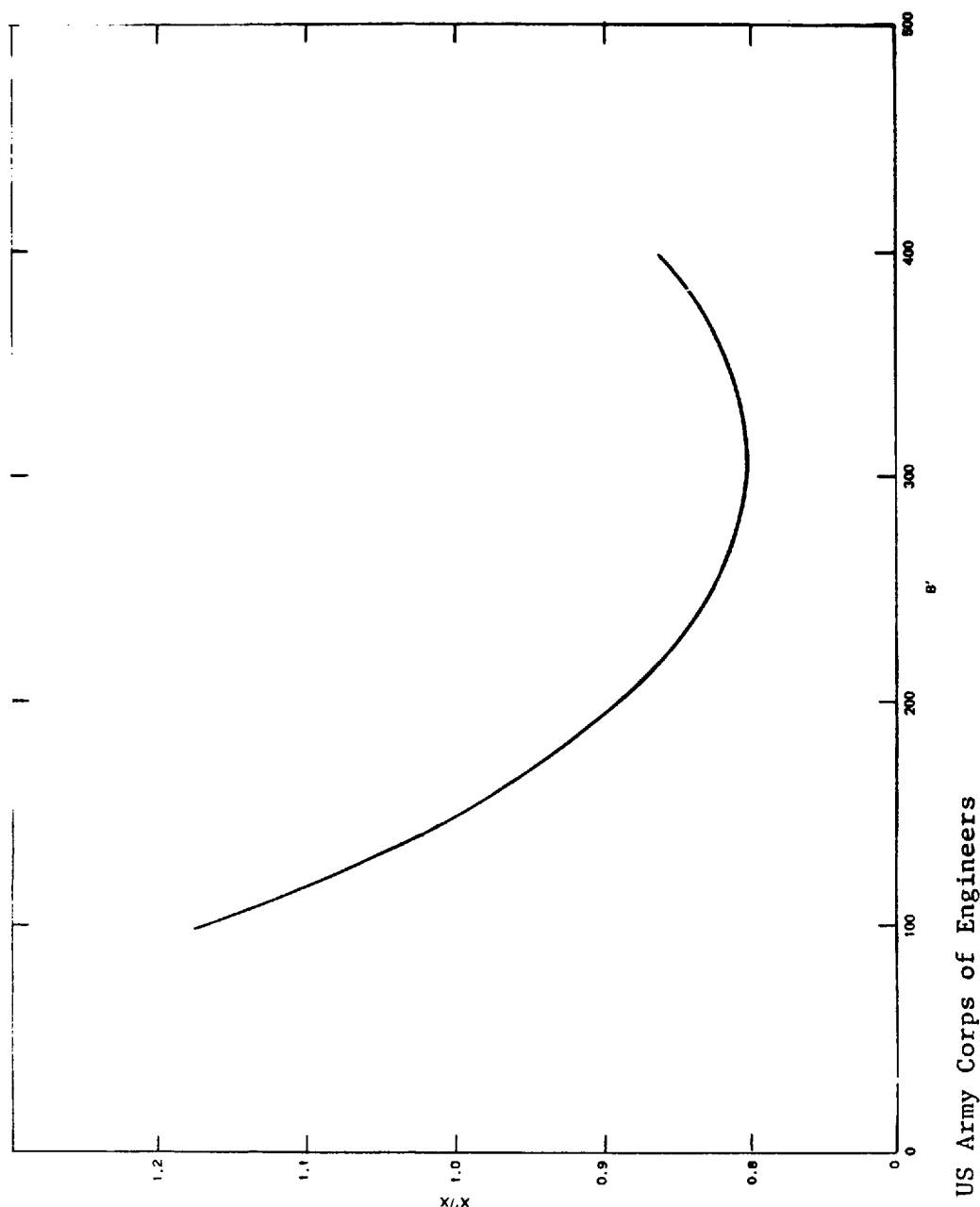
Figure 6–9. Variation of steel penetration with Brinell hardness.

c. *Penetration of concrete.*

(1) Penetration depth. The procedure for calculating the penetration effects in concrete is more involved than that for other materials due to significant spalling which may occur on the rear face. First, it is necessary to calculate the penetration depth into massive concrete by using the following two equations.

$$X = \frac{0.95 \, W_f^{0.37} \, V_{sf}^{0.9}}{f_c'^{0.25}} \quad \text{for } X \leq 1.4 \, W_f^{1/3} \qquad \text{(eq 6-12)}$$

$$X = \frac{0.32 \, W_f^{0.4} \, V_{sf}^{1.8}}{f_c'^{0.25}} + 0.4 \, W_f^{0.33} \quad \text{for } X > 1.4 \, W_f^{1/3} \qquad \text{(eq 6-13)}$$

where f_c' = concrete compressive strength, ksi.

These equations are plotted in figure 6–10 for 3,000–psi concrete.

6-17
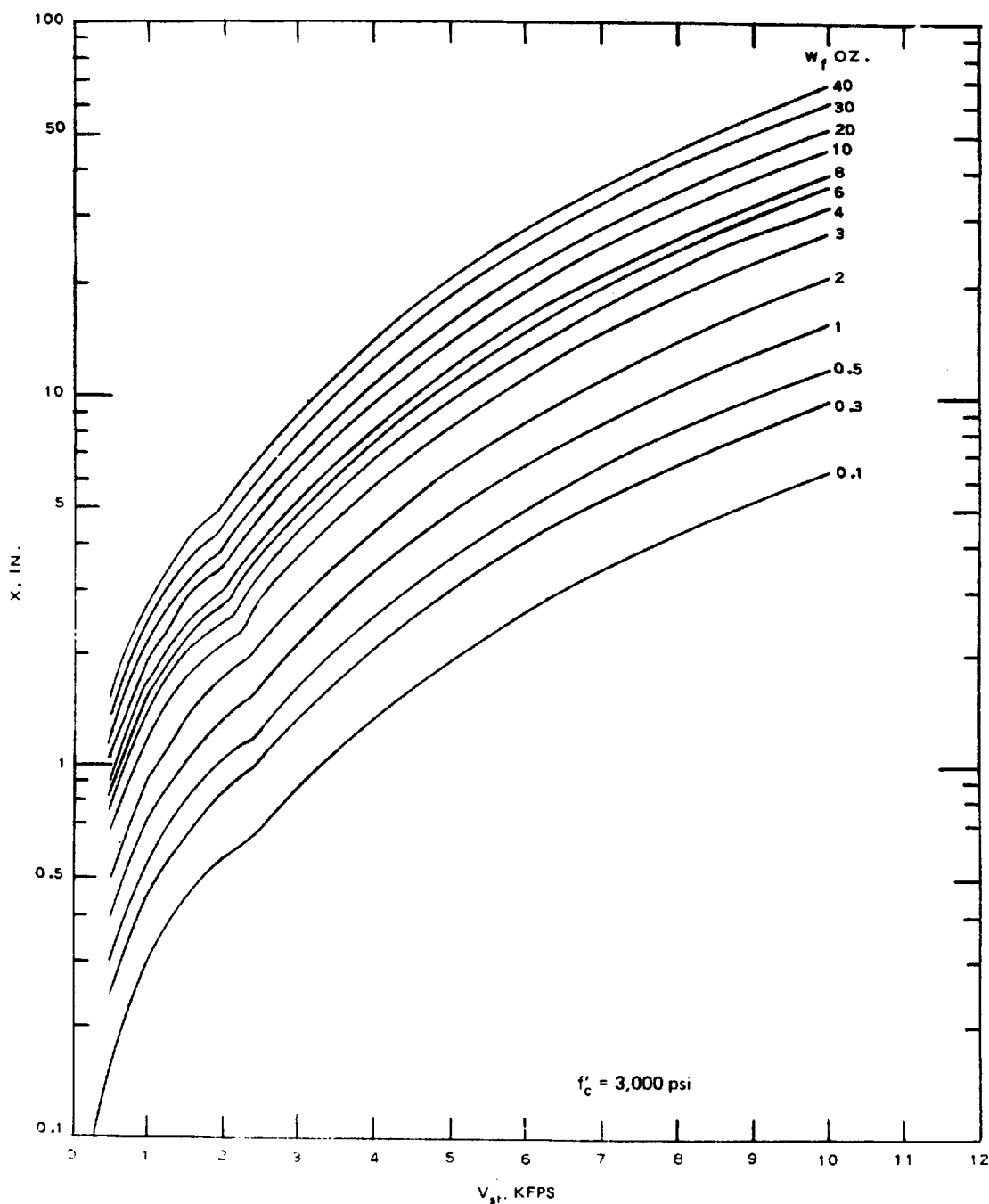
Figure 6-10. Penetration of mild steel fragments into massive concrete.

US Army Corps of Engineers

(2) Thickness of perforation. Next, the thickness of concrete that the fragment is just capable of perforating is calculated from

$$t_{pf} = 1.09 \times W_f^{0.033} + 0.91\, W_f^{0.33}\ , \text{inch} \qquad (eq\ 6\text{-}14)$$

This equation is plotted in figure 6–11. If the actual thickness of the design wall is greater than t_{pf} the fragment will come to rest in the wall. However, the designer should also be aware of the fact that the rear face may still spall and that these spall fragments may be capable of producing damage.
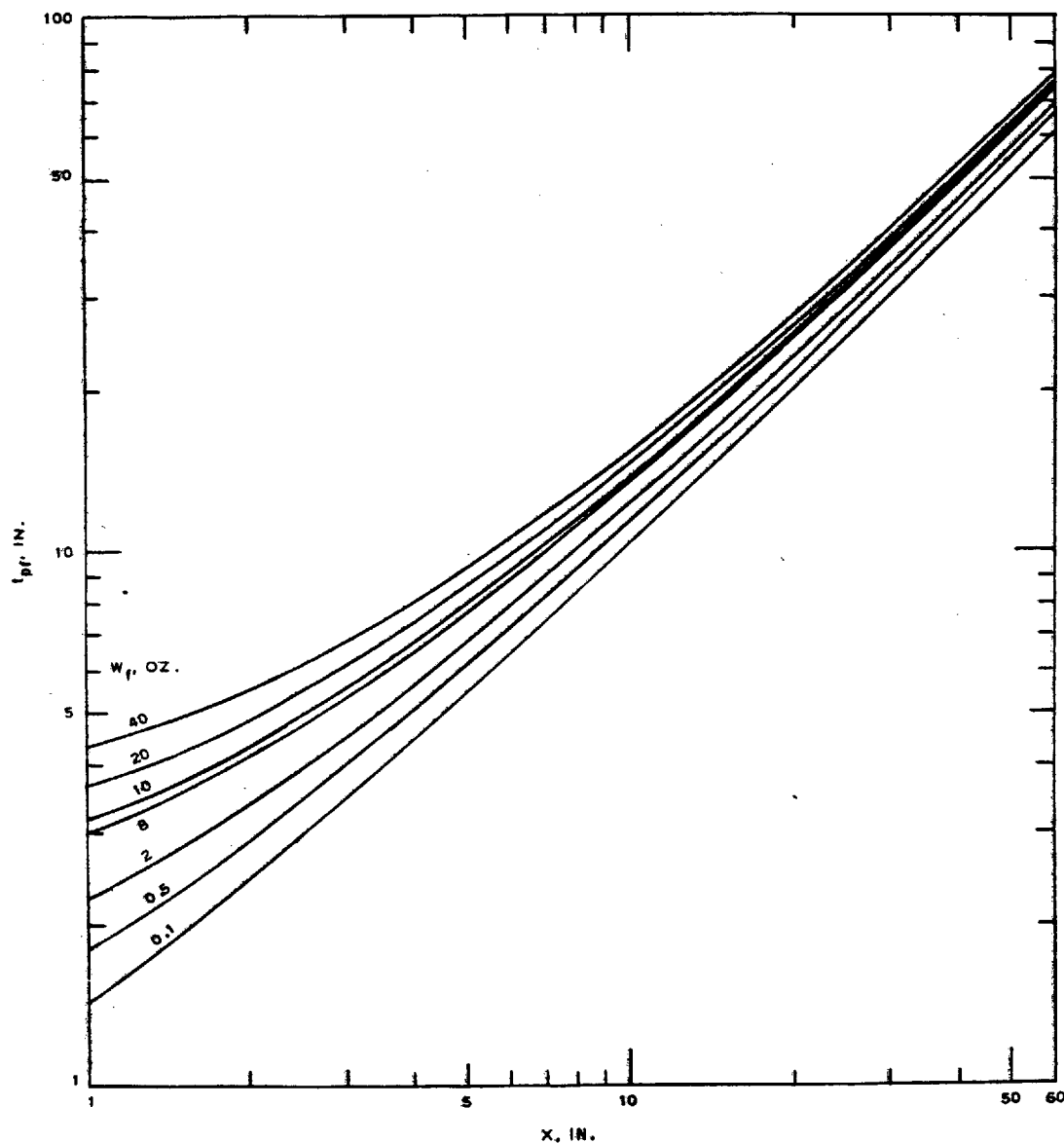
US Army Corps of Engineers

2452

Figure 6–11. Thickness of concrete perforated versus penetration into massive concrete.

(3) Spall protection. If spall protection is desired, the design wall must be thicker than the thickness determined from

$$t_{sp} = 1.17 \times W_f^{0.033} + 1.47 W_f^{0.33} \qquad \text{(eq 6-15)}$$

This equation is plotted in figure 6–12.
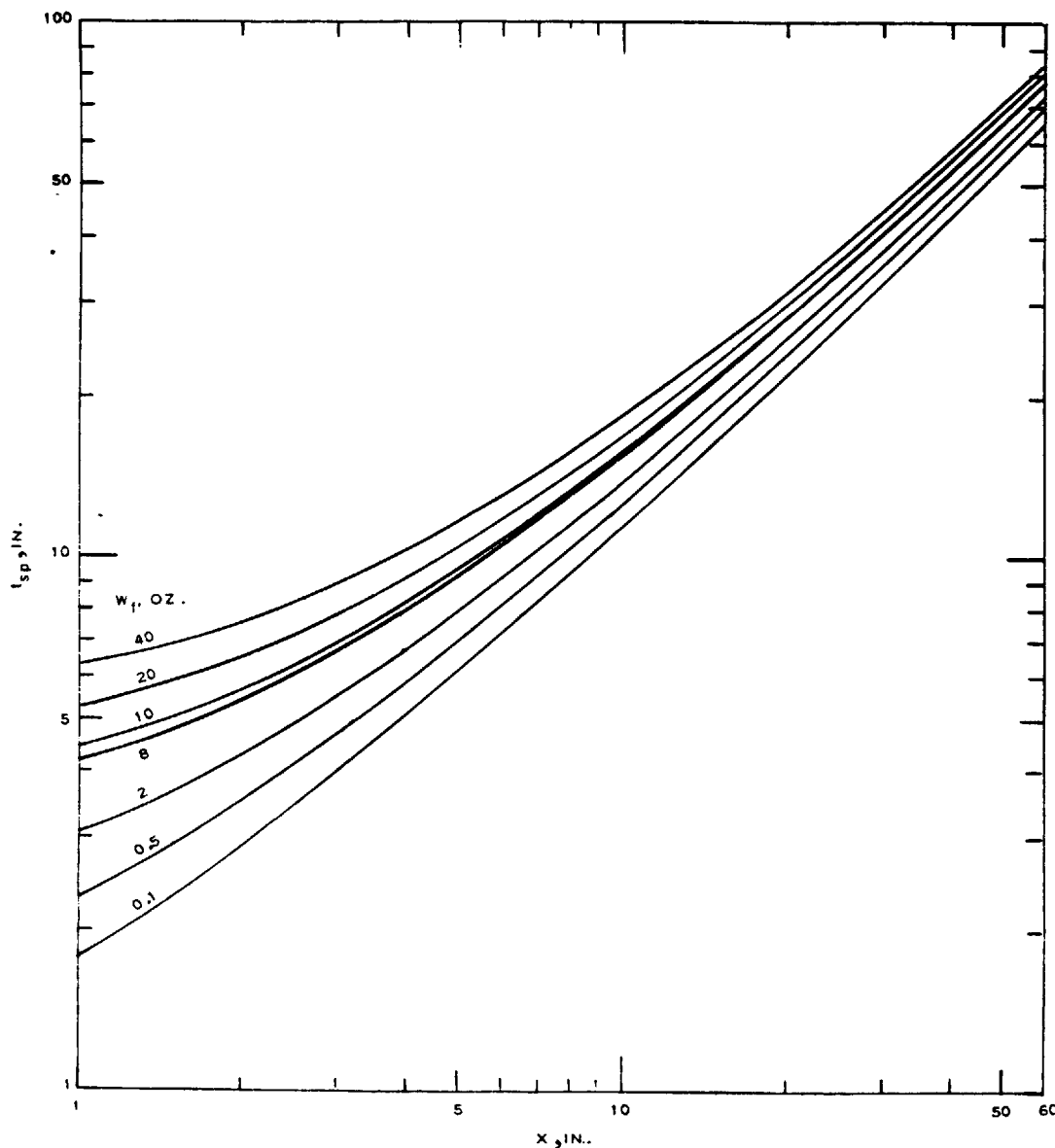
US Army Corps of Engineers

Figure 6-12. Thickness of concrete that will spall versus penetration into massive concrete.

(4) Residual velocity. If the fragment perforates the wall, its residual velocity is given by

$$V_r = V_{sp} \left[1 - \left(\frac{t_s}{t_{pf}} \right)^2 \right]^{0.555} \quad \text{for} \quad X \leq 1.4 \, W_f^{1/3} \quad \text{(eq 6-16)}$$

$$V_r = V_{sp} \left(1 - \frac{t_s}{t_{pf}} \right)^{0.555} \quad \text{for} \quad X > 1.4 \, W_f^{1/3} \quad \text{(eq 6-17)}$$

where t_s is the thickness of the concrete section, in. These equations are plotted in figures 6–13 and 6–14.
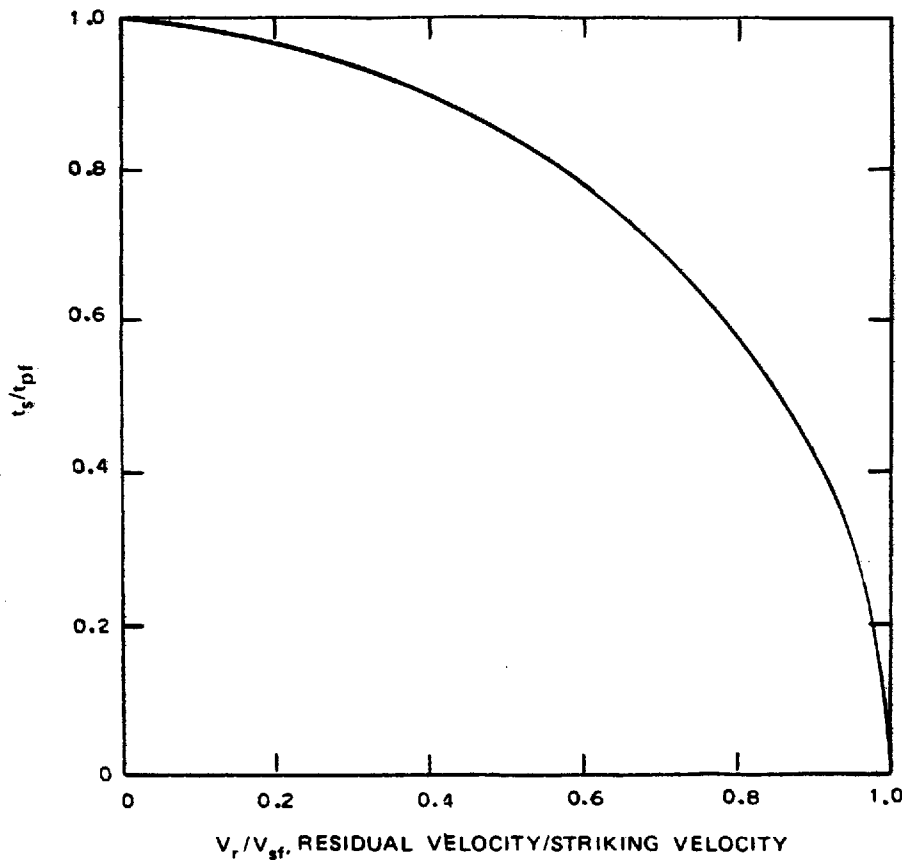
US Army Corps of Engineers

Figure 6–13. Residual fragment velocity upon perforation of concrete barriers for cases where $X \leq 1.4 \, W_f^{1/3}$

2454
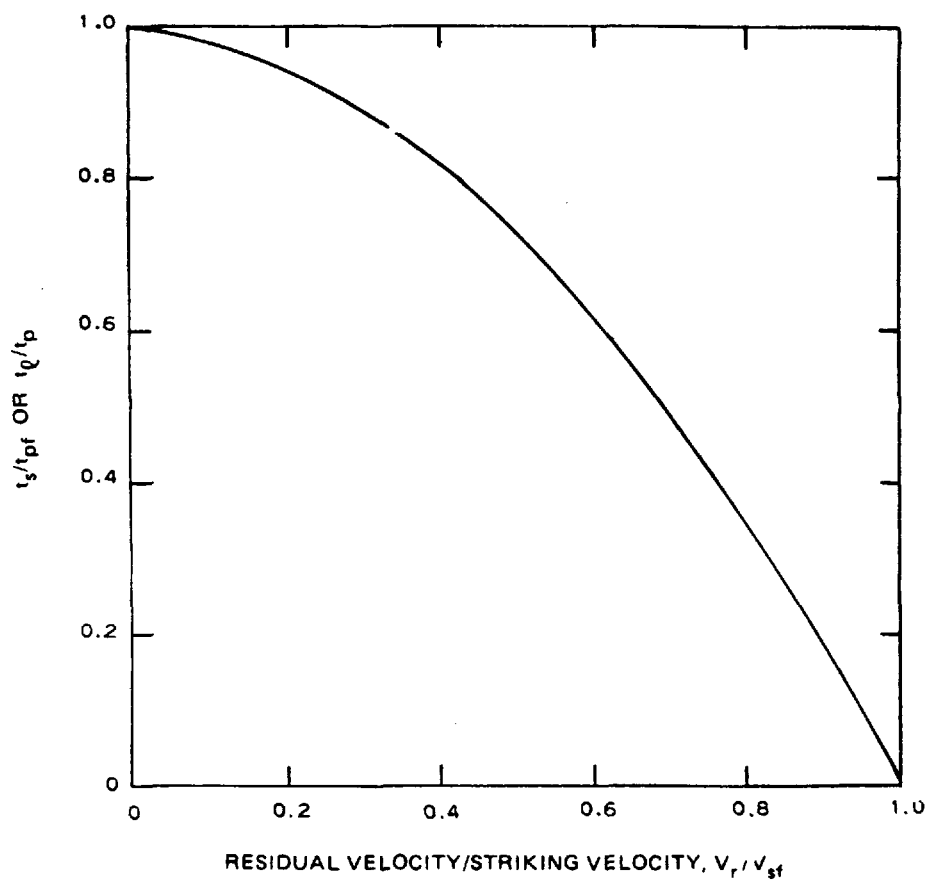
US Army Corps of Engineers

Figure 6-14. Residual fragment velocity upon perforation of concrete barriers for cases where $X \geq 1.4 \ W_f^{1/3}$ and for sand barriers.

d. Penetration of wood. The thickness of wood perforated by fragments of the shape given in paragraph 6–2c. and with normal impact conditions is given by

$$t_p = \frac{1{,}990\, V_s^{0.41}\, W_f^{0.59}}{\rho H^{0.54}} \qquad \text{(eq 6-18)}$$

where

t_p = perforation thickness, in.

V_{sf} = striking velocity, 10^3 fps

W_f = fragment weight, oz

ρ = wood density, pcf, table 6-3

H = wood hardness, lb, table 6-3

If the thickness of wood is less than or equal to t_p, then the fragment will perforate it. The residual velocity after perforation is given by

$$V_r = V_{sf}\left[1 - \left(\frac{t_\ell}{t_p}\right)^{0.5735}\right] \qquad \text{(eq 6-19)}$$

where

V_r = residual velocity, 10^3 fps

t_ℓ = actual thickness of wood, in.

Equation 6-18 is plotted in figure 6-15 for dry fir plywood and equation 6-19 is plotted in figure 6-16.

Table 6-3. Density and hardness of wood targets

Type of Wood	Sample Density pcf	Hardness, lb
Pine, dry	22–25	38.7
Pine, wet	30	51.1
Maple, dry	35	76.9
Maple, wet	40	72.0
Green oak, dry	51–59	88.1
Green oak, wet		72.1
Marine plywood, dry	37	68.9
Marine plywood, wet		58.8
Balsa, dry	6	21.0
Balsa, wet	6	61.5
Fir plywood, dry	30	75.0
Fir plywood, wet		68.9
Corrisa	27	
Hickory, dry	50	74.3
Hickory, wet	55	63.5

2456

6–22

6–23
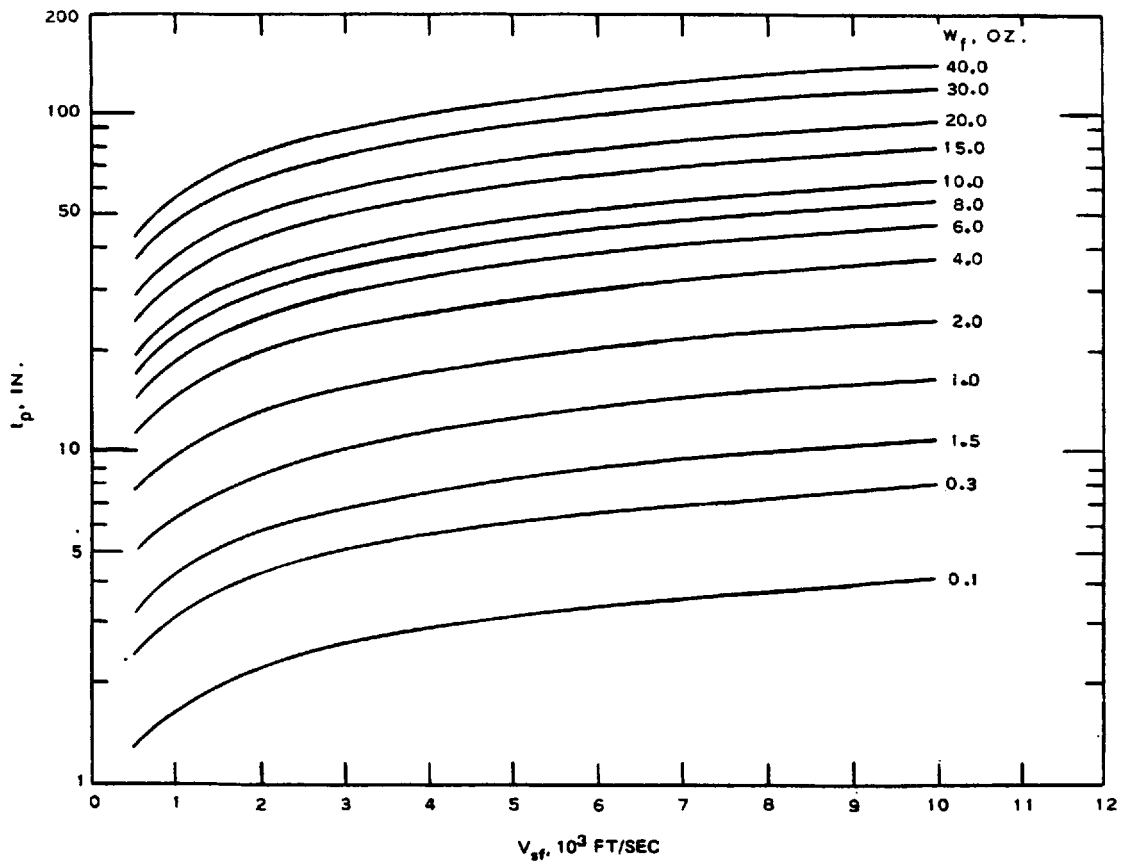
US Army Corps of Engineers

Figure 6-15. Penetration of dry fir plywood (p = 30 pcf, H = 75 lb).
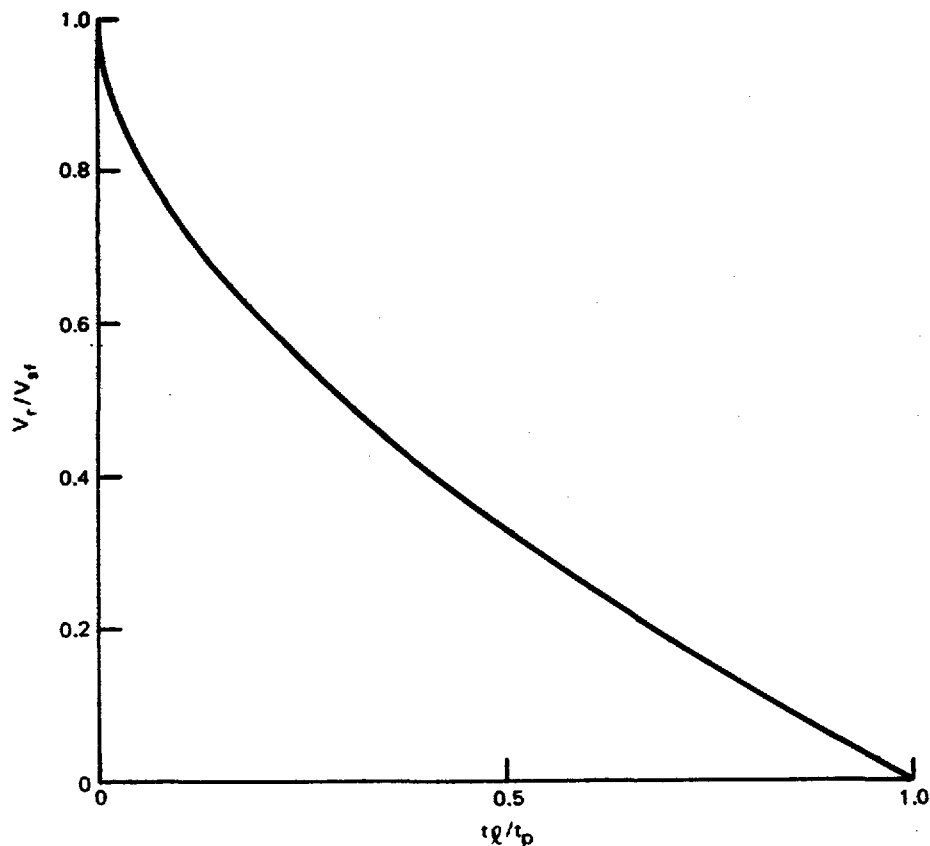
US Army Corps of Engineers

Figure 6-16. Residual velocity after perforation of wood.

e. *Penetration of soil.* The penetration into soil by fragments with the design shape given in figure 6–6 and with normal impact conditions is given by

$$t_p = 1.975 \ W_f^{1/3} \ K_p \ \log_{10} \ (1 + 4.65 \ V_{sf}^2) \qquad \text{(eq 6-20)}$$

where

t_p = thickness perforated, in.

W_f = fragment weight, oz

K_p = soil penetration constant, table 6–4

V_{sf} = striking velocity, 10^3 fps

2458

6–24

The residual velocity of fragments perforating thicknesses less than t_p is given by

$$V_r = V_{sf} \left(1 - \frac{t_\ell}{t_p} \right)^{0.555}$$

where

V_r = residual velocity, 10^3 fps

t_ℓ = actual thickness of soil, in.

This equation is plotted in figure 6–14 for sand.

Table 6–4. Soil penetration constant

Soil Type	Kp (in./oz1/3)
Limestone	0.775
Sandy soil	5.29
Soil containing vegetation	6.95
Clay soil	10.6
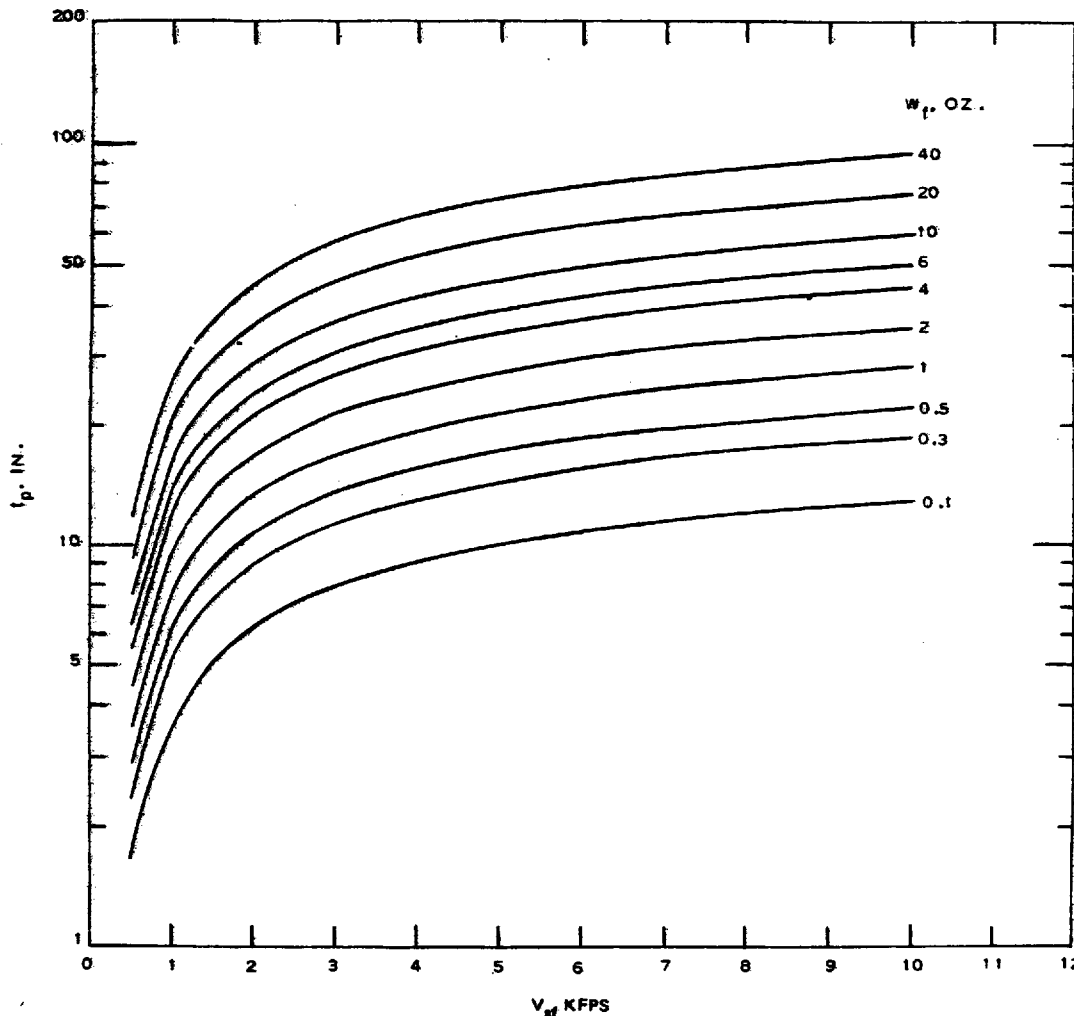
Figure 6-17. Penetration of sand (KP = 5.29).

US Army Corps of Engineers

f. Penetration of composite barriers. The design and analysis of composite barriers is based on the fairly accurate, if not conservative, assumption that there is no interaction between the various materials in the composite so that each materials penetration resistance is not affected by the other materials presence in the composite. This means that one can trace the path of the fragment through each successive layer, calculating whether or not it perforates that layer and if it does, using the appropriate residual velocity equation to obtain a striking velocity for the next layer. Of course, if the fragment comes to rest in any layer, the wall or barrier has successfully defeated perforation. However, if the last layer is concrete and if the fragment enters this layer, the possibility of spalling should be considered by using equation 6–15.

2460

6-36

CHAPTER 7

FIRE, INCENDIARY, AND CHEMICAL AGENTS

7-1. Fire and incendiary phenomena

a. Fire.

(1) Fire generated from flamethrowers generally is used in the assault of fortified positions and in routing defending troops from trenches or caves. Flamethrowers are employed for destructive effect against fortified positions of combustible materials and for neutralizing steel and concrete emplacements. Defenders of a fortification are forced to close embrasures and other openings when the position is attacked by flamethrowers, thus neutralizing the firepower and enabling the assault forces to approach and destroy the position. The intense heat generated by the flaming jet and the ability of the fuel to flow in through openings or cracks causes a fortification to become uninhabitable as a result of a successful attack. Flamethrowers mounted on tanks have proven to be particularly effective. The portable type is adaptable for attacking inaccessible positions.

(2) Flamethrowers installed with multiple jets and provided with centralized control are effective in defense against mobile flamethrowers as well as against assault forces. Experiments have been conducted using water vapor jets or a vapor curtain over pillbox embrasures with no success against flamethrowers.

b. Incendiary bombs. Incendiary bombs are referred to as any missiles containing incendiary or inflammable materials which are dropped by aircraft. These include standard types of incendiary bombs as well as prepared and improvised containers carrying gasoline, napalm, and other materials.

(1) In general, the smaller types of incendiary bombs are the most commonly used against built–up areas. More bombs can be carried and a wider distribution may thus be achieved. Many small fires can be started which will spread before effective fire–fighting equipment can be directed on the area. In covering a large area by incendiary attack, fire–fighting units can be cut off and trapped while attempting to approach the focal point of incendiary fires.

(2) Small and heavily defended areas may be attacked by large incendiary bombs in order to start large fires and to inflict physical damage. The liquid incendiaries are effective in flowing into crevices and underground works. The penetration of incendiary bombs is negligible compared to that of HE bombs.

c. Incendiary projectiles. Incendiary projectiles are used principally for penetrating a resistant target and igniting its contents. They are particularly effective for use by aircraft in attacking enemy aircraft and in strafing ground targets. Fuel supplies and storage tanks, motor transport, and grounded aircraft are vulnerable to the effects of incendiary projectiles. Such projectiles are predominant in smaller calibers, although HE projectiles in larger calibers have some incendiary characteristics.

7-2. Toxic chemical agents.

Toxic chemical agents are primarily designed for use against personnel. They do not destroy materials, supplies, installations, and structures, but may make them unusable for varying lengths of time because of absorption or adsorption of the chemical contaminant. Some agents have a corrosive effect on specific materials. The duration of effectiveness of a chemical agent depends on whether it is disseminated as a vapor or liquid, the volatility of the agent, weather conditions in the target area, and the type of target. Weather, of course, influences chemical agents in vapor form more than it does those in liquid form. In general, V-type nerve agents do not evaporate rapidly or freeze at very low temperatures. Liquid mustard or lewisite evaporates slowly at normal

temperatures; consequently, it remains effective for a considerable time after application. Almost any material, except bright metal and glass, absorbs some mustard and retains it tenaciously. Although toxic chemical agents do not destroy many types of materials, they do present a continuing hazard to personnel working in or around them because of the vapors or gases that are desorbed from the items, in addition to the contact hazard if the material is touched. Logistic problems are involved if decontamination procedures are initiated. Decontamination procedures are generally rather time-consuming and divert personnel from their primary mission.

7-3. Target response

a. *Structures.* Since the vapor of all toxic chemical agents is heavier than air, it has a natural tendency to penetrate to the remotest corners of a structure. For this reason it is of major importance that a nuclear, biological, and chemical (NBC) collective protection structure be sealed effectively against the penetration of vapors and aerosols. It is also essential that air pressure be maintained within ventilated NBC collective protection structures to restrict further penetration of the agent during chemical attacks. The elimination of drafts and the prevention of agent seepage are therefore basic considerations in keeping toxic vapors out of the protected space.

(1) Persons entering a shelter during a chemical agent attack always bring in vapor/liquid agent on their shoes and clothing. This is especially dangerous in the case of mustard since an effective concentration entirely imperceptible to the occupants may be gradually built up. Some vapor is also carried into the air locks upon entrance or exit of personnel. Although contaminated air is cleared from the entrance air locks by ventilation, unless sufficient time is allowed for the air locks to clear between entrances of personnel, contaminated air will enter the protected space. After a chemical attack, a contaminated shelter may be cleared of light concentration of the agent by opening the doors and building a fire inside.

(2) Generally, if liquid blister agents have been carried into structures by shell fire, the buildings must be abandoned for military use in the field. Prolonged concentration of a persistent agent within a structure results from a combination of high absorption and adsorption characteristics with relatively low volatility. However, important installations or buildings can be decontaminated with slurry, a mixture of 50-percent chloride of lime and 50-percent water by weight. Concrete and wood floors readily absorb mustard and may be decontaminated by covering them with a freshly prepared slurry and leaving it on the floors for at least 24 hours. The slurry is then removed by scrubbing with hot soapy water. If walls and ceilings are not too heavily contaminated, the mustard may be neutralized by spraying or swabbing with slurry. A building contaminated with lewisite can be decontaminated with water, preferably sprayed from a high-pressure nozzle. The resulting compound is an arsenic poison and must be washed away. A mixture of mustard and lewisite may be decontaminated with slurry.

(3) Since most chemical agents are highly corrosive (a characteristic which usually is accompanied by high absorption) instruments and equipment are affected seriously by the agent. Material of this type which has been contaminated with blister agents may be decontaminated by using a noncorrosive decontamination agent applied with a swab. Greasy or oily metal surfaces contaminated with mustard or lewisite should first be cleaned with kerosene or gasoline. These solvents do not destroy mustard but dissolve it, so that most of it may be removed. The thin coating of mustard which remains is then destroyed by spraying with a noncorrosive decontamination agent or steam followed by washing with hot soapy water, drying, and following with an application of light oil.

b. *Ammunition.* As a rule, ammunition is stored if possible in single-purpose magazines with reinforced ends and walls. The penetration of incendiary bombs is negligible compared to that of HE bombs. However, incendiary projectiles may penetrate an ammunition storage magazine and initiate sympathetic detonations of stored rounds. Ammunition should be kept in sealed containers in either open or closed storage. Corrosion is likely to occur, particularly on brass parts, if ammunition is contaminated with chemical agents. Ammunition contaminated with liquid mustard or V-type nerve agent should be decontaminated with DS2, and wiped with a gasoline-soaked rag. DS2 or warm soapy water will decontaminate G-type nerve agents. Contaminated ammunition containers may also be decontaminated with DS2, a standard US Army decontamination solution.

c. *Aircraft on the ground.* The relatively thin–skin structure of aircraft is vulnerable to incendiary bombs and projectiles, particularly metal incendiaries that are filled with thermate or thermite. At an airfield, an undamaged plane may be contaminated by toxic chemical agents only

on its exterior surface, provided the plane is closed and the engines are not running. If aircraft are lightly contaminated by spray, they may be decontaminated by aeration. Flying aircraft is one method of aeration of the outer surfaces. A regular fire hose, equipped with fog or spray nozzles, may be used to wash down contaminated aircraft with water. If these special nozzles are not available, the water pressure must be reduced so that the planes are not damaged. Soap or other detergent should be added to the water because it will help to remove contamination that is also attached to greasy or oily surfaces. It may be possible to decontaminate aircraft more completely by using a steam–jet apparatus with a detergent. As an alternative method, the aircraft may be flushed merely with water to physically remove the contamination. The decontamination site then must also be decontaminated. Interior parts of an aircraft should be decontaminated. Interior parts of an aircraft should be decontaminated with hot soapy water and then rinsed with water. Thorough decontamination may be necessary for an aircraft part that must be repaired or replaced in order to provide adequate protection for maintenance personnel. After the external or internal portions of an aircraft have been decontaminated, they should be checked with appropriate detection equipment for adequacy of decontamination.

d. Petroleum, Oil, and Lubricants (POL) facilities. POL facilities consist of tank farms which contain POL stored primarily in bulk. Additional equipment includes large collapsible tanks, rail tank cars, and tank trucks. In many instances large quantities of POL are stored in special structures as described in TM 5–302–1 and TM 5–302–2. A direct hit of incendiary projectiles on exposed metal structures such as those indicated above will, in all probability, penetrate the metal surfaces and ignite the POL mixture. Rail tank cars and tank trucks that are contaminated with liquid chemical agents should only be decontaminated to the extend necessary to safely operate them; that is, decontaminate only those parts that must be touched unless there is gross contamination which may be transferred to clean areas when the fuel is supplied to customers. The decontamination agent DS2 is used for small surface–area decontamination, while slurry should be used if large–scale decontamination is feasible.

e. Enclosed shelters. A pressurized shelter offers complete protection against chemical agents for personnel without masks. Generally, this protection is provided only for special groups, including command and communication personnel and certain emergency recovery teams. Mask–type shelters require that personnel wear masks for protection against chemical agents. Whether a ventilated or unventilated protective shelter is constructed, it is most important that a standard operating procedure be prepared to prevent compromise of the protection of the shelter. TM 3–221 offers guidance to personnel who are responsible for providing field shelters protection against chemical agents.

7-4. Design considerations

a. Flame–type agents. The designer of fortifications must plan all openings so that they provide a positive, armored enclosure which will not permit operation or ready destruction from the exterior. As the greatest hazard to fortified positions from flamethrowers is the entering of burning fuel through embrasure openings, defensive measures should incorporate barbed wire, antitank and antipersonnel mines, and other obstacles in addition to the structural measures.

b. Incendiary weapons. Care must be taken when designing fortification works to locate ventilation shafts and other openings where they will be least vulnerable to attack by incendiary bombs or other incendiary agents. Sumps near entrances or embrasures should be avoided. Buildings of wood construction are inherently vulnerable to all types of weapons, especially to incendiary weapons. Protection against incendiary projectiles is similar to protection against penetration of other projectiles of the same caliber, except that inflammable materials should not be used when they would be exposed to shelling or strafing. Treatment of interior surfaces of fortifications may incorporate fire–resistant materials to the maximum extent consistent with other requirements for such treatments, such as shock and sound treatments. Ammunition storage sites should be designed and constructed as outlined in TM 9–1300–206. The TM 5–302 series describes the characteristics of specially designed structures for storage of bulk petroleum. The vulnerability of aircraft to incendiary weapons can be reduced by dispersion.

c. Toxic chemical agents. Full protection against toxic chemical agents should be provided for command and emergency operations teams. Full protection means that the air will be filtered and masks need not be worn in shelters. The use of wood frame or loosely constructed mortar, brick, or tile buildings requires excessive labor to provide chemical protection and should be avoided. Structures considered suitable for the integration of chemical protection include interior portions of

TM 5-855-1

permanent—type structures such as public buildings, factories, hospitals, and dwellings. Detailed criteria for the construction of collective protection shelters are contained in TM 3–221. Coverings should be used to the fullest possible extend in protecting items such as ammunition or even aircraft stored in the open when there is a high probability that liquid chemical agents may be employed. Plastic types of coverings can be destroyed if they become contaminated.

7-5. References

For more detailed information concerning the effects of fire, incendiary, and chemical agents on structures, selected types of facilities, ammunition, and aircraft, as well as methods of decontamination, consult the Bibliography.

2464

7-4

CHAPTER 8

LOADS ON STRUCTURES

8-1. Introduction

a. The nonuniform highly transient loads produced by the nearby detonation of a conventional weapon, combined with the localized structural response, result in an extremely complex structural analysis problem. The assumptions necessary in developing a simplified analysis procedure usually lead to overly conservative design because they fail to accurately account for the localized nature of the structural response, the large variation of pressure over a relatively small area, and the fact that the pressure does not arrive at every point on the structure at the same time.

b. In this manual, procedures are outlined for determining the average load-time history for a section of a building. These procedures make conservative assumptions about the distribution of pressures across the element and the time phasing of the load. The portion of the building which is chosen for analysis can be extremely important. Normally, walls are analyzed as one-way slabs. The area of slab responding is a function of the standoff distance and the structural geometry. This factor is not considered.

c. Compressive membrane forces generated in the responding structural element can cause significant increases in the strength of that element. No simplified method is available to determine the magnitude of this effect; therefore, this factor is neglected in this manual.

d. If these factors are not considered in the analysis, it is recommended that the loads be divided by 1.5 before the structure is designed. Based on a large number of tests this method will provide a conservative design.

8-2. Buried structures

The type of analysis to be performed for weapons effects depends on the position of the weapon at detonation. The weapon may detonate away from the structure, near the structure, or in contact with the structure. Weapon loads for detonations away from the structure are presented in this section. A near-structure detonation is one that occurs at a scaled range, λ , of less than 1.0. λ is the range (feet) divided by the cube root of the weapon yield (pounds). When a weapon detonates near a structure, failure is likely to be a highly localized breaching. Analyses for breaching are mostly of interest for vulnerability studies and will not be presented in this manual. Methods for sizing members for contact bursts are presented in paragraph 5-2.

a. Free-field pressures. Free-field pressures as a function of distance from the explosion of a conventional weapon were given in chapter 5. If a structure is placed in the free field, these pressures are amplified by reflection. The amount and duration of the amplification depend on the properties and geometries of the soil, structure, and explosives. Recent test data indicate that an average reflection factor of 0.5 is reasonable. Therefore, the total reflected pressure is 1.5 times the incident pressure. The duration of the reflected pulse is a function of either the thickness of the structural element or the distance to the nearest edge of the structure. The smaller of the two numbers should be used in analysis. Experiments on buried structures have shown that the reflected pressure decays in a time equal to approximately six transit times through the reinforced concrete slab. If the reflected pressure is relieved by a tension wave from the free edge, the duration of the reflected pulse is approximately the arrival time at the free edge minus the arrival time at the point under consideration plus the travel time from the free edge to that point. The arrival times are computed using the loading wave velocity in the soil and the travel time is computed using twice the loading wave velocity.

TM 5-855-1

b. Loads on roof. The loads on the roofs of underground structures are not uniform, especially if the depth of burial is shallow. However, uniform loads are needed for the single-degree-of-freedom analysis. Figure 8-1 can be used to obtain an equivalent uniform load. Equivalent uniform loads were obtained by performing a series of static finite-element analyses. These calculations were performed for slabs with various rations A/B of short span to long span.
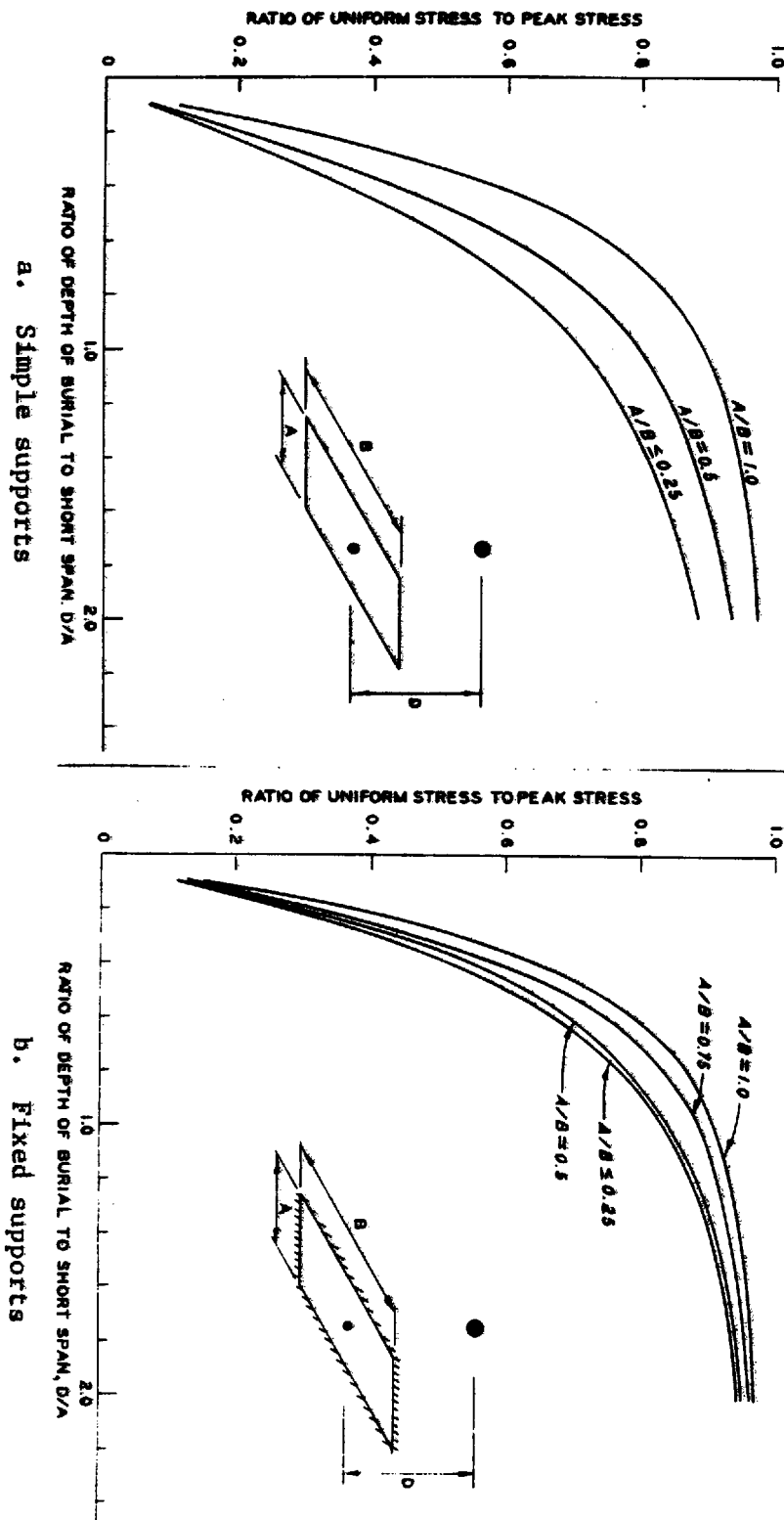
Figure 8-1. Equivalent uniform load in flexure.

2466

8-2

(1) For an explosion originating at a point in a soil medium, the pressure at a given distance is approximately proportional to the inverse of the cube of the distance from the explosion. Equation 8-1 was used to describe such a pressure distribution in the finite element analyses. When a flexural response is expected, the equivalent uniform load is one that will produce the same midpoint deflection as the distributed load given in equation 8-1.

$$P_R = P_{or} (D/R_S)^3 \qquad \text{(eq 8-1)}$$

where

P_R =   pressure on roof at a distance R_S away from weapon

P_{or} =   pressure on the roof directly below the weapon

D =   depth from weapon to roof

R_S =   slant distance from weapon

Equivalent uniform loads in flexure were found for both simply supported and fixed boundary conditions. If the boundary conditions are not known, the fixed boundary conditions should be used since they are more conservative. In order to use this curve the ratio D/A of depth from weapon to roof to the short span of the roof slab is calculated and the appropriate curve is selected according to the A/B ratio.

(2) The duration of the pressure pulse varies with location on the roof slab, and an average value must be used. The worst case loading for a roof slab is when the bomb is directly above the center of the roof. It is recommended that the duration of the equivalent roof pressure be taken equal to the duration of the free-field pressure pulse at the quarter point of the short span along a section at the center of the long span. An equivalent triangular duration for the free-field pulse may be calculated using the equations for free-field impulse and peak pressure as given in chapter 5.

c. *Loads on walls.* The loads on interior walls are the reactions to roof loads and will be discussed in another chapter. Exterior walls must be designed for the case where a bomb detonates at some distance D away from the side of the structure. This procedure is similar to computing an equivalent load for the roof of the structure.

8-3. Aboveground structures

For any given set of free-field incident and dynamic pressure pulses, the forces imparted to an aboveground structure can be divided into three general components:

• the force resulting from the incident pressure,
• the force resulting from the dynamic pressure, and
• the reflected pressure resulting from the shock impinging upon an interfering surface.

The relative significance of each of these components is dependent upon the geometrical configuration and size of the structure and the orientation of the structure to the shock wave. The interaction of the incident blast wave with an object is a complicated process. To reduce the complex problem of blast to reasonable terms, it will be assumed here that (a) the structure is generally rectangular in shape, and (b) the object being loaded is in the region of the Mach reflection.

a. *Front wall.* For a rectangular aboveground structure at low pressure ranges, the variation of pressure with time on the side facing the detonation is illustrated in figure 8-2. At the moment the incident shock front strikes the wall, the pressure is immediately raised from zero to the reflected pressure P_r which is a function of the incident pressure and the angle of incidence between the shock front and the structure face (fig 3-4). The clearing time t_c required to relieve the reflected pressures is represented as

$$t_c = \frac{3S}{U} \qquad \text{(eq 8-2)}$$

where U is the velocity of the shock front and S is equal to the height of the structure H_s, or one-half its width W_s, whichever is smaller. The pressure P_{tc} acting on the front wall after time t_c is the algebraic sum of the incident pressure P_s and the drag pressure $C_D q$.

$$P_{tc} = P_s + C_D q \qquad \text{(eq 8-3)}$$

The drag coefficient C_D gives the relationship between the dynamic pressure q and the total translational pressure in the direction of the wind produced by the dynamic pressure and varies with the Mach number (or with the Reynold's number at low incident pressures) and the relative geometry of the structure. A value of $C_D = 1$ for the front wall is considered adequate for the pressure ranges considered in this manual.
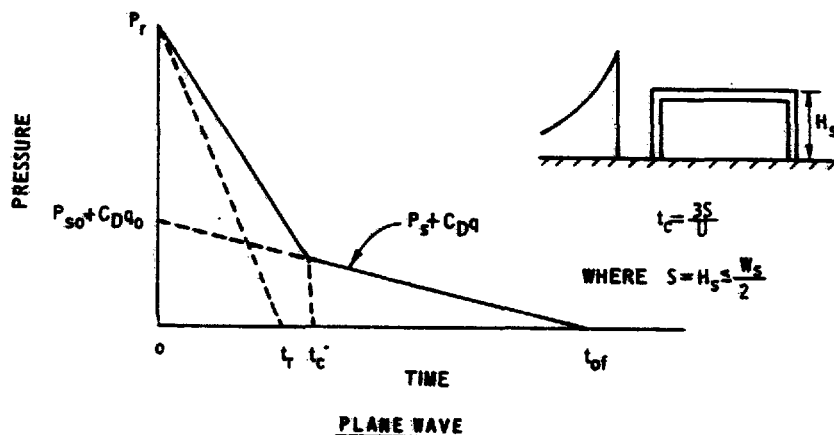
Figure 8-2. Front-wall loading.

US Army Corps of Engineers

(1) At higher pressure ranges, the above procedure may yield a fictitious pressure-time curve because of the extremely short pressure pulse durations involved. Therefore, the pressure-time curve construction must be checked to determine its accuracy. The comparison is made by constructing a second curve (dotted triangle as indicated in fig 8-2), using the total reflected pressure impulse i_r from either figure 3-4 or 3-7 depending upon the shock environment. The fictitious duration t_r of the reflected wave is calculated from

$$t_r = \frac{2 i_r}{P_r} \qquad \text{(eq 8-4)}$$

where P_r is the peak reflected pressure previously used. Whichever curve gives the smallest value of the impulse (area under curve), use that curve in calculating the wall loading. The reflected pressure impulse includes the effects of both the incident and dynamic pressures.

(2) The pressure-time curve (fig 8-2) is based on the assumption that the shock front of the blast wave is essentially parallel to the front surface of the structure (plane wave shock front); the height of the triple point of the shock wave in an airburst shock environment is assumed to be above the top of the wall.

(3) In those cases where the detonation is located relatively close to the structure, the pressure and impulse acting across the wall surface will vary. In these cases, an average pressure-time curve may be constructed over a length of the structure equal to 1.3 times the normal distance between the detonation and the front face of the structure but not greater than 2S. The average pressure and impulse should be determined at midheight of the front face wall.

b. Roof and side walls. As the shock front traverses a structure, a pressure is imparted to the roof slab and side walls equal to the incident pressure at a given time at any specified point reduced by a negative drag pressure. The portion of the surface loaded at a particular time is dependent upon the location of the shock front and the wave lengths (L_W and L_W) of the positive and negative pulses.

(1) To determine accurately the overall loading on a surface where the span direction is perpendicular to the shock front, a step-by-step analysis of the wave propagation should be made. This analysis would include a simultaneous dynamic analysis of the stresses produced in the element at any given time. To simplify this procedure, an approximate method of calculating the pressure-time history has been developed where the actual loading on the surface has been replaced by an equivalent uniform loading which will produce stresses in the element similar to those produced by the actual loading as the blast wave crosses the surface. For this analysis to be valid for reinforced concrete structures, it is assumed that the reinforcement on both faces is continuous across the span length.

(2) The peak value of the incident pressure decays and the wave length increases as the shock wave traverses the roof. As illustrated in figure 8-3, the maximum stress in the member occurs when the shock front is at point d , although the point of maximum stress is located elsewhere. The equivalent uniform loading versus time is shown in figure 8-3 and, to simplify the calculations, has been taken as a function of the blast wave parameters at point b , the back end of the element being considered. The equivalent load factor C_E and the blast wave location ratio D/L are obtained from figure 8-4 as a function of the wave length-span ratio L_{wb}/L . The pressure builds up linearly from the time t_f when the blast wave reaches the beginning of the element (point f) to the time $t_d + t_f$ when the blast wave reaches point d . The peak value P_{or} of the pressure is the sum of the contributions of the equivalent incident and drag pressures.

$$P_{or} = C_E P_{sob} + C_D q_o \qquad \text{(eq 8-5)}$$

where

P_{sob} = peak overpressure occurring at point b

q_{ob} = value of $C_E P_{sob}$

Following the peak, the pressure decays linearly to zero at time $t_b + t_{of}$ where t_b is the time at which the blast wave reaches the end of the element (point b) and t_{of} is the fictitious duration of the positive phase. The negative phase of the equivalent uniform loading, if required, may conservatively be taken as that occurring at point b. The drag coefficient C_D for the roof and side walls is a function of the peak dynamic pressures. Recommended values of the drag coefficient are as follows:

Peak Dynamic Pressure psi	Drag Coefficient
0–25	- 0.40
25–50	- 0.30
50–130	- 0.20
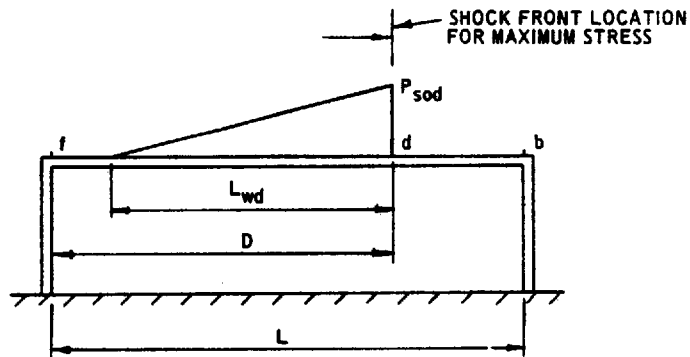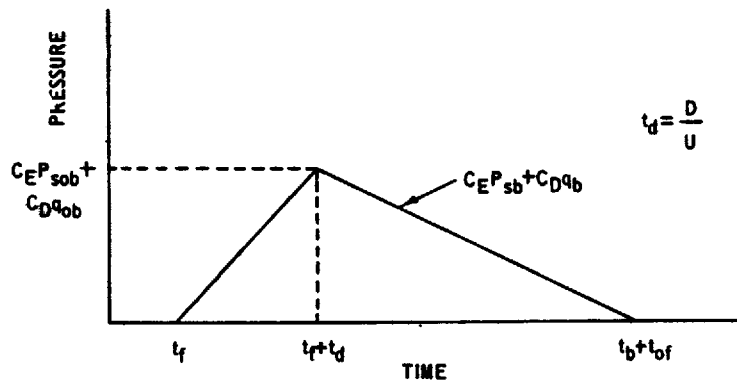
Figure 8-3. Roof and side-wall loading (span direction perpendicular to shock front).

EQUIVALENT LOAD FACTOR $C_E = \dfrac{P_{so}}{P_{sob}}$ AND

BLAST WAVE LOCATION RATIO $\dfrac{D}{L}$
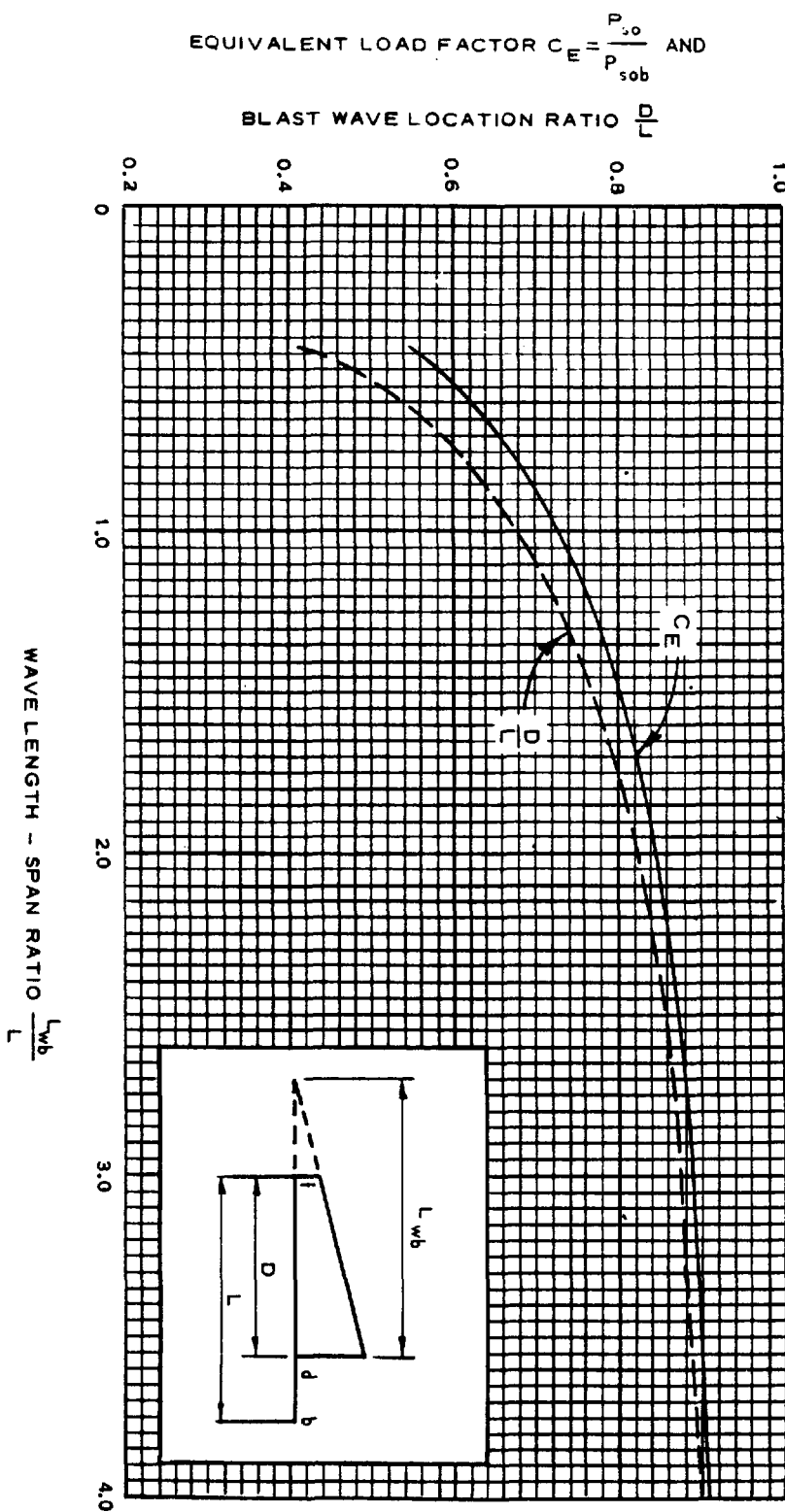
Figure 8-4. *Equivalent load factor and blast wave location ratio versus wave length-span ratio.*

(3) If the span direction of the member is parallel to the shock front, the pressure-time curve shown in figure 8-5 should be used where L is the width of the strip or element being considered.
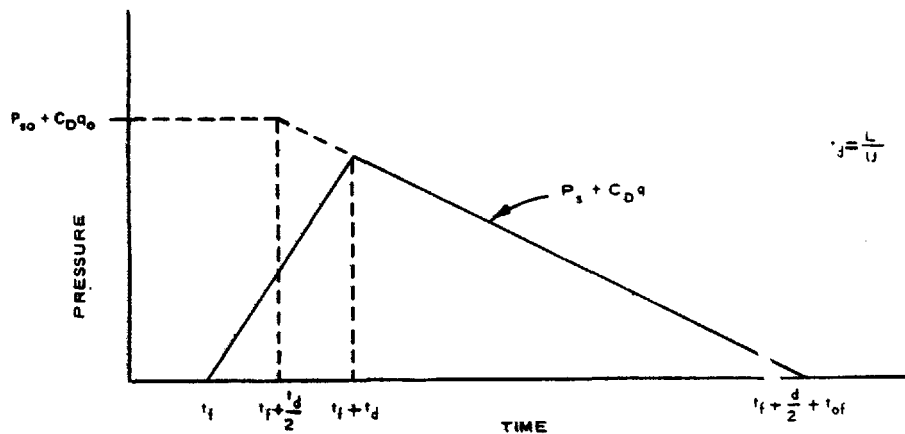
US Army Corps of Engineers

Figure 8-5. Roof and side-wall loading (span direction parallel to shock front).

c. *Rear wall.* As the shock front moves past the rear edges of the roof and/or side walls, the pressure front will expand, forming secondary waves which propagate over the rear wall. In the case of long buildings, this secondary wave enveloping the back wall essentially results from the spillover from the roof, while in short buildings the wall loads arise from the interaction of the spillover both from the roof and the side walls. In both cases, the secondary waves are reinforced due to their impingement with reflecting surfaces. The reinforcement of the spillover wave from the roof is produced by its reflection from the ground surface at the base of the rear wall, whereas the reinforcement of the secondary waves from the side walls is produced by their collision near the center of the wall and/or their interaction with the wave from the roof. Little information is presently available on the overall effects on the rear-wall loading produced by the reflections of the secondary waves.

(1) In most design cases, the primary reason for determining the blast loads acting on the rear wall is to obtain the overall drag effects (both front and rear wall loadings) on the building. For this purpose, a procedure may be used where the blast loading on the wall is calculated using the equivalent uniform method utilized for computing the blast loads on the roof and side walls. Here the peak pressure of the pressure-time curve (b, fig 8-6) is calculated using the peak pressure that would occur at distance H_S (point e on a, fig 8-6) past the rear edge of the roof slab. The equivalent load factor C_E is based on the wave length of the peak pressure above the unsupported length of the rear wall as are the time of rise and the duration.

2472

8—8
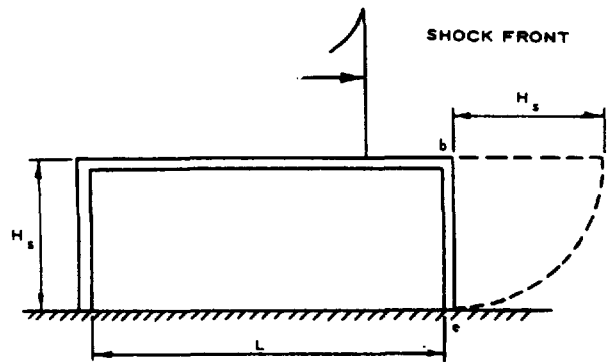
a. SECTION THROUGH STRUCTURE
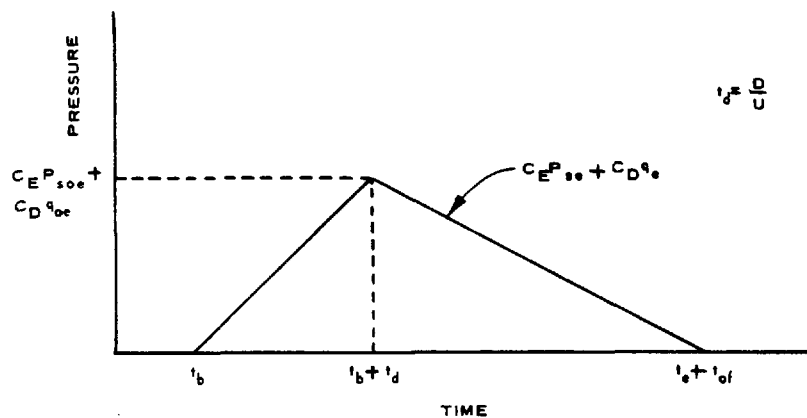
b. AVERAGE PRESSURE — TIME VARIATION

US Army Corps of Engineers

Figure 8-6. Rear-wall loading.

(2) Like the roof and side walls, the blast loads acting on the rear wall are a function of the drag pressures in addition to the incident pressures. The dynamic pressure of the drag corresponds to that associated with the equivalent pressure, while the recommended drag coefficients are the same as used for the roof and side walls.

8-4. Mounded structures

Mounded structures are essentially aboveground structures with an earth covering; however, they are not subject to failure from the airblast of conventional weapons. Mounded structures should be checked for penetration and cratering from direct hits if the design threat includes direct hits.

8-5. Surface-flush structures

Surface-flush structures must be designed to withstand both airblast and ground shock loadings. The roof must be designed to withstand the airblast pressures as described in paragraph 8-3. Also, if the threat includes a direct hit, the roof thickness will be determined by penetration and cratering considerations. The walls and floor must be designed to withstand ground shock as well as the reaction to the airblast loading on the roof.

CHAPTER 9

MECHANICS OF STRUCTURAL ELEMENTS

9-1. Introduction

a. A structure, under the application of external loads, will be deformed, and internal forces will be set up in its members. These internal forces resist the deformation of the structure (movement of its mass) and are defined as the resistance of the structure. For stable structures, as the external loads increase, the deformation increases, and the resistance with displacement is defined as the resistance function of the structure.

b. To satisfy the laws of equilibrium, the vector sum of the external and internal forces acting on a free body must equal zero. The resistance of a structure in equilibrium, therefore, must equal the applied loads. Hence, the resistance function of a structure is numerically equal to the load–deformation function of the structure. The importance of the concept of a structure's resistance to deformation becomes apparent when the structural response (deformation) to dynamically applied loads is discussed.

c. In the design of blast–resistant construction, it is appropriate to employ every material–saving technique available. Depending on the functional requirement of the structure, the material may be strained well into the inelastic range at the critical points. Ultimate strength design concepts are presented so that a preliminary design of structural elements can be undertaken using conventional static load design procedures.

9-2. Properties of steel

Most of the properties of structural grade and reinforcing steel are well known and will not be presented here. However, since the dynamic properties of steel are not so well known and may be important, they are presented. The yield strength of structural steel may be greatly dependent on the strain rate. As the strain rate increases, the yield strength increases, while the modulus of elasticity remains constant.

a. A time to yield of about 1 second is representative of static yield strength. Many classes of structural elements will have time to yield in the range of 0.01 to 0.1 second. For these ranges of time there is an average increase in yield strength, due to strain–rate effects, of about 10 percent. Therefore, it is recommended that a dynamic yield strength 10 percent greater than the static yield strength be used. For high–strength steels without definite yield points, it is recommended that dynamic yield strengths be taken equal to the static values. The dynamic shear yield strength is taken equal to 0.6 times the dynamic strength.

b. Repeated loads on steel structures are generally not a problem and there is some evidence of increased resistance to deformation after the first cycle of loading.

9-3. Properties of concrete

Most of the important properties of concrete are readily available in any concrete design book. One equation which may be useful is the following empirical relationship:

$$E_c = 33W_c^{1.5} \sqrt{f'_c} \qquad \text{(eq 9-1)}$$

where

E_c = modulus of elasticity of concrete, psi

W_c = weight of concrete, pcf

f'_c = compressive strength of concrete, psi

TM 5-855-1

For normal-weight concrete this becomes

$$E_c = 57,000 \sqrt{f'_c} \text{ psi} \qquad \text{(eq 9-2)}$$

a. As was the case with steel structures, the strength of concrete may be increased due to strain rate effects. If no strain rate analyses are to be performed, a 20-percent increase in strength should be used. Strain rate effects should not be considered in checking shear.

b. A small number of load cycles which exceed the elastic limit of the concrete may cause significant change in its resistance. Although no general guidance is possible as to the magnitude of the effect, the designer should be aware that some degradation of resistance can occur under repeated cycles of loading.

9-4. Steel beams

a. *Introduction.* The design or analysis of a structural steel member is generally based upon the inelastic behavior of the member. For steel, the design procedure is referred to as plastic design. Plastic design not only makes use of the plastic theory of bending but also the redistribution of moment due to the formation of plastic hinges. In designing or analyzing the ability of steel members to resist blast effects, many of the concepts and equations developed for the plastic analysis of steel structures under static loads are used. Therefore, an understanding of the conditions and equations governing static behavior is essential.

b. *Flexural strength of structural steel.* Plastic design in structural steel is a standard procedure for protective construction. The flexural strength of structural shapes is obtained from the expression

$$M_p = f_y \cdot Z_x \text{ or } f_y \cdot Z_y \qquad \text{(eq 9-3)}$$

where

M_p = plastic moment

f_y = yield strength of the steel

Z_x, Z_y = plastic section modulus with respect to the major and minor axes, respectively

For rectangular sections of width b and depth h

$$Z_x = \frac{bh^2}{4} = 1.5 \text{ times the elastic section modulus} \qquad \text{(eq 9-4)}$$

(1) For rolled sections, the plastic section modulus is 1.10 to 1.23 times the elastic section modulus. The AISC Manual of Steel Construction includes plastic design selection tables based on the plastic section moduli of rolled sections. The plastic section modulus is the summation of static moments of the tension and compression areas of the structural member about the neutral axis.

(2) An important consideration in the evaluation of the plastic flexural strength of structural steel elements is the lateral support of the beam's compression flange. The compression flange should not buckle before reaching the flexural strength of the beam. This and other restrictions, such as the width/thickness ratio of the projecting elements of the compression flange and the depth/thickness ratio of the web, have led to semiempirical formulas that are specified by the AISC Manual. Design procedures should generally comply with these guidelines in order to preclude premature failure of structural shapes. Equivalent length coefficients for laterally unsupported beams are given in figure 9-1.

c. *Combined flexural and axial loads on structural steel.* In structures subjected to lateral loads imposed by a blast, the columns will be subjected to bending moments as well as axial loads, and they should be treated as beam columns. The maximum allowable load for an axially loaded compression member for plastic design is given as

2475
$$P_{cr} = 1.7 Af_a \qquad \text{(eq 9-5)}$$

where

A = gross area of member

f_a = maximum allowable axial stress dependent on the slenderness ratio of the column

This relationship may also be used for dynamic loads. (AISC <u>Specifications for the Design, Fabrication, and Erection of Structural Steel for Buildings</u>).

(1) Most compression members are also subjected to bending moments and, therefore, act as beam columns. If axially loaded members are sufficiently braced against buckling, the applied moments and axial forces will cause the structural element to go into the plastic range. Insufficient lateral bracing and a large difference between bending stiffnesses about the principal axes will cause the structural element to bend out of the plane of the applied moments and twist at the same time. For columns with intermediate slenderness ratios, this type of buckling takes place when parts of the column have yielded. Recommended spacing of the bracing to avoid this instability is given in the AISC Manual by the following expressions for critical spacing:

$$L_{cr} = \left(\frac{1375}{f_y} + 25 \right) r_y \quad \text{when } + 1.0 > \frac{M}{M_p} > -0.5$$

(eq 9-6)

$$L_{cr} = \frac{1375 \, r_y}{f_y} \quad \text{when} \quad -0.5 \geq \frac{M}{M_p} > -1.0$$

In which

r_y = the radius of gyration of the member about its weak axis

M = the lesser of the moments at the ends of the unbraced segment

M/M_p = the end moment ratio (+ for reverse curvature, - for single curvature)

(2) Width–thickness ratio specifications for single–web shapes and built–up sections are contained in the AISC Manual. For either flange, b_f/t_f should not exceed the following values:

f_y	b_f/t_f
36	17.0
42	16.0
45	14.8
50	14.0
55	13.2
60	12.6
65	12.0

For webs of members subject to plastic bending, d/t_w should not exceed the value given by the following expressions:

$$\frac{d}{t_w} = \frac{412}{\sqrt{f_y}} \left(1 - 1.4 \frac{P_a}{P_y} \right) \quad \text{when} \quad \frac{P_a}{P_y} \leq 0.27$$

(eq 9-7)

$$\frac{d}{t_w} = \frac{257}{\sqrt{f_y}} \qquad \text{when} \qquad \frac{P_a}{P_y} > 0.27$$

(3) Members subject to combined axial load and bending moment should satisfy the following interaction formulas:

$$\frac{P_a}{P_{cr}} + \frac{C_m M_f}{\left(1 - \dfrac{P_a}{P_e}\right)M_m} \leq 1.0 \qquad \text{(eq 9-8)}$$

$$\frac{P_a}{P_y} + \frac{M_f}{1.18 M_p} \leq 1.0 ; \quad M_f \leq M_p \qquad \text{(eq 9-9)}$$

where

P_a = applied axial load

P_y = plastic axial load ($A f_y$)

d = depth of beam

C_m = coefficient applied to bending term

   = $0.6 - 0.4\, M_1 / M_2$, but not less than 0.4 for members in frames braced against sidesway; where M_1 / M_2 is the ratio of smaller to larger end moments (+ for reverse curvature, - for single curvature)

   = 0.85 for members in frames subject to sidesway

   = 0.85 for members in frames braced against sidesway, subjected to transverse loading between supports, and with ends restrained

   = 1.0 for members in frames braced against sidesway, subjected to transverse loading between supports, and with ends unrestrained

M_f = maximum applied moment

P_e = Euler buckling load

t_w = web thickness

$$P_e = \frac{A \pi^2 E_s}{(K_s l_b / r_b)^2}$$

K_s = effective length factor in the plane of bending

l_b = the actual unbraced length in the plane of bending

r_b = radius of gyration

M_m = maximum moment that can be resisted by the member in the absence of axial load

M_m = M_p (columns braced in the weak direction)

(eq 9-10)

$$M_m = \left[1.07 \frac{(L/r_y) \sqrt{f_y}}{3160} \right] M_p \leq M_p \quad \text{(columns unbraced in the weak direction)}$$

(4) In the plane of bending of columns which would develop a plastic hinge at ultimate loading, the slenderness ratio (KL / r) shall not exceed C_c

$$C_c = \sqrt{\frac{2\pi^2 E_s}{f_y}}$$

(eq 9-11)

The axial stress permitted on a compression member in the absence of bending moment is:

$$f_a = \frac{\left[1 - \frac{(KL/r)^2}{2 C_c^2} \right] f_y}{\frac{5}{3} + \frac{3(KL/r)}{8 C_c} - \frac{(KL/r)^3}{8 C_c^3}}$$

(eq 9-12)

where   K = effective length factor given in figure 9-1.

Values of f_a for various slenderness ratios may be obtained from tables in Appendix A of the AISC Manual.

	(a)	(b)	(c)	(d)	(e)	(f)
BUCKLED SHAPE OF COLUMN IS SHOWN BY DASHED LINE						
THEORETICAL K_s VALUE	0.5	0.7	1.0	1.0	2.0	2.0
RECOMMENDED DESIGN VALUE WHEN IDEAL CONDITIONS ARE APPROXIMATED	0.65	0.80	1.20	1.0	2.10*	2.0

END CONDITION CODE		
(rotation fixed symbol)	ROTATION FIXED	TRANSLATION FIXED
(rotation free symbol)	ROTATION FREE	TRANSLATION FIXED
(rotation fixed symbol)	ROTATION FIXED	TRANSLATION FREE
(rotation free symbol)	ROTATION FREE TRANSLATION FREE * TOP END ASSUMED TRULY ROTATION FREE	

US Army Corps of Engineers

Figure 9–1. Effective length factors for various end conditions.

d. Shear strength of structural steel. Shear influences the plastic moment capacity of the member. At rigid or continuous supports, where combined bending and shear exist, the initiation of shear yielding can reduce moment capacity. However, I–shaped beams carry moment predominantly through the flanges and shear through the web, and since combinations of high shear and high moment generally occur at points where the moment gradient is steep, it has been found experimentally that the plastic moment capacity is not appreciably reduced until shear yielding occurs over the full effective depth.

(1) The average stress at which an unreinforced web is fully yielded in pure shear is given by $f_y / \sqrt{3}$. The plastic bending strength of I–beams is maintained until shear yielding occurs over the full effective depth. The static shear strength at yield may be expressed by:

$$V_{up} = \frac{f_y h_e t_w}{\sqrt{3}} = 0.55 f_y h t_w \qquad \text{(eq 9-13)}$$

where

h_e = effective depth of web, distance between centroids of flanges 0.95 h (h is the full depth)

t_w = web thickness

(2) The effect of transverse shear forces is to reduce the full plastic moment. Denote the reduced plastic moment by M_{ps}. Theoretically, it is shown that

$$M_{ps} = M_p - \frac{9}{64} \left(\frac{V_s^2}{f_y} \right) \left(\frac{h_e^2}{Z} \right) \qquad \text{(eq 9-14)}$$

where

M_p = plastic moment

V_s = shear force corresponding to first yield in shear

f_y = yield strength of steel

h_e = effective depth of beam web

Z = plastic section modulus

As an extreme condition, when shear produces full yielding of the web, and if it is assumed that the entire additional shear is taken by the flanges, using equations 9–13 and 9–14 and $V_s = V_{up}$ gives

$$M_{ps} = M_p - \frac{3}{64} \frac{f_y t_w^2 h_e^4}{Z} \qquad \text{(eq 9-15)}$$

or using the full depth h

$$M_{ps} = M_p - 0.038 f_y t_w^2 h^4 / Z \qquad \text{(eq 9-16)}$$

These theoretical equations give conservative results because the implied reduction in moment capacity does not occur owing to strain hardening. It is recommended that, based on test results, no reduction of the plastic moment due to shear be made if the magnitude of the shear force at the ultimate load is less than V_{up}. The static shear capacity of several beam configurations is given in figure 9–2.

MEMBER	FLEXURAL CAPACITY	SHEAR CAPACITY
	$p_f a = 8.0 \dfrac{f_y z}{L^2}$	$p_s a = \dfrac{2V_u}{L}$
	$P_f = 4.0 \dfrac{f_y z}{L}$	$P_s = 2V_u$
	$p_f a = 12.0 \dfrac{f_y z}{L^2}$	$p_s a = \dfrac{2V_u}{L} - \dfrac{2M_p^e}{L^2}$
	$P_f = 6.0 \dfrac{f_y z}{L}$	$P_s = 2V_u - \dfrac{2M_p^e}{L}$
	$p_f a = 16 \dfrac{f_y z}{L^2}$	$p_s a = \dfrac{2V_u}{L}$
	$P_f = 8 \dfrac{f_y z}{L}$	$P_s = 2V_u$

a = WIDTH OF CONTRIBUTORY LOADING AREA
Z = PLASTIC SECTION MODULUS
f_y = STEEL YIELD STRESS
V_{up} = TOTAL SHEAR RESISTANCE OF SECTION (EQ 9-13)

M_p^e = FULLY PLASTIC MOMENT AT END OF SPAN

p_f = UNIFORM LOAD RESISTANCE OF MEMBER BASED ON FLEXURAL CAPACITY
p_s = UNIFORM LOAD RESISTANCE OF MEMBER BASED ON SHEAR CAPACITY
P_f = CONCENTRATED LOAD RESISTANCE OF MEMBER BASED ON FLEXURAL CAPACITY
P_s = CONCENTRATED LOAD RESISTANCE OF MEMBER BASED ON SHEAR CAPACITY

US Army Corps of Engineers

Figure 9-2. Static flexural and shear capacity of steel beams.

e. Ductility. Ductility ratios for steel beams subjected to lateral loads are usually taken as ratios from 10 to 20. If beams are subjected to axial loads other than those imposed by membrane action, ductility ratios of 6 to 8 are recommended. Unless information to the contrary is available, the lower bounds of 10 and 6 should be used.

f. Resistance function. Depending on the degree of indeterminancy, the resistance function of a beam consists of either two or three straight lines (fig 9-3). For the purpose of weapons effects analysis, it is convenient and acceptable to represent the three-part function with an equivalent stiffness K_e. In chapter 10, tables 10-1, 10-2, and 10-3 list equivalent stiffnesses for beams and one-way slabs with various boundary conditions and loadings. Using these values, the resistance function is very easy to construct. The ultimate capacity of the section is computed using figure 9-2. The effective stiffness is obtained from tables 10-1, 10-2, and 10-3. The yield deflection is the ultimate capacity divided by the effective stiffness and the ultimate deflection is the ductility multiplied by the elastic deflection.
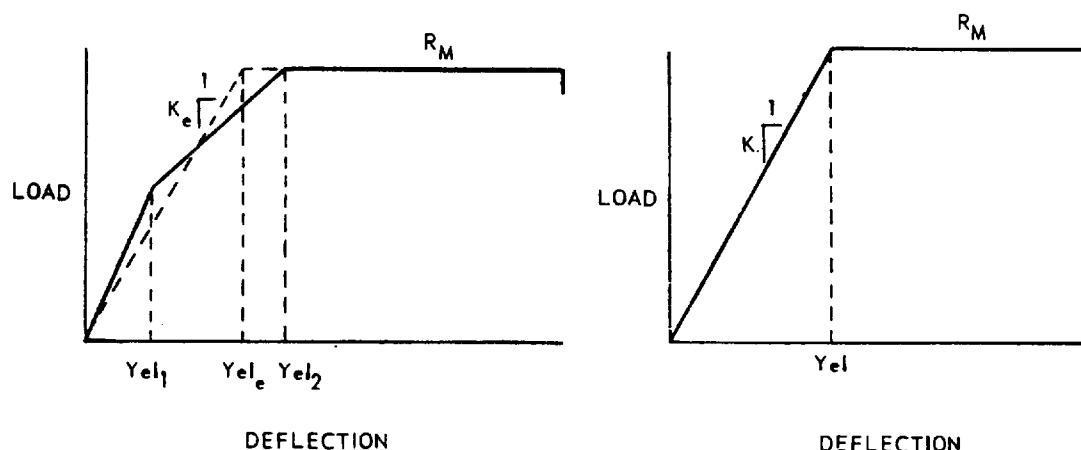
US Army Corps of Engineers

Figure 9-3. Typical resistance functions.

9-5. Reinforced concrete beams.

a. Introduction. Hardened structures should be designed so that failure is caused by yielding of the reinforcing steel. High ductilities cannot be obtained if the structure fails due to compression or shear in the concrete. Reinforced concrete members designed to resist blast and shock resulting from weapons frequently have span-to-depth ratios smaller than those commonly used in conventional structures. In some ways, the behavior of these deep members under load deviates from that observed in members of conventional dimensions. Only limited data are available on the strength and behavior of very deep reinforced concrete members, and the design procedures presented herein are based on these data as well as on studies of the behavior of members of conventional proportions. In general, tests on blast-resistant structures have also shown that construction details based on building code requirements in ACI 318-77 for conventional structures have proven more than adequate for hardened facilities.

b. Flexural strength. The moment capacity of reinforced concrete members can be predicted reasonably well by use of conventional ultimate strength expressions. The design equation presented herein consider only the yield range of the reinforcing steel prior to strain hardening, and if steel percentages are such as to ensure ductile response of the member, consideration of ultimate concrete strain is not necessary in most instances. Ultimate concrete strain could be a factor in those members containing compression reinforcement. After crushing of the concrete, the compression steel may lose its effectiveness because there is no concrete available for bond transfer or prevention of buckling.

(1) The flexural mode of response is heavily dependent upon the percentage of tensile steel employed. If insufficient steel is used, the steel may be incapable of resisting the tensile force carried by the concrete before cracking. For such members, the load deflection relationship is characterized by a sudden rapid increase in deflection when the concrete cracks. If, on the other hand, an excessively large percentage of steel is used, the concrete crushes on the compression side before the tensile steel yields. When this happens, the member loses practically all of its load-carrying capacity and a very brittle failure results. To avoid either of these undesirable failure characteristics and to ensure ductile response, Winter, et al. (1964) recommend that reinforced concrete flexural members having only tensile reinforcing should be proportioned so that $p = 0.75 \, p_b$, where p_b is the

balance point reinforcing ratio. This steel ratio assures that the failure of the cross section is ductile. ACI 318–77 recommends that p be no greater than 0.5 p_b in order to assure that the cross section does not fail during rotation of the plastic section.

$$p \leq \frac{31,400}{87,000 + f_y} \left(\frac{f_c'}{f_y} \right) \qquad \text{(eq 9-17)}$$

where

p = tension reinforcing steel ratio = A_s / bd_f
A_s = cross-sectional area of tension steel
b = width of member
d_f = effective depth of member = distance from extreme compression fiber to center
of tensile steel
f_y = yield strength of steel, psi
f_c' = unconfined compressive strength of concrete, psi

(2) Equation 9–18 is valid for $f_c' \leq 4,000$ psi and decreases by about 6 percent for each 1,000–psi increase in f_c'.

(3) The design moment capacity of a rectangular member with tension reinforcement subjected only to bending is given by:

$$M_p = p f_y b d_f^2 \ (1 - 0.59 p f_y / f_c') \qquad \text{(eq 9-18)}$$

The addition of compression steel normally has little effect on the ultimate moment capacity of under–reinforced members (those meeting criteria of equation 9–17). While compression reinforcement is often provided to increase the ductility or rebound resistance of the member, any increase in flexural resistance therefrom is usually neglected in the design process. When it is considered necessary or desirable to treat compression reinforcement, ACI 318–63 recommends that the following expression for ultimate moment capacity be used.

$$M_p = b d_f^2 \ f_y \ \left\{ \left(p - p' \right) \ \left[1 - \frac{0.59 (p - p') f_y}{f_c'} \right] + p' \left(1 - \frac{d'}{d_f} \right) \right\} \qquad \text{(eq 9-19)}$$

where

p' = compression steel ratio = A_s' / bd_f
A_s' = cross-sectional area of compression steel
d' = depth from extreme compression fiber to center of compression steel

9–10

(4) Equation 9—19 assumes that both compression and tension reinforcing have reached their yield strength. This criterion is satisfied when

$$p - p' \geq \frac{62,900}{87,000 - f_y} \left(\frac{f'_c \, d}{f_y d_f} \right)$$ (eq 9-20)

(5) Equation 9–20 is valid for $f'_c \leq 4,000$ psi and decreases by about 6 percent for each 1,000-psi increase in f'_c. The preceding expressions are based upon both the tension and compression steel having yielded and $p > p'$. When $p = p'$, the strain in the compression steel can be determined by analysis of the section, i.e.,

$$\left(\frac{\bar{x}}{d_f} \right)^2 + \frac{p}{0.72} \left(\frac{E_s}{f'_c} \right) \left(\epsilon_{cu} - \frac{f_y}{E_s} \right) \left(\frac{\bar{x}}{d_f} \right) - \frac{p\epsilon_{cu}}{0.72} \left(\frac{E_s}{f'_c} \right) \left(\frac{d'}{d_f} \right) = 0$$ (eq 9-21a)

$$\epsilon'_s - \frac{\epsilon_{cu} (\bar{x} - d')}{\bar{x}}$$ (eq 9-21b)

where

ϵ'_s = strain in the compression steel

ϵ_{cu} = strain at ultimate concrete stress, normally equal to 0.003

$\bar{x}$ = distance from extreme compression fiber to neutral axis

E_s = modulus of elasticity of steel

The neutral axis is determined by solving the quadratic expression in equation 9–21a for $\bar{x}$ and ϵ'_s is then computed from equation 9–21a and compared with the yield strain. If the compression steel has yielded, equation 9–19 is valid. Otherwise, the moment capacity must be calculated from the section and material properties.

(6) When the flange thickness of the I or T section exceeds the depth to the neutral axis of the member, equation 9–18 can be used to determine the moment capacity. The member width, b , is taken as equal to the overall flange width. If the flange thickness is less than the depth to the neutral axis, Winter , et al. gives the moment capacity as

$$M_p = b'd_f^2 \, f_y \left\{ p_F 1 - \frac{t}{2d_f} + (p_w - p_F) \left[1 - 0.59 (p_w - p_F) \frac{f_y}{f'_c} \right] \right\}$$ (eq 9-22)

where

b = overall flange width

b' = width of web of I or T section

P_f = tensile steel ratio required to balance the compression force in the overhanging portion of the flanges

$$= 0.85 \, \frac{f_c(b-b')t_f}{f_y b' d_f}$$

t_f = flange thickness

p_w = total tensile steel ratio = $A_s / b' d_f$
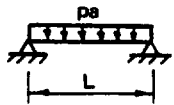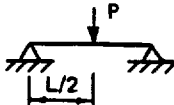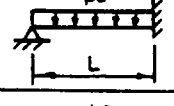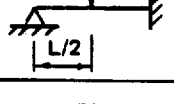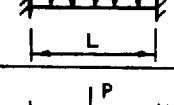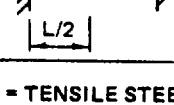
The total tensile steel ratio includes that required to balance the compression force in the overhanging flanges p_F plus that required to balance the compression force in the rectangular section of the beam p_b. As for the rectangular beams, it is desirable to limit the total amount of reinforcing to ensure that yielding of the tensile steel occurs before crushing of the concrete. ACI 318-77 recommends that the total tensile steel ratio be limited to

$$p_w \le 0.5 \, (p_b + p_F) \qquad \text{(eq 9-23)}$$

The steel ratio given by equation 9-17 is equal to $0.5p_b$, thus equation 9-23 can be rewritten as

$$p_w \le p + 0.5p_F \qquad \text{(eq 9-24)}$$

where p is obtained from equation 9-17. Confinement of the concrete in the compression area of flexural members should increase their ductility by allowing greater strains to occur in the concrete before crushing. Because of the possible loss of concrete outside the reinforcing cage, there may be a small decrease in ultimate moment from that calculated from unconfined sections. However, under some conditions strain hardening in the confined section can partially or completely offset this decrease. Static flexural capacities of rectangular reinforced concrete beams and one–way slabs for various beam configurations are given in figure 9–4.

MEMBER	FLEXURAL CAPACITY	SHEAR CAPACITY
	$p_f a = 7.2 p_c f_y b \left(\dfrac{d_f}{L}\right)^2$	$p_s a = \dfrac{2V_u}{L}$
	$P_f = 3.6 p_c \dfrac{b d_f^2}{L} f_y$	$P_s = 2V_u$
	$p_f a = 7.2\left(p_c + \dfrac{p_e}{2}\right) f_y b \left(\dfrac{d_f}{L}\right)^2$	$p_s a = \dfrac{2V_u}{L} - \dfrac{2M_p^e}{L^2}$.
	$P_f = 3.6\left(p_c + \dfrac{p_e}{2}\right)\dfrac{d_f^2}{L} f_y$	$P_s = 2V_u - \dfrac{2M_p^e}{L}$
	$p_f a = 7.2(p_c + p_e) f_y b \left(\dfrac{b d_f}{L}\right)^2$	$p_s a = \dfrac{2V_u}{L}$
	$P_f = 3.6(p_c + p_e)\dfrac{b d_f}{L} f_y$	$P_s = 2V_u$

p_e = TENSILE STEEL RATIO AT THE END

p_c = TENSILE STEEL RATIO AT MID-SPAN

b = BEAM WIDTH

a = WIDTH OF CONTRIBUTORY LOAD AREA

d_f = EFFECTIVE DEPTH

M_p^e = PLASTIC MOMENT CAPACITY AT FIXED END OF BEAM

V_{up} = ULTIMATE SHEAR CAPACITY OF SECTION (EQ 9-44).

f_y = STEEL YIELD STRESS

p_f = UNIFORM LOAD RESISTANCE OF MEMBER BASED ON FLEXURAL CAPACITY

p_s = UNIFORM LOAD RESISTANCE OF MEMBER BASED ON SHEAR CAPACITY

P_f = CONCENTRATED LOAD RESISTANCE OF MEMBER BASED ON FLEXURAL CAPACITY

P_s = CONCENTRATED LOAD RESISTANCE OF MEMBER BASED ON SHEAR CAPACITY

US Army Corps of Engineers

Figure 9-4. Static flexural and shear capacity of rectangular reinforced concrete beams and one-way slabs.

2486

c. Axial loads. The strength of a compression member subjected to pure axial load can be easily obtained. However, slight load eccentricities will likely cause unintentional moments. Therefore, it is recommended that all members subject to axial load be designed in accordance with Section 10–3 of ACI 318–71 which requires that a minimum load eccentricity of at least 1 inch or 0.05h be assumed for spiral columns and 0.10h for tied columns in cases where no moment exists (h is the overall thickness of the member in inches). The procedure for combined flexural and axial loads can then be used to design or analyze the member.

The use of spirals or ties in reinforced concrete compression members increases the allowable stresses and ductility of the member. These increases are derived from lateral confinement of the concrete and lateral support of the longitudinal reinforcement provided by spirals or ties. When required, ACI 318–77 recommends that spiral reinforcement be at least 0.375 inch in diameter for cast–in–place construction. The clear spacing between spirals should not be greater than 3.0 inches nor less than 1.0 inch. The ratio of spiral reinforcing should be

$$P_s = \frac{V_{sp}}{V_c} \geq 0.45 \left(\frac{A_g}{A'_c} - 1 \right) \frac{f'_c}{f_y} \qquad \text{(eq 9-25)}$$

where

V_{sp} = volume of spiral reinforcement

V_c = total volume of core measured out–to–out of spiral

A_g = gross cross-sectional area of member

A'_c = area of core of spirally reinforced concrete member measured to outside diameter of spiral

f_y = yield strength of spiral material, but not more than 60,000 psi

Lateral reinforcement for compression members should be at least No. 3 bars for No. 10 smaller longitudinal reinforcing and at least No. 4 bars for longer size longitudinal reinforcing. The spacing of ties should not exceed 16 longitudinal bar diameters, 48 tie bar diameters, or the least dimension of the column.

d. Combined flexural and axial loads. A member subjected to combined bending and axial loads encompasses both beam and column behavior, and the degree to which either behavior predominates depends upon the relative magnitudes of the two loadings and the sectional properties of the member. The entire range of limiting combinations of moment and axial load may be summarized in an interaction diagram such as that shown in figure 9–5. In this figure, P_o is the ultimate axial load capacity of the member when carrying no moment and M_p is the ultimate moment capacity when no axial forces are present (equations 9–18 and 9–19). M and P , as used in the diagram, are the values of moment and thrust computed for a given loading condition. Any point on the curve abc represents a combination of M and P, which, according to the ultimate strength theory, will just fail the member. Over the range a–b, the member will fail by crushing of the concrete. Point b represents the balance point where limiting strain in the concrete occurs simultaneously with yield stress in the tension steel. In the range b–c, failure is initiated by yielding of the tension steel. Any load combination which falls within the area bounded by the interaction curve and the coordinate axes is considered a safe load. Those falling outside this area are assumed to cause failure of the member. It is evident from figure 9–5 that the presence of a small axial load can substantially increase the moment capacity of an under–reinforced member. Axial compressive forces develop in slabs that are restrained at their edges against longitudinal movement. Sufficient restraint to enhance the flexural capacity of a slab can be provided by surrounding stiff walls or by support friction. For span–to–depth and steel ratios commonly found in hardened facilities, the compressive membrane action can enhance the ultimate flexural capacity by a factor of 1.5. The ultimate axial load capacity is given by

$$P_o = (0.85 f'_c + p_t f_y) A_g \qquad \text{(eq 9-26)}$$

where p_t is the total steel ratio based upon the gross cross–section area of the member A_g .
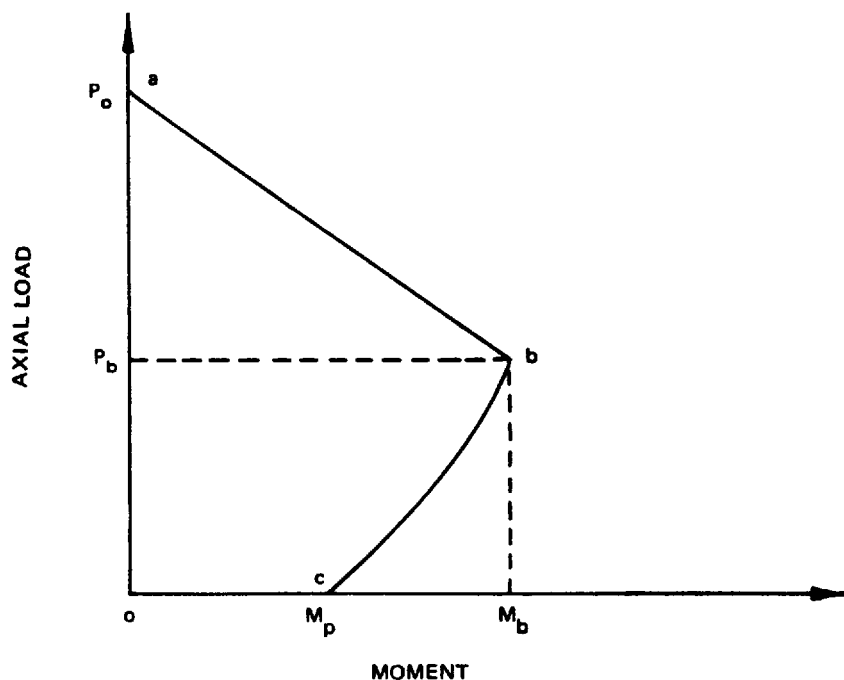
US Army Corps of Engineers

Figure 9–5. Interaction diagram for reinforced concrete beam–column.

(1) In constructing a diagram such as that shown in figure 9–5, values of P_o and M_p can be obtained using equations 9–26 and 9–18 (or 9–19) respectively. For symmetrically reinforced rectangular members, the axial load at the balance point is given by Winter, et al. (1964).

$$P_b = f'_c \, b \, d_f \left(\frac{62,900}{87,000 + f_y} \right), \text{lb} \qquad \text{(eq 9-27)}$$

Equation 9–27 is valid for $f'c \leq 4,000$ psi and decreases by about 6 percen' for each 1,000–psi increase in $f'c$. The moment at the balance point is given by Winter, et al. (1964).

$$M_b = P_b e_b \qquad \text{(eq 9-28)}$$

where

e_b = $(0.20 + 0.91 p_t f_y / f'_c) t_h$ (from plastic centroid)

p_t = total steel ratio for member, A_{st} / A_g

t_h = thickness of member in the direction of bending

(2) The variation of P with M can be assumed to be linear over the range a–b without significant error. Over the range b–c , the axial load capacity under combined axial load and bending, P_u , for a rectangular, symmetrically reinforced member is given by ACI 318-63; that is

$$P_u = 0.85 f'_c \, b d_f$$

$$\left\{ 1 - \frac{e}{d_f} - p + \sqrt{\left(1 - \frac{e}{d_f}\right)^2 + 2p \left[(m-1)\left(1 - \frac{d'}{d_f}\right) + \frac{e}{d_f} \right]} \right\} \qquad \text{(eq 9-29)}$$

where

e = eccentricity of the axial load with respect to the centroid of the tension reinforcement calculated by conventional methods of frame analysis

m = $f_y / 0.85 f'_c$

The corresponding moment in the range b–c is

$$M = P_u e' \qquad \text{(eq 9-30)}$$

where e' is the eccentricity from the plastic centroid of the section calculated by conventional methods of frame analysis. A linear variation of P with M could be taken as a quick approximation over the range b–c and is conservative for design purposes. Interaction curves for typical reinforced concrete members are presented later (fig 9–6).

2489
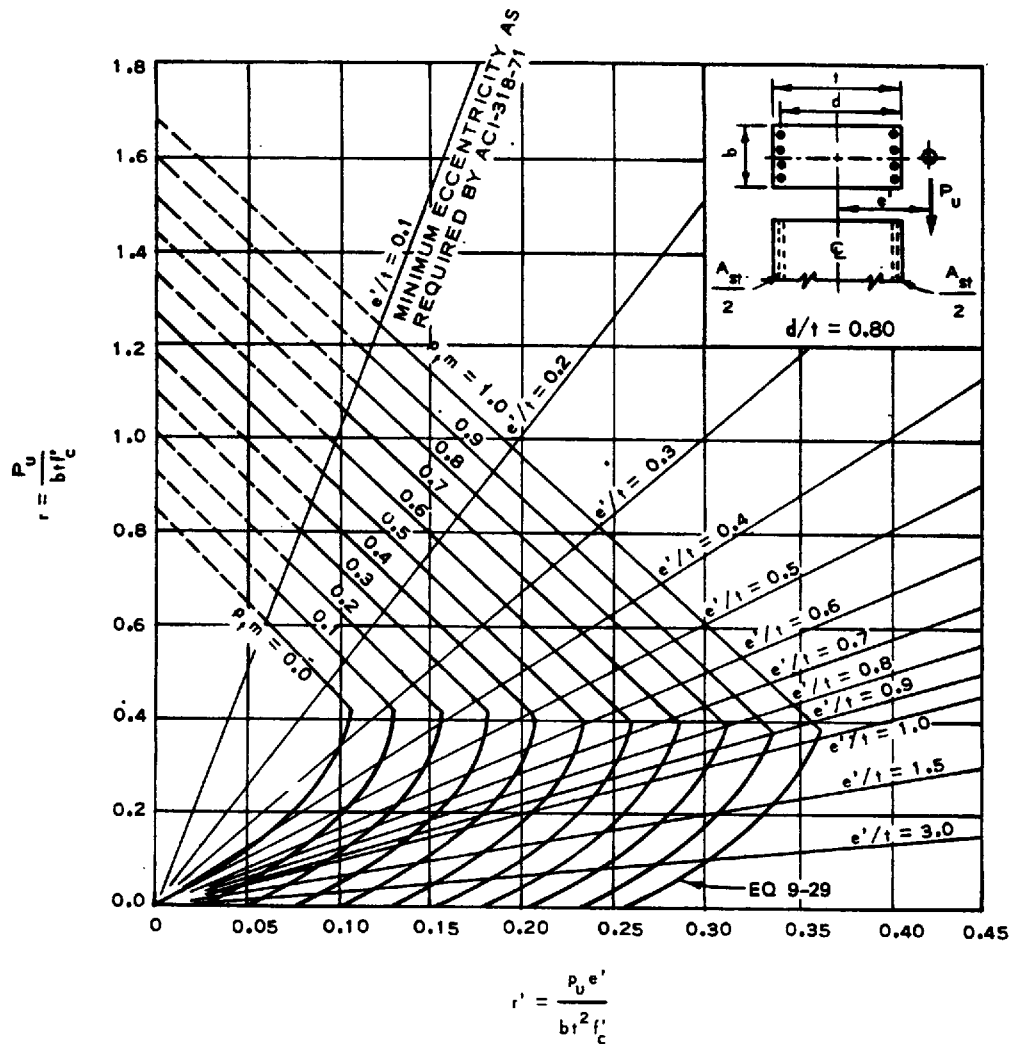
(a) RECTANGULAR SECTION WITH SYMMETRICAL REINFORCEMENT, $d/t = 0.80$

Source: Air Force Weapons Laboratory, "The Air Force
Manual for Design Analysis of Hardened
Structures," TR 74-102

Figure 9-6. Interaction curves for reinforced concrete sections. (Sheet 1 of 4)
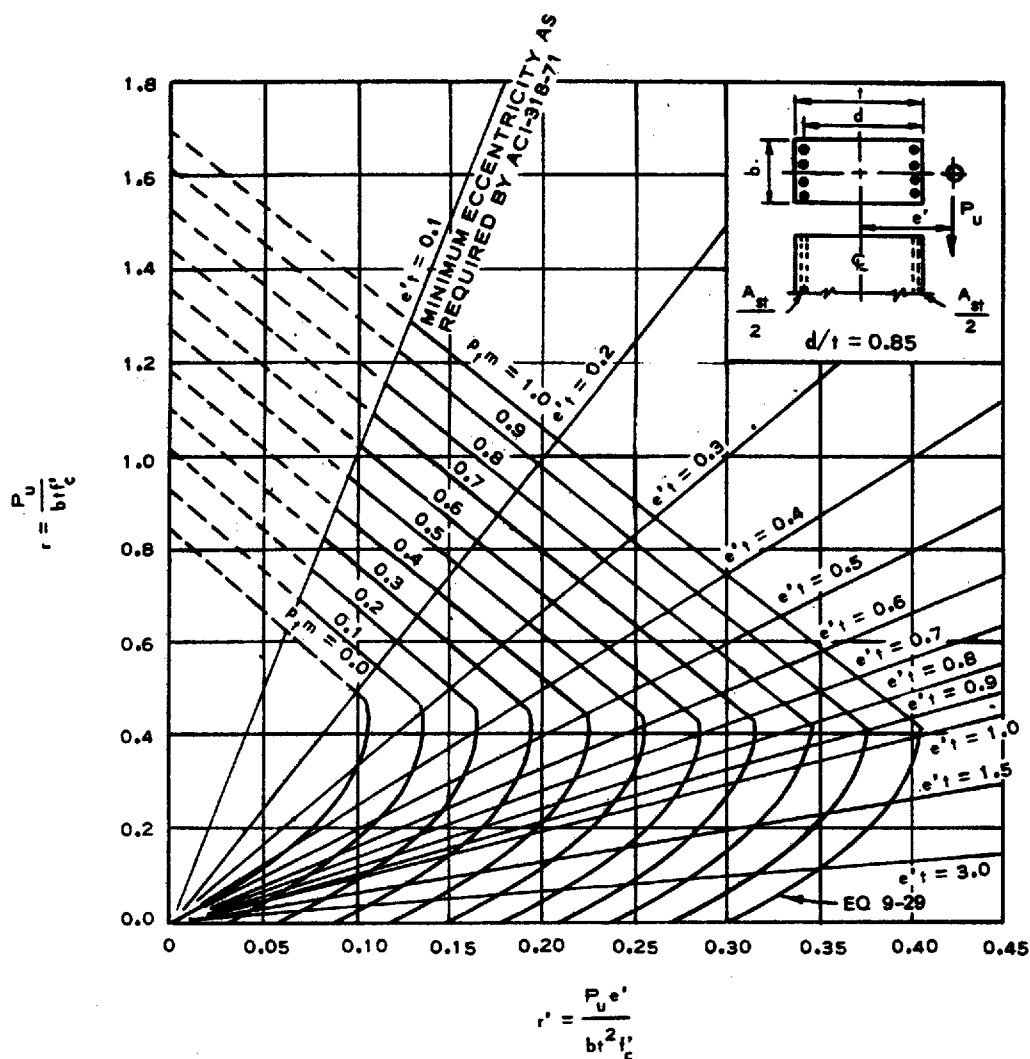
(b) RECTANGULAR SECTIONS WITH SYMMETRICAL REINFORCEMENT, $d/t = 0.85$

Source: Air Force Weapons Laboratory, "The Air Force
Manual for Design Analysis of Hardened
Structures," TR 74-102

Figure 9-6. Interaction curves for reinforced concrete sections. (Sheet 2 of 4)
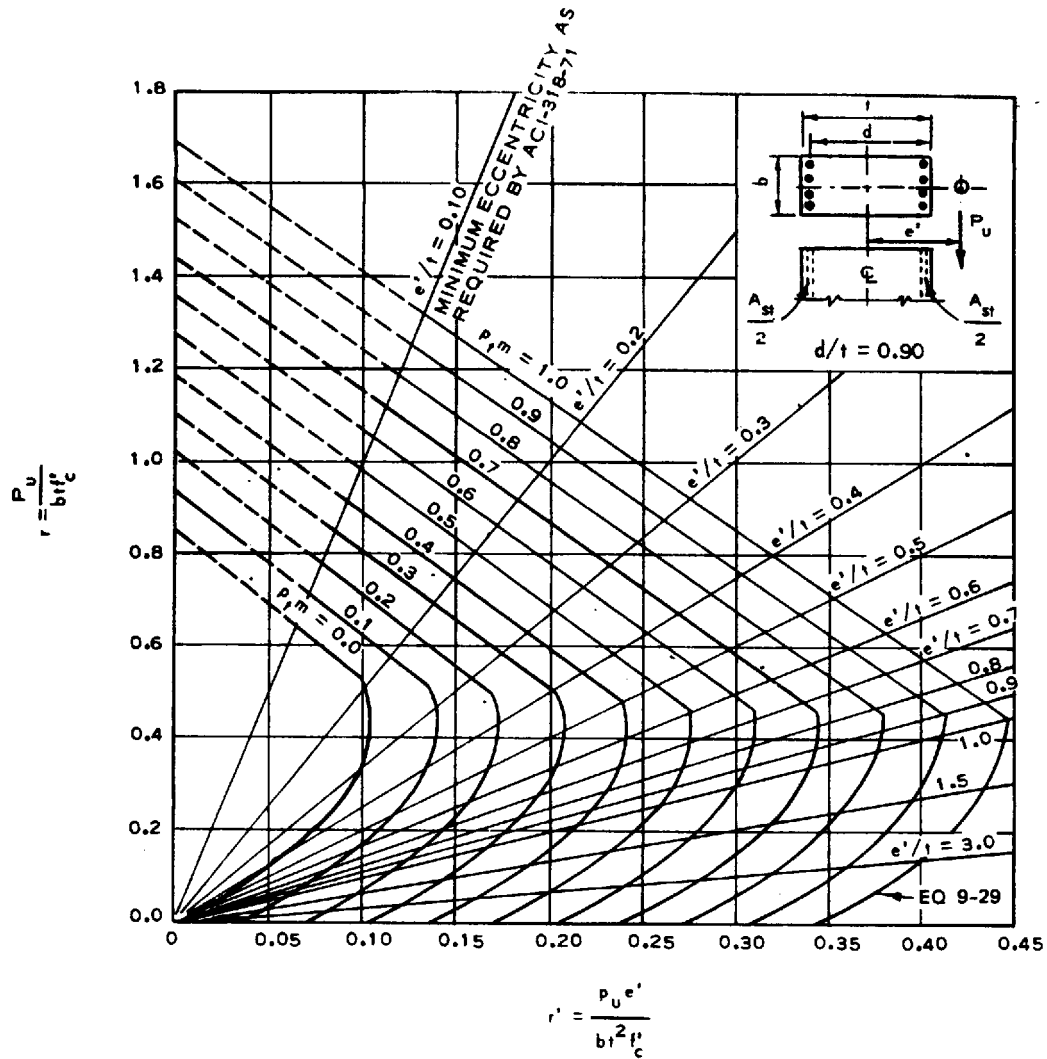
(c) RECTANGULAR SECTIONS WITH SYMMETRICAL REINFORCEMENT, d/t = 0.90

Source: Air Force Weapons Laboratory, "The Air Force
Manual for Design Analysis of Hardened
Structures," TR 74-102

Figure 9–6. Interaction curves for reinforced concrete sections. (Sheet 3 of 4)

TM 5-855-1
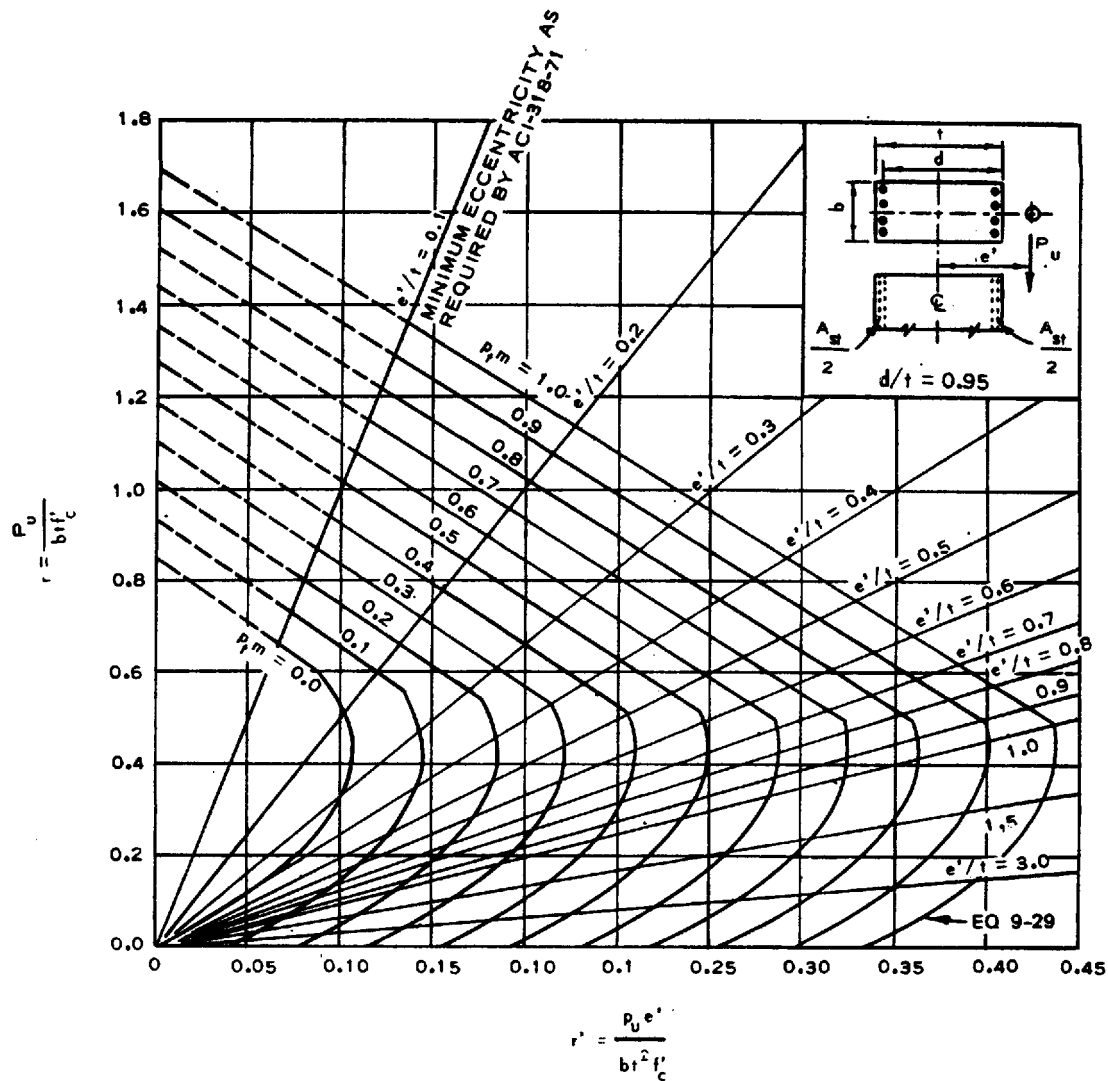
(d) RECTANGULAR SECTIONS WITH SYMMETRICAL REINFORCEMENT, $d/t = 0.95$

Source: Air Force Weapons Laboratory, "The Air Force
           Manual for Design Analysis of Hardened
           Structures," TR 74-102

Figure 9-6. Interaction curves for reinforced concrete sections. (Sheet 4 of 4)

2493

(3) Winter, et al. (1964) gives the following approximate equation for spiral–reinforced circular members. The eccentricity measured from the plastic centroid for the balanced case is given by

$$e_b = (0.24 + 0.46 p_t f_y / f'_c) D_o \qquad \text{(eq 9-31)}$$

where

p_t = ratio of total cross-section area of longitudinal reinforcing to gross cross-section area of member

D_o = outside diameter of concrete section

The eccentricity given by equation 9–31 is with respect to the plastic centroid of the cross section. When the eccentricity of the load is greater than that given by equation 9–31, tensile stresses in the steel govern the strength of the member and the axial load is given by ACI 318–63, that is

$$P_u = 0.85 f'_c D_o^2 \left[\sqrt{\left(\frac{0.85e'}{D_o} - 0.38\right)^2 + \frac{p_t m d_c}{2.5 D_o}} - \left(\frac{0.85e'}{D_o} - 0.38\right) \right] \qquad \text{(eq 9-32)}$$

where d_c is the diameter of the circle through centers of longitudinal reinforcing arranged in a circular pattern.

(4) The preceding expressions, along with virtually all material from ACI318–77 and ACI318–63, are oriented toward design. That is, assumed stress blocks and strains are selected with the objective of providing safe, and rational structures. Consequently, direct use of this material will give misleading results in an attempted failure analysis wherein one must return to basic principles and make assumptions based on failure rather than survival. The allowable load on a compression member is also a function of its slenderness ratio defined by

$$R_s = \frac{K_s L}{r} \qquad \text{(eq 9-33)}$$

where

K_s = an effective length factor

L = the unsupported length of the member

r = the radius of gyration of the member cross section

(5) The unsupported length of a member is defined as the clear distance between floor slabs, beams, girders, or other structural members capable of providing lateral support. Effective length factors are given in figure 9–1 for various types of end restraints. ACI 318–77 recommends that the radius of gyration for reinforced concrete compression members with rectangular cross sections be taken equal to 0.30 times the overall dimension in the direction in which the stability is being considered. For circular cross sections, it is taken equal to 0.25 times the diameter. For compression members braced against sidesway, the effect of slenderness may be neglected when

$$R_s < 34 - 12 M_1 / M_2 \qquad \text{(eq 9-34)}$$

where

M_1 = smaller value of end moment acting on member; sign is positive if member is bent in single curvature

M_2 = larger value of end moment acting on member; sign is always positive

(6) For members not braced against sidesway and Rs less than 22, the effects of slenderness can be neglected; for Rs greater than the above values, the applied moment must be modified to account for the reduced strength of the member. The modified moment is given by:

$$M_m = FM_2 \qquad \text{(eq 9-35)}$$

where

$$F = \frac{C_m}{1 - P_u/P_c} \quad \text{but not less than 1.0} \qquad \text{(eq 9-36)}$$

C_m is defined by equations 9-8 and 9-9, and

$$P_c = \frac{\pi^2 E_c I_c}{(K_s L)^2} \qquad \text{(eq 9-37)}$$

(7) The modulus of elasticity of the concrete E_c is obtained from equation 9-2. The moment of inertia of concrete I_c can be taken equal to the average of that for the cracked and uncracked transformed cross sections. For rectangular sections, it is approximated by

$$I_c = \frac{bd_f^3}{2} \, (5.5p + 0.083) \qquad \text{(eq 9-38)}$$

(8) While the presence of small axial loads can increase the moment capacity of a reinforced concrete member, any axial load decreases its ductility in terms of ultimate curvature. Ductility generally decreases with increasing axial load, and at axial loads corresponding to the balance point for unconfined sections, it may be as low as 1 to 2. Confinement of the concrete by spirals or hoop reinforcement increases the member's ductility, but the same general decrease with axial load is indicated. Since the shell of concrete outside the spiral or hoop reinforcing is considered ineffective in the strain regions at which this lateral reinforcement becomes effective, ultimate moment capacity for a given axial load is reduced in comparison with an unconfined section. The reduction can be significant at loads near the balance point.

(9) Preplotted interaction diagrams for axial and bending loads are a valuable tool in the analysis of reinforced concrete members and can greatly reduce the amount of computation. Figure 9-6 is a series of such diagrams for commonly encountered reinforced concrete sections. Similar diagrams for other sections can be found in most texts on reinforced concrete.

e. Shear. Shear failures are generally brittle in nature with little advance warning of distress in the member. In order to assure ductile behavior of reinforced concrete members, it is necessary that the ultimate strength of the member in shear be greater than its ultimate flexural strength. There are two modes of shear failure, pure shear and diagonal tension. The pure shear mode of failure is characterized by the rapid propagation of a nearly vertical crack through the depth of the member in the region of the support. A minimal amount of horizontal reinforcement inhibits the formation and propagation of such cracks. A few pure shear failures have been observed in members with low span-to-depth ratios, but only at concrete strengths less than 3,000 psi and high reinforcing steel ratios (p > 0.02). Pure shear failures are improbable in members properly proportioned for protective construction applications. The diagonal tension failure mode is characterized by diagonal cracks which propagate through the member from a point near the tensile steel toward the compression face. When the crack has penetrated to the point where the remaining compression zone of the concrete is insufficient to sustain the bending stresses, the concrete crushes

steel toward the compression face. When the crack has penetrated to the point where the remaining compression zone of the concrete is insufficient to sustain the bending stresses, the concrete crushes and the member fails. In order to avoid a diagonal tension failure, the shearing force V on a cross section of the member must be less than a limiting value which is a function of the total load system acting on the member and the physical characteristics of the member, i.e., dimensions, concrete strength, reinforcing, etc.

(1) Conventional members. The ultimate shear capacity of reinforced concrete members can be considered to include two components; that contributed by the concrete alone and that contributed by shear reinforcing. The critical section for shear in members of conventional proportions ($L/d_f > 5$) is assumed to occur at a distance equal to the effective depth of the member df from the face of the support. The ultimate shear capacity is defined in terms of the average shear stress on a cross section of the member.

(a) For rectangular members of conventional proportions, ACI 318-77 gives the ultimate shear capacity contributed by the concrete as

$$V_{uc} = b\,d_f(1.9\sqrt{f'_c} + 2{,}500\,p\,d_f V'/M'),\ lb \qquad \text{(eq 9-39)}$$

where

V' = shear at the critical section, lb
M' = moment at the critical section, in.-lb

Limits on equation 9–39 are as follows:

$$\frac{V_{uc}}{b\,d_f} \quad \text{shall not exceed } 3.5 \ \sqrt{f'_c} \quad psi$$

and

$$\frac{V'}{M'}\,d_f \quad \text{shall not be taken greater than 1.0 in determining } V_{uc}$$

(b) The ACI Manual of Concrete Practice reports a comparison between shear capacity predicted by equation 9–39 and results of 430 tests of beams without web reinforcing. The ratios of tests to calculated strengths varied from 0.65 to 1.91 with an average value of 1.18. Only a very small number of cases fell below 1.0. From these comparisons, it was concluded that equation 9–39 represents a reasonable lower bound to the test data and is adequate for design purposes. The maximum allowable shear stress of $3.5\sqrt{f'_c}$ psi also appears to be reasonable and is recommended for design purposes, although it does not represent a lower bound to the data.

(c) If an axial compressive load is applied to the member, the shear capacity of the concrete increases and is still given by equation 9–39 except that M'' must be substituted for M' and the ratio $V'd/M''$ can have values in excess of 1.0. M'' is given by

$$M'' = M' - Q(4h - d_f)/8 \qquad \text{(eq 9-40)}$$

where

Q = axial load in pounds (positive for compression loads, negative for tensile loads)

Equation 9–39 then becomes

$$V_{uc} = bd_f \left[1.9\sqrt{f'_c} + \frac{20{,}000\,pV'd_f}{8M' - Q(4h - d_f)} \right], \text{lb} \qquad \text{(eq 9-41)}$$

ACI 318-77 states the V_{uc}/bdf calculated from the equation 9-41 cannot exceed

$$3.5\sqrt{f'_c}\,\sqrt{1 + 0.002Q}/bh\ \text{psi}$$

(d) If the member is subjected to a tensile axial load, the reduced shear capacity is given by

$$V_{uc} = 2bd_f(1 + 0.002Q/bh)\sqrt{f'_c},\ \text{lb} \qquad \text{(eq 9-42)}$$

where Q is negative for tensile loads.

(e) Test data reported in the ACI Manual of Concrete Practice indicate that equations 9-41 and 9-42 represent a reasonable lower bound for design purposes with average ratios of actual to predicted strength of 1.29 for compression and 1.57 for tension loads. The total variations in actual to predicted shear capacities were 0.99 to 1.63 for the compression tests and 1.07 to 2.34 in the tension tests. The ratios for the tension tests represent the ratio of actual to predicted axial load at failure with a constant laterally applied load.

(f) The added shear capacity contributed by shear (web) reinforcing is given by

$$V_{us} = d_f\ \frac{A_{vs}f_y}{s} \qquad \text{(eq 9-43)}$$

where

    s = spacing of vertical web reinforcing
    A_{vs} = total cross-sectional area of web reinforcing over distance s

(g) The vertical web reinforcing ratio is defined as the ratio of the area of the vertical web reinforcing to the gross horizontal area, bs . Equation 9-43 assumes that the web reinforcing is placed perpendicular to the longitudinal axis of the member. In using equation 9-43, ACI 318-77 suggests that v_{us}/bd_f should not exceed $8\sqrt{f'_c}$ psi. The total shear capacity is then given by

$$V_{up} = V_{uc} + V_{us} \qquad \text{(eq 9-44)}$$

(h) The ACI Manual of Concrete Practice compared test results to strengths predicted by equation 9-44 but applied a limiting value of $8\sqrt{f'_c}$ psi to equation 9-44 rather than equation 9-43. Only about 5 percent of the test beams exhibited strengths considered a suitable lower bound for design purposes. A limiting value of the web reinforcing contribution to shear strength is not reported in the ACI Manual. Only total shear capacity was determined, and there is no apparent comparison between similar beams with and without web reinforcing. The ratios of actual to predicted shear capacity varied from 0.836 to 2.50. The average ratio was 1.445, and less than 10 percent of the beams tested exceeded the predicted strength by more than 100 percent. On the basis of these tests and the guidance provided in ACI 318-77, it is recommended that the shear stress calculated from equation 9-44 not exceed $11.5\sqrt{f'c}$ psi for design purposes. This limit corresponds to 1.445 times $8\sqrt{fc}$ or the sum of the maximum allowable values of equations 9-39 and 9-43. An additional provision is that the individual limits of equations 9-39 and 9-43 should not be exceeded. ACI 318-77 also places restrictions on the placement and allowable stresses in web reinforcing and should be consulted for detailed design guidance. Only one concrete contribution to total shear capacity is used in equation 9-44. It is obtained from equations 9-39, 9-41, or 9-42, as appropriate.

(i) The limiting value of shear stress given previously is based on tests of beams without axial force. The ACI Manual of Concrete Practice presented no data on beams with web reinforcing and subjected to bending, shear, or axial loads. In the absence of other guidance, it is suggested that the maximum allowable shear stress for members subjected to such loads be taken as the sum of limits for equations 9-41 or 9-42 and 9-43.

(j) Since most test beams exceeded the ultimate shear capacities predicted by equations 9-39 through 9-44, higher capacities are appropriate for analysis. It should also be noted that the ultimate strength of members designed according to the preceding shear criteria will normally be limited by flexural strength. On the basis of test results reported in the ACI Manual, an increase of 50 percent of the shear capacity indicated by equation 9-39 or 9-41 represents a reasonable upper bound to the shear capacity of members without web reinforcing. An increase of 100 percent of the capacity indicated by equation 9-44 represents a reasonable upper bound to the shear capacity of members with web reinforcing. The test results reported in AFWL-TR-71-74 do not suggest an upper bound to the shear capacity of members subjected to axial tension loads.

(2) Deep members. For deep members ($L/d_f \leq 5$) with loads applied to the top surface of the compression region, the shear capacity contributed by the concrete is greater than that predicted by equation 9-39. ACI 318-77 recommends use of

$$V_{uc} = bd_f(3.5 - 2.5M'/V'd_f)(1.9\sqrt{f'_c} + 2{,}500\,pd_fV'/M'), \text{ lb} \qquad \text{(eq 9-45)}$$

with the provisions that

$$1.0 \leq 3.5 - 2.5M'/V'd_f < 2.5$$

and

$$V_{uc}/bd_f \leq 6\sqrt{f'_c} \text{ psi}$$

(a) The critical section for shear in deep members is assumed to occur at a distance of 0.15L from the support for uniformly loaded members, and 0.5 times the distance between a concentrated load and the support for concentrated loads, but not over a distance d for either case. Equation 9-45 represents a conservative lower bound to test results presented in AFWL-TR-71-74 and is suitable for design purposes.

(b) As in the case of conventional members, web reinforcing contributes additional shear capacity. AFWL-TR-71-74 recommends an orthogonal system of reinforcing as the most effective in resisting shear failures in deep members. In such a system, longitudinal web reinforcing is distributed uniformly over the depth of the member. The shear capacity contributed by this system is given by

$$V_{us} = f_yd_f\left[\frac{A_v}{12s}\left(1+\frac{L}{d_f}\right)+\frac{A_{vH}}{12s_H}\left(11-\frac{L}{d_f}\right)\right] \qquad \text{(eq 9-46)}$$

where

A_{vH} = total cross-section area of longitudinal web reinforcing over distance s_H

s_H = vertical spacing of longitudinal web reinforcing

The total shear capacity of the deep member is then given by equation 9-44 as for conventional members. Limits on equation 9-44 for deep members are given by Winter, et al. (1964) as

$$V_u/bd_f \leq 8\sqrt{f'_c} \text{ psi for } L/d_f < 2$$

and

2498

$$V_u/bd_f \leq 0.67 (10+L/d_f) \sqrt{f'_c} \text{ psi for } 2 < L/d_f < 5$$

(c) Since there are no experimental data upon which an evaluation of equation 9–46 can be based, it is necessary to base its evaluation on total shear capacity. In AFWL–TR–71–74 test results are compared with shear capacity predicted by equations similar to equations 9–44, 9–45, and 9–46. ACI 318–77 would permit a maximum total shear stress of $10\sqrt{fc}$ psi for beams with an L/df of 5. None of the test beams which failed in shear exhibited a shear capacity less than predicted. Equations 9–44, 9–45, and 9–46 appear to give a reasonable lower bound to observed results. ACI 318–77 contains additional guidance on minimum amounts and placement of web reinforcing for deep members.

(d) As in the case of conventional members, observed shear capacities exceeded predicted capacities in most instances, and higher values appear appropriate for target analysis. On the basis of the limited data reported in AFWL–TR–71–74, an increase of 50 percent over the shear capacity predicted by equation 9–45 is suggested as an upper bound for members without web reinforcing. An increase of 100 percent over that predicted by equations 9–44, 9–45, and 9–46 is suggested as a reasonable upper bound for members with web reinforcing.

f. Bond. All modes of failure previously discussed are closely coupled to and are, in fact, inseparable from a bond mode of failure. This mode of failure is generally prevented if the reinforcement is well anchored by bond development length, hooks, or mechanical anchorage. If bond failure is not prevented, the bars will not serve their function in other modes of behavior considered. The tension or compression forces in the reinforcement at each section must be developed on each side of that section by an adequate embedment length or end anchorage or a combination of the two. If no mechanical end anchorage is provided, the tension or compression forces in the reinforcing must be resisted by shear–type bond stresses distributed over the contact area between the bars and the concrete. If bars without deformations are used, the resistance consists only of adhesion and mechanical friction between the bar and the concrete. With adequate mechanical end anchorage, the full strength of the bars may be developed, even though the shearing stresses over the contact area between the bars and the concrete cause bond failure. With deformed bars, the projecting ribs bear against the surrounding concrete and provide greatly increased bond strength.

(1) When a bond failure occurs with deformed bars, it generally results in splitting of the concrete along the bars due to a wedging action of the bar deformation. Winter, et al. state that the ultimate resisting bond force, in force per unit length of bar, is largely independent of bar size or perimeter. Since the force in the bar causing bond failure increases with its area, bond is a more serious problem with the larger bars. The critical sections for development of reinforcement in flexural members are generally at points of maximum moment gradient. ACI 318–77 provides guidance as to the required development lengths L_d of deformed bars in tension.

(2) If the reinforcement is placed horizontally in the top of a member with more than 12 inches of concrete below it, the values obtained from ACI 318–77 are multiplied by 1.4. For reinforcement whose yield stress f_y is greater than 60,000 psi, the values obtained from ACI 318–77 are multiplied by the factor 2 - 60,000/f_y. The development length for bars in compression is given by

$$L_D = 0.02 f_y d_b/\sqrt{f'_c} \qquad \text{(eq 9–47)}$$

but not less than $0.0003 f_y d_b$ or 8 inches. Additional guidance on development of bond strength is contained in ACI 318–77. Bends, laps, or welded splices near points of maximum stress are undesirable because of the reduced ductility.

g. Ductility. If the recommended values of tensile and compressive steel are used, a ductility ratio of 5.0 to 10.0 is recommended for flexural design. The ductility of a concrete member which fails in compression or shear may be much lower than for flexure. A ductility of 3.0 to 5.0 may be used for columns in which tension governs; some judgment must be used for columns which are near the balance point. If the larger values of ductility are used, loose concrete may fall off of the structure and concrete dust will probably be generated. If dust and falling concrete present a problem, some means of containing them should be provided or the lower values of ductility should be used.

h. Resistance function. The resistance function for concrete members is obtained using the same procedure as that used for the steel beams. The modulus of elasticity and moment of inertia are obtained by using equations 9–4 and 9–38, respectively. The maximum resistance and effective stiffness are obtained from tables 10–1, 10–2, and 10–3. The deflection is determined by dividing the maximum resistance by the effective stiffness and the failure deflection is obtained by multiplying the yield deflection by the ductility.

9-6. Columns.

Columns are essentially beams with axial loads and these were previously discussed in paragraphs 9–4c, 9–5c, and 9–5d.

9-7. One–way slabs and beams.

a. Reinforced concrete. The moment capacity of a reinforced concrete beam or one–way slab can be obtained from equations 9–18, 9–19, and 9–22. Over the range of recommended steel percentages and obtainable concrete strengths, equation 9–18 can be approximated with little error by

$$M_p = 0.9\, p\, f_y b\, d^2_f \qquad \text{(eq 9-48)}$$

Thus, the flexural resistance of a simply supported rectangular beam of width b and length L in terms of uniformly distributed load P_f is

$$P_f = 7.2\, p\, f_y \left(\frac{b}{a} \right) \left(\frac{d_f}{L} \right)^2 \qquad \text{(eq 9-49)}$$

where a is the width of the area over which the load P_f is applied. For a one–way slab, a is equal to b.

(1) The moment capacity of rectangular beams and one–way slabs with compression reinforcement is given in equation 9–19 and the capacity of T–beams is given by equation 9–22.

(2) If compression reinforcing is neglected, the uniform load corresponding to the ultimate flexural capacity of continuous members with equal end moment capacities is given by

$$P_f = \frac{8}{L^2_a} \left(M^c_p + M^e_p \right) = 7.2\, (p_c + p_e)\, f_y \left(\frac{b}{a} \right) \left(\frac{d_f}{L} \right)^2 \qquad \text{(eq 9-50)}$$

where

M^c_p and M^e_p = fully plastic moment capacities at the center and ends

p_c and p_e = tensile steel ratios at the center and ends

(Equation 9-50 is applicable only to under-reinforced members.

9-27

(3) Equations applicable to other support and load conditions can be derived by equating the appropriate expression for moment capacity to the expression for maximum moment in the member. Figure 9–4 presents expressions for several of the more common load and support conditions.

(4) Expressions for flexural capacity of indeterminate members assume the formation of plastic hinges at the supports and midspan. For other load and support conditions, a structural analysis should be performed to obtain the significant moments and these moments equated to the flexural capacities given by the appropriate equation in paragraph 9–5b.

(5) Figure 9–4 also includes approximate expressions for the shear capacity of a beam or one–way slab. These expression are approximate since they are based upon shear at the support rather than at the critical points referred to in paragraph 9–5e. The ultimate shear resistance V_{up} is determined from equations 9–39 and 9–43 for conventional beams and equations 9–45 and 9–46 for deep members.

(6) If the beam or slab is subjected to an axial load, equations 9–41 and 9–42 can be used to obtain the section shear capacity. The effect of axial load on moment capacity of the beam or slab can be determined in accordance with the procedures of paragraph 9–5d.

(7) In order to assure ductile response of the member, the tension reinforcing steel ratio should be limited to the range of 0.0025 to 0.02 wherever possible. The ratio should be at least 0.0025 for any flexural member. The difference between the compression and tension steel ratios should not exceed 0.0125.

(8) Some vertical web reinforcing should be provided for all flexural members subjected to blast loads. A minimum of 50–psi shear stress capacity should be provided by shear steel in the form of stirrups. In those cases where analysis indicates a requirement for vertical shear reinforcing, it should be provided in the form of stirrups.

(9) If the recommended reinforcement ratios are used, ductility factors recommended for reinforced concrete beams may be used.

b. Steel. Figure 9–2 gives expressions for the flexural capacity of steel beams for several support and load conditions. With the exception of the propped cantilever subjected to a uniform load, the expressions for indeterminate members assume the formation of plastic hinges at the fixed ends and center of the spans. In the case of the propped cantilever subjected to a uniform load, the plastic hinges form at the fixed end and a point 0.414L from the propped end. Also shown in figure 9–2 are beam capacities based upon the shear capacity given by equation 9–13. Since superposition does not hold in plastic analysis, the expressions of figure 9–2 cannot be combined to obtain results for other loading conditions. For other loading and support conditions, the critical moments and shears can be obtained from the applied loads through a structural analysis. These quantities can then be compared to the moment and shear capacities of the member as given by equations 9–3 and 9–13.

$$M_p \quad = \quad f_y Z \qquad\qquad (eq~9\text{-}51)$$

9–8. Two–way slabs and plates.

a. Reinforced concrete.

(1) Recommended design. Tensile steel ratios ranging from 0.0025 to 0.02 should be used for two–way slabs. A compressive steel ratio should be at least 0.0025, and the difference between the compressive and tensile steel ratios should be no greater than 0.0125.

(2) Flexural resistance. Tests have verified that the ultimate capacity of reinforced concrete slabs can be predicted with confidence by the Yield–Line Theory (Hognestad 1963). Furthermore, according to Hognestad, the results are always on the conservative side for design purposes, i.e., the calculated ultimate load being 80 to 90 percent of the actual ultimate load. It is thought that this results from strain hardening of the reinforcement together with membrane action of the slab when the slab experiences relatively large deflections near failure.

(a) The Yield–Line Theory is well covered in the literature (Hognestad 1963, Jones 1963, Ferguson 1958). For the general case of a rectangular two–way slab, continuous over all four supports (fig 9–7) and subjected to a uniform load, Jones gives the following expressions for the required ultimate moment capacity at the center.

$$M_{sc} = \frac{w \alpha^2 L^2}{6\gamma^2_{34}} \left[\sqrt{3 + \gamma_c \left(\frac{\alpha\gamma_{12}}{\gamma_{34}}\right)^2} - \frac{\alpha\gamma_{12} \sqrt{\gamma_c}}{\gamma_{34}} \right]^2 \qquad \text{(eq 9-52)}$$

where

M_{sc} = ultimate moment capacity per unit width of slab at the center of and in the direction of the short span

α = ratio of the short span to the long span

γ_c = ratio of ultimate moment capacity in long span direction to that in short span direction at center of slab

$\gamma_{12} = \sqrt{1 + i_1} + \sqrt{1 + i_2}$

$\gamma_{34} = \sqrt{1 + i_3} + \sqrt{1 + i_4}$

i_1, i_2 = ratios of ultimate moment capacities at supports 1 and 2 to that at center of long span

i_3, i_4 = ratios of ultimate moment capacities at supports 3 and 4 to that at center of short span

w = uniform load applied to slab
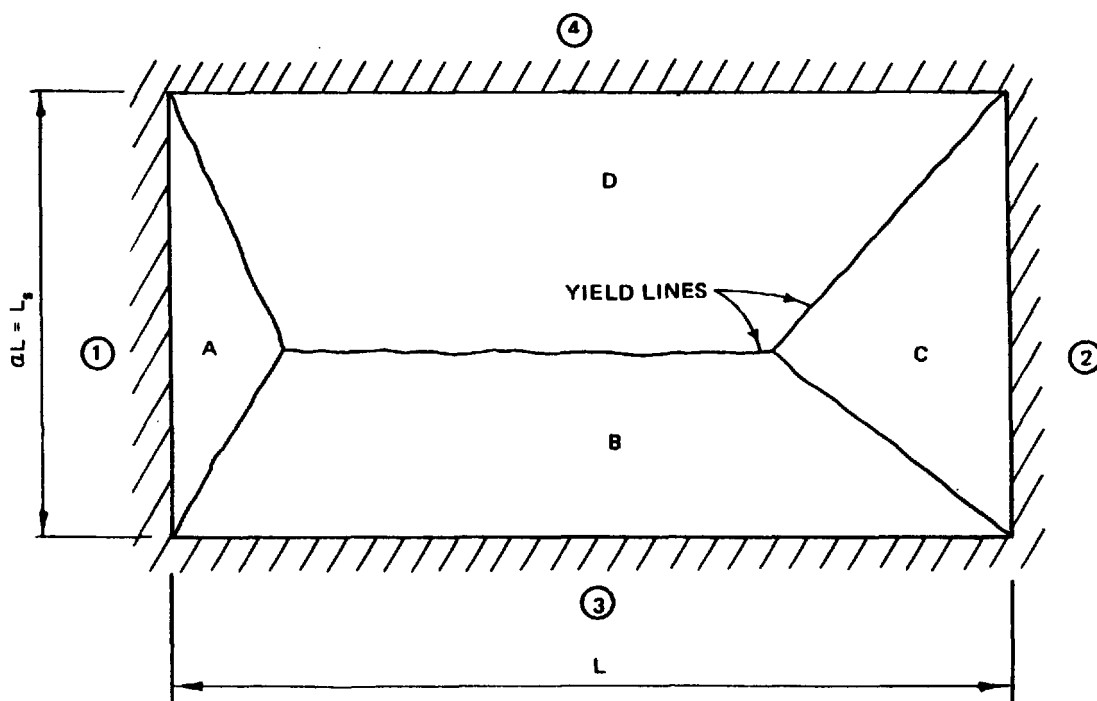
US Army Corps of Engineers

Figure 9–7. Yield lines for a general rectangular slab.

(b) If it is assumed that the moment capacities are equal at both supports of each span, equation 9–52 can be rearranged to give ultimate load capacity in terms of the moment capacities at the supports and midspan. Thus,

$$P_f = \frac{24(M_{sc}+M_{se})}{L_s^2} \left[\sqrt{3+\alpha^2 \frac{M_{Lc}+M_{Le}}{M_{sc}+M_{se}}} - \alpha \sqrt{\frac{M_{Lc}+M_{Le}}{M_{sc}+M_{se}}} \right]^{-2} \qquad \text{(eq 9-53)}$$

where

M_{se} = ultimate moment capacity per unit width of slab at the supports of and in the direction of the short span

M_{Lc} = ultimate moment capacity per unit width of slab at the center of and in the direction of the long span

M_{Le} = ultimate moment capacity per unit width of slab at the supports of and in the direction of the long span

(c) The ultimate moment capacities at the critical sections can be obtained from equation 9–18 or 9–48 using appropriate properties of the slab. Equations 9–52 and 9–53 can also be applied to simply supported slabs by setting moment capacity at the edges equal to zero.

(d) For rectangular slabs of reasonable relative dimensions and steel percentages, the critical yield line pattern can be assumed to be symmetrical, i.e., it intersects the corners at 45 deg, area A equals area C, and area B equals area D (fig 9–7). The resistance, expressed as a uniformly distributed load, corresponding to this yield line pattern can be obtained by considering the equilibrium of segments A and B. Since the true yield lines depend on slab properties, agreement between the resistances obtained for the two segments would be a fortuitous case. Newmark and Haltiwanger (1962) suggest using an average value weighted on the basis of the areas of the two segments. The resulting resistance is given by

$$P_f = 10.8 \, (p_{se}+p_{sc}) \left[\alpha \left(\frac{p_{le}+p_{lc}}{p_{se}+p_{sc}} \right) + \frac{2-\alpha}{3-2\alpha} \right] f_y \left(\frac{d_f^2}{L_s} \right) \qquad \text{(eq 9-54)}$$

where

p_{se} = average tensile steel ratio at the edge spanning in short direction

p_{sc} = average tensile steel ratio at the center spanning in short direction

p_{le} = average tensile steel ratio at the edge spanning in long direction

p_{lc} = average tensile steel ratio at the center spanning in long direction

(e) Results obtained from equation 9–54 may, in some instances, overestimate the resistance of the slab, but generally not in amounts sufficient to warrant analysis by a more refined application of the Yield–Line Theory in preliminary analyses (Hognestad 1963 and Ferguson 1958). Edge panels, however, or other cases where unsymmetrical support conditions exist, should be checked for adequacy.

(f) For the case of a circular slab subjected to a uniform load and continuously supported at its edges, the flexural resistance is given by

$$P_f = \frac{6\left(M^c_p + M^e_p\right)}{R_r^2}$$

where

M^c_p = ultimate moment capacity per unit width of slab at center of slab

M^e_p = ultimate moment capacity per unit width of slab at edge of slab

R_r = radius of the slab

According to Newmark and Haltiwanger (1962), equation 9–55 can also be defined in terms of the reinforcing steel ratios at the center and edges of the slab.

$$P_f = 5.4\, f_y \left(\frac{d_f}{R_r}\right)^2 (p_c + p_e) \qquad \text{(eq 9-56)}$$

where

pc = average tension steel ration at center of slab

pe = average tension steel ratio at edge of slab

(g) Since the yield line patterns for two–way slabs are similar for simple or continuous supports, equations 9–52 through 9–56 are also applicable to simply supported slabs. For these cases, the moment capacity at the supports is simply set equal to zero. Jones (1963) and Ferguson (1958) treat other support conditions in some detail.

(h) Under some conditions the reinforced concrete slab may be subjected to both axial and lateral components of load. For example, the walls of a shallow–buried structure subjected to ground shock loading will transmit significant axial compressive components of load to the structure's roof slab. These loads can significantly increase the flexural resistance of the roof slab. A similar condition arises in the case of roof loads transmitted to side walls. The effect of such axial loads on slab resistance can be estimated by application of the principles described in paragraph 9–5d. Careful consideration, however, must be given to whether the possible time–phasing of the axial and flexural load components will be more likely to produce beneficial or harmful results.

(3) Shear resistance. Shear failures in two–way slabs with dimensions encountered in normal construction are unlikely due to the large perimeter area available to resist the shearing forces. Exceptions are those cases where concentrated loads are applied to the slab through columns or other similar structural members. In some instances, it may be necessary to provide additional reinforcement at column–to–slab connections to prevent shear failures. In some protective construction applications, two–way slabs carry loads of very high intensity, and the possibility of shear failure increases.

(a) Shear is the governing mode of failure for deep, square, two–way slabs. As in the case of beams and one–way slabs, there are differences in the shear behavior of conventional and deep (L /d ≤ 5) two–way slabs. In either slab, the shear resistance can be expressed as

$$P_s = C_v \sqrt{f'_c}\, A_{SH} / A_L \qquad \text{(eq 9-57)}$$

where

p_s = shear resistance of slab (expressed as uniform load)

C_v = an empirical constant

A_{SH} = area resisting shear (fig 9-8)

A_L = loaded area producing shear (fig 9-8)

The shear mode of failure was typically found to be a circular cone–shaped section as indicated in figure 9–8 being forced out from the center of the slab.
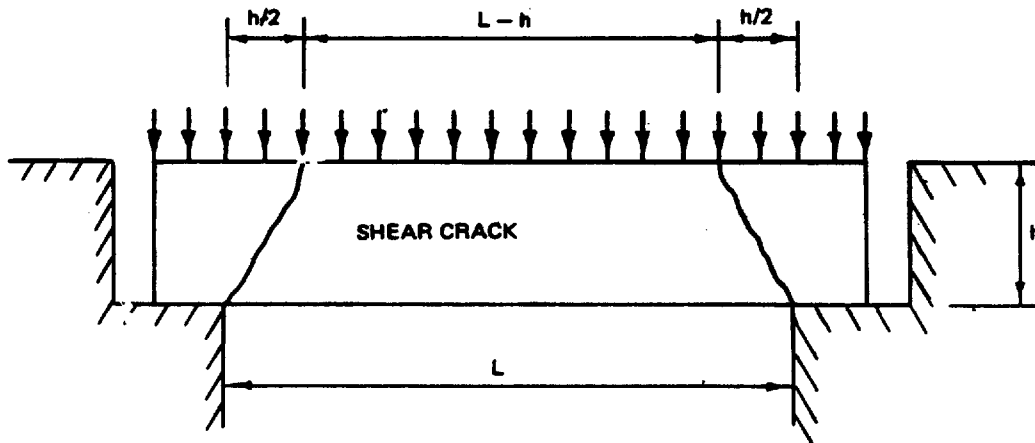
A_{SH} = SHEAR AREA = $\pi h(L - h)$

A_L = LOADED SHEAR AREA = $\frac{\pi}{4}(L - h)^2$

US Army Corps of Engineers

Figure 9–8. Two–way slab shear mode of failure.

(b) ACI 318–77b suggests that the critical section for shear occurs at a distance of d/2 from the reaction and $C_v = 4.0$. It is recommended that these criteria be applied to two–way slabs of conventional ($L / d_f > 5$) proportions. For square slabs, equation 9–57 becomes

$$P_s = 16 \sqrt{f'_c} \ \frac{d_f}{L - d_f} \ \text{psi} \qquad \text{(eq 9- 58)}$$

where L is the clear span of the slab.

(c) Experimental data indicate that deep slabs can sustain higher shear stresses than allowed by equation 9–58. It is recommended that

$$P_s = 12 \sqrt{f'_c} \, A_{SH}/A_L \ \text{psi} \qquad \text{(eq 9-59)}$$

as a lower bound to deep slab test results. For a deep square slab, equation 9–59 becomes

$$P_s = 48 \sqrt{f'_c} \ \frac{h}{L-h} \ \text{psi} \qquad \text{(eq 9-60)}$$

where h is the total depth of the slab and other terms are as previously defined.

(d) Equations 9–59 and 9–60 are based on an earlier experimental study by Gamble (1967) of deep circular slabs. A lower bound to test data for deep circular slabs is given by

$$P_s = 36 \sqrt{f'_c} \ \frac{h}{L-2h} \ \text{psi} \qquad \text{(eq 9-61)}$$

Equations 9–59 and 9–61 are suggested for design of deep slabs. An upper bound to the experimental data, which is appropriate for analysis, is obtained by changing the coefficient 12 in equation 9–59 to 19 and the coefficient 36 in equation 9–61 to 54. For rectangular slabs, it is suggested that equation 9–60 be used, with L taken as the average of the two spans. If the ratio of short–to–long span is less than 5.0, the shear resistance of the two–way slab spanning in the short direction.

(e) It is noted that equations 9–59 through 9–61 do not consider the effect of tension reinforcing on shear capacity. Test data indicate that although the shear resistance of deep slabs is slightly higher with tension reinforcing, it is relatively insensitive to the tension reinforcement ratio over the range $0.001 \leq p < 0.015$. In the slab tests bounded by equation 9–59, the tension reinforcement ratio varied from 0 to 0.015 in each direction and the compression reinforcement ratio varied from 0 to 0.005. Although the strength of the slabs tested did not vary significantly over the range of tension reinforcing, the presence of reinforcing steel was found to affect the severity of the failure. In most cases, those slabs with no reinforcing broke into small fragments. Those with reinforcing, although severely damaged, did tend to stay together.

(f) Gamble (1967) indicates that moment and axial forces affect the shear strength of deep two–way slabs in a way similar to that observed for beams and one–way slabs. Increasing moment at the critical section will generally decrease the allowable shear stress. Compressive axial loads increase and axial tension loads lower shear capacity of concrete sections. If moment and axial tension loads lower shear capacity of concrete sections. If moment and axial loads can be determined with reasonable confidence, it is suggested that a unit width of the two-way slab be analyzed as a beam column spanning in the short direction using the procedures described in

2506

Provided by IHS
No reproduction or networking permitted without license from IHS

Sold to:ARSALAN GHAHRAMANI, W0685154
Not for Resale,2009/5/25 8:10:11 GMT

9–33

paragraph 9–5e. The shear capacity of the two-way slab can be estimated as 2/3 (1 + α) , but not less than one, times that of the beam.

(g) In the event shear capacity is required above that provided by the concrete alone, additional strength can be provided in the form of vertical and / or horizontal web reinforcing. The amount of reinforcing required can be determined from equation 9–43 or 9–46 as appropriate.

(4) Supporting beams. The beams supporting a slab must be designed for the actual load distribution on the beam, which varies as the edge shear of the support slab. For a square slab, the flexural resistance of supporting beams with symmetrical support restraints can be determined by assuming a triangular load distribution with the maximum load intensity at the center of the beam. For this case, the support beam resistance, expressed as a uniform load on the slab, is

$$p_f = 10.8 (p_e + p_c) f_y \left(\frac{b}{a}\right) \left(\frac{d_f}{L}\right)^2 \qquad \text{(eq 9-62)}$$

where a = center-to-center distance between adjacent slabs. For the beam under the long side of a two-way slab, the loading may be assumed trapezoidal, which leads to

$$p_f = 7.2 (p_e + p_c) f_y \left(\frac{b}{a}\right) \left(\frac{d_f}{L}\right)^2 \left[\frac{1}{1 - \frac{1}{3}(\omega)^2}\right] \qquad \text{(eq 9-63)}$$

where the terms are as previously defined except that a is the center-to center distance between adjacent long beams. The flexural resistance of the beam under the short span of a rectangular slab is obtained from equation 9-62 with a taken as equal to the short span. The shear resistance of beams supporting a two-way slab can be determined using the equations of paragraph 9-5e.

(5) Ductility of two-way concrete slabs. If recommended steel ratios are used, a ductility ration of 5.0 to 10.0 is recommended for flexural design.

b. Steel. For some structural elements, steel plate is a more practical material than reinforced concrete. Access doors, hatches, and cover plates are examples of the types of structural elements which lend themselves to fabrication from steel plate. The maximum deflections and stresses in these elements will be affected by plate geometry and the type of support provided at the edges of the plates. Unless it is combined with a system of stiffeners, a flat plate provides very low flexural resistance to lateral loads. In most cases, large deflections of the plate will result in the applied loads being carried primarily through membrane action. The flexural load capacity of steel plates can be estimated from equation 9-52 and 9-55 by inserting the appropriate moment capacities at the critical sections. The large deflections of simple flat plates can be reduced by use of grillages of beams or stiffeners. The basic relationships could be applied with moment capacities based on the properties of the grillage. Torsional effects should be investigated in all cases.

9-9. Reinforced concrete shear walls.

In most one-story buildings, external walls designed to carry loads in flexure will be adequate to serve as shear walls in the other direction. INterior walls designed to take vertical loads will also be adequate as shear walls. ACI 318-77 gives the horizontal load which causes first cracking in a shear wall as

$$R_c = 0.1 f'_c L t \qquad \text{(eq 9-64)}$$

where

R_c = force required to cause first cracking

L = wall length

t = wall thickness

Because of the limited data on shear walls, the length used in equation 9-64 should not be greater than three times the height. If the load is greater than the cracking load, the wall thickness may be increased or the procedures in TM 5-856-2 may be used to calculate ultimate capacity.

CHAPTER 10

DYNAMIC RESPONSE OF STRUCTURES

10-1. Introduction

Basic theory regarding the dynamic response of structures is well covered in the literature. Therefore, the theory of dynamic response will not be covered in this manual. Instead, this chapter will focus on the analysis of structures under blast-induced loads. The analysis of structural systems using a large number of modes can be very complex. Problems that involve oscillatory type loads, such as earthquakes, often require a multi-degree-of-freedom analysis. However, for nonoscillatory loads, such as blast loads, and when only the peak response is required, many structural systems may be sufficiently analyzed using one mode. This chapter provides guidance for the use of single-degree-of-freedom (SDOF) systems for the analysis of structures under blast-induced loads.

10-2. SDOF systems.

The relationship between deflection and stress is the same under both static and dynamic conditions. Therefore, once the deflections are determined, the basic principles of structural analysis can be used to determine moments and stresses for the analysis and/or design of a given structure. The approach to dynamic analysis used in this manual will be to reduce a given structure or structural element to an "equivalent" SDOF system and determine its dynamic deflections. Deflections determined from the SDOF system will always be equivalent to the deflection of a specified point in the real structure or structural element. With the deflections known, basic structural analysis principles can then be used to proceed with the analysis is and/or design.

  a. An SDOF system will consist of a mass, a damper, and a resistance element, as shown in figure 10-1. The resistance element will usually be a linear spring up to some maximum resistance R_m and then offer a constant resistance with further deformation. Such a resistance element can be described with a bilinear resistance function. The mass and spring will be selected so that the frequency of the SDOF system will be equal to the expected response frequency of the equivalent structure.
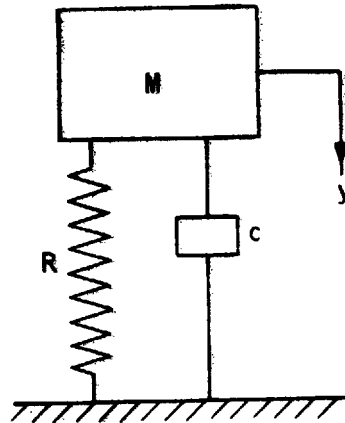
US Army Corps of Engineers

Figure 10-1. Single-degree-of-freedom system.

b. For nonoscillatory loads, when only the maximum response is needed, structural damping can normally be ignored. The exception to this may be in the case of a buried structure when radiation damping into the soil can occur. However, since damping will always decrease the computed deflections, it can be conservatively ignored when designing protective structures.

(1) Pressure-time history (load function). The pressure-time histories of weapons are not known exactly; however, simple approximations to their shape can be used as long as the peak pressure and total impulse are preserved. These approximate pressure-time histories are generally represented by a triangular pulse with zero rise time that preserves peak pressure and total impulse characteristics. In case of aboveground structures, a two-part triangular pulse is sometimes needed.

(2) Response of an SDOF system. The resistance function for these analyses will either be elastic or elasto-plastic. If the system is undamped, the following equation must be satisfied.

$$F(t) - R_R - M_s \ddot{y} = 0 \qquad \text{(eq 10-1)}$$

where

$F(t)$ = forcing function (function of time t)

R_R = resistance function = Ky for an elastic system

y = displacement

M_s = mass

$\ddot{y}$ = acceleration

(a) Elastic systems. For an elastic system with very simple load-time functions, equation 10-1 is easily solved. The solution to equation 10-1 is sometimes presented in a nondimensional form as a Dynamic Load Factor (DLF). The DLF is the ratio of the dynamic deflection at any time to the deflection which would have been caused by the static application of the maximum value of the load. Equations 10-2 and 10-3 give the DLF's as a function of time for rectangular and triangular pulses, respectively, with rise time of zero.

$$DLF = 1 - \cos(\omega t) = 1 - \cos\left(\frac{2\pi t}{T}\right) \text{ for } t \leq t_d \qquad \text{(eq 10-2)}$$

$$DLF = \cos[\omega(t - t_d)] - \cos(\omega t) \text{ for } t \geq t_d$$

$$= \cos\left[2\pi\left(\frac{t}{T} - \frac{t_d}{T}\right)\right] - \cos 2\pi\frac{t}{T}$$

$$DLF = 1 - \cos(\omega t) + \frac{\sin(\omega t)}{\omega t_d} - \frac{t}{t_d} \text{ for } t < t_d \qquad \text{(eq 10-3)}$$

$$DLF = \frac{1}{\omega t_d}[\sin(\omega t) - \sin[\omega(t - t_d)] - \cos(\omega t) \text{ for } t \geq t_d$$

where

ω = natural circular frequency of system (discussed in paragraph 10-3 below)

t = time

T = natural period = $\frac{2\pi}{\omega}$ (discussed in paragraph 10-3 below)

t_d = duration of rectangular or triangular pulse

Solutions for the rectangular and triangular pulses are also given in figure 10-2 where the maximum DLF is plotted for varying ratios (t_d / T) of pulse duration to the natural period of the structure. Given the ratio (t_d / T), the maximum DLF may be determined. The maximum values of stresses and displacement in a dynamically loaded structure may be determined by performing a static analysis using the maximum value of the load and multiplying the static values by the maximum DLF. Figure 10-2 also shows the plot of the ratio (t_m / T) of time to peak response to the natural period as a function of t_d / T where t_m is the time to peak response.

TM 5-855-1
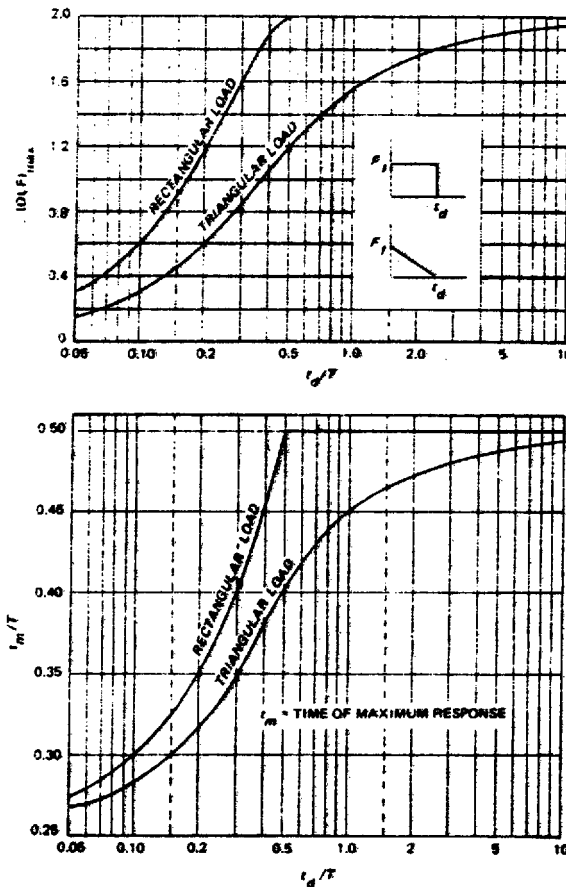
US Army Corps of Engineers

Figure 10-2. *Maximum response of single-degree, undamped elastic system subjected to rectangular and triangular load pulses having zero rise time.*

(b) Elasto-plastic systems. Equation 10-1 may also be solved for nonlinear elasto-plastic systems. For a bilinear resistance, the response is now broken up into three parts: the elastic response with $R = Ky$, the plastic response with $R = R_m$ (the maximum resistance), and the rebound response, which occurs after maximum displacement. As was the case for elastic systems, these equations have been solved in a nondimensional form. The peak response of an undamped elasto-plastic system to a suddenly applied triangular load is plotted in figure 10-3. This figure is a family of curves in which each curve represents a different ratio (R_m / F) of static capacity to peak dynamic load. For each curve the ductility ratio μ is plotted for a range of values of the ratio (t_d / T) of the pulse duration to the natural period of the structure (fig 10-3a). The ductility μ is the ratio (Y_m / Y_e) of the maximum deflection to the deflection. Figure 10-3b shows the ratio (t_m / t_d) of time to peak response to the load duration.
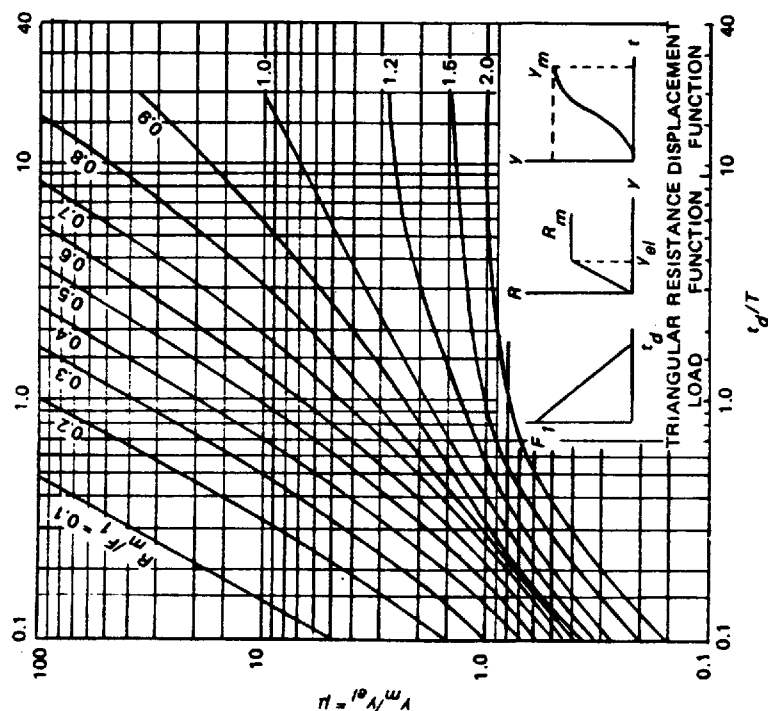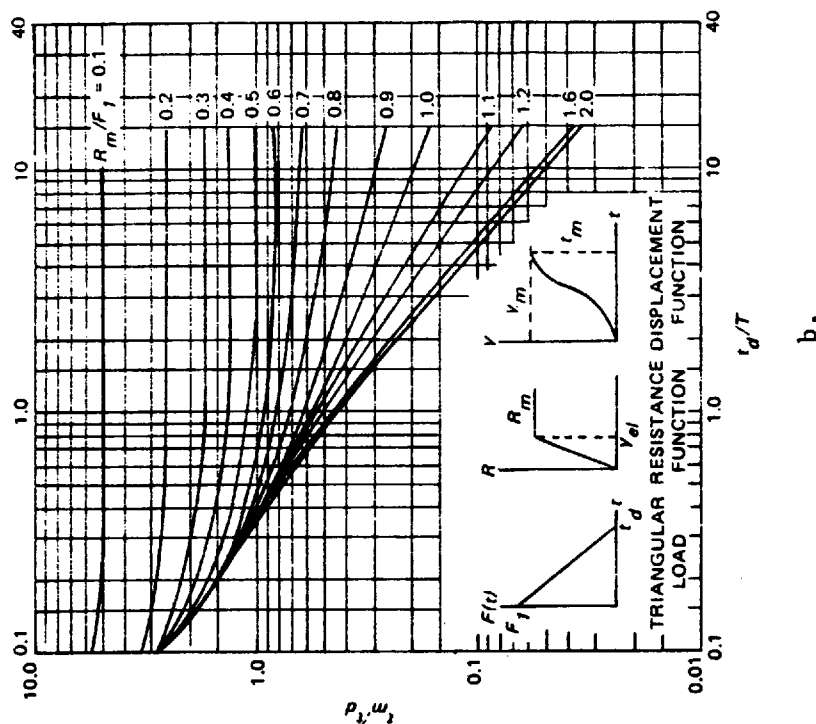
Figure 10-3. *Maximum response of elasto-plastic, undamped, single-degree systems due to triangular load pulses with zero rise time.*

US Army Corps of Engineers

(c) Response to impulsive loads. If the ratio (t_d / T) of duration to period is smaller than those in figure 10-3, the load may be considered to be impulsive and the following equation may be used.

$$\text{Required } R_m = \frac{i\,\omega}{\sqrt{2\mu - 1}} \qquad \text{(eq 10-4)}$$

where

i = impulse of load-time history
ω = natural circular frequency
μ = ductility ratio

The equation may be rearranged to give

$$\mu = 1/2 \left(\frac{i^2 \omega^2}{R_m^2} + 1 \right) \qquad \text{(eq 10-5)}$$

Note that equation 10-4 is an iterative design equation. Structural properties must be assumed in order to calculate the natural frequency, ω . These structural properties also determine the static capacity R_m. Therefore, iterations must be made to yield a structure whose natural frequency and static capacity reasonably satisfy equation 10-4.

  (d) *Response to instantaneously applied constant load.* If the ratio is greater than those given on the chart, the load may be considered to be an instantaneously applied constant load equal to F_1 . The response is defined by equation 10-6 and 10-7.

$$\text{Required } R_m = F1 \left(\frac{1}{1 - 1/2\mu} \right) \qquad \text{(eq 10-6)}$$

or

$$\mu = \frac{1}{2(1 - F_1/R_m)} \qquad \text{(eq 10-7)}$$

  (e) *Response to two-part pressure pulse.* If a bilinear pressure-time history like the one shown in figure 10-4 is used, the following approximate relationship conservatively predicts the response:

$$\frac{(F_1)_1}{R_m} C_1(\mu) + \frac{(F_1)_2}{R_m} C_2(\mu) = 1 \qquad \text{(eq 10-8)}$$

$C_1(\mu)$ and $C_2(\mu)$ are the values of R_m / F corresponding to a certain value of ductility ratio and the ratios of duration to period t_{d1}/T t_{d2}/T , respectively. A trial-and -error procedure must be used to determine the ductility. With the period and maximum resistance known, ductilities may be changed until the equation is satisfied.

2514
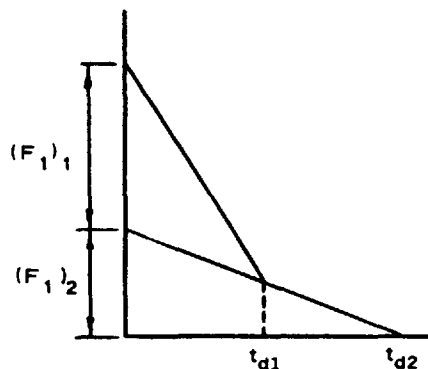
US Army Corps of Engineers

Figure 10-4. Bilinear load function.

10-3. Natural period.

The importance of the natural period to the response of a structure has already been shown in paragraph 10-2b. The following is a brief discussion of the natural period and which natural periods will be given.

a. If the mass if figure 10-1 is displaced downward and released, the mass will oscillate up and down through its initial equilibrium position. The time required for each cycle is constant and is known as the natural period T. The natural frequency f is the inverse of the natural period and is normally expressed in radians per second and is defined by :

$$\omega = 2\pi / T \qquad \text{(eq 10-9)}$$

b. A structure such as a beam, slab, etc., has an infinite number of degrees of freedom and therefore has an infinite number of natural frequencies. With each natural frequency there is associated a characteristic (modal) shape. It can be shown that any configuration assumed by the structure can be described by a linear combination of the characteristic shapes. For most load cases and structures considered in this manual, the major contribution to the deformed shape will be from only one mode. Therefore, the structure can be approximated by an SDOF system that has a frequency associated with the deformed shape of the structure.

(1) General equation for natural period. The period of any system may be calculated using the following expression.

$$T = 2\pi \sqrt{\frac{K_{LM}M_s}{k_f}} \qquad \text{(eq 10-10)}$$

where

K_{LM} = the load mass factor

M_s = the mass of the structure

k_f = the stiffness of the structure

Values for K_{LM} and formulas for k_f are given for several common structural elements in tables 10-1, 10-2, and 10-3. For a spring-mass system $K_{LM} = 1$, M_s = total mass, k_f = spring constant.

2515

Table 10-1. Transformation factors for beams and one-way slabs, simply supported boundary condition

Simply-Supported

Loading Diagram	Strain Range	Load Factor K_L	Mass Factor K_M		Load-Mass Factor K_{LM}		Maximum Resistance R_m	Spring Constant k	Dynamic Reaction V
			Concentrated Mass*	Uniform Mass	Concentrated Mass*	Uniform Mass			
$P = pl$	Elastic	0.64		0.50		0.78	$\dfrac{8M_P}{L}$	$\dfrac{384EI}{5L^3}$	$0.39R + 0.11P$
	Plastic	0.50		0.33		0.66	$\dfrac{8M_P}{L}$	0	$0.38R_m + 0.12P$
P	Elastic	1	1.0	0.49	1.0	0.49	$\dfrac{4M_P}{L}$	$\dfrac{48EI}{L^3}$	$0.78R - 0.28P$
	Plastic	1	1.0	.49	1.0	0.33	$\dfrac{4M_P}{L}$	0	$0.75R_m - 0.25P$
$F \quad F$	Elastic	0.87	0.76	0.52	0.87	0.60	$\dfrac{6M_P}{L}$	$\dfrac{56.4EI}{L^3}$	$0.525R - 0.25F$
	Plastic	1	1.0	0.56	1.0	0.56	$\dfrac{6M_P}{L}$	0	$0.52R_m - 0.02F$
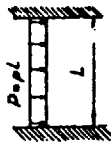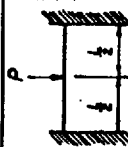
* Equal parts of the concentrated mass are lumped at each concentrated load

U S Army Corps of Engineers

M_{Ps} = Ultimate moment capacity at support
M_{Pm} = Ultimate moment capacity at midspan

Fixed Ends

Table 10-2. Transformation factors for beams and one-way slabs, fixed end boudary conditions

Loading Diagram	Strain Range	Load Factor K_L	Mass Factor K_M		Load-Mass Factor K_{LM}		Maximum Resistance R_m	Spring Constant k	Effective Spring Constant k_E	Dynamic Reaction V
			Concentrated Mass*	Uniform Mass	Concentrated Mass*	Uniform Mass				
	Elastic	0.53		0.41		0.77	$\dfrac{12M_{Ps}}{L}$	$\dfrac{384EI}{L^3}$		$0.36R+0.14P$
	Elasto-Plastic	0.64		0.50		0.78	$\dfrac{8(M_{Ps}+M_{Pm})}{L}$	$\dfrac{384EI}{5L^3}$	$\dfrac{307\,EI}{L^3}$	$0.39R+0.11P$
	Plastic	0.50		0.33		0.66	$\dfrac{8(M_{Ps}+M_{Pm})}{L}$	0		$0.38R_m+0.12P$
	Elastic	1	1.0	0.37	1.0	0.37	$\dfrac{4(M_{Ps}+M_{Pm})}{L}$	$\dfrac{192EI}{L^3}$		$0.71R-0.21P$
	Plastic	1	1.0	0.33	1.0	0.33	$\dfrac{4(M_{Ps}+M_{Pm})}{L}$	0		$0.75R_m-0.25P$

* Concentrated mass is lumped at the concentrated load.

US Army Corps of Engineers

TM 5-855-1

Table 10-3. *Transformation factors for beams and one-way slabs, simply supported and fixed end boundary conditions*

M_{Ps} = Ultimate moment capacity at support
M_{Pm} = Ultimate moment capacity at midspan

Simply-Supported and Fixed — L

Loading Diagram	Strain Range	Load Factor K_L	Mass Factor K_M Concentrated Mass*	Mass Factor K_M Uniform Mass	Load-Mass Factor K_{LM} Concentrated Mass	Load-Mass Factor K_{LM} Uniform Mass	Maximum Resistance R_m	Spring Constant k	Effective Spring Constant k_E	Dynamic Reaction V
(P=pL)	Elastic	0.58		0.45		0.78	$8M_{Ps}/L$	$185EI/L^3$	$\dfrac{160EI}{L^3}$	$V_1 = 0.26R+0.12P$ $V_2 = 0.43R+0.19P$
	Elasto-Plastic	0.64		0.50		0.78	$\dfrac{4(M_{Ps}+2M_{Pm})}{L}$	$\dfrac{384EI/L^3}{5}$		$V = 0.39R+0.11F\pm M_{Ps}/L$
	Plastic	0.50		0.33		0.66	$\dfrac{4(M_{Ps}+2M_{Pm})}{L}$	0		$V = 0.38R_m+0.12F\pm M_{Ps}/L$
(P)	Elastic	1.0	1.0	0.43	1.0	0.43	$16M_{Ps}/3L$	$107EI/L^3$	$\dfrac{160}{L^3}$	$V_1 = 0.25R+0.07F$ $V_2 = 0.54R+0.14F$
	Elasto-Plastic	1.0	1.0	0.49	1.0	0.49	$\dfrac{2(M_{Ps}+2M_{Pm})}{L}$	$48EI/L^3$		$V = 0.78R-0.28F\pm M_{Ps}/L$
	Plastic	1.0	1.0	0.33	1.0	0.33	$\dfrac{2(M_{Ps}+2M_{Pm})}{L}$	0		$V = 0.75R_m-0.25F\pm M_{Ps}/L$
(P/2, P/2)	Elastic	0.81	0.67	0.45	0.83	0.55	$6M_{Ps}/L$	$132EI/L^3$	$\dfrac{122EI}{L^3}$	$V_1 = 0.17R+0.17P$ $V_2 = 0.33R+0.33P$
	Elasto-Plastic	0.87	0.76	0.52	0.87	0.60	$\dfrac{2(M_{Ps}+3M_{Pm})}{L}$	$\dfrac{56EI}{L^3}$		$V = 0.52R-0.025F\pm M_{Ps}/L$
	Plastic	1.0	1.0	0.56	1.0	0.56	$\dfrac{2(M_{Ps}+3M_{Pm})}{L}$	0		$v = 0.52R_m-0.02F\pm M_{Ps}/L$

* Equal parts of the concentrated mass are lumped at each concentrated load.

US Army Corps of Engineers

(2) Boundary conditions of structural elements. In most structural systems the boundary conditions are neither simple nor fixed supports, and the period of the beam, slab, arch, or other structure will be somewhere in between the fixed case and the simple case. Unless it can be shown that the boundary conditions are truly simply supports, the fixed boundary conditions or the methods of paragraph 10-3B (5) below, should be used. In the dynamic analysis of conventional weapons effects, it is generally conservative to use the lower period. Therefore, assuming the beam or slab to be fixed is a conservative assumption.

(3) Beams and one-way slabs. For beams and one-way slabs K_{LM} and k_f are given in tables 10-1, 10-2, and 10-3 for various beam fixity conditions and loadings. The constants are given for elastic, plastic, and sometimes elastic-plastic ranges of strain. For most analyses, the elastic-plastic range using the effective spring constant is recommended. If these values are not given, the elastic values should be used. If an elastic analysis is to be performed, the elastic values should be used. If M_s is the mass of structure or mass/unit width, the period is then defined by

$$ T = 2\pi \sqrt{\frac{K_{LM} M_S}{k_f}} \qquad \text{(eq 10-11)} $$

(4) Two-way slabs. The period of two-way slabs may be calculated in the same manner as one-way slabs using the values in 10-4 through 10-7. For two-way slabs the effective spring constant is not given but may be constructed so that the area under the elastic-plastic portion of the resistance curve is the same.

Table 10-4. Transformation factors for two-way slabs, simple supports, uniform load for Poisson's ratio = 0.3
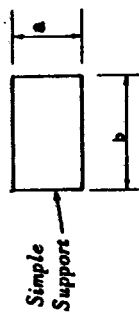
M_{Pfa}, M_{Pfb} = Total positive ultimate moment capacity along midspan section parallel to edges a and b, respectively
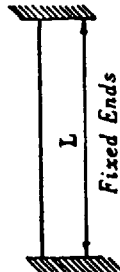
Strain Range	a/b	Load Factor K_L	Mass Factor K_M	Load-Mass Factor K_{LM}	Maximum Resistance	Spring Constant k	Dynamic Reactions V_A	Dynamic Reactions V_B
Elastic	1.0	0.45	0.31	0.68	$\frac{12}{a}(M_{Pfa}+M_{Pfb})$	$252\,EI_a/a^2$	0.07P+0.18R	0.07P+0.18R
	0.9	0.47	0.33	0.70	$\frac{1}{a}(12M_{Pfa}+11M_{Pfb})$	$230\,EI_a/a^2$	0.06P+0.16R	0.08P+0.20R
	0.8	0.49	0.35	0.71	$\frac{1}{a}(12M_{Pfa}+10.3M_{Pfb})$	$212\,EI_a/a^2$	0.06P+0.14R	0.08P+0.22R
	0.7	0.51	0.37	0.73	$\frac{1}{a}(12M_{Pfa}+9.8M_{Pfb})$	$201\,EI_a/a^2$	0.05P+0.13R	0.08P+0.24R
	0.6	0.53	0.39	0.74	$\frac{1}{a}(12M_{Pfa}+9.3M_{Pfb})$	$197\,EI_a/a^2$	0.04P+0.11R	0.09P+0.26R
	0.5	0.55	0.41	0.75	$\frac{1}{a}(12M_{Pfa}+9.0M_{Pfb})$	$201\,EI_a/a^2$	0.04P+0.09R	0.09P+0.28R
Plastic	1.0	0.33	0.17	0.51	$\frac{12}{a}(M_{Pfa}+M_{Pfb})$	0	$0.09P+0.16R_m$	$0.09P+0.16R_m$
	0.9	0.35	0.18	0.51	$\frac{1}{a}(12M_{Pfa}+11M_{Pfb})$	0	$0.08P+0.15R_m$	$0.09P+0.18R_m$
	0.8	0.37	0.20	0.54	$\frac{1}{a}(12M_{Pfa}+10.3M_{Pfb})$	0	$0.07P+0.13R_m$	$0.01P+0.20R_m$
	0.7	0.38	0.22	0.58	$\frac{1}{a}(12M_{Pfa}+9.8M_{Pfb})$	0	$0.06P+0.12R_m$	$0.10P+0.22R_m$
	0.6	0.40	0.23	0.58	$\frac{1}{a}(12M_{Pfa}+9.3M_{Pfb})$	0	$0.05P+0.10R_m$	$0.01P+0.25R_m$
	0.5	0.42	0.25	0.59	$\frac{1}{a}(12M_{Pfa}+9.0M_{Pfb})$	0	$0.04P+0.08R_m$	$0.11P+0.27R_m$

Simple Support

US Army Corps of Engineers

Table 10-5. Transformation factors for two-way slabs, fixed supports, uniform load for Poisson's ratio = 0.3
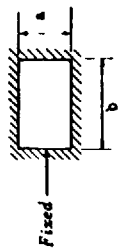
M_{Psa}, M_{Psb} = Total negative ultimate moment capacity along edges a and b, respectively

M^o_{Psa}, M^o_{Psb} = Negative ultimate moment capacity per unit width at edges a and b, respectively

Strain Range	a/b	Load Factor K_L	Mass Factor K_M	Load-Mass Factor K_{LM}	Maximum Resistance	Spring Constant k	Dynamic Reactions V_A	V_B
Elastic	1.0	0.33	0.21	0.63	$29.2 M^o_{Psb}$	$810 EI_a/a^2$	$0.10P+0.15R$	$0.10P+0.15R$
	0.9	0.34	0.23	0.68	$27.4 M^o_{Psb}$	$743 EI_a/a^2$	$0.09P+0.14R$	$0.10P+0.17R$
	0.8	0.36	0.25	0.69	$26.4 M^o_{Psb}$	$706 EI_a/a^2$	$0.08P+0.12R$	$0.11P+0.19R$
	0.7	0.38	0.27	0.71	$26.2 M^o_{Psb}$	$692 EI_a/a^2$	$0.07P+0.11R$	$0.11P+0.21R$
	0.6	0.41	0.29	0.71	$27.3 M^o_{Psb}$	$724 EI_a/a^2$	$0.06P+0.09R$	$0.12P+0.23R$
	0.5	0.43	0.31	0.72	$30.2 M^o_{Psb}$	$806 EI_a/a^2$	$0.05P+0.08R$	$0.12P+0.25R$
Elasto-Plastic	1.0	0.46	0.31	0.67	$\frac{1}{a}[12(M_{Pfa}+M_{Psa})+12(M_{Pfb}+M_{Psb})]$	$262 EI_a/a^2$	$0.07P+0.18R$	$0.07P+0.18R$
	0.9	0.47	0.33	0.70	$\frac{1}{a}[12(M_{Pfa}+M_{Psa})+11(M_{Pfb}+M_{Psb})]$	$230 EI_a/a^2$	$0.06P+0.16R$	$0.08P+0.20R$
	0.8	0.49	0.35	0.71	$\frac{1}{a}[12(M_{Pfa}+M_{Psa})+10.3(M_{Pfb}+M_{Psb})]$	$212 EI_a/a^2$	$0.06P+0.14R$	$0.08P+0.22R$
	0.7	0.51	0.37	0.73	$\frac{1}{a}[12(M_{Pfa}+M_{Psa})+9.8(M_{Pfb}+M_{Psb})]$	$201 EI_a/a^2$	$0.5P+0.13R$	$0.08P+0.24R$
	0.6	0.53	0.39	0.74	$\frac{1}{a}[12(M_{Pfa}+M_{Psa})+9.3(M_{Pfb}+M_{Psb})]$	$197 EI_a/a^2$	$0.04P+0.11R$	$0.09P+0.26R$
	0.5	0.55	0.41	0.75	$\frac{1}{a}[12(M_{Pfa}+M_{Psa})+9.0(M_{Pfb}+M_{Psb})]$	$201 EI_a/a^2$	$0.04P+0.09R$	$0.09P+0.28R$
Plastic	1.0	0.33	0.17	0.51	$\frac{1}{a}[12(M_{Pfa}+M_{Psa})+12(M_{Pfb}+M_{Psb})]$	0	$0.09P+0.16R_m$	$0.09P+0.16R_m$
	0.9	0.35	0.18	0.51	$\frac{1}{a}[12(M_{Pfa}+M_{Psa})+11(M_{Pfb}+M_{Psb})]$	0	$0.08P+0.15R_m$	$0.09P+0.18R_m$
	0.8	0.37	0.20	0.54	$\frac{1}{a}[12(M_{Pfa}+M_{Psa})+10.3(M_{Pfb}+M_{Psb})]$	0	$0.07P+0.13R_m$	$0.10P+0.20R_m$
	0.7	0.38	0.22	0.58	$\frac{1}{a}[12(M_{Pfa}+M_{Psa})+9.8(M_{Pfb}+M_{Psb})]$	0	$0.06P+0.12R_m$	$0.10P+0.22R_m$
	0.6	0.40	0.23	0.58	$\frac{1}{a}[12(M_{Pfa}+M_{Psa})+9.3(M_{Pfb}+M_{Psb})]$	0	$0.05P+0.10R_m$	$0.10P+0.25R_m$
	0.5	0.42	0.25	0.59	$\frac{1}{a}[12(M_{Pfa}+M_{Psa})+9.0(M_{Pfb}+M_{Psb})]$	0	$0.04P+0.08R_m$	$0.11P+0.27R_m$

Fixed

US Army Corps of Engineers

TM 5-855-1

Table 10-6. Transformation factors for two-way slabs: short edges fixed – long edges simply supported for Poisson's ratio = 0.3

Strain Range	a/b	Load Factor K_L	Mass Factor K_M	Load-Mass Factor K_{LM}	Maximum Resistance	Spring Constant k	Dynamic Reactions V_A	V_B
Elastic	1.0	0.39	0.26	0.67	$20.4 M^o_{Psa}$	$575\,EI_a/a2$	$0.09P+0.16R$	$0.07P+0.18R$
	0.9	0.41	0.28	0.68	$10.2 M^o_{Psa} + \frac{11}{a} M_{Pfb}$	$476\,EI_a/a2$	$0.08P+0.14R$	$0.08P+0.20R$
	0.8	0.44	0.30	0.68	$10.2 M^o_{Psa} + \frac{10.3}{a} M_{Pfb}$	$396\,EI_a/a2$	$0.08P+0.12R$	$0.08P+0.22R$
	0.7	0.46	0.33	0.72	$9.3 M^o_{Psb} + \frac{9.7}{a} M_{Pfb}$	$328\,EI_a/a2$	$0.07P+0.11R$	$0.08P+0.24R$
	0.6	0.48	0.35	0.73	$8.5 M^o_{Psb} + \frac{9.3}{a} M_{Pfb}$	$283\,EI_a/a2$	$0.06P+0.09R$	$0.09P+0.26R$
	0.5	0.51	0.37	0.73	$7.4 M^o_{Psb} + \frac{9.0}{a} M_{Pfb}$	$243\,EI_a/a2$	$0.05P+0.08R$	$0.09P+0.28R$
Elasto-Plastic	1.0	0.46	0.31	0.67	$\frac{1}{a}[12(M_{Pfa}+M_{Psa})+12(M_{Pfb})]$	$271\,EI_a/a2$	$0.07P+0.18R$	$0.07P+0.18R$
	0.9	0.47	0.33	0.70	$\frac{1}{a}[12(M_{Pfa}+M_{Psa})+12(M_{Pfb})]$	$248\,EI_a/a2$	$0.06P+0.16R$	$0.08P+0.20R$
	0.8	0.49	0.35	0.71	$\frac{1}{a}[12(M_{Pfa}+M_{Psa})+10.3(M_{Pfb})]$	$228\,EI_a/a2$	$0.06P+0.14R$	$0.08P+0.22R$
	0.7	0.51	0.37	0.72	$\frac{1}{a}[12(M_{Pfa}+M_{Psa})+9.7(M_{Pfb})]$	$216\,EI_a/a2$	$0.05P+0.13R$	$0.08P+0.24R$
	0.6	0.53	0.37	0.70	$\frac{1}{a}[12(M_{Pfa}+M_{Psa})+9.3(M_{Pfb})]$	$212EI_a/a2$	$0.04P+0.11R$	$0.09P+0.26R$
	0.5	0.55	0.41	0.74	$\frac{1}{a}[12(M_{Pfa}+M_{Psa})+9.0(M_{Pfb})]$	$216\,EI_a/a2$	$0.04P+0.09R$	$0.09R+0.28R$
Plastic	1.0	0.33	0.17	0.51	$\frac{1}{a}[12(M_{Pfa}+M_{Psa})+12M_{Pfb})]$	0	$0.09P+0.16R_m$	$0.09P+0.16R_m$
	0.9	0.35	0.18	0.51	$\frac{1}{a}[12(M_{Pfa}+M_{Psa})+11M_{Pfb})]$	0	$0.08P+0.15R_m$	$0.09P+0.18R_m$
	0.8	0.37	0.20	0.54	$\frac{1}{a}[12(M_{Pfa}+M_{Psa})+10.3M_{Pfb})]$	0	$0.07P+0.13R_m$	$0.10P+0.20R_m$
	0.7	0.38	0.22	0.58	$\frac{1}{a}[12(M_{Pfa}+M_{Psa})+9.7M_{Pfb})]$	0	$0.06P+0.12R_m$	$0.10P+0.22R_m$
	0.6	0.40	0.23	0.58	$\frac{1}{a}[12(M_{Pfa}+M_{Psa})+9.3 M_{Pfb})]$	0	$0.05P+0.10R_m$	$0.10P+0.25R_m$
	0.5	0.42	0.25	0.59	$\frac{1}{a}[12(M_{Pfa}+M_{Psa})+9.0M_{Pfb})]$	0	$0.04P+0.08R_m$	$0.11P+0.27R_m$

Simple Support — Fixed, b, a

US Army Corps of Engineers

Table 10-7.
Transformation factors for two-way slabs: short sides simply supported – long sides fixed
for Poisson's ratio = 0.3

Strain Range	a/b	Load Factor K_L	Mass Factor K_M	Load-Mass Factor K_{LM}	Maximum Resistance	Spring Constant k	Dynamic Reactions V_A	Dynamic Reactions V_B
Elastic	1.0	0.39	0.26	0.67	$20.4\,M^o_{Pab}$	$575\,EI_a/a^2$	$0.07P+0.187R$	$0.09P+0.16R$
	0.9	0.40	0.28	0.70	$19.5\,M^o_{Pab}$	$600\,EI_a/a^2$	$0.06P+0.16R$	$0.10P+0.18R$
	0.8	0.42	0.29	0.69	$19.5\,M^o_{Pab}$	$610\,EI_a/a^2$	$0.06P+0.14R$	$0.11P+0.19R$
	0.7	0.43	0.31	0.71	$20.2\,M^o_{Pab}$	$662\,EI_a/a^2$	$0.05P+0.13R$	$0.11P+0.21R$
	0.6	0.45	0.33	0.73	$21.2\,M^o_{Pab}$	$731\,EI_a/a^2$	$0.04P+0.11R$	$0.12P+0.23R$
	0.5	0.47	0.34	0.72	$22.2\,M^o_{Pab}$	$850\,EI_a/a^2$	$0.04P+0.09R$	$0.12P+0.25R$
Elasto-Plastic	1.0	0.46	0.31	0.67	$\frac{1}{a}[12M_{Pfa}+12(M_{Psb}+M_{Pfb})]$	$271\,EI_a/a^2$	$0.07P+0.18R$	$0.07P+0.18R$
	0.9	0.47	0.33	0.70	$\frac{1}{a}[12M_{Pfa}+11(M_{Psb}+M_{Pfb})]$	$248\,EI_a/a^2$	$0.06P+0.16R$	$0.08P+0.20R$
	0.8	0.49	0.35	0.71	$\frac{1}{a}[12M_{Pfa}+10.3(M_{Psb}+M_{Pfb})]$	$228\,EI_a/a^2$	$0.06P+0.14R$	$0.08P+0.22R$
	0.7	0.51	0.37	0.73	$\frac{1}{a}[12M_{Pfa}+9.8(M_{Psb}+M_{Pfb})]$	$216\,EI_a/a^2$	$0.05P+0.13R$	$0.06P+0.24R$
	0.6	0.53	0.39	0.74	$\frac{1}{a}[12M_{Pfa}+9.3(M_{Psb}+M_{Pfb})]$	$212\,EI_a/a^2$	$0.04P+0.11R$	$0.09P+0.26R$
	0.5	0.55	0.41	0.74	$\frac{1}{a}[12M_{Pfa}+9.0(M_{Psb}+M_{Pfb})]$	$216\,EI_a/a^2$	$0.04P+0.09R$	$0.09P+0.26R$
Plastic	1.0	0.33	0.17	0.51	$\frac{1}{a}[12M_{Pfa}+12(M_{Psb}+M_{Pfb})]$	0	$0.09P+0.16R_m$	$0.09P+0.16R_m$
	0.9	0.35	0.18	0.51	$\frac{1}{a}[12M_{Pfa}+11(M_{Psb}+M_{Pfb})]$	0	$0.08P+0.15R_m$	$0.09P+0.18R_m$
	0.8	0.37	0.20	0.54	$\frac{1}{a}[12M_{Pfa}+10.3(M_{Psb}+M_{Pfb})]$	0	$0.07P+0.13R_m$	$0.10P+0.20R_m$
	0.7	0.36	0.22	0.58	$\frac{1}{a}[12M_{Pfa}+9.8(M_{Psb}+M_{Pfb})]$	0	$0.06P+0.12R_m$	$0.10P+0.22R_m$
	0.6	0.40	0.23	0.58	$\frac{1}{a}[12M_{Pfa}+9.3(M_{Psb}+M_{Pfb})]$	0	$0.05P+0.10R_m$	$0.10P+0.25R_m$
	0.5	0.42	0.25	0.59	$\frac{1}{a}[12M_{Pfa}+9.0(M_{Psb}+M_{Pfb})]$	0	$0.04P+0.08R_m$	$0.11P+0.27R_m$

Fixed / Simple / a / b

US Army Corps of Engineers

(5) Box structures. Finite element calculations, backed up by experimental data, were used to determine the natural frequencies of box structures with various span–to–thickness and aspect ratios. The height of the box was equal to the width of the box, the thickness of the roof was equal to the thickness of the floor and walls, and 1–percent tensile and compressive steel was used. These analyses show that for a span–to–effective_depth ratio L/df of 4, the period of the roof is nearly the same as the period of a simply supported slab while the period of the roof with an L/dv of 10 is more like a fixed slab. Most protective structures will have an L/df within these limits, and their frequency may beated using the following equation.

$$ f = \frac{\sqrt{p}}{C_s} \left(\frac{1}{L_s/d_f} \right) \left(\frac{1}{L_s} \right) \left(\frac{L_s^2 + B_L^2}{B_L^2} \right) \qquad \text{(eq 10-12)} $$
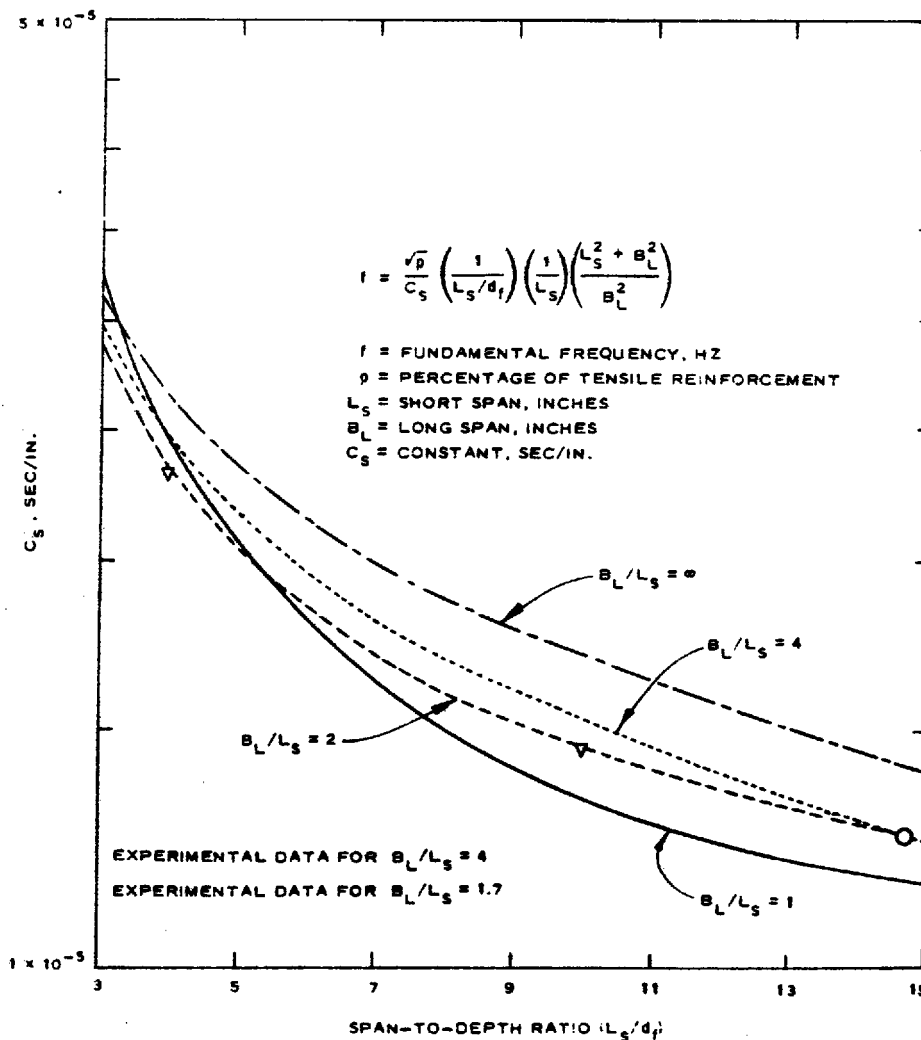
US Army Corps of Engineers

Figure 10-5 is a plot of the constant Cs for various Ls/df ratios, and all other variables are defined.

(6) Frames.

(a) Transformation factors can be obtained for frames such as the one shown in figure 10–6. The masses m_1 and m_2 are uniformly distributed along the roof and sides and the dynamic load includes a concentrated force at roof level plus a uniformly distributed load on one wall surface. The frame is assumed to deflect horizontally as shown in figure 10–6 with the side walls remaining straight. The displacement of the replacement system is taken to be equal to that at the top of the frame, and the mass of the equivalent system is given by

$$M_{eq} = m_1 L + \frac{2 m_2 h}{3} \qquad \text{(eq 10-13)}$$

This equivalent force is equal to

$$F_{eq} = F(t) + p(t)\frac{h}{2} \qquad \text{(eq 10-14)}$$

The equivalent stiffness k_{eq} is equal to the actual stiffness of the frame referred to a horizontal load applied at the top of the frame, and is concentrated force required to produce a unit horizontal displacement of the roof.
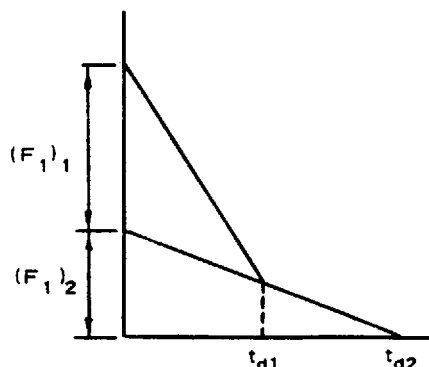
US Army Corps of Engineers

Figure 10–6. Equivalent SDOF system.

(b) The maximum resistance of both the actual and equivalent system is simply the maximum horizontal force which can be carried by the frame. If the girders are rigid compared to the columns (the more common case), then

$$R_m = R_{m_{eq}} = \frac{4M_{uc}}{h} \qquad \text{(eq 10-15)}$$

where M_{uc} = ultimate bending moment capacity of each column. With the properties of equivalent system shown in figure 10-6c established, the next step is an SDOF analysis to obtain frame deflections and, from these deflections, stresses within the frame. For multistory frames, it is generally sufficiently accurate to lump the load and mass at the floor levels on the basis of tributary wall area.

(7) Effect of earth cover on natural frequency. Recent experiments have shown that earth cover has very little if any effect on the natural period of slabs and arches. The only effect which the soil could have on the period would be to provide additional mass which would increase the period of the structure. For the type of blast loads considered in this manual, it is conservative to consider the period unaffected by soil cover.

10-4 Dynamic reaction

The dynamic reactions for beams and one—way slabs and two—way slabs are given in tables 10-1 through 10-7. Both R and F in the equations for dynamic reaction are functions of time. If the maximum values of both R and F are used, the value of the dynamic reaction is an upper bound and in many cases a very conservative estimate.

CHAPTER 11

IN–STRUCTURE SHOCK

11-1. Introduction

The major concern in the design of a protective structure is to prevent structural failure. However, the operation of sophisticated electronic gear within a facility such as a command and control center may be impaired at shock levels much less than those required to fail the structure, thus preventing the center from completing its mission. In order to economically design shock isolation devices to protect the various components within the structure, the internal shock environment must be well defined. For long motions associated with nuclear events, the procedure for the modification of the free–field ground motion to predict the in–structure motion is well documented. However, procedures for predicting the in–structure shock environment in the case of short–duration ground shock, such as that generated by conventional weapons, are not so well established.

11-2. Rectangular buried structures

a. Side burst load case. The simplified methods given below will take into account the attenuation of the ground shock as it traverses the structure. The computed value for in–structure acceleration, velocity, and displacement will be in the horizontal direction at the center of the structure. Experimental evidence indicates that vertical acceleration, velocity, and displacement will be approximately 20 percent of the horizontal values in the case of a side burst. Also, the horizontal motions are very uniform over the entire floor of the structure, while the vertical motions at the leading edge are twice the midspan values.

(1) In–structure accelerations, velocities, and displacements may be predicted by modifying the free–field values. The acceleration of a structure, such as the structure shown in figure 11–1, may be predicted by using the average value of free–field acceleration over the span of the structure.
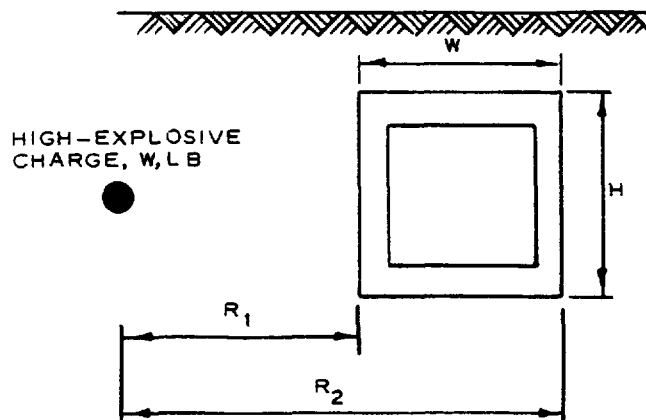
US Army Corps of Engineers

Figure 11–1. Average acceleration for side burst load case of a buried rectangular structure.

(2) The average value of acceleration is found by integrating the acceleration–range function given in chapter 5 over the span of the structure. The average acceleration for the structure is the uniform acceleration which yields the same integral across the structure. The average velocity and displacement are obtained using the same method. Equations 11–1, 11–2, and 11–3 give the average free–field acceleration, velocity, and displacement, respectively, across a rectangular buried structure.

$$A_{avg} \times W^{1/3} = \frac{50 f c W^{[(n+1)/3]} \left[R_1^{-n} - R_2^{-n} \right]}{n(R_2 - R_1)} \text{, lb}^{1/3} \text{ g's} \qquad \text{(eq 11-1)}$$

$$V_{avg} = \frac{160 f W^{(n/3)} \left[R_1^{(-n+1)} - R_2^{(-n+1)} \right]}{(n-1)(R_2 - R_1)} \text{, fps} \qquad \text{(eq 11-2)}$$

$$\frac{d_{avg}}{W^{1/3}} = \frac{500 f W^{[(n-1)/3]} \left[R_1^{(-n+2)} - R_2^{(-n+2)} \right]}{c(n-2)(R_2 - R_1)} \text{, } \frac{ft}{lb^{1/3}} \qquad \text{(eq 11-3)}$$

where

A_{avg} = average free-field acceleration across structure, g's
W = weapon yield
f = coupling factor, from chapter 5
c = seismic velocity, fps, from chapter 5
n = attenuation coefficient, from chapter 5
R_1 and R_2 = range, ft (fig 11-1)
V_{avg} = average free-field velocity across structure, fps
d_{avg} = average free-field displacement across structure, ft

(3) The average free–field values of acceleration and velocity overpredict the in–structure values. The information shown in figure 11–2 may be used to reduce these values. The reduction factor RF was determined as the ratio of the pressure ordinate for an equivalent uniformly distributed load to the maximum pressure ordinate from the actual load distribution. The equivalent uniform load was determined over a wall with dimension of H and L .

(4) In–structure accelerations may be predicted by obtaining the average free–field acceleration from equation 11–1 and multiplying this average by the reduction factor given in figure 11–2. Test data have shown this method to be conservative for rectangular buried structures. Velocities are predicted using equation 11–2 and figure 11–2. Test data have shown that this method yields results close to experimental values.

2528
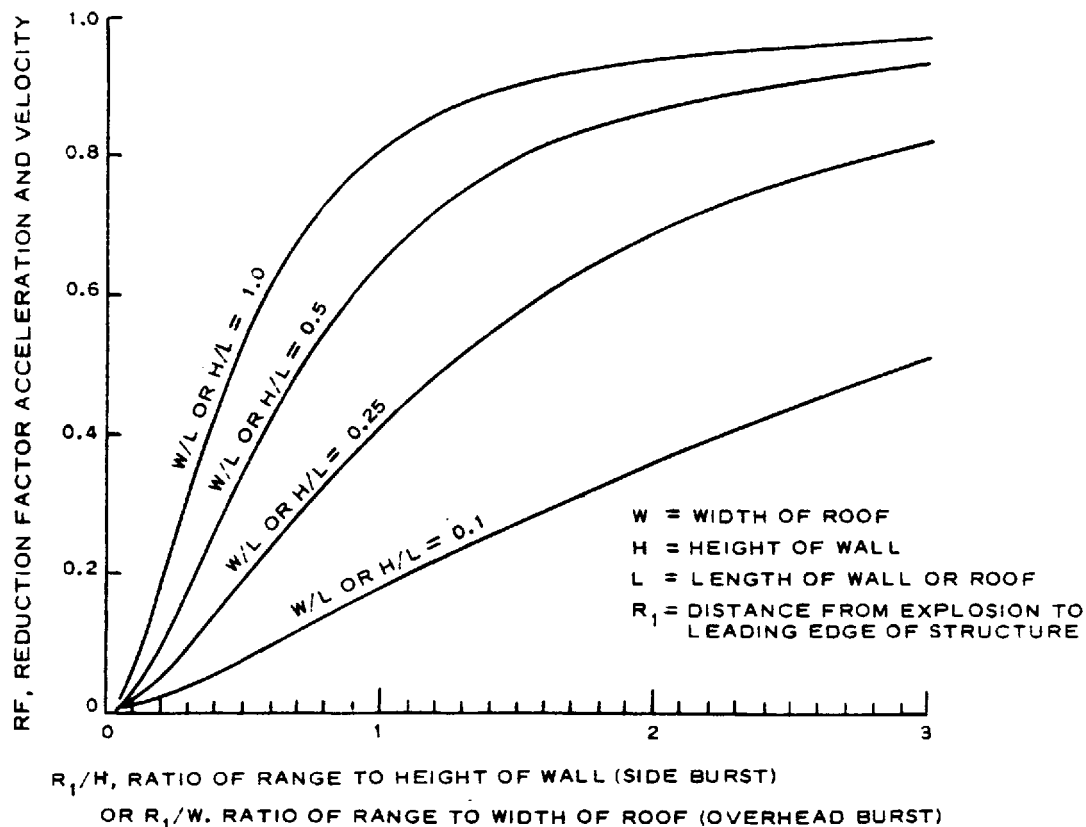
Figure 11-2. Reduction factor for in-structure acceleration and velocity.

(5) Equation 11-3 should be used to predict the in-structure displacement with no reduction factor.

b. Overhead burst. The same equations used for side bursts should be used for an overhead burst. R_1 and R_2 are now defined by figure 11-3. These values must be modified by a reduction factor obtained from figure 11-2, using the roof dimensions of W and L . For large structures, some judgment is required in selecting the dimensions W , H , and L for a burst that is not symmetrically located over the structure roof for an overhead burst and exterior wall for a side burst. Figure 11-4 shows an example in which the dimensions of one bay in a multibay structure were used to calculate in-structure shock.

HIGH-EXPLOSIVE
CHARGE, W, LB
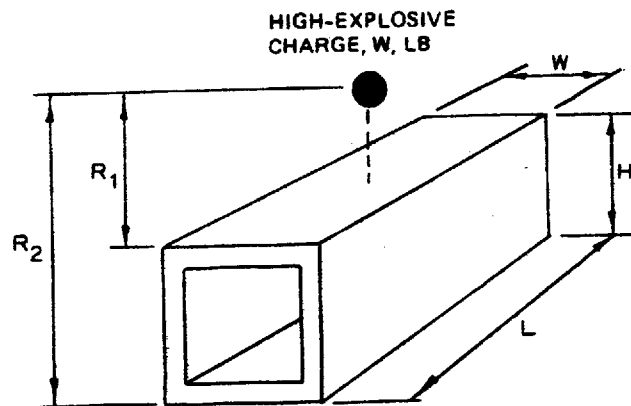
US Army Corps of Engineers

Figure 11–3. Average acceleration for overhead burst on a rectangular buried structure.
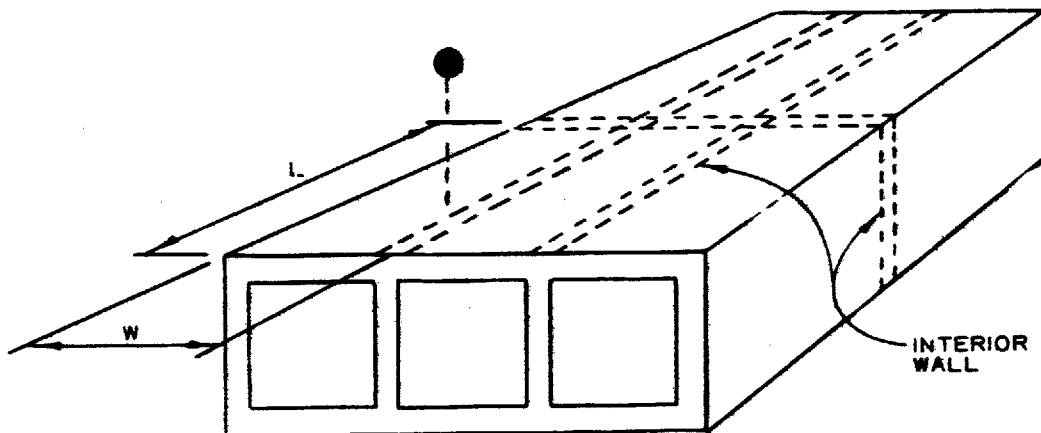
US Army Corps of Engineers

Figure 11–4. Roof dimensions for overhead burst on a buried multibay structure.

c. In–structure shock spectra. Once the peak values for in–structure acceleration, velocity, and displacement have been determined, they can be used to develop an approximate in–structure shock spectra.

(1) Let D be the maximum relative displacement between a simple spring–mass oscillator and the floor of the structure. The relations between the maximum relative displacement D , the pseudovelocity V , and the pseudoacceleration A are as follows:

$$V = {}_\omega D \tag{eq 11-4}$$

$$A = {}_\omega V = {}_\omega{}^2 D \tag{eq 11-5}$$

where ω is the natural circular frequency of the oscillator in radians per second. The pseudovelocity V is nearly equal to the maximum relative velocity for systems with moderate or high frequencies, but may differ considerably from the maximum relative velocity for very low frequency systems. The acceleration A is exactly equal to the maximum acceleration for systems with no damping and is not greatly different from the maximum acceleration for systems with moderate amounts of damping.

(2) In general, D , V , and A will be larger than the peak values for the floor motion. A conservative estimate for D , V , and   A can be made by multiplying the floor motions by the appropriate amplification factors. A limited amount of data from high–explosive tests on model structures indicate average amplification factors for systems damped at 5 percent of critical of approximately 1.2, 1.5, and 1.6 for displacement, velocity, and acceleration, respectively. For lightly damped systems (5 to 10 percent of critical damping) respective amplification factors of 1, 1.5, and 2.0 for relative displacement, pseudovelocity, and acceleration are generally used for earthquake–generated ground motions. Therefore, for developing an approximate in–structure design shock spectra for damping equal to 5 to 10 percent of critical, respective amplification factors of 1.2, 1.5, and 2.0 for relative displacement, pseudovelocity, and acceleration are recommended.

11–3. Contact bursts on buried structures

Because of the tamping effect of the soil backfill, shock levels in underground structures exposed to contact bursts can be extremely high; therefore, these situations should be avoided if possible. A reinforced concrete burster slab, or a burster layer comprised of rubble, placed flush with the ground can prevent the weapon from penetrating the backfill material and detonating adjacent to the structure.

CHAPTER 12

AUXILIARY SYSTEMS

12-1. Equipment protection

Equipment installed in facilities covered by this manual will be operated in a shock environment when the facilities come under enemy attack. Therefore, designers must consider equipment protection during design so that the installed equipment will not be misaligned or overstressed.

   a. *General.* Ideally, a knowledge of the upper limit of the shock environment which the equipment can tolerate (i.e., equipment fragility level) is desirable. With this information, sufficiently rugged equipment to withstand the potential shock environment can be selected. Unfortunately, the cost for testing of equipment to establish such data could be prohibitive. Further, because of constraints of procurement procedures, the designer has limited control over the exact model and make of equipment that will eventually be installed in the facility. In practice, the best information the designer can rely on is the test data and experience gained from previous military programs. The data base is still rather limited in terms of the types of equipment tested and probably does not contain the identical model and make of equipment that will eventually be installed in the facilities being designed. If a large number of standard facilities are planned, the designer can specify the type of shock test and require the manufacturer to demonstrate that his equipment will survive the specified environment.

   (1) This chapter provides information and guidance for making use of available data to the best advantage for equipment protection considerations during facility design. It should be recognized, however, that shock testing of some items of critical equipment may still be required for hardness verification.

   (2) Table 12-1 provides designers with information for designing or specifying equipment details that significantly affect shock resistance of various types of equipment. The information in the table is obtained from many sources which document the experience gained from several previous military programs. The itemized format will permit the designer to select appropriate items for incorporation into equipment design or procurement specifications.

TM 5-855-1

Table 12-1 Characteristics of shock-resistant equipment

Materials

1. Do not use cast iron.

2. Do not use porcelain plumbing fixtures

3. Do not use low strength insulating materials such as transite and cold molded products.

4. Pipe nipples (1-1/2 inches and smaller): Use extra strong pipe or better of steel, Monel, or copper nickel.

5. Bolts: Use materials having high yield strength to minimize stretching under shock that will loosen the joint.

6. Dowel pins and receptacles should be made of steel.

7. Cathode ray tube supports should be made of firm rubber.

8. Do not use sheet metal for structural members.

9. Do not use cast aluminum to support transformers.

10. Do not use carbon pump seals. They have demonstrated a low resistance to shock.

11. Do not use ceramics and other rigid, brittle materials as insulators. Shock may crack and destroy such insulators. Use more flexible materials for insulators.

Fasteners

12. Provide positive means of locking nuts to prevent loosening.

13. Where possible, use fitted bolts to reduce slippage.

14. Do not use friction due to weight of equipment or spring clips to keep equipment in place.

15. Small bolts have less strength under shock than larger bolts.

16. Avoid bolts and nuts having abrupt changes in shape, such as shoulders, fillets, notches, grooves, and holes since the stress risers at these points contribute to a lower shock resistance.

17. Shock resistance in bolts can be improved by undercutting the shank diameter to slightly less than the root of the thread

18. Fine threaded bolts are more resistant to loosening by shock and vibration than are coarse threaded bolts.

19. Bolts connecting friction joints should be torqued down until slight yielding takes place in the bottom threads, thus ensuring maximum tightness. Preloading resulting from torquing can be estimated from the following formula

2533

$$M = 0.2DF \text{ inch-pounds}$$

where M = torque applied to bolt, inch-pounds

D = diameter of bolt, inches

F = preload tension in bolt, pounds

Periodically the preload must be checked to prevent loosening.

20. Bolt locking devices that depend on friction tend to lose their effectiveness through repeated use and should be avoided.

21. Lock washers with sawtooth edges with an axial set to the teeth that prevent loosening by wedge action are not suitable for use in equipment subjected to severe shock.

22. Dowel pins and receptacles: (a) Should be between 1/4 to 1/2 inch in diameter and no longer than an inch, (b) receptacles should be made with a close fit to the pin, (c) between cabinet and chassis: located pin on cabinet frame and receptacle on chassis.

23. Do not use quick release fasteners to carry large loads. Quick releases fasteners may be used to fasten light inspection covers or plates.

24. Do not use quick release fasteners on light plates that retain filters in filter racks in an air handling unit.

25. Fasteners used to attach door to cabinets must be capable of resisting combined shear and tensile loads resulting from shock. This section presents a procedure for doing this.

26. Door hinges and latches must also be designed to take the loads imposed by shock. This section presents a procedure for doing this.

27. Use bolts, nuts, and washers, to fasten sheet metal parts. Do not use sheet metal screws since they strip out when shocked. Fastener holes in sheet metal should be at least 1/2 inch form the edge to prevent tearing.

28. Rivets: (a) Do not use cold-driven rivets, (b) Hot-driven rivets may be used, but in general rivets should be avoided.

29. All latching surfaces should be well fitted.

Welding and Brazing

30. Welded or brazed joints when done properly are highly shock resistant and more desirable than bolted joints. Strict quality control must be observed, however, or these types of joints will be more susceptible to shock than bolted joints. Strict quality control must be observed, however, or these types of joints will be more susceptible to shock than bolted joints.

31. Use full depth welds and avoid crevasses and sharp corners where stress concentrations can build up.

32. Avoid short intermittent welds less than 1.5 inches long and with spacing less than or equal to 4 inches.

33. Welded joints are usually the tightest and therefore are desirable from this aspect.

34. Do not use spot welds to connect structural load bearing members.

2534

TM 5-855-1

35. Spot welds can be used to fasten a metal skin to a structural framework, if: (a) accepted quality control methods are used and followed stringently, (b) frequent tests are conducted to show that proper welding conditions exist.

Equipment (General)

36. Do not cantilever equipment parts (e.g., flywheels, extended shafts, castings, motors, and large protrusions, in general).

37. Equipment parts should be located far enough apart to prevent collision or impact during shock.

38. Shock resistance can be improved by using stiffer member, smaller masses, and large clearances.

39. To prevent billiard ball action, rubber or low frequency spring should be placed between two movable parts.

40. Equipment having long shafts that can experience large deflections during shock should possess positive means of preventing the large deflections that may dislodge the shaft from its bearings or temporarily or permanently disengage the gears.

Equipment (Mechanical)

41. Cooling coils: Quality control should ensure that all foreign material such as weld material is removed from the final product to prevent puncturing the coil.

42. Fans: If possible, provide positive means of preventing fan belts from from jumping off pulleys.

43. Provide positive means of clamping air conditioning filters into their racks. Spring or friction clips are not acceptable.

44. Fan motors should be mounted on the floor or a rigid support structure. If a manufacturer provides motor mounts on the air handling unit structure, always locate the motor as close to the base of the unit as possible to increase shock resistance. Preferably, the motor should be attached to the structure supporting the air handling unit.

45. If vibration isolators are required on small fans at the attachment points, use bulkhead grommets since they have demonstrated the best shock resistance.

46. Tanks: Manufacturer-designed support legs should have cross bracing between legs and be designed to take the shock loads and remain in the elastic range. This section presents a procedure for computing the equivalent static load that must be resisted.

47. Equipment structure should be checked to ensure that equipment will survive the shock loads. Where it does not, the structure must be strengthened so that it remains in the elastic range. This section presents a procedure for computing the equivalent static load that must be resisted.

48. Fan impellers should have ample clearance between the impellers and the housing and support braces to prevent impact or rubbing during shock.

49. Avoid pump couplings that use rubber inserts between cogs, since rubber inserts are sensitive to shock and may be destroyed by shock resulting in metal-to-metal contact.

2535

50.   Air diffusers, dampers, etc., in critical air systems (e. g., those cooling electrical equipment) should be provided positive means of retaining the vanes, doors, etc., in the desired position, otherwise shock will change the position. Friction is not considered a positive means of retaining. Also remove the slack in vane operators.

51.   Do not use heat-sensitive straps that are looped through a ring to activate fire doors in air ducts. Such devices are susceptible to slipping out of the loop during shock and causing an undesirable closing of the fire door.

52.   Large cantilevered pieces of equipment should be provided support or not be used.

53.   Air filters installed in combustion air systems for engines must be capable of taking the overpressure generated by bombs detonating near the intake. Standard air conditioning filters may not take these pressures. Shock tube testing should be performed if theses filters must remain in the air stream during an attack. A better solution is to bypass these filters during an attack and isolate them from the airstream.

54.   Ensure that the equipment support foundation (that part made by the manufacturer) is designed to accommodate the type of tiedown to be used. For example, if bearing-type bolts are used, then the equipment foundation must be used, then the equipment foundation must be designed to develop the full potential of this type bolt.

55.   High speed motors are more shock resistant than low speed motor.s

Equipment (Electrical)

56.   Avoid stress in concentrations in insulating materials. Common sources of stress concentrations are sharp reentrant corners, sudden changes in cross-section, transverse holes, and insufficient bearing area under metal bolts and clamps holding plastic or ceramic pats.

57.   Electrical components that are fitted into sockets or clips should be provided with positive means to tie the component down.

58.   Electrical chassis should be as rigid as possible. For example, chassis formed from cast light metal (e.g., aluminum or magnesium) are acceptable. Chassis constructed of sheet metal are too flexible and require stiffening to increase rigidity.

59.   Electrical components mounted on a sheet metal chassis. If a heavy component (e.g., transformer) cannot be mounted adjacent to a corner, it should be mounted adjacent to an edge. If it must be mounted near the center of the chassis, a stiffener should be provided on the lower side of the chassis.

60.   It is preferable to mount components on a retractable chassis or directly on the cabinet structure or not on a door or hinged panel.

61.   Retractable chassis must be designed not to bounce and must transfer load directly to the frame of the cabinet. For example, testing shows that interface contacts for retractable air circuit breakers are destroyed when the circuit breaker bounces due to shock.

62.   Numerous front panel fasteners spaced at regular intervals must be placed around the periphery of the front panel to develop maximum stiffness.

63.   If ball bearing slides are used for retractable chassis, the weight of the chassis in the locked-up position must be carried by dowel pins and the front panel fasteners.

64.   Small cathode ray tube appear more shock resistant than larger tubes.

TM 5-855-1

65. Electron tubes, when used, must be held in place by screws, or that possess a threaded stud that can be screwed into the chassis, are highly shock resistant. Other types should be clamped down.

67. Transformers should be supported at the top as well as the bottom to prevent failure of the weak supports common to off-the-shelf transformers.

68. Capacitors should be supported at the leads. Instead, positive means of clamping the capacitor to the chassis should be provided.

69. Resistors of 1/3- to 2-watt rating may be supported by their leads if the structure supporting the resistor is rigid and if the length of each lead is less than or equal to 3/8 inch. Resistors with rating of 2 watts and greater must be clamped to the support structure.

70. Printed circuit boards should be stiffened by a metal chassis, conformal coating, or complete potting in plastic.

71. Cabinets should be designed to remain in the elastic range during shock.

72. Do not use plastic-cased batteries. Use battery casings that are designed for impact.

73. Battery support racks must be designed to take the shock.

74. Batteries must be securely strapped to the support rack.

75. Air circuit breakers: Design should incorporate positive means of locking the contacts into position to prevent movement during shock. Linkages should be designed in accordance with the directives in this table.

76. Transformer supports should be designed to remain in the elastic range during shock. Transformers should be supported the the tip as well as the bottom to prevent failure of the weak supports common to commercial transformers.

77. Electrical devices: Wiring in these devices should not pass between two metal plates without some protection such ar rubber spacers; without such protection, shock may sever the wires and render the device inoperable.

78. Control cabinets: Where possible, provide automatic restart of controlled equipment so equipment can quickly be brought back on line following a shutdown due to shock.

79. Provide supports at the ends of cantilevered cabinet-mounted devices.

80. Do not support cabinet-mounted devices with small-diameter pipes that are part of the equipment.

81. Provide plug-in devices and connectors with positive means of tiedown and clamping to prevent separation due to shock.

82. Magnetic motor overload devices are shock sensitive and should be avoided in equipment exposed to shock. Use a thermal motor overload device.

Equipment (Relays, Motor Starters, and Switchgear)

83. Devices used for control only: These devices can be make shock resistant by providing positive locking latches or shock-actuated locking latches to prevent contact chatter or change the position due to shock. Some common latching devices are magnetic latch, inertia latches, and manual latches.

2537

84. Dampers can be effective in preventing malfunction of these devices.

85. Relays, motor starters, and switchgear that use a crack to open and close the contacts are shock resistant if overcentering is used. Overcentering consists of setting the mechanism that opens and closes the contacts beyond dead center and against a stop at the extremes of its movement.

86. Malfunction of these devices can be prevented by using irreversible mechanisms; for example, using a worm gear to open and close electrical contacts.

87. Another method of preventing the opening or closing of contacts during shock is to use two contacts to close one set of contacts while opening the other set.

88. Statically balancing pivoted or hinged relay, motor starter, or switchgear armatures about the pivot or hinge increases the shock resistance of these devices.

89. Energized relays are more shock resistant than deenergized relays.

90. Clapper-type relays should be avoided since they are inherently unbalanced and sensitive to shock.

91. Indicator flags on these devices and on circuit breakers should be firmly locked into place. This prevents flags from dripping into another position during shock, giving false indication of the true status of the device.

92. Sudden pressure relays are sensitive to shock and should be avoided, if possible.

93. Motor starters having thermally actuated overload relay heater elements (particularly NEMA size 1 starters) can be made more shock resistant by increasing the rating of the heater elements by 15 to 25 percent above maximum motor operating current but equal to or less than motor full-load current.

Mechanisms Such as Control Linkages

94. Positive locking devices such as pins and keys should be used to lock mechanisms in place to prevent changing positions during shock.

95. Avoid knife edge and pivot bearings. Use sleeve bearing or well-designed plastic hinges.

96. Clearances and backlash should be minimized.

97. Linkages or groups of linkages or groups of linkages should be statically balance so that CG is on the axis of the pivot.

Electrical Wiring

98. Electrical cables passing through holes in chassis should be protected by grommets.

99. Shock and vibration resistance can be increased by binding adjacent cables together and properly supporting the harness to prevent loading termination points.

100. Electrical wires between two closely spaced terminals that *do not move relative* to one another should be as short as possible.

101.   Electrical wires between terminals that are too closely spaced and *do move* relative to one another should have some slack. Stranded insulated wire is preferred in this case due to its inherent damping.

102.   Electric wires that are soldered should be clamped near the soldered connecti .. to prevent failure due to shock.

103.   Electrical cables can be protected from failure at the terminal points by a restricting sleeve that prevents severe cable bending.

104.   All wiring bundles in electrical equipment and in cable trays should be tied down to prevent placing loads on electrical components and to prevent impacting electrical components during shock.

Piping Components

105.   When pipe nipples (1-1/2 inch or smaller) are required, use pipe of extra strength or better (steel, Monel, or copper nickel).

106.   Automatic air vents: internal linkages must be constrained to remain in the operating range of the device. Also, the comments under "Mechanisms Such as Linkages," in this table should apply.

107.   Check valves should be of the non-slam type.

108.   Components should be 300# rated and flanged.

Instrumentation

109.   Gages: When possible, specify gages designed to resist shock, such as those approved for use on Navy ships.

110.   Monitoring and control devices mounted in long-term vibration environments should be designed to withstand the vibration.

111.   Instrumentation using cams, gears, etc., must be provided positive means of preventing parts from disengaging.

112.   The internal workings of instrumentation should be statically balanced so that the initial setting will not be changed due to shock.

Light Fixtures

113.   The shock resistance of commercial fluorescent light fixtures varies drastically between manufacturers. Light fixtures procured for this type of facility should be shock tested and retrofitted until they pass the design shock environment with no failure and with all structural parts remaining in the elastic range.

114.   Weak areas in commercial fluorescent light fixtures are:

a.   Fluorescent light tubes pop out of sockets and break.

b.   Separation of ballast and reflector due to shock.

c.   Structure fastened with a few screws and a number of bent tabs.

2539

115. Methods of improving shock resistance:

a. Do not use bent tabs to connect parts; use nuts, bolts, and washers as recommended in the directives on fasteners contained in this table.

b. Use positive locking devices to lock light tubes into sockets.

Quality Control

116. Manufacturers must have strict quality control program to reduce the number of defective items purchased for use in this type facility.

      (3) Table 12–2 and figure 12–1 provide quantitative data on the shock resistance of 32 categories of equipment in terms of vertical and horizontal shock response spectra. It is a condensation of data obtained in testing about 300 pieces of equipment under the SAFEGUARD program. Reports on these tests are listed in the Bibliography. The tests were conducted during 1971–1973. With this information, an evaluation can be made to determine whether shock isolation is needed for equipment protection.

2541

Table 12-2. Equipment Shock Resistance

Item	Limitation	Environments (Figure 12-1) Horizontal	Vertical
		1	1
1. Air conditioning units	1. Small 5-ton compressor and air handling unit	1	1
2. Air handling units	2. None	4	4
3. Air conditioning and CB filters	3. None	4	2
4. Fans	4. Centrifugal and axial flow	5	2
5. Dampers, diffusers, and extractors	5. None	6	7
6. Piping components	6. Valves (manual, control, pneumatic actuated), sediment strainers, flex hoses, fluid filters, moisture traps, expansion joints, autpomatic air vents, flow orifices, attenuators, etc.	19	3
7. Pumps	7. a. Sump pumps b. Peripheral turbine, centrifugal and positive displacement	8 4	10 9
8. Heat exchangers	8. None	19	11
9. Heating and cooling coils	9. None	12	2
10. Air compressors, storage tanks, instrument air dryers	10. None	13	14
11. Water chillers	11. None	16	15
12. Water purification units	12. None	17	18
13. Heat-sensing devices	13. None	19	20
14. Indicators	14. Pressure, flow, temperature, level	4	21
15. Instrument panels	15. None	19	22
16. Control panels	16. a. Generator surge pak b. All others	24 24	23 25
17. Monitoring and control	17. Current trips, regulator filters, switches, probes, transmitters, transducers, power supplies, controllers, thermostats, etc.	26	27
18. Motor generators	18. None	28	29

2542

TM 5-855-1

Table 12-2. Equipment Shock Resistance

Item	Limitation	Environments (Figure 12-1) Horizontal	Vertical
19. Diesel engine generators	19. Diesel engine generator, pumps, governors, control linkage, pneumatic actuators	30	30
20. Gas turbine generators	20. None	31	4
21. Generator accessories	21. Neutral resistor, neutral breaker, static exciter regulator	32	32
22. Circuit breakers	22. a. Molded-case circuit breakers b. All other types	34 33	34 33
23. Relays	23. a. Hardmounted to rigid surface b. Cabinet mounted – structural limit c. Cabinet mounted – relay chatter limit	35 37 36	38 37 36
24. Electric motor control	24. a. Structural limit b. Relay chatter limit	39 41	39 40
25. Metal clad switchgear	25. Environments are those the switchgear passed structurally. At these environments the switchgear changed state and indicator flags dropped down giving false information.	42	42
26. Dry transformers	26. None	44	43
27. Electrical panel boards	27. Circuit breakers, relays, meters, RFI filters, motor starters, air circuit breakers a. Panelboards with air circuit breakers b. Panelboards without air circuit breakers	45 45	46 46
28. Station battery sets	28. a. Batteries b. AC switchboards and DC power supply	48 49	48 49
29. Unit substations	29. Transformers, voltage, regulators, circuit breakers, motor controls, motor starter	30	37
30. Light fixtures	30. a. OCE type F10-B modified b. OCE type F-4 modified	50 52	51 2
32. Communications equipment	32. None	55	56

2543
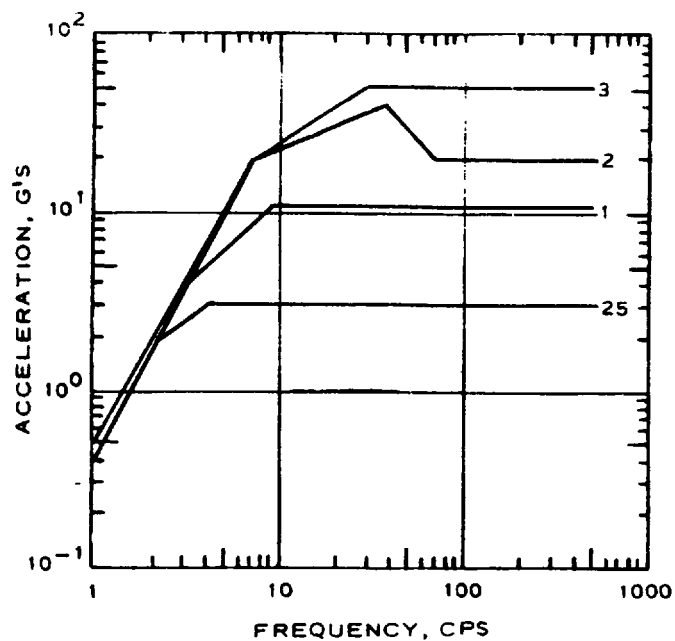
US Army Corps of Engineers

Figure 12–1. Equipment shock resistance. (Sheet 1 of 10)
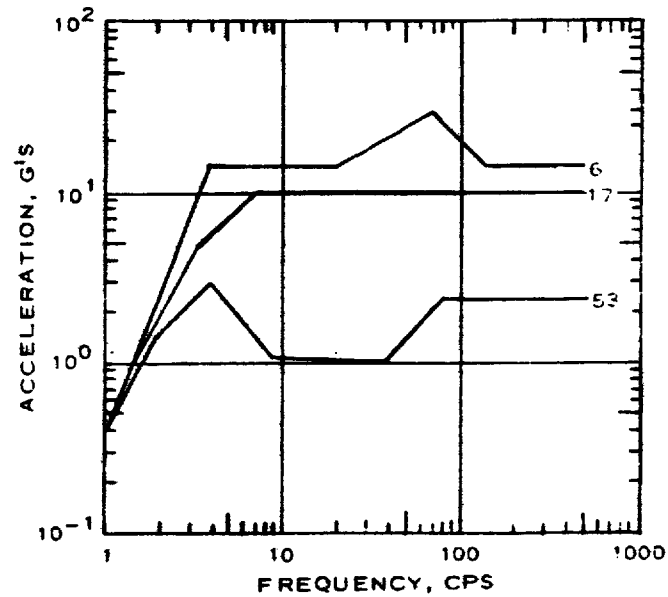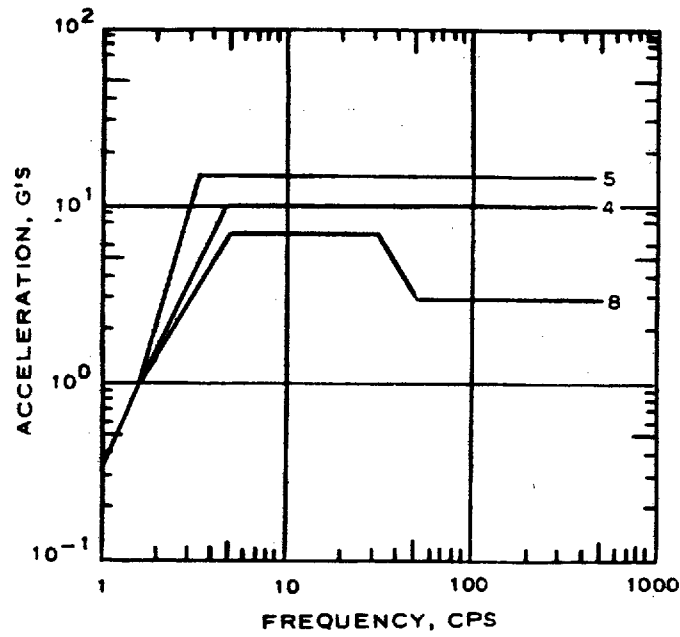
US Army Corps of Engineers

Figure 12–1. Equipment shock resistance. (Sheet 2 of 10)

2545
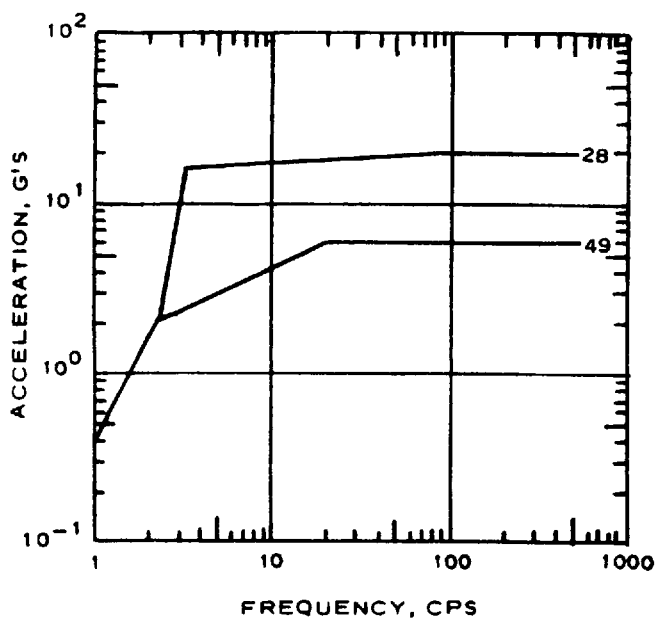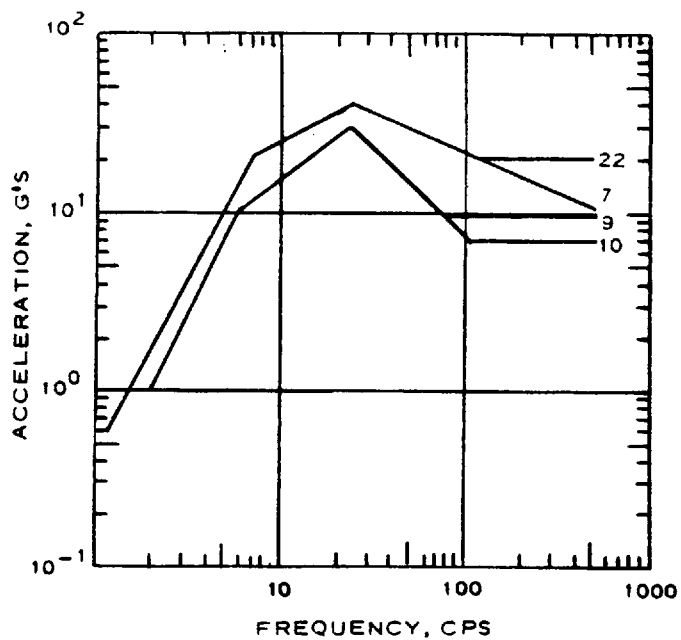
US Army Corps of Engineers

Figure 12–1. Equipment shock resistance. (Sheet 3 of 10)

2546
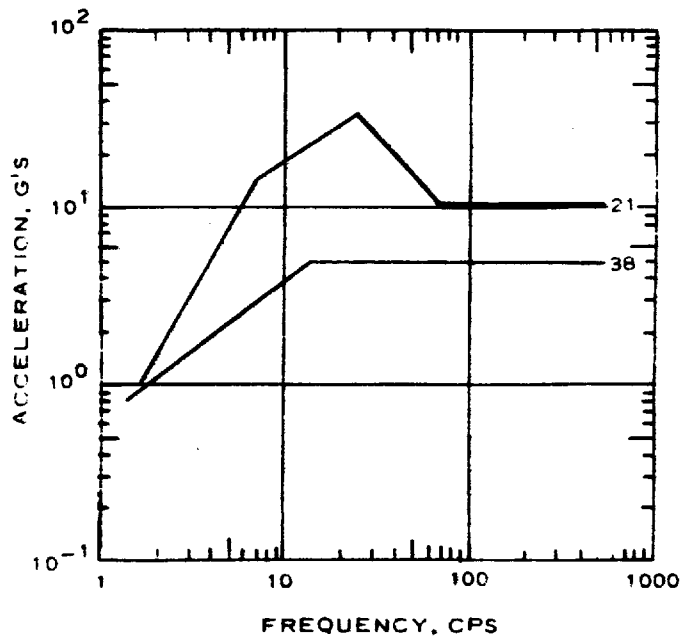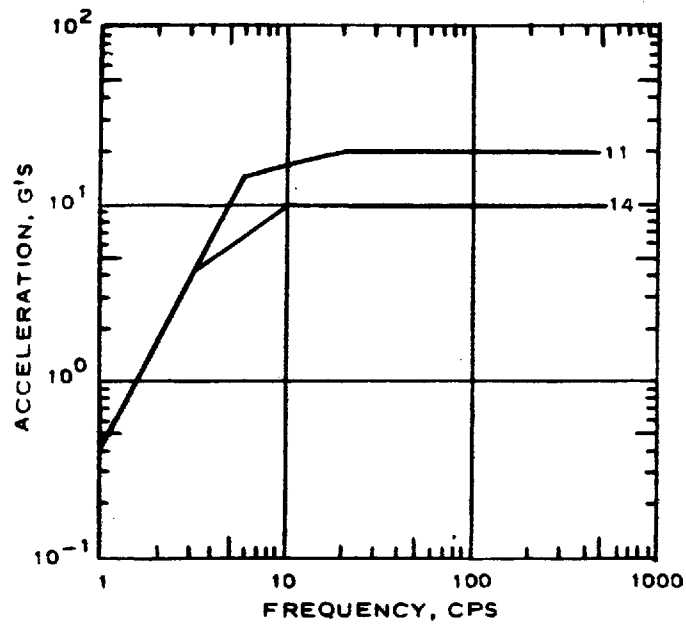
TM 5-855-1

US Army Corps of Engineers

Figure 12-1. Equipment shock resistance. (Sheet 4 of 10)

2547

2548
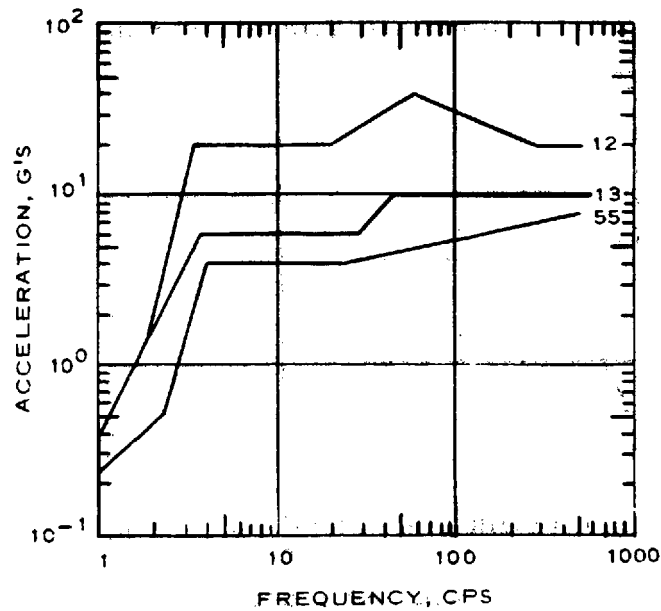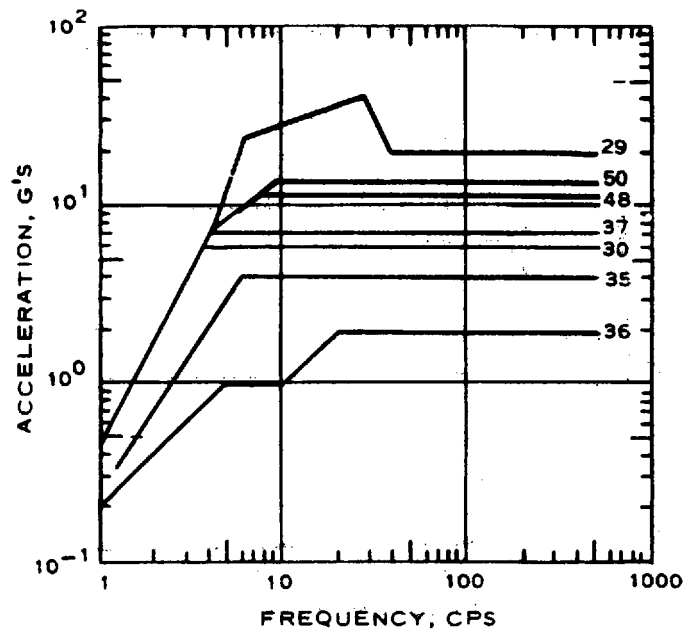
US Army Corps of Engineers

Figure 12–1. Equipment shock resistance. (Sheet 5 of 10)

TM 5-858-1
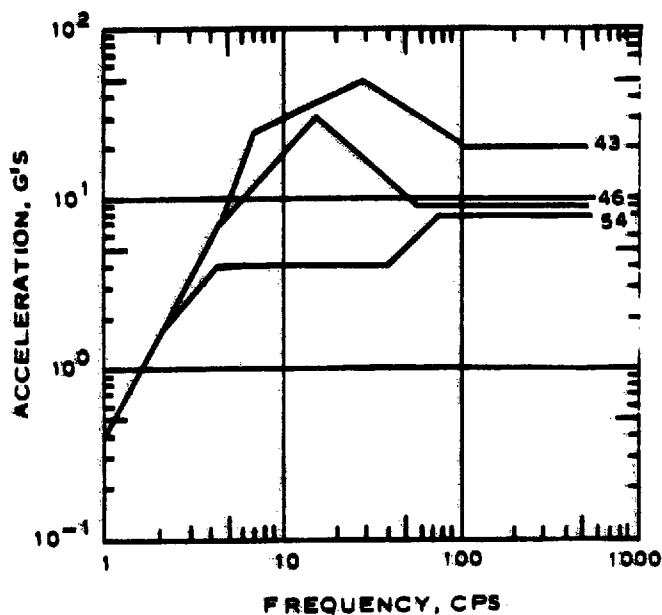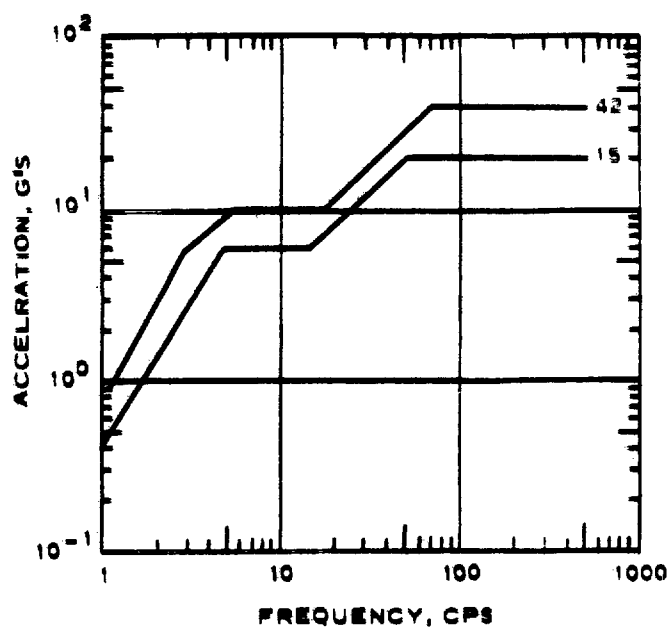
US Army Corps of Engineers

Figure 12-1. Equipment shock resistance. (Sheet 6 of 10)

2549
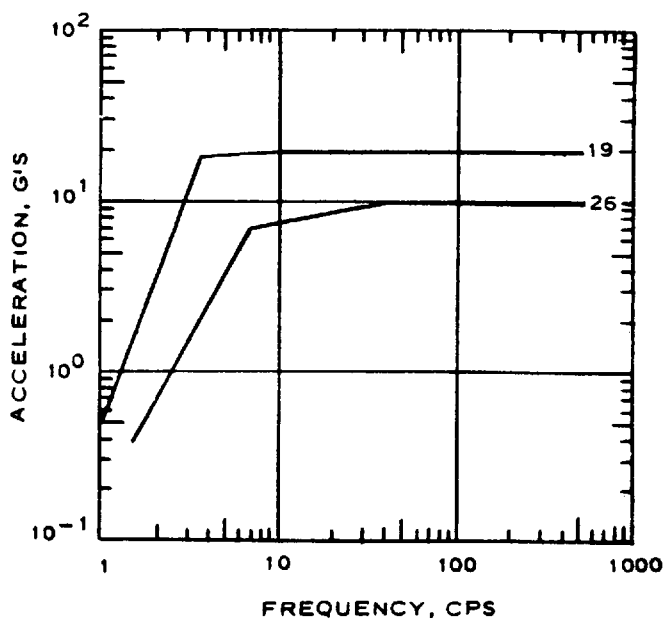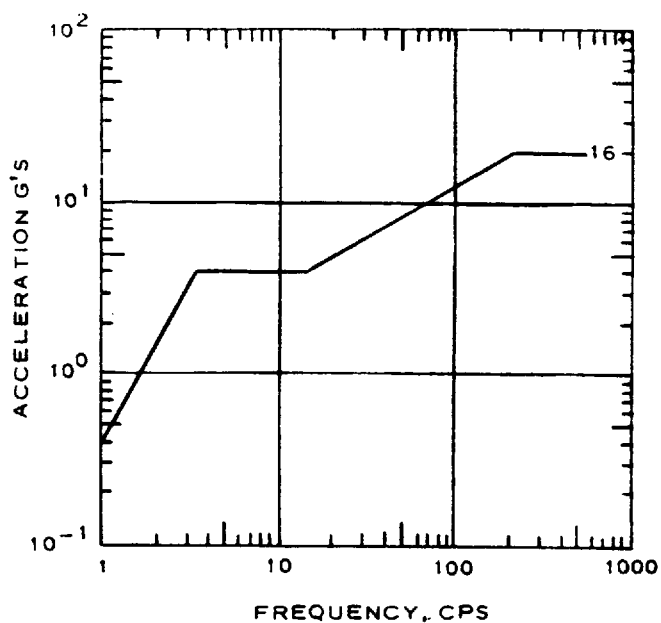
US Army Corps of Engineers

Figure 12-1. Equipment shock resistance. (Sheet 7 of 10)

TM 5-855-1
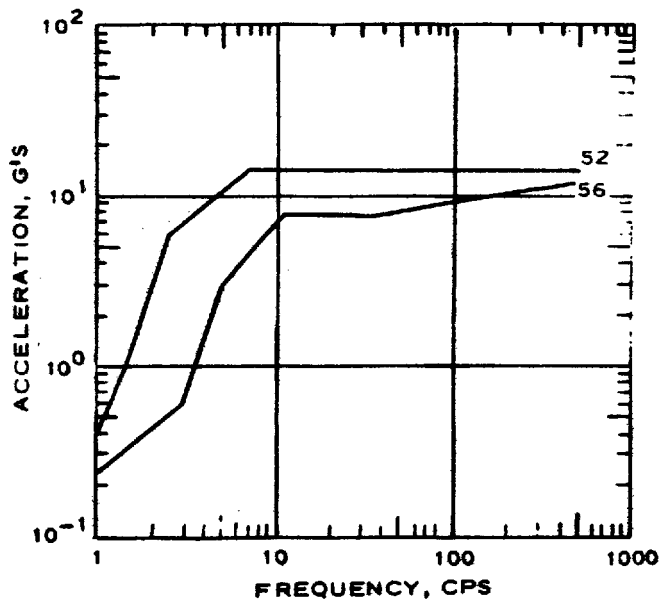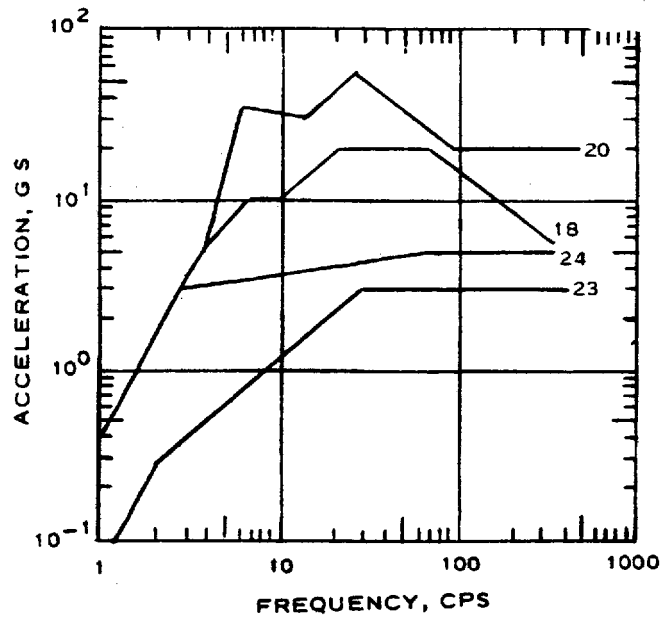
US Army Corps of Engineers

Figure 12–1. Equipment shock resistance. (Sheet 8 of 10)

2551
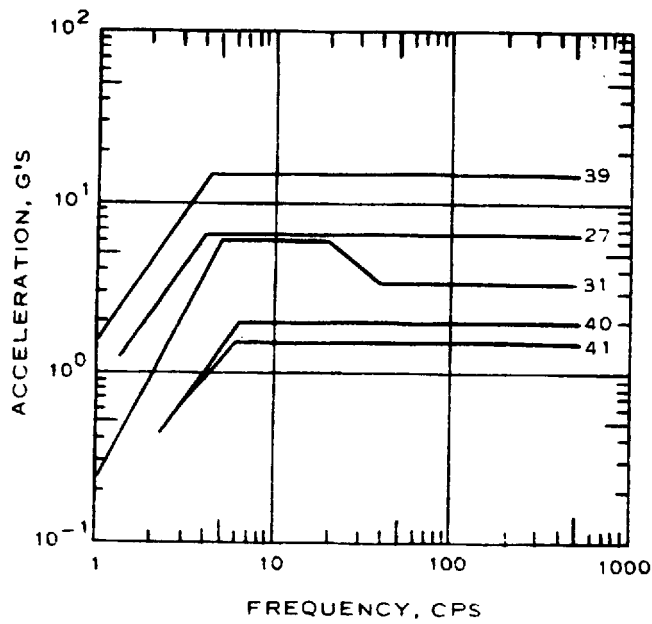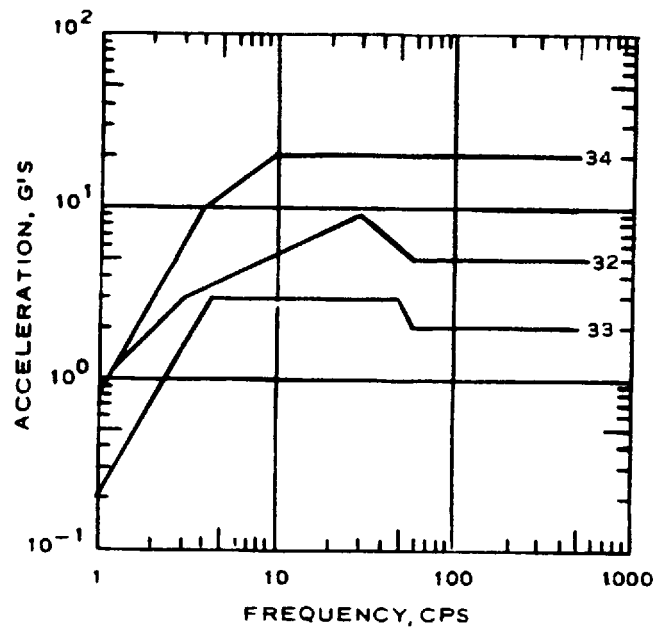
US Army Corps of Engineers

Figure 12-1. Equipment shock resistance. (Sheet 9 of 10)
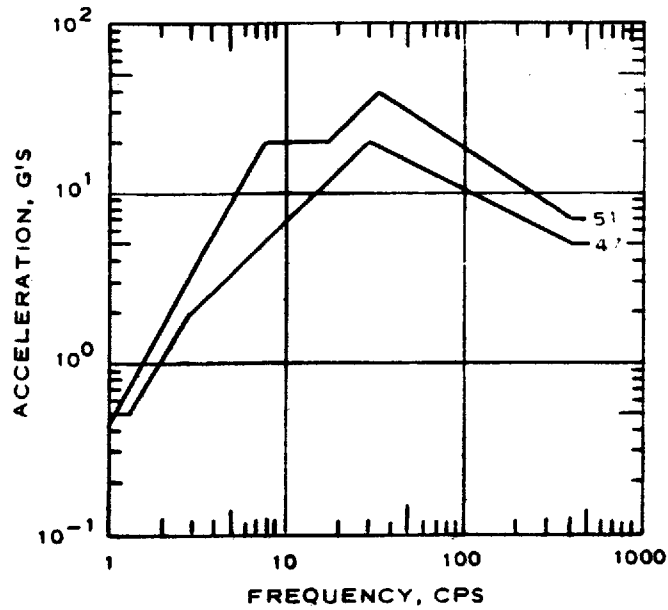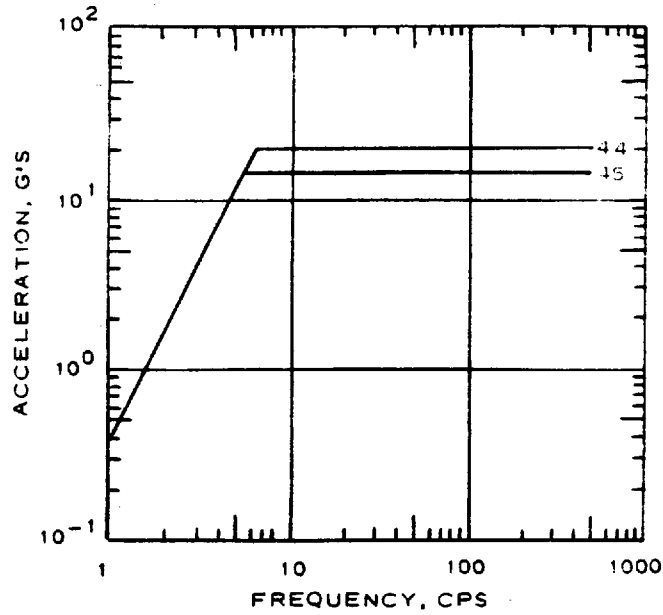
US Army Corps of Engineers

Figure 12–1. Equipment shock resistance. (Sheet 10 of 10)

(4) The hardness (or shock resistance) of a subsystem consisting of several items of electrical or mechanical equipment can often be enhanced by designing around the weak links in the system. Table 12–3 provides such information for system design based on experience gained during the SAFEGUARD program.

Table 12-3. System Design Guidance

Power Protective Circuits (Switchgear, Unit Substations, etc.)

Provide bypass circuit directly to the critical equipment during attack.

Control Circuits (Motor Control Centers, Equipment Control Cabinets, etc.)

(1) A device sensitive to shock can be used to initiate an automatic restart cycle when the equipment shuts down during a shock.

(2) Where possible, circuits containing relays sensitive to shock can be bypassed during attack.

(3) Relays that are highly shock resistant (solid state relays, Navy-tested relays, etc.) can be used.

(4) Make effective use of time-delay relays.

(5) Limit the use of seal in relays.

Monitoring Systems

(1) Physically separate the critical and the no-critical monitoring functions on the control console, so operators can focus on the critical functions during an attack.

(2) When under attack, electrically bypass warning bells, buzzers, etc., activated by non-critical monitoring circuits to reduce confusion.

(3) Use time-delay relays in critical monitoring circuits to prevent false alarms due to contact chatter.

(4) Do not locate continuous readout devices (gages, meters, etc.) necessary for proper operation of piping systems on the piping. Past test experience frequently shows that devices mounted on piping provide unreliable readouts following shock. Shock resistance of these devices is greatly increased by locating them on instrument panels with a sensor line to the piping.

Pneumatic Systems

(1) Control Systems - design controlled device to fail in position necessary for mission accomplishment.

(2) Monitoring Systems - provide adequate storage capacity to operate critical systems until air supply can be reestablished.

Light Fixtures

When light fixtures are suspended from the ceiling with steel rods, provide swivels at the ceiling to prevent large bending loads in rod.

(5) The following sections provide guidance for using the tables. In addition, design considerations for proper equipment positioning, tiedown, and for equipment maintenance are also provided.

b. Technical provisions for equipment procurement specifications. Shock testing experience frequently shows that minor, seemingly insignificant failures can result in loss of critical mechanical and electrical systems. Therefore, careful attention to subtle points of equipment design can greatly increase equipment shock resistance. The objective in this section is not to require new designs or to solve the total equipment protection problem, but to reduce the amount of shock–sensitive equipment purchased. Commercial equipment varies considerably in ability to resist shock. Shock testing experience shows that most but not all commercial mechanical equipment is shock resistant. Electrical equipment (especially light fixtures, relays, switchgear, air circuit breakers, and motor starters) are less shock resistant as a group, but shock–resistant electrical equipment is available commercially. Therefore, designers can greatly increase equipment protection by writing technical provisions in equipment procurement specifications that will require purchase of equipment with shock–resistant features. Table 12–1 is a list of characteristics possessed by shock–resistant equipment. The characteristics are based on extensive shock and vibration testing of commercial equipment installed in hardened structures. Designers should study this table and select the applicable characteristics for use in their procurement specifications.

(1) Relays, switchgear, and motor starters are particularly sensitive to shock since their function depends on an armature operating about a pivot. Malfunction occurs when shock causes the armature to rotate and change position (opening or closing electrical contacts). Previous testing experience shows that usually these devices are not damaged by the shock, but they frequently change position, causing a disruption of the electrical function. Designers of facilities exposed to nonnuclear threats must prevent this type of malfunction from occurring since it causes confusion and temporary loss of the affected systems every time the facility experiences the design shock loading. Therefore, designers are especially encouraged to include the characteristics for these devices in table 12–1 in their equipment procurement specifications.

(2) Air circuit breakers usually are devices with considerable amounts of mechanical linkages and used to operate and protect the contacts of the breaker. The electrical contacts are spring loaded and are "floppy" from a shock–sensitive viewpoint. As a result, shock may cause the contacts to change positions. This situation must be prevented for the same reasons given above and the designer is encouraged to avoid using this type of device or include the requirements of table 12–1 in the procurement specification.

(3) Previous testing shows that commercial fluorescent light fixtures differ significantly between manufacturers in their ability to survive shock. Two weaknesses frequently showed up: (1) methods used to fasten parts together generally are not equal to the standards required for fasteners in table 12–1 and (2) light tubes in fluorescent light fixtures may be dislodged during shock. Both of these can be easily eliminated by requiring purchase of fixtures that follow the guidelines for fasteners in table 12–1 and by providing locking devices on the light tubes to prevent dislodgement during shock. Since loss of lighting during an attack is undesirable as well as hazardous from a debris viewpoint, designers are encouraged to require shock testing of light fixtures to ensure that the items actually purchased will in fact survive the design shock. Lighting fixtures using light bulbs screwed into a socket have been designed and tested for shipboard use. If these types of lighting fixtures are used, the designers should specify fixtures certified for Navy shipboard use or require shock testing to verify their shock resistance.

(4) The designer will notice that several of the characteristics in table 12–1 would require manufacturers to analyze their equipment support structures to verify that they will remain in the elastic range under shock loads. This can be done simply and quickly by the following procedure:

(a) Estimate, compute, or measure the weight of the equipment.

(b) Obtain the equivalent static loads by multiplying the weight by the highest g–level reached by the response spectrum computed from chapter 11 for the location where the equipment will be installed. This will result in vertical and horizontal loads, F_V and F_H, where

$$F_V = W_w g_v$$

$$F_H = W_w g_h \qquad \text{(eq 12-1)}$$

where

W_w = the weight of the equipment, tank, door, or equipment cover

g_v = maximum vertical acceleration from the vertical response spectrum for the location where equipment is located, g's

g_h = maximum horizontal acceleration from the horizontal response spectrum for the location where equipment is located, g's

c. Optimizing cost of limiting in–structure shock and equipment protection. A severe in–structure shock environment may require that all equipment be isolated. In a large facility this may not be cost–effective and may be unnecessary. Using design configurations that prevent close proximity detonation of bombs, the in–structure shock can be reduced. It is the job of the designer to determine the most cost–effective combination of in–structure shock, shock isolation, and shock testing. Guidance is given below for determining the following parameters for a given in–structure shock environment: (1) Equipment which must be shock isolated; (2) Equipment which can be bolted to the floor (hardmounted); (3) Equipment which must be shock tested. Table 12–2 has ben prepared for this purpose.

(1) Table 12–2 contains a list of equipment commonly found in military facilities. Associated with each item is a horizontal and a vertical undamped in–structure shock response spectrum that the representative equipment may be expected to survive without structural damage. The undamped response spectrum is a plot of the maximum responses of a series of SDOF oscillators to a complex shock–time history that describes the motion of the floor where the equipment is mounted. Response spectra are commonly used in the shock testing community to portray the shock level to which the equipment has been tested. By comparing the shock spectra in table 12–2 to undamped in–structure shock response spectra at the location where the equipment is to be installed, a decision can be made as to whether shock isolation is required. At this point the designer should be warned that this procedure does not guarantee with absolute certainty that all equipment will survive the environments in table 12–2. The reason is that each piece of equipment is unique and has its own sensitive frequencies and characteristics. But the results presented in table 12–2 represent considerable testing (about 300 items). Also, approximately 30,000 items of similar but untested equipment have been qualified as shock resistant to a high degree of confidence using these test results.

(2) Before discussing the procedure for determining what should be isolated, shock tested, or hardmounted, a few comments about table 12–2 are in order. Dampers, diffusers, and extractors (Item 5) are installed in air ducts and will never be shock isolated. Piping components (Item 6) are installed in piping systems and will always be hardmounted. For Items 5 and 6, shock testing will be required when the environments in table 12–2 for these items are exceeded. The procedure for determining whether shock isolation, shock testing, or a hardmount is appropriate is as follows:

d. Procedure.

2557

(1) Step 1 – equipment classification. Designers must first classify the equipment as follows:

(a) Mission–critical equipment that must function during **and** after each shock (Criticality A).

(b) Mission–critical equipment that does **not** have to function during each shock but **must** function **following** each shock (Criticality B).

(c) Equipment not critical to the mission that does not have to function during or following an attack (Criticality C). Criticality A and B equipment must be protected against shock. Items with Criticality C will be hardmounted and securely attached to the building structure to prevent hazards to personnel or mission–critical equipment. All equipment controls and system monitoring devices, remote and local, must be either Criticality A or B. If they are Criticality B, they must return to their original state following shock without requiring operators to reset, restart, or readjust. This prevents confusion following each shock because of false alarms or equipment shutdown requiring operators to restart machinery and readjust each system.

(2) Step 2 – in-structure shock environment. Compute and plot the horizontal and vertical in–structure shock response spectra as described in chapter 11. Remember, this is not the actual floor environment but the maximum response of a lightly damped system of SDOF oscillators to in–structure shock.

(3) Step 3 – equipment selection. Locate the item of equipment being considered from table 12–2 and find the shock environments it will survive.

(4) Step 4 – shock environment comparison. Compare the horizontal and vertical spectra obtained from Step 3 with the horizontal and vertical in–structure response spectra from Step 2 at the location where the equipment is installed.

(5) Step 5 – hardmount or shock isolate?

(a) All equipment except relays, electric motor control centers, and metal–clad switchgear. If the design shock environment (Step 2) falls below the environment in table 12–2, the equipment can be hardmounted. If it exceeds the environment in table 12–2, the designer has two options: shock isolate the equipment or shock test and retrofit if required until it survives the in–structure shock environment.

(b) Relays and electric motor control centers. Two environments are listed for these items on table 12–2. One represents the environment the equipment can be expected to survive structurally and mechanically. At this level there will be considerable relay chatter that may result in electrical malfunction. If the higher level is used, the designer must design electrical circuitry for Criticality A equipment to prevent the loss or disruption of critical functions during shock motions. If the higher level is used for Criticality B equipment, the designer must design electrical circuitry to prevent loss of the critical function following shock motions. The lower environment must be used if circuitry cannot be designed to prevent disruption due to relay chatter. Once the proper environment is selected from table 12–2, proceed as instructed in Step 5 (a).

(c) Metal-clad switchgear. These devices are very sensitive to any level of shock. Environments in table 12—2 are levels these devices have survived structurally and mechanically. At these levels considerable contact chatter and change of state took place. Therefore, these devices must be protected by one of the following: 1. circuitry designed to prevent disruption of Criticality A functions and to prevent loss of function requiring resetting or restarting for Criticality B functions; 2. shock isolation; 3. shock tests and retrofit until the switchgear survives the environment; 4. use of another piece of already hardened equipment that provides the same service.

Using this procedure the designer can identify the amount of shock isolation and shock testing for a particular in–structure shock environment. Cost tradeoffs can be made between the cost of equipment protection (shock isolation and shock testing) and the cost of reducing in–structure shock. Each time the in–structure shock environment changes, Steps 2 through 5 should be repeated until an optimum is obtained.

e. Positioning and tiedown of equipment. Proper equipment positioning and tiedown are important steps in protecting equipment. Careful attention to positioning and tiedown will prevent unexpected impact loading that may cause equipment failure or malfunction. To avoid this possibility, the following guidelines should be observed.

(1) Position equipment properly.

(a) Avoid bolting equipment to exterior walls or roof (exception: light fixtures).

(b) Avoid attaching equipment to more than one surface (ceiling and wall, wall and floor, floor and ceiling, or two walls).

(2) Tiedown of equipment.

(a) Provide a means of tiedown (bolts or welds) that resists the shock loading without failure or yielding. The procedure for computing the equipment static loading is the same as that used for the equipment support structure.

(b) Cast–in–place bolts, expansion–type concrete anchor bolts, and welding to cast–in–place plates are the three methods used to tie down equipment. Cast–in–place bolts are the most desirable but also the most impractical method for two reasons. First, once their position is established, the designer loses the flexibility of shifting equipment later in the construction process. Expansion–type concrete anchor bolts are the most practical method since they give the greatest flexibility. If bolts are used to tie equipment down, the bolt holes in the equipment and the bolts should be fitted to reduce the possibility of slippage. If fitted bolts are not used, then provide some other means of preventing shifting of the equipment such as grouting or stops. Also, if bolts are used, then washers should be provided to distribute the load under the nuts.

Welding is another less frequently used method of equipment tiedown. Welded joints provide the best and most shock–resistant tiedown when properly done. When using welds as tiedowns, follow the guidelines for welding in table 12–1. If welds are used to tie equipment down to the floor, cast–in–place steel beams or plates designed to resist the shock loads must be provided in the design. The disadvantage of this method is that equipment weight and center of gravity are rarely available and must be estimated in the design phase. Also, it is difficult to remove equipment for repair or replacement.

f. System design guidance. Shock vibration can cause temporary or permanent loss of system performance information necessary for controlling the system. This is an undesirable situation since the loss of critical systems means that the mission is not performed. There are, however, design methods that can be used to prevent the loss of critical functions. A few possibilities are presented in table 12–3, but the designer is not limited to these. As long as designers satisfy the objective of preventing loss of critical systems, other methods may be used. The designer should also refer to table 12–1 for design guidance, since many of the entries are applicable to this paragraph.

(1) Power protective circuits contain many relays that may open or close (contact chatter) during shock. Sometimes the contact chatter lasts long enough to cut power to critical equipment. An effective method of preventing this is to provide a bypass circuit (table 12–3) around the protective relay circuit directly to the operating equipment. When the facility is warned of or under attack, a manual switch in the control room can be thrown to activate all bypass circuits. The U. S. Navy uses this design approach on all combat ships when the ships are engaged in combat. It was also used in the design of the SAFEGUARD Ballistic Missile Defense System.

(2) Control circuits also contain relays that may experience contact chatter during shock. Previous shock testing shows that this contact chatter frequently results in shutting the equipment down. Since this is undesirable, the designer should design the circuitry to prevent this possibility. Table 12–3 presents several possible solutions.

(3) Monitoring systems gather the information necessary for operators to effectively control the operation of the facility. Some of the monitoring systems are critical (i.e., necessary) for mission accomplishment; others are not. Those that are critical should be designed so that false alarms are prevented during shock. Noncritical monitoring systems should be designed to function following an attack since the diagnostic information may be needed to repair any resulting damage. Several ways to eliminate problems with monitoring systems are presented in table 12–3.

g. Maintenance. Maintenance is one of the important aspects of an effective equipment protection design. Unfortunately, it is usually given low priority in design. This might be tolerable in civilian facilities, but not in military facilities designed to resist shock. Effective maintenance requires access to the areas requiring attention. In a military facility, it may also mean providing a means of conducting maintenance while the system is in operation. Take, for example, a piping system containing shock attenuators (protect equipment from hydraulic transient pressures due to

shock). Criteria may require continuous system operation for one year, while attenuators may require maintenance every six months. The obvious solution is to provide a bypass around the attenuator. In this case, failure to consider the maintenance requirements results in loss of the equipment protection provided by the attenuator. This may seem trivial, but it actually happened in a major military facility. Since maintenance of equipment protection devices had lower priority than Operations, the maintenance was not performed, thereby casting uncertainty on the facility's ability to resist shock. Neglect of maintenance considerations in the design can nullify the design features provided for equipment protection. Therefore, designers must identify equipment protection maintenance requirements and include them in the design criteria. Several maintenance–related points to be considered in design are listed below:

(1) Provide access to shock isolators so maintenance or replacement can take place without shutting the facility down.

(2) Provide corrosion protection for all equipment, equipment tiedowns, and support structures.

(3) Provide bypass around equipment requiring maintenance more frequently than regular system shutdown periods.

(4) Where cost–effective, design systems so that the equipment protection maintenance required is minimized.

12–2. Piping, air ducting, and electrical cable

Piping, air ducting, and electrical cable systems run extensively throughout a facility, passing between floors and equipment and outside the building. Supports for these systems experience different relative motions when the building is shocked. Therefore, the design must provide sufficient flexibility between the termination points to prevent failure at high stress points. Also, protection devices must be installed in piping and air ducting penetrating the facility exterior walls to prevent entry of blast debris, air blast, and chemical and biological (CB) warfare agents.

 a. Piping. Piping systems designed for hardened facilities must have the following features:

(1) Piping should be connected to equipment with flexible connections or the piping should be rigidly supported to prevent movement close to the attachment to the equipment. This prevents loading the equipment due to pipe movements (fig 12–2).

(2) Hardmounted piping connected to shock–isolated equipment must have flexible connections or expansion joints between the last rigid support and the first pipe support on the platform. The allowable movement of the flexible connectors must be sufficient to allow the platform to move within its design limits with minor resistance.

(3) Gages cantilevered off piping should be supported or a flexible line used. This prevents failure of the sensing line where it attaches to the piping resulting in loss of fluid.

(4) Small–diameter threaded pipe should not be directly screwed into the tops of tall tanks. Testing shows that the relative movement between the top of the tank and the pipe results in failure of the pipe threads. In pneumatic systems this is undesirable, since air pressure is lost. Instead, follow the advice in (1) above and use flexible connections.

(5) Heavy items such as valves must never be totally supported by small–diameter (1 inch or smaller) threaded pipe. Tests show that the pipe fails at the threads and the device falls out of the line. To prevent this, the item must be completely supported by some other means.

(6) Where possible, flanged connections should be used since they are stronger than screwed connections.

(7) Heavier–duty pipe and flanges should be used in hardened piping systems.

(8) Great care must be taken to ensure that piping does not enter the required rattlespace for shock–isolation systems. For example, drainage lines for isolated equipment must not empty into drains under the platform unless this has been accounted for when determining the required rattlespace.

(9) Flexible hoses or expansion joints must be installed between rigid supports on two different floors to avoid large stresses due to relative movements induced by shock (fig 12–2).

TM 5-855-1
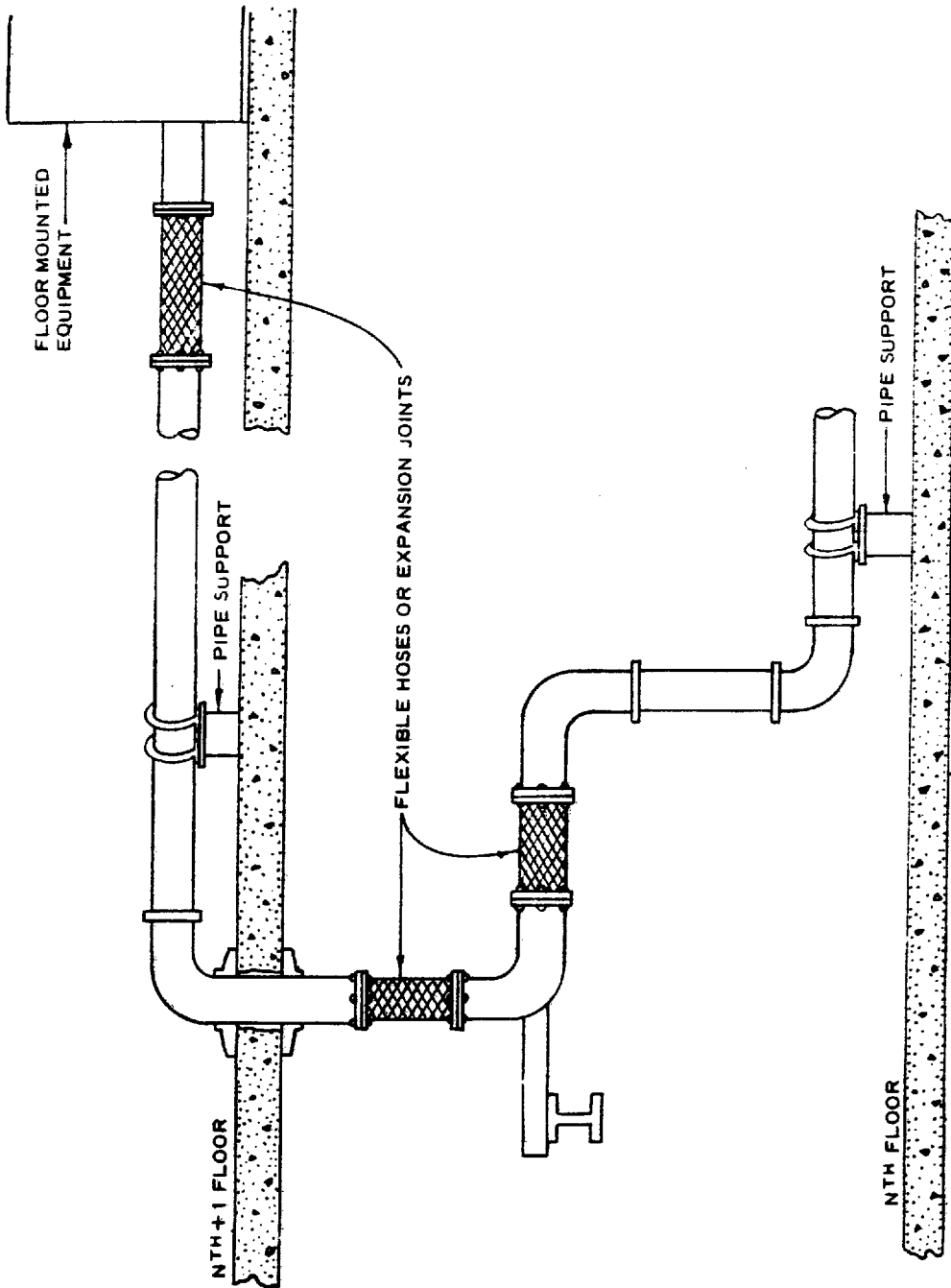
Figure 12-2. *Piping between floors.*

2561

(10) Piping penetrating a building and running to nearby hardened structures must be designed to withstand the relative movement between the soil and the building during shock motion. Figure 12–3 shows one method of accomplishing this.
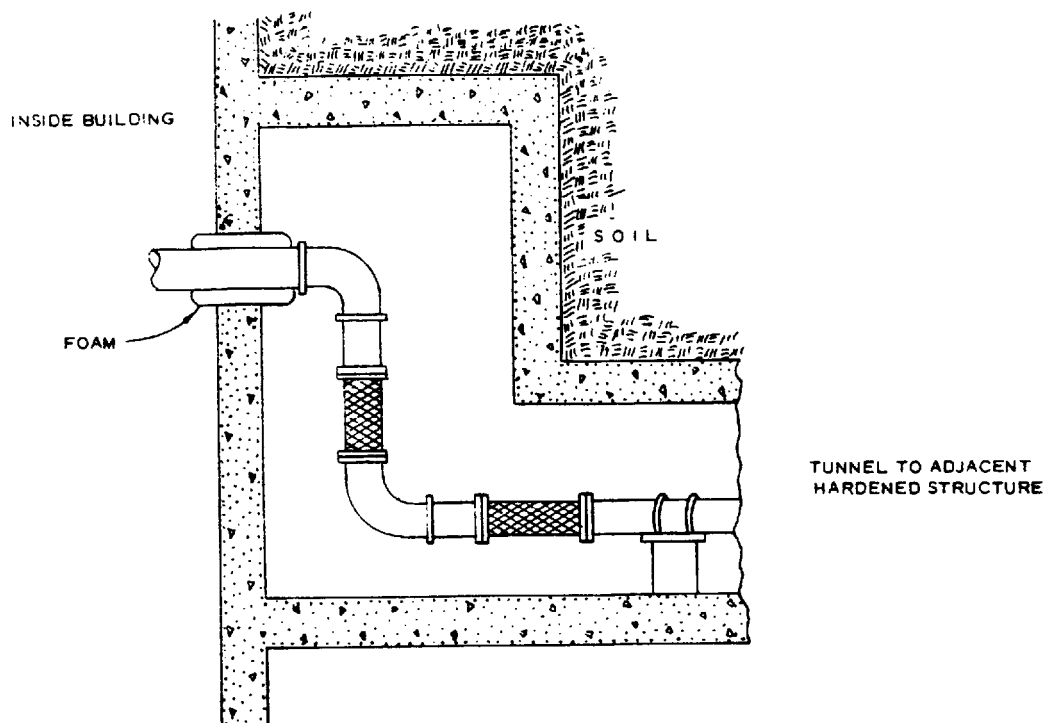
US Army Corps of Engineers

Figure 12–3. Exterior wall penetration.

TM 5-855-1

(11) A remotely controlled valve should be installed in the piping system just prior to the point where the pipe exits the building. This allows the interior piping system to be isolated from exterior piping. If the exterior piping is not designed to survive the ground shock, this valve should be closed when an attack is expected.

(12) Piping systems designed to resist shock should be designed to resist the hydraulic transient pressures induced by shock motions. The HYTRAN computer program was developed to compute these pressures when a piping system is shaken. When the analysis shows that the transient pressure plus the static pressure exceeds the allowable pressure of the piping and/or equipment, hydraulic attenuators should be installed. Computer codes are available that have the capability of analyzing the system and locating attenuators. There are several types of attenuators, but the most effective type is the one shown in figure 12-4.

CHARGING
VALVE

END FLANGES
TO SUIT SERVICE

AIR OR NITROGEN PRE-CHARGE

FLEXIBLE BARRIER

PERFORATED FLOW TUBE

FLEXIBLE BARRIER IN EXTENDED POSITION

OUTER SHELL
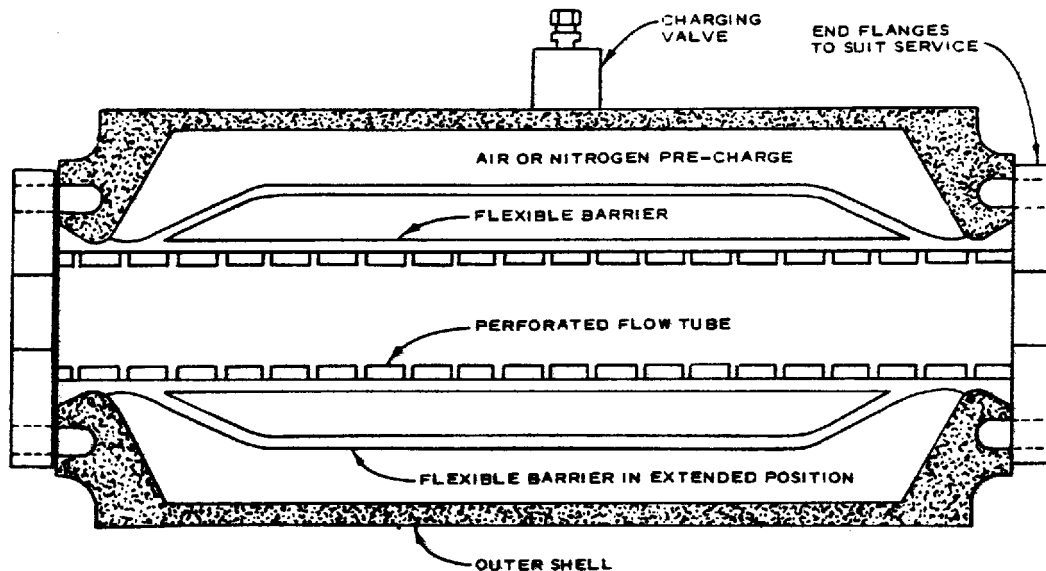
US Army Corps of Engineers

Figure 12-4. In-line accumulator with a perforated flow tube.

2563

(13) Pipe supports should be designed to resist the following load:

$$L_i = W_w g \qquad \text{(eq 12–2)}$$

where

L_i = load

W_w = weight of piping

g = maximum acceleration (g's) obtained from the response spectrum

(14) The maximum acceleration (g's) is taken off the horizontal and vertical response spectra at the attachment point of the supports. The load should be applied in each orthogonal direction.

b. *Air ducts*. Air ducts should have the following features:

(1) Duct can be constructed of standard–gauge sheet metal ducting reinforced with angles. Schedule–10 pipe, welded at the joints, can also be used.

(2) Ducts should be rigidly attached to the structure.

(3) Flexible ducts should be used between ducts supported on different floors or ducts supported from the wall and the floor to prevent damage due to relative movement.

(4) Flexible ducts should be installed between hardmounted ducts and shock–isolated ducts. The flexible ducts must deflect enough to freely move within the design limits.

(5) Supports for ducts should be designed in a manner similar to pipe supports.

(6) Air intake ducts that supply ventilation air from the outside must have CB filters installed in the ducts near the entrance to eliminate CB threats to the facility.

(7) Air ducts to the outside environment must have remotely controlled blast valves installed immediately inside the facility at the entrance points. These valves should be closed when an attack is expected to prevent airblast overpressure propagating into the facility. Another way to achieve this is by shock–actuated blast valves, but these types are not recommended for a nonnuclear threat.

The following formula can be used to compute time of safe occupancy while the valve is closed:

$$T_c = 0.04 \, V_v / N \qquad \text{(eq 12–3)}$$

where

T_c = time after closure, hr

V_v = shelter volume, ft^3

N = number of people in the facility

(8) Care should be taken to ensure that ducting does not enter the required rattlespace for shock isolation platforms.

(9) Combustion air systems and exposed ventilation ducts must be designed to withstand the design airblast pressure.

(10) Air intake stacks and ventilation ducts should be designed to prevent the possibility of a conventional bomb physically entering the stack before detonating.

(11) Two widely separated ventilation air intake and exhaust ducts should be provided to reduce the chance of a bomb destroying the ventilation system.

c. *Electrical cable*. Electrical cable systems should have the following features:

TM 5-855-1

(1) Cable trays should be securely attached to the building structure.

(2) Cables should be secured so they will not fall out of the cable trays during shock.

(3) Cables passing between floors and equipment should have sufficient slack to account for relative motion due to shock.

(4) Cables exiting the building must be designed to resist and survive the relative movement between the ground and the structure during ground shock.

12-3. Protection against CB warfare agents

CB protection is accomplished by filtration, pressurization, and personnel decontamination. The U.S. Army Chemical Corps has developed CB filters that remove all known chemical and biological contaminants. These filters are composed of a particulate filter and an activated carbon filter. Table 12-4 is a list of available filter sizes. The CB filters should be preceded by a commercial prefilter and a blast valve to protect the filter from blast. The static pressure level inside the facility should be maintained above the outside ambient air pressure level to prevent migration of CB agents into the facility. A decontamination facility should be located inside the blast door to prevent CB-contaminated personnel from bringing CB agents into the protected facility. CB protection should be designed according to TM 5-855-2.

Table 12-4. Filter specifications

Nomenclature		Capacity CFM	Size, in. A B C	Air Resistance in., H_2O	Weight lb
Filter, Particulate	C-18	600	24 x 24 x 5-7/8	1.00	18
Filter, Gas	C-22	600	25-1/2 x 25-1/2 x 5-7/8	1.25	275
Filter, Particulate	C-19	1,200	24 x 24 x 11	1.75	40
Filter, Gas	C-32	1,200	25-1/2 x 25-1/2 x 54	1.25	530
Filter, Particulate	C-30	2,500	24 x 46-1/2 x 11	1.75	64
Filter, Gas	C-29	2,500	25-1/2 x 48 x 54	1.75	1,000
Filter, Particulate	C-20	5,000	48 x 48 x 11	1.75	120
Filter, Gas	C-23	5,000	48 x 48 x 51	1.25	2,100

12-4. Nonnuclear blast doors

Blast doors require that certain criteria and protection requirements be determined before a design analysis can be made. Those requirements must be ascertained regardless of the door type, whether hinged, sliding, personnel, equipment, etc. For utmost protection, personnel blast doors should be arranged in tandem and be provided with interlocks so that only one door can be opened at a time. This is especially imperative for nuclear-type blast doors. Design criteria requirements include:

- Equivalent static overpressure.
- Equivalent static rebound pressure (1/2 of overpressure).
- Horizontal (G) force from shock.
- Vertical (G) force from shock.
- Intended use.

Protection is to be provided against:

- Blast overpressure.
- Shock overloading.
- Security intrusion.
- CB.

CB protection is provided by a seal which is installed in a machine groove in the door, and which seals against the machined surface of the frame.

APPENDIX

REFERENCES

Government Publications.

Departments of the Army and the Air Force

FM 5–25	Explosives and Demolitions
FM 21–40	NBC (Nuclear, Biological, and Chemical) Defense
TM 3–221	Field CBR Collective Protection
TM 5–302–1	Army Facilities Components System–Design; Vol I
TM 5–302–2	Army Facilities Components System–Design; Vol II
TM 5–855–2	Protection Against Chemical and Biological Agents and Radiological Fallout
TM 5–856–2	Design for Structures to Resist the Effects of Atomic Weapons; Strength of Materials and Structural Elements
TM 9–1300–206	Care, Handling, Preservation, and Destruction of Ammunition

Air Force Weapons Laboratory, Kirtland AFB, NM

AFSWC–TDR–62–138	Principles and Practices for Design of Hardened Structures
AFWL–TR–70–127	Protection from Nonnuclear Weapons
AFWL–TR–71–74	Static and Dynamic Shear Behavior of Uniformly Loaded Reinforced Concrete Deep Beams
SAMSO–RT–67015	A Study of Launch Facility Closures

US Army Ballistic Research Laboratory Research and Development Center, Aberdeen Proving Ground, MD

| BRL MR 1809 | Attenuation of Peaked Air Shock Waves in Smooth Tunnels |

US Army Corps of Engineers Huntsville Division, HNDED-ES, PO Box 1600, Huntsville, AL 35807–4301

| HNDM 1110–1–2 | Suppressive Shields Design and Analysis Handbook |

Nongovernment Publications.

American Concrete Institute (ACI), PO Box 19150, Detroit, MI 48219

ACI 318–63	Building Code Requirements for Reinforced Concrete, 1963
ACI 318–71	Building Code Requirements for Reinforced Concrete, 1971
ACI 318–77	Building Code Requirements for Reinforced Concrete, 1977
ACI Journal, March, 1963	Yield Line Theory for the Ultimate Strength of Reinforced Concrete Slabs

American Institute of Steel Construction (AISC), Inc., 400 North Mighican Ave., Chicago, IL
60611

Manual of Steel Construction
Specifications for the Design, Fabrication, and Erection of Structural Steel for Buildings
Manual of Concrete Practice, Part 2.

Interscience Publishers, New York, NY

Ultimate Load Analysis of Reinforced and Prestressed Concrete Structures

John Wiley and Sons, Inc., New York, NY

Reinforced Concrete Fundamentals with Emphasis on Ultimate Strength

2567

A–2

BIBLIOGRAPHY

A. BOOKS:

Archer, D. H. R., ed., Jane's Infantry Weapons. Franklin Watts, Inc., New York (1978).

Baker, Wilfred E., Pete S. Westine, and Franklin T. Dodge, Similarity Methods in Engineering Dynamics. Haden Book Company, Inc., Rochelle Park, New Jersey (1973).

Biggs, J. M., Introduction to Structural Dynamics. McGraw–Hill Book Co., New York (1964).

Bonds, R., ed., The Soviet War Machine. Salamander Books Ltd., London, United Kingdom (1977).

Foss, C. F., Artillery of the World. Ian Allen Ltd., Shepperton, Surrey, United Kingdom (1976).

Harris, Cyril M. and Charles E. Crede, Shock and Vibration Handbook, Volume 3. McGray–Hill Book Co., New York.

Henrych, Josef, The Dynamics of Explosions and Its Use. Elsevier Publishing Company, New York (1979).

Owen, J., ed., Brassey's Infantry Weapons of the World. Crane Russak and Company, Inc., New York (1979).

Pretty, R. T., ed., Jane's Weapon Systems, 9th Edition. Jane's Publishing Company, London, New York (1977).

Pretty, R. T., ed., Jane's Weapon Systems, Jane's Yearbooks. Franklin Watts, Inc., New York (1978).

Roark, R. J., Formulas for Stress and Strain. McGraw–Hill Book Co., New York (1965).

Vaile, R. B., Jr., Underground Explosion Tests at Dugway. Stanford Research Institute, Stanford, California (1952).

Weeks, Col. J., ed., Jane's Infantry Weapons, 7th Edition. Jane's Publishing Company, London, New York (1981).

B. ARTICLES:

Boyd, M. A. and C. C. Huang, "Experiences on Shock Isolation of Equipment in the SAFEGUARD System." Shock and Vibration Bulletin, No. 47, Part 1, pp 151–161 (1977).

Cherikov, N., "Soviet Aircraft Cannon." International Defense Review.

Deere, D. U., "Technical Description of Rock Cores for Engineering Purposes." Rock Mechanics and Engineering Geology, Vol. I, No. 1, pp 16–22 (1964).

Eubanks, R. A., and Bernard R. Juskie, "Shock Hardening of Equipment." Shock and Vibration Bulletin, No. 32, Part 3, pp 23–73 (1963).

Huang, C. C., R. J. Bradshaw, and H. H. Yen, "Piping Design for Hydraulic Transient Pressure." Shock and Vibration Bulletin, No. 44, Part 3, pp 141–156 (1974).

C. MANUALS:

The Air Force Manual for Design and Analysis of Hardened Structures. R. E. Crawford, C. J. Higgins, and E. H. Bultman. Air Force Weapons Laboratory (1974).

AISC Manual of Steel Contruction, 6th Edition. "Eccentric Loads on Fastener Groups." AISC (1963).

Commentary on Plastic Design in Steel, Manual of Engineering Practice 41. American Society of Civil Engineering (1961).

FM 9-13. "Ammunition Handbook." U. S. Department of the Army (1981).

FM 10-18. "Petroleum Terminal and Pipeline Operations." U. S. Department of the Army (1974).

FM 10-207. "Petroleum Pipeline Terminal Operating Company. " U. S. Department of the Army (1981).

FM 21-40. "Chemical, Biological, Radiological, and Nuclear Defense." U. S. Department of the Army (1977).

TM 3-220. "Chemical, Biological, Radiological (CBR) Decontamination." U. S. Department of the Army (1967).

TM 5-855-2. "Protection Against Chemical and Biological Agents and Radiological Fallout." U. S. Department of the Army (1961).

TM 5-856-3. "Design of Structures to Resist the Effects of Atomic Weapons: Principles of Dynamic Analysis and Design." USAE Waterways Experiment Station (1957).

TM 9-1300-200. "Ammunition, General." U. S. Department of the Army (1969).

TM 9-1300-203. "Artillery Ammunition." U. S. Department of the Army (1967).

D. REPORTS:

Albritton, G. E., et al., Technical Report N–69–2, Report No. 1.
"Response of Deep Two–Way Reinforced and Unreinforced Concrete Slabs to Static and Dynamic Loading." U. S. Army Engineer Waterways Experiment Station, Vicksburg, Mississippi (1969).

Albritton, G. E., et al., Technical Report N–69–2, Report No. 2.
"Response of Deep Two–Way Reinforced and Unreinforced Concrete Slabs to Static and Dynamic Loading." U. S. Army Engineer Waterways Experiment Station, Vicksburg, Mississippi (1969).

Albritton, G. E., et al., Technical Report N–69–2, Report No. 3.
"Response of Deep Two–Way Reinforced and Unreinforced Concrete Slabs to Static and Dynamic Loading." U. S. Army Engineer Waterways Experiment Station, Vicksburg, Mississippi (1969).

Albritton, G. E., et al., Technical Report N–69–2, Report No. 4.
"Response of Deep Two–Way Reinforced and Unreinforced Concrete Slabs to Static and
Dynamic Loading." U. S. Army Engineer Waterways Experiment Station, Vicksburg,
Mississippi (1969).

Ball, J. W., DNA PR 0026 WES TR N–76–10, "ESSEX–Diamond Ore Research Program;
Damage Predictions for Contact Bursts on Reinforced Concrete Bridge Piers Project ESSEX
III." USAE Waterways Experiment Station, Vicksburg, Mississippi (1976).

Clark, R. O. and G. A. Coulter, BRL 1278. "Attenuation of Air Shock Waves in Tunnels."
Ballistic Research Laboratories, Aberdeen Proving Ground, Maryland (1960).

Department of the Army, BRL Memorandum Report No. 1344. "Air Blast Parameters Versus
Distance for Hemispherical TNT Surface Burst." Ballistic Research Laboratories, Aberdeen
Proving Ground, Maryland (1961).

Department of the Army, BRL Memorandum Report No. 1390 (DASA 1273). "Information
Summary of Blast Patterns in Tunnels and Chambers." Ballistic Research Laboratories,
Aberdeen Proving Ground, Maryland (1962).

Dishon, J. F., WES MP N–77–2. "Cratering Kenetics, Project ESSEX I, Phase I," U. S. Army
Engineer Waterways Experiment Station, Vicksburg, Mississippi.

Grabarek, C. L., BRL MR 2134. "Penetration of Armor by Steel and High Density Penetrators."
Ballistic Research Laboratories, Aberdeen Proving Ground, Maryland (1971).

Healey, J., et al., Technical Report 4903. "Primary Fragment Characteristics and Impact Effect
on Barriers." Picatinny Arsenal, Alabama (1975).

Ingram, J. K., TR N–77–6. "CENSE Explosion Tests Program–CENSE 2, Explosions in Soil."
U. S. Army Engineer Waterways Experiment Station, Vicksburg, Mississippi (1977).

Joachim, C. E. and L. K. Davis, TR SL–81 (draft). "Project MBCE–Munitions/Bare Charge
Equivalence in Soils." U. S. Army Engineer Waterways Experiment Station, Vicksburg,
Mississippi (1981).

Kintzinger, P. R., SC–RR–64–549. "Air Vent Phase I–Earth Particle Motion." Sandia
Laboratory, Albuquerque, New Mexico (1964).

Kriebel, A. R., URS 7050–2 or DASA 1200–12 Supplement 1. "Airblast in Tunnels and
Chambers." URS Research Company, San Mateo, California (1972).

Lampson, C. W., NDRC A–479. "Final Report on Effects of Underground Explosions." National
Defense Research Committee, Washington, D. C. (1946).

Perret, W. R. and R. C. Bass, SAND 74–0252. "Free–Field Ground Motion Induced by
Underground Explosions." Sandia Laboratories, Albuquerque, New Mexico (1975).

Perret, W. R., et al., TID–4500. "Project Scooter." Sandia Laboratories, Albuquerque, New
Mexico (1963).

Rhomberg, E. J., AFWL–TR–68–126. "Shear Strength of Deep Reinforced Concrete Slabs." Air
Force Weapons Laboratory, Kirtland AFB, New Mexico (1969).

Rowe, R. D., AWRE Report No. E2/65. "A Survey of Blast Valve Design." United Kingdom
Atomic Energy Authority Atomic Weapons Research Establishment (1966).

TM 5-855-1

Sonneburg, P. N. and R. J. Bradshaw, HNDTR–78–35–ED–SR. "Life Cycle Maintenance for PAR Site Shock Isolation Systems." U. S. Army Corps of Engineers, Huntsville Division, Huntsville, Alabama (1978).

True, D. G., Technical Report R–608, AD 680429. "Design for Flexible Utility Connections." Naval Civil Engineering Laboratory, Port Hueneme, California (1963).

U. S. Army Corps of Engineers, HNDTR–73–42–ED–R. "Shock Test Program, Dynamic Analysis Diesel Engine Generator, for SAFEGUARD TSE Systems and Equipment." Huntsville Division, Huntsville, Alabama (1973).

U. S. Army Corps of Engineers, HNDTR–75–22–ED–SR. "Shock Test Program, Dynamic Analysis–Air Compressor (P01CR), for SAFE–GUARD TSE Systems and Equipment." Huntsville Division, Huntsville, Alabama (1975).

U. S. Army Corps of Engineers, HNDTR–77–29–ED–SR. "Shock Test Program, Revised Hydraulic Transients Program, for SAFEGUARD TSE Systems and Equipment HYTRAN USERS MANUAL." Huntsville Division, Huntsville, Alabama (1977).

U. S. Army Corps of Engineers, HNDTR–77–30–ED–SR. "Shock Test Program, Dynamic Analysis of a 660–Ton Chiller, for SAFEGUARD TSE Systems and Equipment." Huntsville Division, Huntsville, Alabama (1977).

U. S. Defense Intelligence Agency, DST–1160W–029–76. "Projectile Fragment Identification Guide–Foreign." Washington, D. C. (1976).

U. S. Navy Department Bureau of Ships, NAVSHIPS 250–660–30. "A Guide for Design of Shock Resistant Naval Equipment." Washington, D. C. (1949).

Welch, W. P., NAVSHIPS 250–660–26. "Mechanical Shock on Naval Vessels." Washington, D. C. (1946).

Young, C. W., Report SC–DR–72 0523. "Empirical Equations for Predicting Penetration Performance in Layered Earth Materterials for Complex Penetrator Configuration." Sandia Laboratories, Albuquerque, New Mexico (1972).

E. PAPERS:

Bernard, R. S., Misecllaneous Paper S–77–16. "Empirical Analysis of Projectile Penetration in Rock." U. S. Army Engineer Waterways Experiment Station, Vicksburg, Mississippi (1977).

Brown, J. W., et al., MP SL–80–7. "Propogation of Explosive Shock Through Rubble Screens." U. S. Army Engineer Waterways Experiiment Station, Vicksburg, Mississippi (1980).

Day, J. D. and C. E. Joachim, MP SL–81–19. "Cable Vulnerability Study." U. S. Army Engineer Waterways Experiment Station, Vicksburg, Mississippi (1981).

Drake, J. L., "Ground Shock Threat to Buried Structures from Conventional Weapons." Presented at the Protective Design Symposium, Brussels, Belgium, September 22–23, 1975.

Flathau, W. J. and J. L. Drake, "Loading of Buried Structures for Conventional Bombs." Presented at the 100th Symposium on Weapons Effects on Protective Structures, Mannheim, Germany, November 14–16, 1978.

Sachs, D. C. and L. M. Swift, AFSWP–291. "Small Explosion Tests–Project MOLE." Stanford Research Institute, Stanford, California (1955).

U. S. Army Corps of Engineers, Huntsville, <u>HNDSP–71–57–ED–R</u>. "Shock Test Program, Relay –Fragility Test, for SAFEGUARD TSE Systems and Equipment," Huntsville, Alabama (1972).

U. S. Army Corps of Engineers, Huntsville, <u>HNDSP–71–58–ED–R</u>. "Shock Test Program, Air Conditioner Test, for SAFEGUARD TSE Systems and Equipment," Huntsville, Alabama (1972).

U. S. Army Corps of Engineers, Huntsville, <u>HNDSP–72–64–ED–R</u>. "Shock Test Program, Electrical Panelboards Tests, for SAFEGUARD TSE Systems and Equipment," Huntsville, Alabama (1972).

U. S. Army Corps of Engineers, Huntsville, <u>HNDSP–72–69–ED–R</u>. "Shock Test Program, Station Battery System, for SAFEGUARD TSE Systems and Equipment," Huntsville, Alabama (1972).

U. S. Army Corps of Engineers, Huntsville, <u>HNDSP–72–70–ED–R</u>. "Shock Test Program, Water Purification Units, for SAFEGUARD TSE Systems and Equipment," Huntsville, Alabama (1973).

U. S. Army Corps of Engineers, Huntsville, <u>HNDSP–72–77–ED–R</u>. "Shock Test Program, Fluorescent Light Fixtures, for SAFEGUARD TSE Systems and Equipment," Huntsville, Alabama (1973).

U. S. Army Corps of Engineers, Huntsville, <u>HNDSP–72–77–ED–R</u>. "Shock Test Program, Fluorescent Light Fixtures, for SAFEGUARD TSE Systems and Equipment," Huntsville, Alabama (1974).

U. S. Army Corps of Engineers, Huntsville, <u>HNDSP–73–85–ED–R</u>. "Shock Test Program, Heat Exchanger, for SAFEGUARD TSE Systems and Equipment," Huntsville, Alabama (1973).

U. S. Army Corps of Engineers, Huntsville, <u>HNDSP–73–86–ED–R</u>. "Shock Test Program, Air Conditioning and CBR Filters, for SAFEGUARD TSE Systems and Equipment," Huntsville, Alabama (1973).

U. S. Army Corps of Engineers, Huntsville, <u>HNDSP–73–87–ED–R</u>. "Shock Test Program, Centrifugal Fans and Axial Fans, for SAFEGUARD TSE Systems and Equipment," Huntsville, Alabama (1973).

U. S. Army Corps of Engineers, Huntsville, <u>HNDSP–73–88–ED–R</u>. "Shock Test Program, Waste Disposal Pumps, for SAFEGUARD TSE Systems and Equipment," Huntsville, Alabama (1973).

■■ 3515789 0225035 080 ■■

U. S. Army Corps of Engineers, Huntsville, HNDSP–73–89–ED–R. "Shock Test Program, Heating and Cooling Coils, for SAFEGUARD TSE Systems and Equipment," Huntsville, Alabama (1973).

U. S. Army Corps of Engineers, Huntsville, HNDSP–73–91–ED–R. "Shock Test Program, Switchgear Cabinet–Transfer Function Tests, for SAFEGUARD TSE Systems and Equipment," Huntsville, Alabama (1973).

U. S. Army Corps of Engineers, Huntsville, HNDSP–73–95–ED–R. "Shock Test Program, Water Chiller, for SAFEGUARD TSE Systems and Equipment," Huntsville, Alabama (1973).

U. S. Army Corps of Engineers, Huntsville, HNDSP–73–97–ED–R. "Shock Test Program, Peripheral Turbine Pumps, for SAFEGUARD TSE Systems and Equipment," Huntsville, Alabama (1973).

U. S. Army Corps of Engineers, Huntsville, HNDSP–73–158–ED–R. "Hardness Program – NON–EMP, Heat Exchanger Dynamic Response Analysis, for SAFEGUARD TSE Ground Facilities," Huntsville, Alabama (1973).

U. S. Army Corps of Engineers, Huntsville, HNDSP–73–159–ED–R. "Hardness Program – NON–EMP, Test Report, for SAFEGUARD TSE Ground Facilities Shock Test Program, Fragility Testing Electric Motor Control Centers (ITCs E06MC, E52MC, E87MC, and E89MC), Volumes 1 and 2," Huntsville, Alabama (1973).

U. S. Army Corps of Engineers, Huntsville, HNDSP–73–160–ED–R. "Hardness Program – NON–EMP, Pump Piping Appurtenance, Shock Response Analysis, for SAFEGUARD TSE Ground Facilities," Huntsville, Alabama (1973).

U. S. Army Corps of Engineers, Huntsville, HNDSP–73–300–ED–R. "Shock Test Program, Dry Transformers, for SAFEGUARD TSE Systems and Equipment," Huntsville, Alabama (1973).

U. S. Army Corps of Engineers, Huntsville, HNDSP–73–302–ED–R. "Shock Test Program, Monitoring and Control Components, for SAFEGUARD TSE Systems and Equipment," Huntsville, Alabama (1973).

U. S. Army Corps of Engineers, Huntsville, HNDSP–73–304–ED–R. "Shock Test Program, Compressor–Instrument Air Dryer, for SAFEGUARD TSE Systems and Equipment," Huntsville, Alabama (1973).

U. S. Army Corps of Engineers, Huntsville, HNDSP–73–305–ED–R. "Shock Test Program, Metal-Clad Switchgear, for SAFEGUARD TSE Systems and Equipment, Volume 1, Book 2- 5HK350 Test Data," Huntsville, Alabama (1973).

U. S. Army Corps of Engineers, Huntsville, HNDSP–74–305–ED–R. "Shock Test Program, Metal-Clad Switchgear, for SAFEGUARD TSE Systems and Equipment, Volume I, Book 1, Basic Report and 5HK75 Test Data," Huntsville, Alabama (1974).

U. S. Army Corps of Engineers, Huntsville, HNDSP–74–306–ED–R. "Shock Test Program, Piping Segments, for SAFEGUARD TSE Systems and Equipment," Huntsville, Alabama (1974).

U. S. Army Corps of Engineers, Huntsville, <u>HNDSP–74–307–ED–R</u>. "Shock Test Program, Monitoring and Control-Duct Mounted Equipment, for SAFEGUARD TSE Systems and Equipment," Huntsville, Alabama (1974).

U. S. Army Corps of Engineers, Huntsville, <u>HNDSP–74–308–ED–R</u>. "Shock Test Program, 660-Ton Chiller Components, for SAFEGUARD TSE Systems and Equipment," Huntsville, Alabama (1974).

U. S. Army Corps of Engineers, Huntsville, <u>HNDSP–74–309–ED–R</u>. "Shock Test Program, Air Compressor Control Panel and Drive Motor, for SAFEGUARD TSE Systems and Equipment," Huntsville, Alabama (1974).

U. S. Army Corps of Engineers, Huntsville, <u>HNDSP–74–310–ED–R</u>. "Shock Test Program, Generator Control Panel, for SAFEGUARD TSE Systems and Equipment," Huntsville, Alabama (1974).

U. S. Army Corps of Engineers, Huntsville, <u>HNDSP–74–312–ED–R</u>. "Shock Test Program, Generator Neutral Breaker, for SAFEGUARD TSE Systems and Equipment," Huntsville, Alabama (1974).

U. S. Army Corps of Engineers, Huntsville, <u>HNDSP–74–315–ED–R</u>. "Shock Test Program, Electric Motor Control Centers (E52MC) (E87MC) for SAFEGUARD TSE Systems and Equipment," Huntsville, Alabama (1974).

U. S. Army Corps of Engineers, Huntsville, <u>HNDSP–74–316–ED–R</u>. "Shock Test Program, Instrument Air Dryer, for SAFEGUARD TSE Systems and Equipment," Huntsville, Alabama (1974).

U. S. Army Corps of Engineers, Huntsville, <u>HNDSP–74–321–ED–R</u>. "Shock Test Program, Thermal Water Valve, for SAFEGUARD TSE Systems and Equipment," Huntsville, Alabama (1974).

U. S. Army Corps of Engineers, Huntsville, <u>HNDSP–74–323–ED–R</u>. "Shock Test Program, Generator Static Exciter/Regulator, for SAFEGUARD TSE Systems and Equipment," Huntsville, Alabama (1974).

U. S. Army Corps of Engineers, Huntsville, <u>HNDSP–74–324–ED–R</u>. "Shock Test Program, Diesel Engine Components and M&C Components, for SAFEGUARD TSE Systems and Equipment," Huntsville, Alabama (1974).

U. S. Army Corps of Engineers, Huntsville, <u>HNDSP–74–325–ED–R</u>. "Shock Test Program, Air Handling Unit (H06AU), for SAFEGUARD TSE Systems and Equipment," Huntsville, Alabama (1974).

U. S. Army Corps of Engineers, Huntsville, <u>HNDSP–74–326–ED–R</u>. "Shock Test Program, Three Piping Segments (P0ZPC), for SAFEGUARD TSE Systems and Equipment," Huntsville, Alabama (1974).

U. S. Army Corps of Engineers, Huntsville, <u>HNDSP–74–327–ED–R</u>. "Shock Test Program, Piping Segment (P39PC), for SAFEGUARD TSE Systems and Equipment," Huntsville, Alabama (1974).

U. S. Army Corps of Engineers, Huntsville, <u>HNDSP–74–328–ED–R</u>. "Shock Test Program, Piping Segment (P30PC), for SAFEGUARD TSE Systems and Equipment," Huntsville, Alabama (1974).

U. S. Army Corps of Engineers, Huntsville, <u>HNDSP–74–329–ED–R</u>. "Shock Test Program, Gas Turbo–Generator Assembly (E01GT), for SAFEGUARD TSE Systems and Equipment," Huntsville, Alabama (1974).

U. S. Army Corps of Engineers, Huntsville, <u>HNDSP–74–330–ED–R</u>. "Shock Test Program, Unit Substation Switch-Transformer-Voltage Regulator-Circuit Breaker (E0455), for SAFEGUARD TSE Systems and Equipment," Huntsville, Alabama (1974).

U. S. Army Corps of Engineers, Huntsville, <u>HNDSP–74–332–ED–R</u>. "Shock Test Program, Unit Substation Voltage Regulator-Circuit Breaker (E0555)-B, for SAFEGUARD TSE Systems and Equipment," Huntsville, Alabama (1974).

U. S. Army Corps of Engineers, Huntsville, <u>HNDSP–74–333–ED–R</u>. "Shock Test Program, Unit Substation Motor Control Center (E1255), for SAFEGUARD TSE Systems and Equipment," Huntsville, Alabama (1974).

U. S. Army Corps of Engineers, Huntsville, <u>HNDSP–74–334–ED–R</u>. "Shock Test Program, Unit Substation Transformer (E1655), for SAFEGUARD TSE Systems and Equipment," Huntsville, Alabama (1974).

U. S. Army Corps of Engineers, Huntsville, <u>HNDSP–74–335–ED–R</u>. "Shock Test Program, Unit Substation Transformer (E2755), for SAFEGUARD TSE Systems and Equipment," Huntsville, Alabama (1974).

U. S. Army Corps of Engineers, Huntsville, <u>HNDSP–74–336–ED–R</u>. "Shock Test Program, Unit Substation Circuit Breakers (E2955), for SAFEGUARD TSE Systems and Equipment," Huntsville, Alabama (1974).

U. S. Army Corps of Engineers, Huntsville, <u>HNDSP–74–337–ED–R</u>. "Shock Test Program, Motor Generator Set (E03GM), for SAFEGUARD TSE Systems and Equipment," Huntsville, Alabama (1974).

U. S. Army Corps of Engineers, Huntsville, <u>HNDSP–74–338–ED–R</u>. "Shock Test Program, Motor Generator Set (E12GM), for SAFEGUARD TSE Systems and Equipment," Huntsville, Alabama (1974).

U. S. Army Corps of Engineers, Huntsville, <u>HNDSP–74–340–ED–R</u>. "Shock Test Program, Compressor Control Oil Shutdown Switch, for SAFEGUARD TSE Systems and Equipment," Huntsville, Alabama (1974).

U. S. Army Corps of Engineers, Huntsville, <u>HNDSP–74–342–ED–R</u>. "Shock Test Program, Pressure Control Valve (P83VE), for SAFEGUARD TSE Systems and Equipment," Huntsville, Alabama (1974).

U. S. Army Corps of Engineers, Huntsville, <u>HNDSP–74–344–ED–R</u>. "Shock Test Program, Dynamic Analysis–Motor Generator Set–ITC–E12GM, for SAFEGUARD TSE Systems and Equipment," Huntsville, Alabama (1974).

U. S. Army Corps of Engineers, Huntsville, <u>HNDSP–74–345–ED–R</u>. "Shock Test Program, Heat Sensing Device Assembly, for SAFEGUARD TSE Systems and Equipment," Huntsville, Alabama (1974).

U. S. Army Corps of Engineers, Huntsville, <u>HNDSP–75–22–ED–SR</u>. "Shock Test Program, Dynamic Analysis–Air Compressor (P01CR), for SAFEGUARD TSE Systems and Equipment," Huntsville, Alabama (1975).

U. S. Army Corps of Engineers, Huntsville, <u>HNDSP–75–349–ED–R</u>. "Shock Test Program,

Fragility Tests of Twenty–Two Electrical Components, for SAFEGUARD TSE Systems and Equipment," Huntsville, Alabama (1975).

GLOSSARY

Abbreviations

AC	Alternating current
AISC	American Institute of Steel Construction
AP	Armor piercing
API	Armor piercing incendiary
BHN	Brinell Hardness Number
BP	Homogeneous bulletproof armor
Cal	Caliber
CB	Chemical and biological
CEV	Combat engineer vehicle
cfm	Cubic feet per minute
CL	Confidence level
CPS	Cycles per second
DC	Direct current
DLF	Dynamic load factor
DOB	Depth of burst
FAE	Fuel air explosive
FHBP	Face-hardened bulletproof armor
fps	Feet per second
FRAG	Fragmentation
GP	General purpose
GPF	General purpose fragmentation (weapon)
GZ	Ground zero
HE	High explosive
HEAT	High explosive antitank
HOB	Height of burst
in	Inch
lb	Pound
LC	Light case
m	Meter
mm	Millimeter
MDOF	Multi degree of freedom
MQ	Machinable quality homogeneous soft armor
MS	Mild steel
NBC	Nuclear, biological, and chemical
OCE	Office, Chief of Engineers
pcf	Pounds per cubic feet
POL	Petroleum, oil, and lubricants
psf	Pounds per square foot
psi	Pounds per square inch
RAP	Rocket-assisted projectiles
RQD	Rock quality designation

SAP	Semi armor piercing
SDOF	Single degree of freedom
STS	Special-treatment steel
yd	Yard
%	Percent

List of Symbols

a	Width of the area over which the load p_f is applied; also, short span of slab; also, center-to-center distance between adjacent slabs
a_0	Peak acceleration, g's
A	Gross area of member
A	Acceleration
A'_c	Area of core of spirally reinforced concrete member measured to outside diameter of spiral
A'_s	Cross-sectional area of compression steel
A_{avg}	Average free-field acceleration across structure, g's
A_g	Gross cross-sectional area of number
A_i	Internal vented surface area, ft^2
A_L	Loaded area producing shear
A_{SH}	Area resisting shear
A_{vH}	Total cross-sectional area of longitudinal web reinforcing over distance s_H
A_{vS}	Total cross-sectional area of web reinforcing over distance s
A_o	Area of openings, ft^2
A_s	Cross-sectional area of tension steel
A_m	Maximum cross-sectional area of projectile, in.2
A_v	Vent areas of structure
A_w	Wall areas of structure
A_1, A_2	Areas of tunnel sections
b	Long span of slab; also, width of member; also, flange width; also, width of rectangular section
b_f	Flange width
b'	Width of web of I or T section
B	Back-face crater diameter, feet; also, Brinell hardness of common mild structural steel (taken as 150)
B'	Brinell hardness of other than mild steel
B_L	Long span, inches
B_x	Explosive constant
c	Seismic velocity, fps
C	Ambient sound velocity in air, fps; also, damper
C_D	Drag coefficient
$C_D q$	Drag pressure
C_E	Equivalent load factor
C_L	Leakage pressure coefficient (a function of pressure difference P-P; where P = pressure applied to the exterior of the structure)
C_m	Coefficient applied to bending term
$C_{r\alpha}$	Peak reflected pressure coefficient
C_s	Constant, sec/in.
C_v	Empirical constant
C_1	Seismic velocity of upper level

$C_{1(\mu)}, C_{2(\mu)}$	Values of R_m/F corresponding to a ductility (μ) and ratios t_{d1}/T and t_{d2}/T, respectively
C_2	Seismic velocity of lower layer
d	Linear dimension of fragment; also, location of shock front when maximum stress in roof occurs; also, diameter or caliber of bomb or projectile, inches; also, depth of steel beam; also, diameter of shaped charge, mm
d'	Depth from extreme compression fiber to center of compression steel
d_a	Apparent crater depth
d_{avg}	Average free-field displacement across structure, ft
d_c	Diameter of circle through centers of longitudinal reinforcing arranged in a circular pattern
d_f	Effective depth of member (distance from extreme compression fiber to center of tensile steel)
d_i	Average inside diameter of casing, inches
d_o	Peak displacement, ft
d_t	True depth
D	Diameter of bolt, inches; also, maximum relative displacement between a simple spring-mass oscillator and the floor of the structure; also, depth from weapon to roof; also, depth of explosion in soil or detonation slab
D/L	Blast wave location ratio
D_d	Caliber density
DLF	Dynamic load factor
D_o	Outside diameter of concrete section
D_t	Tunnel diameter, feet
e	Eccentricity of the axial load with respect to the centroid of the tension reinforcement calculated by conventional methods of frame analysis; also, eccentricity measured from the plastic centroid for the balanced case
e'	Eccentricity from the plastic centroid of the section calculated by conventional methods of frame analysis
e_h	Thickness of homogeneous armor (BHN 360-440), inches
E_c	Modulus of elasticity of concrete, psi
E_s	Modulus of elasticity of steel
f	Coupling factor; also, natural frequency, cycles/sec
f'_c	Concrete compressive strength, psi or ksi
f_a	Axial stress permitted on a compression member in the absense of bending moment (dependent on slenderness ratio)
f_i	Coupling factor for each component material; i.e., air, soil, concrete
f_y	Yield strength of steel, psi
F	Peak dynamic load; also, preload tension in bolt, pounds
$F(t)$	Forcing function (function of time t)
F_{eq}	Equivalent force
F_H	Horizontal load
F_v	Vertical load
F_1	Magnitude of instantaneously applied constant load
g	Gravitational acceleration; also, maximum acceleration (g's) obtained from the response spectrum
g_h	Maximum horizontal acceleration from the horizontal response spectrum for the location where equipment is located, g's
g_v	Maximum vertical acceleration from the vertical response spectrum for the location where equipment is located, g's
G	Gurney explosive energy constant

TM 5-855-1

h	Total depth of slab; also, overall thickness of member (inches); also, depth of rectangular section; also, thickness of layer; also, height of frame
h_e	Effective depth of beam web, distance between centroids of flanges $\approx 0.95d$ (d is the full depth)
H	Wood hardness, pounds; also, height of wall
H_s	Height of structure
i	Impulse of load-time history
i_r	Reflected pressure unit impulse, psi-ms
i_s	Incident unit impulse for positive phase, psi-ms
i_1, i_2	Ratios of ultimate moment capacities at supports 1 and 2 to that at center of long span
i_3, i_4	Ratios of ultimate moment capacities at supports 3 and 4 to that at center of short span
I	Average impulse transmitted to structure by a particle
$I/W^{1/3}$	Scaled impulse of a reference explosion
I_c	Average of cracked and uncracked moment of inertia of concrete
I_o	Impulse, lb-sec/in.^{2}
K	Spring constant; also, stiffness
K_{eq}	Equivalent stiffness
K_E	Effective spring constant
K_f	Stiffness of the structure
K	Reflection coefficient from the lower layer; also, effective length factor in the plane of bending
KL/r	Slenderness ratio
K_e	Equivalent stiffness
K_L	Load factor
K_{LM}	Load mass factor
K_M	Mass factor
K_p	Soil penetration constant
K_s	Effective length factor
l_b	Actual unbraced length in the plane of bending
l_d	Linear dimension of an idealized particle shape
L	Penetration path length of weapon in soil, feet; also, total weapon length; also, width of the strip or element being considered; also, length of column; also, unsupported length of the member; also, wall length; also, width of frame; also, clear span of slab
L/d	Slenderness ratio of bomb
L_a	Length of charge in contact with air
L_c	Length of charge in contact with concrete
L_{cr}	Recommended bracing spacing for columns
L_d	Required development lengths of deformed bars
L_D	Development length for bars in compression
L_i	Length of weapon in contact with each material; also, load
L_s	Short span, inches
L_W	Positive phase wave length, ft
L_W^-	Wave length of the negative pulse
L_{wb}/L	Wave length-span ratio
m	$f_y / 0.85f_c$
m_1	Mass of top member of frame
m_2	Total mass of both side members of single bay frame

Glossary—4

M	Stiffness or modulus of soil; also, moment; also, torque applied to bolt, inch-pounds; also, mass; also, lesser of the moments at the ends of the unbraced segment; also, constant for a given munition
$\bar{M}$	Average particle momentum
M'	Moment at the critical section, in.–lb.
M''	Moment at the critical section adjusted for axial load
M^c_p	Ultimate moment capacity per unit width of slab at edge of slab; also, ultimate moment capacity at the center of a beam
M^e_p	Ultimate moment capacity per unit width of slab at edge of slab; also, ultimate moment capacity at the end of the member
M_b	Balance point moment
M_{eq}	Mass of the equivalent system
M_f	Maximum applied moment
M_{Lc}	Ultimate moment capacity per unit width of slab at the center of and in the direction of the long span
M_{Le}	Ultimate moment capacity per unit width of slab at the supports of and in the direction of the long span
M_m	Modified moment; also, maximum moment that can be resisted by the member in the absence of axial load
M / M_p	End moment ratio (+ for reverse curvature, - for single curvature)
M_p	Plastic moment capacity; also, moment capacity of member
M_{ps}	Reduced plastic moment
M_s	Mass of the structure
M_{sc}	Ultimate moment capacity per unit width of the slab at the center of and in the direction of the short span
M_{se}	Ultimate moment capacity per unit width of slab at the supports of and in the direction of the short span
M_{uc}	Ultimate bending moment capacity of column
M_1	Smaller value of end moment acting on member; sign is positive if the member is bent in single curvature
M_2	Larger value of end moment acting on member; sign is always positive
n	Attenuation coefficient; also, number of 90-degree turns in a tunnel
N	Number of people in the facility
N_f	Number of fragments with weight greater than W/f
N_m	Number of fragments with weight greater than the fragment weight m
N_s	Nose shape factor; also, fragment shape factor
N_T	Total number of fragments
p	Tension reinforcing steel ratio
p'	Compression steel ratio = A'_s / bd_f
$p(t)$	Intensity of uniform load on wall of frame (function of time)
p_b	Balance point reinforcing ratio
p_c	Tensile steel ratio at the center of the member; also, average tension steel ratio at center of slab
p_e	Tensile steel ratio at the end of the member; also, average tension steel ratio at end of slab
p_f	Uniformly distributed load
p_F	Tensile steel ratio required to balance the compression force in the overhanging portion of the flanges
p_{lc}	Average tensile steel ratio at the center spanning in the long direction
p_{le}	Average tensile steel ratio at the end spanning in the long direction

Glossary–5

p_s	Shear resistance of slab
p_{sc}	Average tensile steel ratio at the center, spanning in the short direction
p_{se}	Average tensile steel ratio at the edge, spanning in the short direction
p_t	Total steel ratio based upon the gross cross-section area of the member A_g
p_w	Total tensile steel ratio
P	Steel armor penetration by shaped charge, mm; also, applied blast pressures acting on the surface surrounding an opening; also, axial load
$P(t)$	Shock stress
P_a	Applied axial load; also, ambient pressure, psi
P_b	Balance point load
P_{cr}	Maximum allowable load for an axially loaded compression member for plastic design
P_d	Directly transmitted stress
P_e	Euler buckling load
P_f	Concentrated load resistance of member based on flexural capacity; also, ultimate load capacity of a two-way slab
P_i	Leakage pressure inside a structure
$P-P_i$	Pressure differential at the openings of a structure
P_n	Peak pressure after n turns or bends in a tunnel
Po	Ultimate axial load capacity of a member when carrying no moment; also, peak pressure
P_{or}	Pressure on the roof directly below the weapon
P_p	Sectional pressure of the bomb or projectile (weight in pounds divided by the maximum cross-sectional area in square inches)
P_{qs}	Peak quasi-static pressure
P_r	Peak positive reflected pressure
P_R	Pressure on roof at a distance R_S away from weapon
P_s	Incident pressure; also, stress reflected from the surface; also, concentrated load resistance of member based on shear capacity
P_{se}	Incident pressure at point e , a function of time
P_{so}	Peak overpressure in the tunnel just ahead of the first turn; peak incident pressure
P_{sob}	Peak overpressure occurring at point b
P_{soe}	Peak overpressure occurring at point e
P_{tc}	Pressure acting on the front wall after time t_c
P_T	Transmitted shock overpressure
P_u	Axial load capacity under combined axial load and bending
P_y	Plastic axial load ($A\ f_y$)
P_ℓ	Stress reflected from a lower layer
q	Dynamic pressure
q_e	Dynamic pressure at point e (a function of time)
q_o	Peak dynamic pressure
q_{ob}	Value of $C_t\,P_{sob}$
q_{oe}	Peak dynamic pressure at point e
Q	Axial load, pounds (positive for compression loads, negative for tensile loads)
r	Horizontal distance to the point on the structure; also, radius of gyration of the member cross section
r_a	Apparent crater radius
r_b	Radius of gyration

Glossary–6

r_t	True crater radius
r_y	Radius of gyration of the member about its weak axis
R	Resistance (a function of time); also, distance from the explosion, ft
R_c	Force required to cause first cracking of shear wall
R_d	Path length traveled by the directly transmitted wave to any point on the wall
R_f	Distance traveled by fragment, ft
R_G	Horizontal or ground distance from weapon to structure wall
R_m	Static capacity
R_r	Radius of the slab
R_R	Resistance function (K_y for an elastic system)
R_s	Slenderness ratio; also, total path length of a wave reflected from the ground surface
R_1, R_2	Range, feet; also, distance from explosion to leading edge of structure
R_l	Total path length of a wave reflected from a deeper layer
s	Spacing of vertical web reinforcing; also, thickness scabbed
s_H	Vertical spacing of longitudinal web reinforcing
S	Height of the structure (H_s) or one–half its width (W_s), whichever is smaller
S_i	Soil penetrability index
t	Wall thickness; also, time
t_o	Positive phase duration
t_o^-	Negative phase duration
t_a	Arrival time
t_b	Time at which the quasi–static pressure returns to ambient; also, time at which the blast wave reaches the end of the element (point b)
t_c	Clearing time; also, average casing thickness, in.
t_d	Positive phase duration of directly transmitted ground shock; also, duration of rectangular or triangular pulse; also, time when the blast wave reaches point d
t_{dy}	Duration of dynamic loading
t_e	Time when the blast wave reaches point e
t_f	Time then the blast wave reaches the beginning of the element (point f); also, flange thickness
t_h	Thickness of member in the direction of bending
t_l	Positive phase duration of pressure wave reflected from lower layer
t_m	Time to peak response
t_o	Duration of applied pressure, positive phase duration
t_o^-	Duration of negative phase
t_{of}	Fictitious duration of the positive phase or equivalent triangular duratin
t_p	Perforation thickness, inches
t_{pf}	Thickness of concrete that a fragment is just capable of perforating, inches
t_r	Duration of initial reflected pulse; also, rise time
t_s	Positive phase duration of pressure wave reflected from surface; also, steel plate thickness or concrete slab thickness, inches
t_{sp}	Thickness of concrete that will spall, inches
t_t	Total effective thickness of composite plates
t_w	Web thickness
t_ℓ	Actual thickness, inches
T	Natural period; also, pier thickness, feet
T_c	Time after closure, hours

T_c	Time after closure, hours
u	Velocity of gas molecules making up a shock
U	Velocity of the shock front
$\underline{V_a}$	Percent volume of air voids
$\overline{V}$	Average vertical velocity during deformation
V	Particle velocity; also, striking velocity in units of 1,000 fps; also, shearing force; also, pseudovelocity; also, dynamic reaction
V'	Shear at the critical section, pounds
V_A	Percent volume of air voids; also, dynamic reaction on short side of slab
V_B	Dynamic reaction on long side of slab
V_{avg}	Average free-field velocity across structure, fps
V_c	Total volume of core measured out–to–out of spiral
V_f	Final velocity
V_i	Impact velocity
V_I	Internal volume of structure, ft^3
V_L	Ballistic limit velocity, fps
V_o	Peak value of particle velocity, fps; also, volume of structure, ft^3
V_{oI}	Initial fragment velocity, 10^3 fps
V_r	Residual velocity, 10^3 fps
V_s	Shear force corresponding to first yield in shear; also, striking velocity, fps
V_{sf}	Striking velocity of fragment, 10^3 fps
V_{sp}	Volume of spiral reinforcement
V_u	Total shear resistance of section
V_{uc}	Total shear strength of beam; also, ultimate shear resistance; also, static shear strength
V_{us}	Added shear capacity contributed by shear steel
V_v	Shelter volume, ft^3
W	Uniform load applied to slab; also, width of roof; also, charge weight, pounds
W_a	Weight of charge in contact with air
W_c	Total casing weight, ounces; also, weight of concrete, pcf; also, weight of charge in contact with concrete
W_f	Design fragment weight, ounces
W_i	Weight of the charge in contact with each component material
W_p	Particle weight
W_s	Weight of the charge in contact with soil; also, width of structure
W_w	Weight of piping; also, weight of the equipment, tank, door, or equipment cover
$\overline{x}$	Distance from extreme compression fiber to neutral axis; also, adjusted scaled ground range
X	Penetration of weapon into concrete, inches; also, penetration depth in common structural steel of fragments, inches
X'	Penetration into other than mild steel
X_f	Final penetration depth of bomb into soil, feet
y	Displacement
$\ddot{y}$	Acceleration
y_e	Yield deflection
y_m	Maximum deflection
Y	Unconfined compressive strength of the intact rock, psi
Y_m	Maximum deflection
z	Depth of the point on the structure from the ground surface

Glossary–8

Z	Depth of penetration, calibers; also, scaled depth of burial, ft / lb $^{1/3}$; also, plastic section modulus
Z_x, Z_y	Plastic section modulus with respect to the major and minor axes, respectively
α	Angle of incidence; also, ration of the short span to the long span; also, time constant
β	Time constant
∂_e	Vent area ratio
ΔP_i	Interior pressure increment, psi
Δt	Time increment, ms
ε'_s	Strain in the compression steel
ε_{cu}	Strain at ultimate concrete stress, normally equal to 0.003
Θ	Angle of obliquity
λ	Scaled distance or scaled range $(R/W^{1/3})$
λ_D	Scaled depth of explosion
λ_x	Scaled ground range
μ	Ductility ratio
γ	Total unit weight, pcf
γ_c	Ratio of the ultimate moment capacity in long span direction to that in short span direction at center of slab
γ_{dry}	Dry unit weight, pcf
γ_{12} γ_{34}	$\dfrac{\sqrt{1+i_1} + \sqrt{1+i_2}}{\sqrt{1+i_3} + \sqrt{1+i_4}}$
ρ	Target bulk density, pcf; also, wood density; also, mass density
ρc	Acoustic impedance, psi / fps
ρ'	Specific gravity of soil
ρ_o	Mass density of soil, lb-sec^2 / ft^4
ρ_s	Density of steel
ρ_t	Density of material for which penetration is desired
ρ_2	Mass density of lower layer
τ_i	Time intercept (a function of the charge weight and distance from the explosion to the tunnel entrance
ω	Natural circular frequency of system, radius per second

> The proponent agency of this manual is the Office of the Chief of Engineers, United States Army. Users are invited to send comments and suggested improvements on DA Form 2028 (Recommended Changes to Publications and Blank Forms) directly to HQDA (DAEN-ECE-T), WASH DC 20314-1000.

By Order of the Secretary of the Army:

JOHN A. WICKHAM, JR.
General, United States Army
Chief of Staff

Official:

R. L. DILWORTH
Brigadier General, United States Army
The Adjutant General

DISTRIBUTION:
To be distributed in accordance with DA Form 12–34B requirements for
TM 5–855–Series: Protective Designs–CBR/Nuclear.

* U.S. GOVERNMENT PRINTING OFFICE : 1988 - 201-421 (71452)